

EXPERIMENTAL AND THEORETICAL
STUDIES OF GREEN ENERGY BUILDING
USING VARIOUS BUILDING MATERIALS
AND ORIENTATION

Thesis

Submitted in partial fulfillment of the requirement for the degree of

DOCTOR OF PHILOSOPHY

by

S. SABOOR



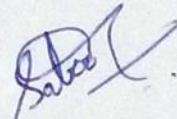
DEPARTMENT OF MECHANICAL ENGINEERING
NATIONAL INSTITUTE OF TECHNOLOGY KARNATAKA
SURATHKAL, MANGALORE – 575025

October, 2016

DECLARATION

by the Ph.D. Research Scholar

I hereby *declare* that the Research Thesis entitled "Experimental and Theoretical Studies of Green Energy Building using Various Building Materials and Orientation" which is being submitted to the National Institute of Technology Karnataka, Surathkal in partial fulfillment of the requirements for the award of the Degree of Doctor of Philosophy in Mechanical Engineering is a bonafide report of the research work carried out by me. The material contained in this Research Thesis has not been submitted to any University or Institution for the award of any degree.



S. Saboor

Reg. No. ME11F05

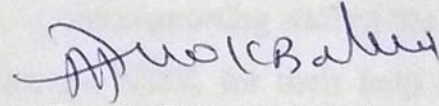
Department of Mechanical Engineering

Place: NITK - Surathkal

Date: 15-10-2016

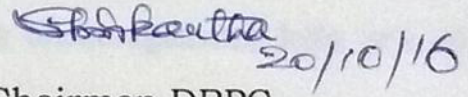
CERTIFICATE

This is to certify that the Research Thesis entitled "Experimental and Theoretical Studies of Green Energy Building using Various Building Materials and Orientation" submitted by Mr. S. Saboor (Register Number ME11F05) as record of the research work carried out by him, is accepted as the Research Thesis submission in partial fulfillment of the requirements for the award of degree of Doctor of Philosophy.



Dr. T. P. Ashok Babu

Research Guide and Professor,
Department of Mechanical Engineering



20/10/16

Chairman DRPC

Department of Mechanical Engineering



ACKNOWLEDGEMENT

First and foremost, I express my sincere heartfelt thanks and deepest gratitude to my beloved research guide Prof. T. P. Ashok Babu, Department of Mechanical Engineering for his esteemed guidance and kind cooperation throughout the project, which has helped me to complete this project satisfactorily. Apart from the technical guidance, it was his constant encouragement, affection, support and solace during the moments of despair that have been behind the successful completion of this report. This project would not have been possible without his guidance and invaluable suggestions.

I am extremely thankful to Research Progress Assessment Committee members, Prof. A. U. Ravi Shankar, Department of Civil Engineering and Dr. Kumar G.N., Department of Mechanical Engineering, NITK, for their invaluable comments and critical suggestions.

I acknowledge my thanks to Prof. K. V. Gangadharan, Head of Department of Mechanical Engineering for providing the necessary facilities. I express my heart full thanks to the Director of NITK Surathkal for providing the grants/funds to carry out this research work. I also thank all the teaching and supporting staff of the Mechanical Engineering and Civil Engineering Departments, NITK for their help and support provided during the research work.

I would like to thank my dearest friends G. Kiran Kumar and S. Sharmas Vali for their help during the research work. I would also like to thank my fellow research scholar Kezia Buruga of Chemical Engineering department and other research scholars of various departments for continuous encouragement, help and support during the course of my research work.

I lovingly acknowledge my parents, brothers and my relatives for their invaluable cooperation and support during every single day of my life. They have always been a source of inspiration for me. Finally, I am grateful to everybody those, who have helped and encouraged me during this research work.

- SABOOR SHAIK

ABSTRACT

The cooling of buildings by using passive methods has evoked great interest. Passive cooling is one of the methods to keep the building cool and to reduce the load on the air conditioner. The most prominent building elements that ensure energy efficiency in buildings are building enclosures such as walls and roofs. Passive cooling demands the study of the thermal characteristics of walls or roofs such as admittance, transmittance, decrement factor, time lag, surface factor and surface factor time lags. For the computation of these unsteady state characteristics, one dimensional heat flow diffusion equation with convective periodic boundary conditions was solved using matrix algebra and a computer program was developed using MATLAB to compute unsteady state thermal characteristics of homogeneous and typical composite walls. Natural building materials depreciate negative ecological impact and promote environmental sustainability. Hence, it is imperative to dedicate attention to the thermal performance of natural and sustainable building materials. Laterite stone is a locally available and natural building material in South-West coastal India. The thermal properties of laterite stone exposed to various humidity and temperature levels of ambient air were measured experimentally and their impact on unsteady thermal response characteristics of the laterite walls was studied in detail. The results showed that the increase in the relative humidity from 0% RH to 98% RH decreases the decrement factor by 8.35% and increases the time lag by 2.88%, whereas, the increase in the temperature from 0°C to 60°C decreases the decrement factor by 14.5% and increases the time lag by 8.3%. The effect of thermal properties of building materials, insulation location, air space thickness and air space location on unsteady state thermal characteristics was studied. From this study, It is concluded that fly ash brick composite walls with jute felt insulation located at the mid plane of the wall give greater time lags (11.17h) and fly ash brick composite walls with coir board insulation located at the outer side of the wall give the lowest value of decrement factor (0.17) among hundred configurations of the walls studied. Optimum wall thicknesses of building and insulating materials were computed. From the results, it is concluded that mud phuska and coconut pitch are the most recommended

homogeneous building and insulation materials, respectively, among studied building and insulating materials, from lower decrement factor and higher time lag point of view. It is also found that the insulation materials are highly responsive to short wave radiation than that of building materials. The impact of the divided air space thickness within the wall on thermal performance of the wall was also investigated. From the results, it is observed that the decrement factor decreases and time lag increases with the increase in the divided air space thickness within the composite wall for all building materials. The effect of unventilated continuous vertical air space location in the wall on unsteady state thermal response characteristics of composite walls was also studied. From this study, it is observed that Fly ash brick composite wall with air space located at the outer side and the mid center plane and fly ash brick with air space located at outer and inner sides of the composite walls are the recommended composite walls due to their highest time lag (11.28 h) and lowest decrement factor (0.166), respectively among studied building materials. The influence of the insulation location in the roof on thermal performance was investigated. The results reveal that the roof with insulation placed at the outer side and at the mid center plane of the roof is the most energy efficient from the lower decrement factor point of view and the roof with the insulation placed at the mid center plane and the inner side of the roof is the best from highest time lag point of view among seven studied configurations. The unsteady thermal response characteristics of hollow and stuffed bricks were also studied. From the results, it is observed that thermal admittance, surface factor time lag, decrement factor time lag and areal thermal heat capacity values increase with the increase in the number of air gaps in hollow bricks, whereas thermal transmittance and decrement factor reduces with the increase in the number of air gaps in the hollow bricks. The effect of wind velocity on the dynamic thermal performance of various composite walls was also reported. This research aids in designing energy efficient and environment friendly buildings for passive cooling.

Keywords: Decrement factor, Time lag, Admittance, Surface factor, Optimum insulation thickness, Laterite stone, Optimum insulation location, Air space thickness, Air space location, Hollow bricks, Stuffed bricks, Wind velocity, Admittance procedure.

CONTENTS

ACKNOWLEDGEMENTS.....	i
ABSTRACT.....	ii
CONTENTS.....	iv
LIST OF FIGURES.....	xiv
LIST OF TABLES.....	xxiv
NOMENCLATURE.....	xxx
CHAPTER 1	
INTRODUCTION.....	1
1.1 OVERVIEW.....	1
1.2 OPTIMUM ORIENTATION.....	2
1.3 ROOM SPACE ARRANGEMENT (THERMAL BUFFER ZONE (or) BUFFER SPACES).....	3
1.4 PLACING OF BUILDING OPENINGS.....	4
1.5 SHADING DESIGN.....	4
1.5.1. Shading of facades.....	4
1.5.2. Shading of fenestration.....	4

1.6 CLIMATE ZONES OF INDIA.....	4
1.7 ORGANIZATION OF DESSERTATION.....	7
CHAPTER 2	
REVIEW OF LITERATURE.....	9
2.1 INTRODUCTION.....	9
2.2 MOTIVATION.....	21
2.3 OBJECTIVES OF THE PRESENT STUDY.....	22
CHAPTER 3	
UNSTEADY STATE THERMAL CHARACTERISTICS OF THE WALLS.....	24
3.1 INTRODUCTION	24
3.2 ADMITTANCE PROCEDURE	24
3.2.1 Thermal transmittance	31
3.2.2 Thermal admittance	31
3.2.3 Time lead for thermal admittance.....	31
3.2.4 Decrement factor	32
3.2.5 Decrement delay	32
3.2.6 Surface factor	33
3.2.7 Time lag for the surface factor	33
3.2.8 Thermal heat capacity.....	34

3.2.9 Penetration length.....	34
3.2.10 Phase velocity	34
3.2.11 Optimum fabric thickness	35

CHAPTER 4

DYNAMIC THERMAL RESPONSE CHARACTERISTICS OF LATERITE WALLS.....	36
---	----

4.1 INTRODUCTION.....	36
-----------------------	----

4.2 THE EFFECT OF AIR RELATIVE HUMIDITY AND TEMPERATURE ON THERMAL PROPERTIES AND DYNAMIC THERMAL RESPONSE CHARACTERISTICS OF LATERITE WALLS	39
--	----

4.2.1 Morphology and chemical composition of laterite rocks.....	39
--	----

4.2.2 Pore structure and heat transfer through a moist pore of the laterite rocks.....	42
--	----

4.2.3 Effect of moisture in ambient air on thermal properties of laterite rocks.....	44
--	----

4.2.4 Effect of ambient air temperature on thermal properties of laterite rock.....	47
---	----

4.2.5 Effect of moisture and temperature on admittance and transmittance of laterite rocks.....	48
---	----

4.2.6. Effect of moisture and temperature on thermal heat capacity of laterite rocks.....	49
---	----

4.2.7. Effect of moisture and temperature on decrement factor and time lag of laterite rocks.....	51
---	----

4.2.8.Effect of moisture and temperature on surface factor and surface factor time lags.....	52
4.2.9. Effect of moisture, temperature and outside convective heat transfer coefficient on decrement factor and decrement time lags.....	54
4.3 THE DECREMENT FACTOR AND TIME LAG OF LATERITE AND CONCRETE BUILDINGS IN FOUR DIFFERENT CLIMATIC ZONES OF INDIA	56
4.3.1 Thermal properties and methodology.....	56
4.3.2 Decrement factor and time lag of buildings in hot and dry climatic zones (ahmedabad) of india.....	59
4.3.3 Decrement factor and time lag of buildings in moderate climatic zones (bangalore) of india.....	63
4.3.4 Decrement factor and time lag of buildings in composite climatic zones (hyderabad) of india.....	66
4.3.5 Decrement factor and time lag of buildings in warm and humid climatic zones (mangalore) of india.....	69
4.4 SUMMARY.....	72
CHAPTER 5	
EFFECT OF THERMAL PROPERTIES OF BUILDING MATERIALS, INSULATION LOCATION, AIR SPACE THICKNESS AND AIR SPACE LOCATION WITHIN WALL ON DYNAMIC THERMAL PROPERTIES OF WALLS.....	74

5.1 INTRODUCTION.....	74
5.2 EFFECT OF THERMAL PROPERTIES OF BUILDING AND INSULATING MATERIALS ON DYNAMIC THERMAL PROPERTIES OF WALLS.....	76
5.2.1 Thermal properties and unsteady thermal response characteristics of building and insulating materials.....	76
5.2.2 Optimum fabric thickness of building and insulating materials.....	79
5.2.3 Decrement factor and it's time lag of building and insulating materials.....	81
5.2.4 Surface factor and it's time lag of building and insulating materials.....	82
5.2.5 Decrement factor and it's time lag of composite walls.....	82
5.3 EFFECT OF INSULATION LOCATION WITHIN WALL ON DYNAMIC THERMAL PROPERTIES OF WALLS.....	84
5.3.1 Unsteady state thermal characteristics of building and insulating materials....	84
5.3.2 Optimum fabric energy storage of building and insulating materials.....	87
5.3.3 Effect of thickness on time lag and decrement factor of building and insulating materials.....	88
5.3.4 Effect of thickness on surface factor and it's time lag of building and insulating materials.....	88
5.3.5 Effect of insulation location on decrement factor and it's time lag of composite walls.....	89

5.4 Effect of air space thickness within wall on dynamic thermal properties of walls.....	94
5.4.1 Building material thermal properties and their unsteady thermal response characteristics.....	94
5.4.2 Thermal transmittance and admittance of homogeneous building materials.....	98
5.4.3 Decrement factor and time lag of building materials.....	99
5.4.4 Effect of air space thickness on thermal transmittance and thermal admittance.....	100
5.4.5 Effect of air space thickness on decrement factor and time lag.....	101
5.5 EFFECT OF AIR SPACE LOCATION WITHIN WALL ON DYNAMIC THERMAL PROPERTIES OF WALLS.....	102
5.5.1 Thermal properties and unsteady thermal characteristics of building materials.....	102
5.5.2 Optimum wall thicknesses of the building materials.....	106
5.5.3 Effect of wall thickness on decrement factor and it's time lag of building materials.....	107
5.5.4 Effect of wall thickness on surface factor and it's time lag of building materials.....	108
5.5.5 Effect of air space location in the wall on decrement factor and it's time lag of	

composite walls.....110

5.6 SUMMARY.....112

CHAPTER 6

EFFECT OF INSULATION LOCATION WITHIN ROOF ON DYNAMIC THERMAL PROPERTIES OF THE ROOFS.....116

6.1 INTRODUCTION.....116

6.2 THERMAL PROPERTIES AND UNSTEADY THERMAL RESPONSE PARAMETERS OF ROOF MATERIALS.....117

6.3 OPTIMUM FABRIC ENERGY STORAGE THICKNESS120

6.4 DECREMENT FACTOR AND TIME LAG OF ROOFING AND INSULATING MATERIALS.....121

6.5 SURFACE FACTOR AND SURFACE FACTOR TIME LAG OF ROOFING AND INSULATING MATERIALS122

6.6 EFFECT OF INSULATION POSITION IN THE COMPOSITE ROOF ON DECREMENT FACTOR AND TIME LAG.....123

6.7SUMMARY.....125

CHAPTER 7

DYNAMIC THERMAL PERFORMANCE OF HOLLOW AND STUFFED BRICKS.....127

7.1 INTRODUCTION.....	127
7.2 DYNAMIC THERMAL PERFORMANCE OF HOLLOW BRICKS.....	129
7.2.1 Dynamic thermal response of solid and hollow bricks.....	129
7.2.2 Decrement factor and time lag of solid bricks.....	132
7.2.3 Admittance and transmittance of solid bricks.....	132
7.2.4 Admittance and transmittance of hollow bricks.....	133
7.2.5 Surface factor and it's time lag of hollow bricks.....	134
7.2.6 Decrement factor and it's time lag of hollow bricks.....	135
7.2.7 Areal thermal heat capacity of hollow bricks.....	135
7.3. DYNAMIC THERMAL PERFORMANCE OF STUFFED BRICKS.....	137
7.3.1 Thermal properties and dynamic thermal parameters of bricks.....	137
7.3.2 Thermal transmittance and admittance of insulation filled bricks.....	141
7.3.3 Decrement factor and time lag of insulation filled bricks.....	144
7.3.4 Areal thermal heat capacity of insulation filled bricks.....	146

7.4 SUMMARY	147
-------------------	-----

CHAPTER-8

EFFECTS OF WIND VELOCITY ON DYNAMIC THERMAL CHARACTERISTICS OF OUTER BUILDING ENCLOSURES	150
--	-----

8.1 INTRODUCTION	150
------------------------	-----

8.2 BUILDING MATERIAL THERMAL PROPERTIES AND THEIR UNSTEADY THERMAL RESPONSE CHARACTERISTICS	151
--	-----

8.3 EFFECT OF WIND VELOCITY ON TRANSMITTANCE AND ADMITTANCE OF HOMOGENEOUS WALLS	155
--	-----

8.4 EFFECT OF WIND VELOCITY ON DECREMENT FACTOR AND TIME LAG OF HOMOGENEOUS WALLS	156
---	-----

8.5 EFFECT OF WIND VELOCITY ON SURFACE FACTOR AND SURFACE FACTOR TIME LAG OF HOMOGENEOUS WALLS	157
--	-----

8.6 EFFECT OF WIND VELOCITY ON AREAL THERMAL HEAT CAPACITY OF HOMOGENEOUS WALLS	158
---	-----

8.7 EFFECT OF WIND VELOCITY ON TRANSMITTANCE AND ADMITTANCE OF COMPOSITE WALLS	159
--	-----

8.8 EFFECT OF WIND VELOCITY ON DECREMENT FACTOR AND TIME LAG OF COMPOSITE WALLS	163
---	-----

8.9 SUMMARY.....	171
------------------	-----

CHAPTER-9

CONCLUSIONS AND FUTURE SCOPE.....	173
-----------------------------------	-----

REFERENCES.....	177
-----------------	-----

APPENDIX- I.....	184
------------------	-----

BIO-DATA.....	185
---------------	-----

LIST OF FIGURES

Figure 1.1 Schematic diagram of solar-passive building design (GRIHA 2011).....	2
Figure 1.2 Orientation of the building.....	3
Figure 1.3 Buffer spaces arrangement in building envelopes.....	3
Figure 1.4 Climatic Classification of India	5
Figure 1.5 Incident solar radiation in different orientations during summer in India	5
Figure 1.6 Incident solar radiation in different orientations during winter in India	6
Figure 3.2.1 Schematic diagram of homogeneous wall with boundary conditions	26
Figure 3.2.2 Homogeneous building element with outside and inside conditions	28
Figure 4.2.1 SEM images of laterite stone: (a) Laterite overview, (b) Porous area in Fe-rich laterite, (c) Details of Fe-rich matrix around a pore of (b), (d) Dark colored Fe-rich aggregates around a pore of (b).....	40
Figure 4.2.2 EDS Mapping of laterite: (a) Pore in Fe-rich matrix of laterite, (b) Pore lined with yellowish white clay, (c) Details of surface for EDS mapping. (d) Carbon distribution over a surface of (c), (e) Oxides distribution over a surface of (c), (f) Al distribution over a surface of (c), (g) Si distribution over a surface of (c), (h) Fe distribution over a surface of (c).....	41

Figure 4.2.3 EDS spectrum of laterite rocks containing oxides of C, Al, Si and Fe...	41
Figure 4.2.4 Heat transfer mechanism in the pore structure of a moist laterite rock walls.....	43
Figure 4.2.5 Equilibrium moisture content of laterite rocks in relation to the relative humidity of ambient air at 23°C.....	43
Figure 4.2.6 Experimental set up for thermal property measurement at various relative humidity levels.....	45
Figure 4.2.7 Thermal properties at constant temperature: (a) Thermal conductivity of laterite rocks as a function of relative humidity of ambient air, (b) Specific heat of laterite rocks as a function of relative humidity of ambient air.....	47
Figure 4.2.8 Admittance and Transmittance: (a) Admittance and transmittance of laterite rocks as a function of relative humidity of ambient air and thickness at constant temperature, (b) Admittance and transmittance of laterite rocks as a function of temperature and thickness at constant relative humidity.....	49
Figure 4.2.9 Thermal heat capacity: (a) Thermal heat capacity of laterite rocks as a function of relative humidity of ambient air and thickness at constant temperature, (b) Thermal heat capacity of laterite rocks as a function of temperature and thickness at constant relative humidity.....	50
Figure 4.2.10 Decrement factor and it's time lag at constant temperature: (a) Decrement factor of laterite rocks as a function of relative humidity and thickness, (b)	

Time lag of laterite rocks as a function of relative humidity and thickness.....52

Figure 4.2.11 Decrement factor and it's time lag at constant relative humidity: (a) Decrement factor of laterite rocks as a function of temperature and thickness, (b) Time lag of laterite rocks as a function of temperature and thickness.....52

Figure 4.2.12 Surface factor and it's time lag at constant temperature: (a) Surface factor of laterite rocks as a function of humidity and thickness, (b) Surface factor time lag of laterite rocks as a function of humidity and thickness.....53

Figure 4.2.13 Surface factor and it's time lag at constant relative humidity: (a) Surface factor of laterite rocks as a function of temperature and thickness, (b) Surface factor time lag of laterite rocks as a function of temperature and thickness.....54

Figure 4.2.14 Decrement factor and it's time lag at constant temperature: (a) Decrement factor of laterite rocks as a function of humidity and heat transfer coefficient, (b) Time lag of laterite rocks as a function of humidity and heat transfer coefficient.....55

Figure 4.2.15 Decrement factor and it's time lag at constant relative humidity: (a) Decrement factor of laterite rocks as a function of temperature and heat transfer coefficient, (b) Time lag of laterite rocks as a function of temperature and heat transfer coefficient.....55

Figure 4.3.1 Sun path diagrams on peak summer day: (a) Ahmedabad climatic region, (b) Bangalore climatic region, (c) Hyderabad climatic region, (d) Mangalore climatic region.....57

Figure 4.3.2 Surface temperatures of Eastern laterite wall: (a) Outside wall surface

temperatures, (b) Inside wall surface temperatures.....58

Figure 4.3.3 Surface temperatures of Western laterite wall: (a) Outside wall surface temperatures, (b) Inside wall surface temperatures.....58

Figure 4.3.4 Surface temperatures of Northern laterite wall: (a) Outside wall surface temperatures, (b) Inside wall surface temperatures.....59

Figure 4.3.5 Surface temperatures of Southern laterite wall: (a) Outside wall surface temperatures, (b) Inside wall surface temperatures.....59

Figure 4.3.6 Decrement factor of laterite and dense concrete building walls in hot and dry climatic zones (Ahmedabad) of India.....61

Figure 4.3.7 Time lag of laterite and dense concrete building walls in hot and dry climatic zones (Ahmedabad) of India.....62

Figure 4.3.8 Decrement factor of laterite and dense concrete building walls in moderate climatic zones (Bangalore) of India.....64

Figure 4.3.9 Time lag of laterite and dense concrete building walls in moderate climatic zones (Bangalore) of India.....65

Figure 4.3.10 Decrement factor of laterite and dense concrete building walls in composite climatic zones (Hyderabad) of India.....67

Figure 4.3.11 Time lag of laterite and dense concrete building walls in composite climatic zones (Hyderabad) of India.....68

Figure 4.3.12 Decrement factor of laterite and dense concrete building walls in warm

and humid climatic zones (Mangalore) of India.....	70
Figure 4.3.13 Time lag of laterite and dense concrete building walls in warm and humid climatic zones (Mangalore) of India.....	71
Figure 5.2.1 Configuration of composite wall. (BM: Building material, IM: Insulating material, P: Plaster).....	79
Figure 5.2.2 (a) Optimum wall thickness of Building materials, (LS, MBC, IBC, SL and BB) (b) Optimum wall thickness of Building materials (MB, RB, BT, MP and CNC).....	80
Figure 5.2.3 (a) Optimum wall thickness of Insulation materials, (SD, RH, CRB, JF and JFB) (b) Optimum wall thickness of Insulation materials (CPI, SB, AF, WB and CHB).....	80
Figure 5.2.4 (a) Decrement factor of Building materials, (b) Time lag of Building materials.....	81
Figure 5.2.5 (a) Decrement factor of Insulation materials, (b) Time lag of Insulation materials.....	81
Figure 5.2.6 (a) Surface factor of Building materials, (b) Surface factor Time lag of Building materials.....	83
Figure 5.2.7 (a) Surface factor of Insulation materials, (b) Surface factor Time lag of Insulation materials.....	83
Figure 5.2.8 (a) Decrement factor of composite walls, (b) Time lag of composite walls.....	84
Figure 5.3.1 Configurations of Composite walls.....	87

Figure 5.3.2 (a) Optimum fabric energy storage thickness of Building materials, (b) Optimum fabric energy storage thickness of insulating materials.....	90
Figure 5.3.3 (a) Decrement factor of Building materials, (b) Time lag of Building materials.....	91
Figure 5.3.4 (a) Decrement factor of Insulating materials, (b) Time lag of Insulating materials.....	91
Figure 5.3.5 (a) Surface factor of Building and insulating materials, (b) Surface factor time lag of Building and insulating materials.....	92
Figure 5.3.6 (a) Effect of insulation location on decrement factor of LS, (b) Effect of insulation location on time lag of LS.....	92
Figure 5.3.7 Effect of Insulation location on Decrement factor and its time lag for different configurations.....	94
Figure 5.4.1 Configuration of composite walls with different air spaces.....	95
Figure 5.4.2 Wall structure with divided air space.....	96
Figure 5.4.3 Thermal transmittance and admittance of building materials as a function of thickness.....	99
Figure 5.4.4 (a) Decrement factor of building materials, (b) Time lag of building materials as a function of thickness.....	100
Figure 5.4.5 Effect of air space thickness on thermal transmittance and admittance of composite.....	101

Figure 5.4.6 (a) Effect of air space thickness on decrement factor, (b) Effect of air space thickness on time lag.....	102
Figure 5.5.1 Configurations of Composite walls.....	106
Figure 5.5.2 Optimum fabric thickness of Building materials.....	107
Figure 5.5.3 Decrement factor of Building materials.....	108
Figure 5.5.4 Time lag of Building materials.....	109
Figure 5.5.5 Surface factor of Building materials.....	109
Figure 5.5.6 Surface factor time lag of Building materials.....	110
Figure 5.5.7 (a) Decrement factor of composite walls, (b) Time lag of composite walls	112
Figure 6.2.1 Configurations of Composite roofs.....	119
Figure 6.2.2 Images of roofing and insulation materials.....	119
Figure 6.3.1 Optimum fabric thickness: (a) Roofing materials, (b) Insulation materials.....	121
Figure 6.4.1 Decrement factor and time lag of homogeneous materials: (a) Decrement factor of roofing and insulating materials, (b) Time lag of roofing and insulating materials.....	122
Figure 6.5.1 Surface factor and surface factor time lag of homogeneous materials: (a) Surface factor of roofing and insulating materials, (b) Surface factor time lag of roofing and insulating materials.....	123

Figure 6.6.1 Decrement factor and time lag of composite roofs: (a) Effect of insulation location on decrement factor, (b) Effect of insulation location on time lag.....	125
Figure 7.2.1 Configurations of the bricks. (All dimensions are in “m”).....	130
Figure 7.2.2(a) Decrement factor of solid brick as a function of thickness, (b) Time lag of solid brick as a function of thickness.....	133
Figure 7.2.3 Admittance and transmittance of solid brick as a function of thickness.....	133
Figure 7.2.4 Admittance and transmittance of hollow bricks.....	134
Figure 7.2.5 Surface factor and it’s time lag of hollow bricks.....	135
Figure 7.2.6 (a) Decrement factor of hollow bricks, (b) Time lag of hollow bricks.....	136
Figure 7.2.7 Areal thermal heat capacity of hollow bricks.....	136
Figure 7.3.1 Configurations of bricks.....	138
Figure 7.3.2 Thermal transmittance and admittance of bricks filled with foam glass insulation.....	143
Figure 7.3.3 Thermal transmittance and admittance of bricks filled with asbestos fibre insulation.....	143
Figure 7.3.4 Decrement factor and time lag of bricks filled with foam glass	

Insulation.....	145
Figure 7.3.5 Decrement factor and time lag of bricks filled with asbestos fibre Insulation.....	145
Figure 7.3.6 Areal thermal heat capacity of bricks filled with foam glass insulation.....	147
Figure 7.3.7 Areal thermal heat capacity of bricks filled with asbestos fiber insulation.....	147
Figure 8.2.1 Building and insulation materials.....	152
Figure 8.2.2 Configuration of composite walls with expanded polystyrene insulation.....	153
Figure 8.3.1 Effect of wind velocity on transmittance and admittance of homogeneous walls.....	156
Figure 8.4.1 Effect of wind velocity on: (a) Decrement factor of homogeneous walls, (b) Time lag of homogeneous walls.....	157
Figure 8.5.1 Effect of wind velocity on: (a) Surface factor of homogeneous walls, (b) Surface factor time lag of homogeneous walls.....	158
Figure 8.6.1 Effect of wind velocity on areal thermal heat capacity of homogeneous walls.....	158
Figure 8.7.1 Effect of wind velocity on transmittance and admittance of composite burnt brick walls.....	161

Figure 8.7.2 Effect of wind velocity on transmittance and admittance of composite mud brick walls.....	162
Figure 8.7.3 Effect of wind velocity on transmittance and admittance of composite laterite walls.....	162
Figure 8.7.4 Effect of wind velocity on transmittance and admittance of composite cinder concrete walls.....	163
Figure 8.8.1 Effect of wind velocity on decrement factor of composite burnt brick walls.....	164
Figure 8.8.2 Effect of wind velocity on time lag of composite burnt brick walls.....	165
Figure 8.8.3 Effect of wind velocity on decrement factor of composite mud brick walls.....	166
Figure 8.8.4 Effect of wind velocity on time lag of composite mud brick walls.....	167
Figure 8.8.5 Effect of wind velocity on decrement factor of composite laterite walls.....	168
Figure 8.8.6 Effect of wind velocity on time lag of composite laterite walls.....	169
Figure 8.8.7 Effect of wind velocity on decrement factor of composite cinder concrete walls.....	170
Figure 8.8.8 Effect of wind velocity on time lag of composite cinder concrete walls.....	171

LIST OF TABLES

Table 2.1.1 Literature review on decrement factor and time lag.....	10
Table 2.1.2 Literature review on building roofs.....	15
Table 2.1.3 Literature review on natural ventilation.....	19
Table 2.1.4 Literature review on laterite stone.....	21
Table 3.2.1 The external, internal and air space surface resistances.....	30
Table 3.2.2 Comparison of dynamic thermal response characteristics of composite brick wall results with CIBSE results	35
Table 4.2.1 Experimentally measured thermal properties of laterite rocks at various humidity levels and constant temperature.....	46
Table 4.2.2 Experimentally measured thermal properties of laterite rocks at various temperatures and constant relative humidity.....	48
Table 4.3.1 Thermo physical properties of building materials.....	57
Table 4.3.2 Decrement factor and time lag of laterite buildings in Ahmedabad climatic region.....	62
Table 4.3.3 Decrement factor and time lag of dense concrete buildings in Ahmedabad climatic region.....	63

Table 4.3.4 Decrement factor and time lag of laterite buildings Bangalore climatic region.....	65
Table 4.3.5 Decrement factor and time lag of dense concrete buildings Bangalore climatic region.....	66
Table 4.3.6 Decrement factor and time lag of laterite buildings in Hyderabad climatic region.....	68
Table 4.3.7 Decrement factor and time lag of dense concrete buildings in Hyderabad climatic region.....	69
Table 4.3.8 Decrement factor and time lag of laterite buildings in Mangalore climatic region.....	71
Table 4.3.9 Decrement factor and time lag of dense concrete buildings in Mangalore climatic region.....	72
Table 5.2.1 Thermo physical properties of building materials	77
Table 5.2.2 Thermo physical properties of insulating materials.....	77
Table 5.2.3 Unsteady state thermal characteristics of building materials.....	78
Table 5.2.4 Unsteady state thermal characteristics of insulating materials.....	78
Table 5.2.5 Configuration of composite walls.....	78
Table 5.2.6 Unsteady state thermal characteristics of composite walls.....	79
Table 5.3.1 Thermal properties and Optimum thickness values of Building and Insulating materials.....	85

Table 5.3.2 Composite wall configuration and Thickness.....	86
Table 5.3.3 Unsteady state thermal characteristics of Building and Insulating materials.....	86
Table 5.4.1 Thermo physical properties of building materials.....	95
Table 5.4.2 Composite wall configuration with different air space thicknesses.....	95
Table 5.4.3 Divided airspace resistances for horizontal heat flow	96
Table 5.4.4 Effect of air space thickness on unsteady thermal characteristics of Laterite walls.....	96
Table 5.4.5 Effect of air space thickness on unsteady thermal characteristics of Mud brick walls.....	97
Table 5.4.6 Effect of air space thickness on unsteady thermal characteristics of Cellular concrete walls.....	97
Table 5.4.7 Effect of air space thickness on unsteady thermal characteristics of Dense concrete walls.....	97
Table 5.4.8 Effect of air space thickness on unsteady thermal characteristics of Cinder concrete walls.....	98
Table 5.5.1 Thermo physical properties of building materials.....	103

Table 5.5.2 Unsteady thermal response characteristics of laterite stone composite walls.....	103
Table 5.5.3 Unsteady thermal response characteristics of burnt brick composite walls.....	103
Table 5.5.4 Unsteady thermal response characteristics of mud brick composite walls.....	104
Table 5.5.5 Unsteady thermal response characteristics of reinforced brick composite walls.....	104
Table 5.5.6 Unsteady thermal response characteristics of fly ash brick composite walls.....	104
Table 5.5.7 Unsteady thermal response characteristics of concrete block composite walls.....	105
Table 5.5.8 Composite wall configuration and thickness.....	105
Table 6.2.1 Thermal properties of materials at 50°C.....	117
Table 6.2.2 Unsteady thermal response parameters of homogeneous materials at 0.15 m thickness.....	117
Table 6.2.3 Configurations of the composite roof with thicknesses.....	118

Table 7.2.1 Thermo physical properties of brick materials.....	129
Table 7.2.2 Composite wall configuration with different air space thicknesses.....	130
Table 7.2.3 Unsteady thermal response characteristics of Dense concrete blocks...	130
Table 7.2.4 Unsteady thermal response characteristics of burnt bricks.....	131
Table 7.2.5 Unsteady thermal response characteristics of mud bricks.....	131
Table 7.2.6 Unsteady thermal response characteristics of cinder concrete.....	131
Table 7.2.7 Unsteady thermal response characteristics of cellular concrete blocks.....	132
Table 7.3.1 Thermal properties of brick and insulation materials.....	138
Table 7.3.2 Brick configurations and Thickness.....	139
Table 7.3.3 Dynamic thermal parameters of mud bricks filled with foam glass insulation.....	139
Table 7.3.4 Dynamic thermal parameters of mud bricks filled with asbestos fiber insulation.....	139
Table 7.3.5 Dynamic thermal parameters of burnt bricks filled with foam glass insulation.....	140
Table 7.3.6 Dynamic thermal parameters of burnt bricks filled with asbestos fiber insulation.....	140

Table 7.3.7 Dynamic thermal parameters of dense concrete blocks filled with foam glass insulation.....	140
Table 7.3.8 Dynamic thermal parameters of concrete blocks filled with asbestos fiber insulation.....	141
Table 7.3.9 Dynamic thermal parameters of fly ash bricks filled with foam glass insulation.....	141
Table 7.3.10 Dynamic thermal parameters of fly ash bricks filled with asbestos fiber insulation.....	141
Table 8.2.1 Thermo physical properties of building materials.....	152
Table 8.2.2 Effect of wind velocity on dynamic thermal characteristics of homogeneous burnt brick walls.....	153
Table 8.2.3 Effect of wind velocity on dynamic thermal characteristics of homogeneous mud brick walls.....	154
Table 8.2.4 Effect of wind velocity on dynamic thermal characteristics of homogeneous laterite stone walls.....	154
Table 8.2.5 Effect of wind velocity on dynamic thermal characteristics of homogeneous cinder concrete walls.....	155

NOMENCLATURE

ba	Airspace breadth (m)
Cp	Specific heat (J/kgK)
Cs	Wind speed (m/s)
d	Optimum Fabric thickness (m)
E	Emissivity factor
f	Decrement Factor
F	Surface Factor
G	Imperfect thermal contact condition
hc	Convective heat transfer coefficient at external surface (W/m ² K)
hr	Radiative heat transfer coefficient (W/m ² K)
k	Thermal Conductivity (W/mK)
K	Geometric constant
P	Time period (s)
P ₀	Output power in sensor (W)
r	Sensor radius (m)
q	Heat Flux (W/m ²)
R	Surface Resistance (m ² K/W)
t	Time (s)
ta	Air space thickness (m)
T	Temperature (°C)
u	Cyclic Transmittance (Dimensionless)
U	Thermal Transmittance (W/m ² K)
v	Velocity of heat wave (m/s)
X	Thickness of the wall (m)
Y	Thermal Admittance (W/m ² K)

Greek Letters

α	Thermal Diffusivity (m ² /s)
Δ	differential

ϵ	Emissivity of the surface
Θ	Characteristic time (Dimensionless)
ρ	Density (kg/m^3)
σ	Stefen boltzman constant ($5.67 \times 10^{-8} \text{ W/m}^2\text{K}^4$)
σ_L	Penetration length (m)
τ	Dimensionless Time
ϕ	Decremental Delay (h)
χ	Thermal Heat Capacity ($\text{J/m}^2\text{K}$)
ψ	Time lag for Surface factor (h)
ω	Time lead for Thermal Admittance (h)
ω_v	Heat waves angular frequency ($2\pi/P$) (s^{-1})

Subscripts

e	Exterior surface
i	Interior surface
se	External air surface
si	Internal air surface

Abbreviations

AF	Asbestos fiber
BB	Burnt brick
BT	Brick tile
CB	Coir board
CHB	Chip board
CLC	Cellular concrete
CNC	Cinder concrete
CNCB	Concrete block

CPI	Coconut pitch insulation
DC	Dense concrete
EP	Expanded polystyrene
FAB	Fly ash brick
FG	Foam glass
GHG	Green house gases
IBC	Indore Black clay
JF	Jute felt
JFB	Jute fiber
LS	Laterite Stone
MB	Mud brick
MBC	Madras black clay
MP	Mud phuska
P	Plaster
RB	Reinforced brick
RBMW	Resin bonded mineral wool
RCC	Reinforced cement concrete
RH	Rice husk
RW	Rockwool
SB	Straw board
SD	Saw dust
SL	Slate
WB	Wall board

CHAPTER-1

INTRODUCTION

1.1 OVERVIEW

Buildings consume a substantial amount of energy for air conditioning and day lighting. The construction rate in India is increasing rapidly and accounting for massive consumption of fossil fuels that result in a lot of environmental damage. Thus, it is imperative to pay attention to the crucial aspect of energy efficiency in the design of building itself. According to US green building council, buildings are consuming about 40% of total energy use in the world and they are responsible for 40% of greenhouse gas emissions. The building sector represents about 33% of power consumption in India, with the commercial sector and residential sector accounting for 8% and 25% respectively (ECBC 2009). Buildings are also responsible for carbon dioxide emissions with a consequential impact on global warming. Climate responsive design of buildings becomes an extremely important aspect in the process of constructing an energy efficient building. Though India has a large variety of climate types, it is predominantly a country with tropical climate (NBC 2005). Approximately, 90% of the area has hot-dry, warm-humid, and composite climate. Therefore, climate responsive buildings, in this context, are designed to avoid the heat gain, but at the same time allow adequate daylight into the living space. Most of the buildings that are presently being designed and constructed in India are far from being green or sustainable (GRIHA 2011). The energy consumption and imposition of the buildings on natural resources are massive. In order to reduce energy demand of space conditioning, an energy efficient design of building envelopes is needed. The building envelopes or enclosures such as, walls and roofs should be designed in such a way that internal built environment must be in a comfortable condition, even when the outside ambient conditions are outside the comfort range. The building envelope is

the physical barrier that separates the interior of the building from the outdoor environment. The purpose of the envelope of a building is to act as a passive climate modifier to help in maintaining an indoor environment more suitable for habitation than the outdoors. Building materials serve as thermal mass in passive building design. The energy efficient and environment friendly building and insulating materials have become an extremely important aspect of energy efficient building construction. Figure 1.1 shows a schematic diagram of solar-passive building design.

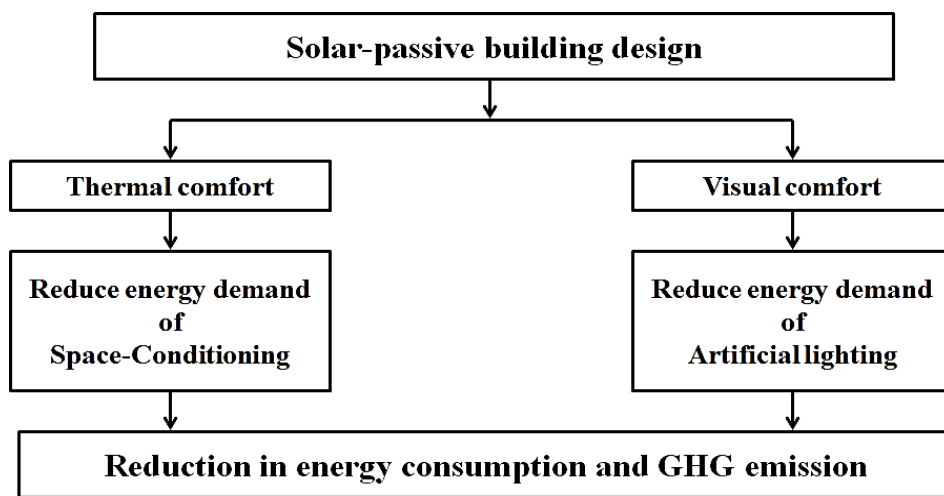


Figure 1.1 Schematic diagram of solar-passive building design (GRIHA 2011)

1.2 OPTIMUM ORIENTATION

The orientation of the building plays very significant role in the design of solar passive buildings. The optimum orientation of buildings is essential to maintain comfortable indoor conditions. The total incident radiation falling on the surface of the building changes with the orientation of the building. The passive building should be designed in such a way that it should receive less radiation in summer and maximum radiation in winter. The information relating to peak summer and winter conditions and thermal properties of building materials are significant in designing of passive buildings. Figure 1.2 shows the long facades of building facing least radiation sides for Indian Latitudes.

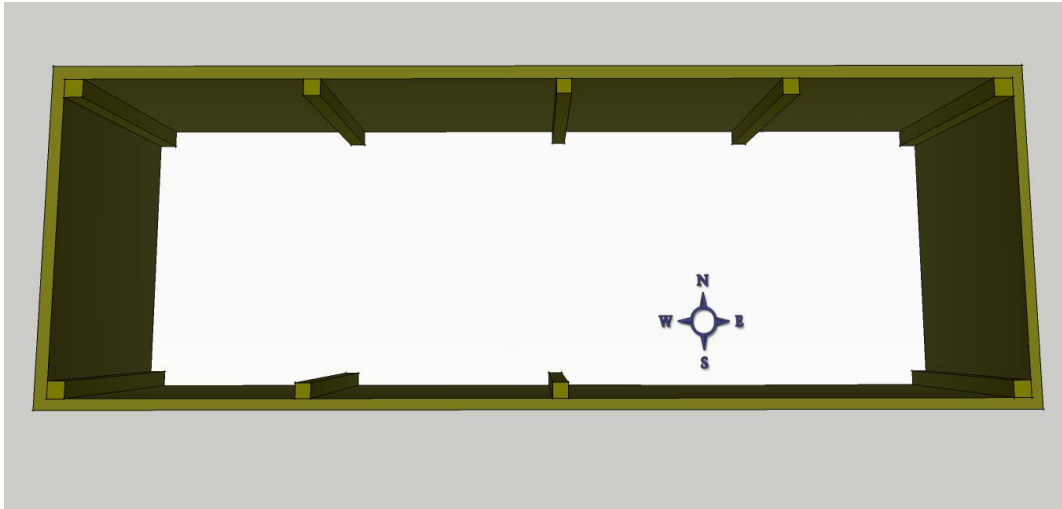


Figure 1.2 Orientation of the building

1.3 ROOM SPACE ARRANGEMENT (THERMAL BUFFER ZONE (or) BUFFER SPACES)

The living room should be shielded by the thermal buffer zones or buffer space such as staircases, lifts, corridors, toilets, rest rooms, store rooms, balconies, and other service areas to reduce heat gain during the summer seasons. With the help of these buffer zones solar radiation passing through the walls of the living room can be reduced or eliminated. These concepts should be incorporated during the building design stage itself. Figure 1.3 depicts the buffer space arrangement in building envelopes.

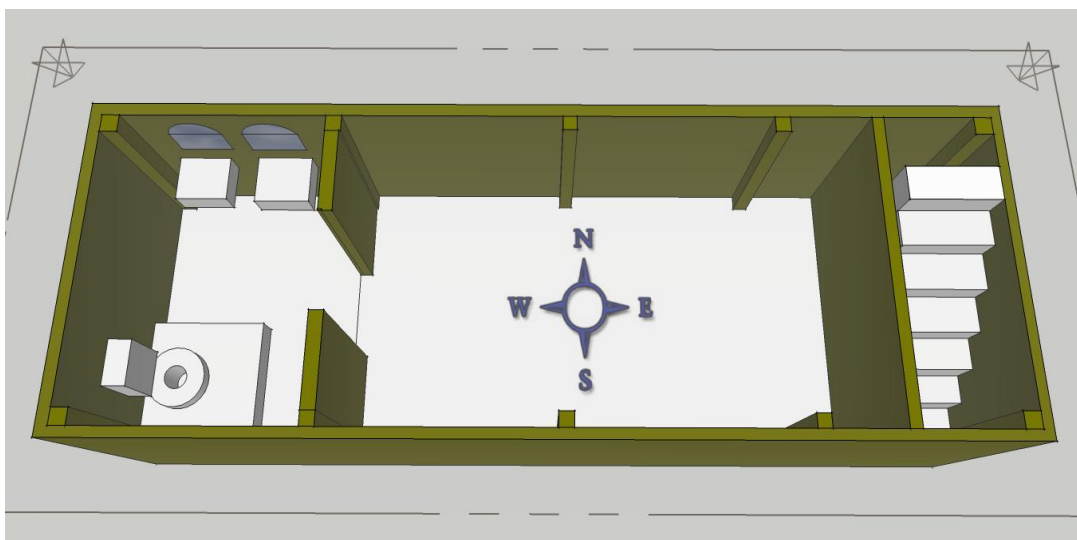


Figure 1.3 Buffer spaces arrangement in building envelopes

1.4 PLACING OF BUILDING OPENINGS

The placing of building openings helps in further reduction of heat gain in the buildings. The building openings must be placed on the facades with the minimum insolation. The openings of the buildings must be placed in such a way that they allow adequate day lighting with comfortable indoor conditions without increasing cooling loads.

1.5 SHADING DESIGN

There are two shading design types (i) Facade shading (ii) Fenestration shading for reducing heat gain or for reducing cooling loads into the buildings.

1.5.1. Shading of facades

The maximum solar radiation passes through roofs, east walls and west walls. If the critical surfaces such as, roofs, east walls and west walls are shaded externally then cooling loads can be reduced drastically. Due to **lower altitude** of the sun, east and west walls are subjected to the low angle of solar radiation with respect to the wall surface. Shading these surfaces helps to cut down the maximum heat gain into the buildings.

1.5.2. Shading of fenestration

The openings are the major source of heat gain into the buildings. The shading devices for the openings require external shading devices for effectively preventing unwanted heat gain into the buildings. They should be designed in such a way that they keep summer sunlight out and allow winter sunshine.

1.6 CLIMATE ZONES OF INDIA

India has a large variety of climatic conditions ranging from extremely hot to severe cold conditions. Automatic weather stations located currently across India are 233 to record monthly mean data of incident solar radiation, ambient temperature, air humidity, precipitation, wind velocity, wind direction, sky conditions and rainfall in different climates of India. India has six climatic zones namely; (i) Hot and Dry (ii) Hot and Humid (iii) Composite (iv) Cold (v) Moderate. Figure 1.4 shows the climatic zones of India.

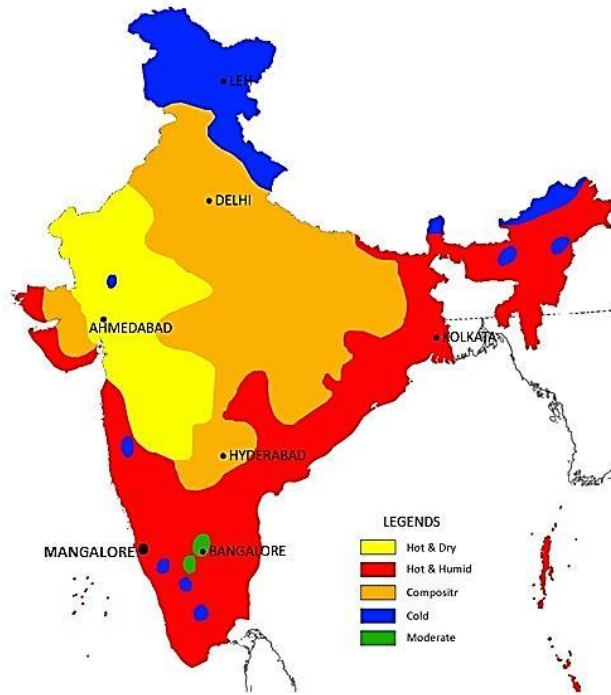


Figure 1.4 Climatic Classification of India (ECBC 2009)

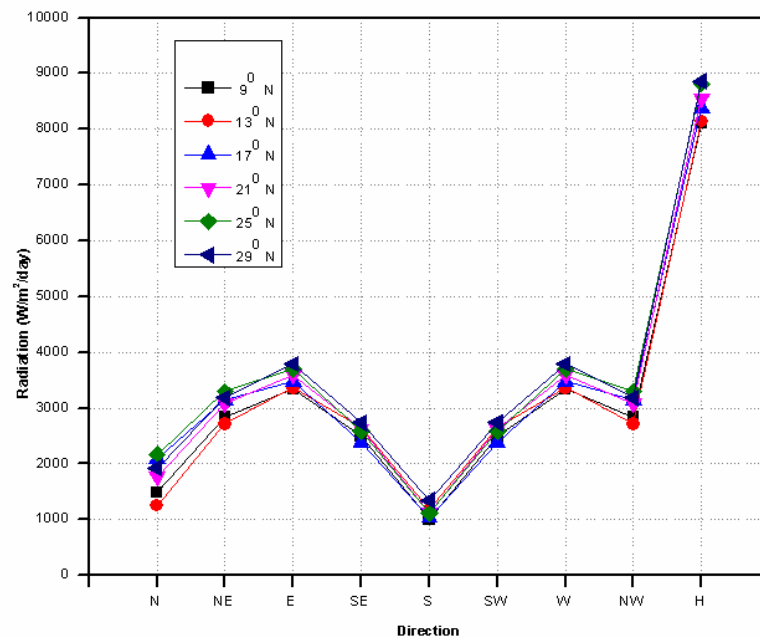


Figure 1.5 Incident solar radiation in different orientations during summer in India (NBC 2005)

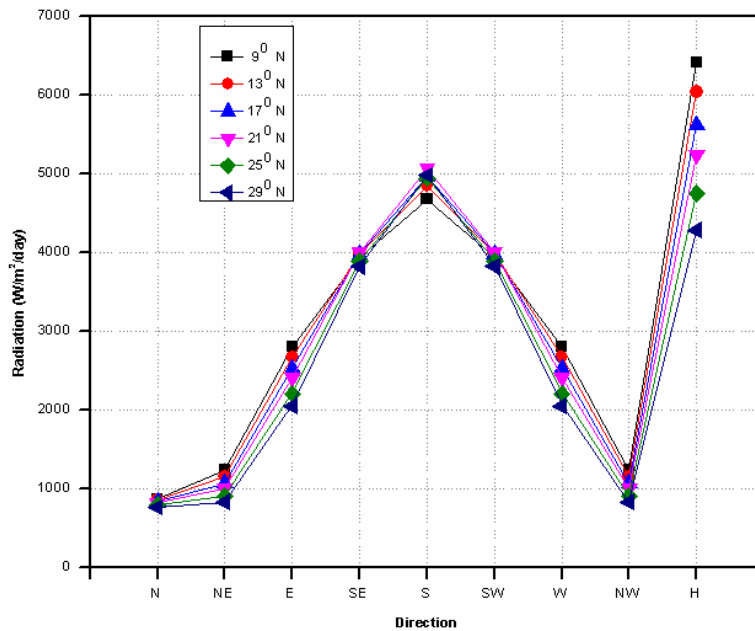


Figure 1.6 Incident solar radiation in different orientations during winter in India

The total incident solar radiation (direct plus diffused radiation) incident on various surfaces of the buildings during summer in India is shown in Figure 1.5. This graph presents the total incident solar radiation for 22 June, which is representative of the summer solstice. From this it is clear that during summer the total incident solar radiation is maximum on horizontal surfaces such as roof, terrace, and so on. Among the facades, west and east orientations are significant in summer for maximum solar radiation as compared to south and north orientations.

The total incident solar radiation (direct plus diffused radiation) incident on various surfaces of the buildings during winter in Indian latitudes is shown in Figure 1.6. This graph presents the total incident solar radiation for 22 December, which is representative of winter solstice. From this, it is clear that during winter the total incident solar radiation is maximum on the south surface, which can be allowed inside the room to maintain comfortable conditions in winter.

1.7 ORGANIZATION OF DESSERTATION

This dissertation consists of nine chapters and a list of references. Chapters one and two are the introduction and literature review, chapter three presents the analytical solution to the diffusion equation under periodic convective heat transfer boundary conditions and this chapter describes the unsteady state thermal characteristics of walls. Each chapter from chapter four to nine deals with one of the current project objectives. Summary for each chapter is presented below.

Chapter two gives the review of literature on the work carried out by various researchers in this field. This chapter summarizes the past work carried out on decrement factor and time lag of the building walls, different building roofs, natural ventilation and laterite stone walls. The objectives of the present work are listed at the end of this chapter.

Chapter three presents the unsteady state thermal characteristics of the walls exposed to convective periodic variations such as thermal transmittance, thermal admittance, decrement factor, time lag, surface factor, surface factor time lag and areal thermal heat capacity. The procedure for solving the diffusion equation for the cyclic admittance procedure is presented. A computer program has been developed using MATLAB and the validation of the program is presented.

Chapter four presents the experimentally measured thermal properties of locally available, natural and sustainable building material, i.e., laterite stone for the first time. Use of natural laterite stone as building material reduces the negative ecological effect and promotes environmental sustainability. The effect of relative humidity and temperature of ambient air on unsteady thermal response characteristics has been investigated. This chapter also presents the effect of wall orientation on decrement factor and time lag of laterite and concrete walls in four different climatic zones of India.

Chapter five deals with the analytical computation of thermal response characteristics of various homogeneous building and insulating materials used in India. The best building and the best insulating materials from unsteady thermal response characteristic perspective is presented. This chapter also presents the optimum position of the insulation location within the composite wall from unsteady thermal state characteristics point of view. The effect of air space thickness on unsteady

thermal characteristics of the composite walls such as thermal transmittance, thermal admittance, decrement factor and time lag were also reported in the chapter. The effect of vertical air spaces within the composite walls on unsteady thermal response characteristics was also studied. The optimum location of vertical air spaces within the composite wall to be maintained has been presented. In addition, the investigation summary has been presented.

Chapter six deals with the dynamic thermal characteristics of external roofs exposed to sinusoidal periodic heat transfer. The effect of insulation material position within the roof on dynamic thermal properties of roofs was investigated in detail. The optimum insulation location inside the composite wall for reducing cooling loads in buildings has been presented based on unsteady state thermal characteristics.

Chapter seven is the investigation of dynamic thermal performance of hollow and stuffed bricks. The thermal performance of hollow and stuffed bricks exposed to periodic solar thermal excitation was studied in detail. The summary of the significant outcomes was reported.

Chapter eight presents the effect of wind velocity on the dynamic thermal performance of various homogeneous and composite wall configurations. This chapter focuses on presenting the best composite wall configuration at higher wind velocities.

The conclusions of the dissertation and the scope for future work have been presented in the chapter nine.

The list of the cited references has been provided after chapter nine.

CHAPTER-2

REVIEW OF LITERATURE

2.1 INTRODUCTION

Worldwide concern about depletion of energy resources has stressed the need of energy conservation strategies. The impact of the building industry is significant in energy consumption. Buildings annually consume more than 20% of the electricity used in India. The need of conserving primary resources has led to an increased awareness of the need of energy savings in cooling and heating of the buildings. Efforts should be made to minimize the use of primary energy, within the constraints of human comfort, economy and architectural design. This chapter presents a survey of past work done in the field of energy saving buildings.

During summer, the heat transfer takes place from outside surface of the wall to the inside surface of the wall. During this process, outside sinusoidal heat wave progresses through the wall. The heat wave has two parameters; these are amplitude and wavelength. The amplitude of the heat wave indicates the temperature magnitude and wavelength of the heat wave indicates the time. The outside amplitude of the heat wave is depending on solar radiation and convection between the outside surface of the wall and atmospheric air. The amplitude of the heat wave decreases as it progresses from outside of the wall to the inside of the wall due to the thermal mass of the wall material. The attenuation of heat wave from outside to inside is called decrement factor and time taken by the heat wave to progress through the wall is called the time lag (Duffin 1984). The comfortable conditions can be maintained inside the room by a low decrement factor and high time lag materials (Knowles 1983). Table 2.1.1 presents the literature survey on decrement factor and time lag.

Table 2.1.1 Literature review on decrement factor and time lag

No.	Author/Year	Summary
1.	Asan (1998)	<ul style="list-style-type: none"> • Numerical investigations were carried out by the author to find the effect of building wall's insulation thickness and insulation position in the wall on time lag and decrement factor using Crank-Nicolson method. • Overall wall thickness studied was 20 cm. • Insulation materials used were polyurethane foam, cork board and rubber for brick and wooden walls.
2.	Asan and San (1998)	<ul style="list-style-type: none"> • The Crank-Nicolson method under periodic convective boundary conditions was used to compute decrement factor and time lag. • The effects of thermo physical properties of building materials and thickness on decrement factor and it's time lag were studied and the authors concluded that the influence of thermo physical properties of building materials is significant on decrement factor and it's time lag.
3.	Asan (2000)	<ul style="list-style-type: none"> • The Crank-Nicolson method was used to optimize insulation position inside the wall from lower decrement factor and higher time lag point of view. • The author concluded that half insulation placed at the mid of the wall and another half placed at the outer surface of the wall were observed to be optimum from lower decrement factor and higher time lag perspective.
4.	Ulgen (2002)	<ul style="list-style-type: none"> • Analytically computed values of decrement factor and time lag were compared with the

		experimental results by the author.
5.	Asan (2006)	<ul style="list-style-type: none"> • Twenty six building materials were investigated by the author using Crank-Nicolson method for decrement factor and time lag. • Decrement factor and time lag values were computed for different thickness of the walls ranging from 0.001 m to 1 m. The author found that the thickness of the wall has important effects on decrement factor and time lag.
6.	Kontoleon and Bikas (2007)	<ul style="list-style-type: none"> • The wall with south orientation in the Mediterranean region during the winter season was investigated. • The effect of outdoor absorption coefficient on decrement factor and time lag was studied. • The authors observed that the increase in the solar absorptivity up to 0.2 increases the time delay and further increase in the solar absorptivity decreases the time lag. It was also observed that time lag decreases with the increase in the solar absorptivity.
7.	Ozel and Pihili (2007)	<ul style="list-style-type: none"> • The implicit finite difference method was used to calculate decrement factor and time lag in summer and winter seasons of Turkey. • Total twelve configurations of the walls with different insulation location were investigated. • The optimum values of decrement factor and time lag were obtained by placing one insulation at the outdoor surface of the wall, second insulation at the mid centre plane of the wall and third insulation at indoor surface of the wall.
8.	Kontoleon and	<ul style="list-style-type: none"> • A thermal network model was developed by the

	Eumorfopoulou (2008)	<p>authors using the nodal method to determine thermal inertia parameters.</p> <ul style="list-style-type: none"> • This study was carried out in Greek region, which is the mild Mediterranean climate. • The effects of wall orientation and outside solar absorptivity on decrement factor and time lag were studied.
9.	Hall and Allinson (2008)	<ul style="list-style-type: none"> • The authors modified the admittance method to incorporate the moisture dependant unsteady parameters such as admittance, transmittance, decrement factor and time lag.
10.	Soon-ching et al. (2011)	<ul style="list-style-type: none"> • The authors studied the decrement factor and it's time lag of aerated lightweight concrete. • The inside and outside temperatures were recorded at every 3 min interval in a day. From these surface temperatures, decrement factor and it's time lag values were computed. • From the results of the authors, it was observed that an increase in the thermal diffusivity increases the decrement factor and decreases the time lag values.
11.	Jin et al. (2012)	<ul style="list-style-type: none"> • This paper describes the heat flux decrement factor and heat flux time lag of various building materials. • The results of the article showed that the heat flux decrement factor decreases with the increase in the thermal capacity and thermal conductivity of the wall whereas, heat flux time lag values increase with the increase in the thermal capacity and decrease in the thermal conductivity of the wall.

12.	Mavromatidis et al. (2012)	<ul style="list-style-type: none"> • The decrement factor and time lag values of multi-layer thermal insulation in Athens and Yerevan climatic conditions were computed numerically by explicit control volume discretisation.
13.	Ruivo et al. (2013)	<ul style="list-style-type: none"> • A numerical model using finite difference method was developed for computing decrement factor and time lag. • The authors found that the azimuth angle of the wall considerably affects the time lag values.
14.	Sun et al. (2013)	<ul style="list-style-type: none"> • The Crank-Nicolson's scheme was employed to calculate decrement factor and time lag of twelve different types of envelopes used in China. • The authors observed that the decrement factor and time lag values change with mean outside temperatures.
15.	Evola and Marletta (2013)	<ul style="list-style-type: none"> • The admittance method was used to explore surface factor. • The authors provided the information about the response of a wall to periodic heat transfer on the internal surface of the wall.
16.	Kontoleon et al. (2013)	<ul style="list-style-type: none"> • The authors investigated the influence of density and thermal conductivity of concrete on decrement factor and time lag using nodal approach.
17.	Alavez-Ramirez et al. (2014)	<ul style="list-style-type: none"> • A coconut fiber filled Ferro cement prototype house was constructed to study the time lag and decrement factor in Oaxaca, Mexico. • The authors concluded that coconut fiber Ferro cement offers the higher resistance to the flow of heat at peak times than the concrete slab roofing.

18.	Najim (2014)	<ul style="list-style-type: none"> • In this paper thermal performance of residential buildings in Iraq climatic conditions was studied. • The author observed that the binding material does not affect the thermal performance of the walls and air cavities have a significant effect on thermal performance.
19.	Zhang et al. (2014)	<ul style="list-style-type: none"> • A Matlab code was developed for two dimensional energy equation using finite difference method • A temperature change hot chamber was made for experimentation. • The authors observed that wall thermal performance is good with thermal conductivity of building wall 1 W/mK if it is greater than this value, then the thermal capacity must be increased for energy efficient thermal performance of the wall.
20.	Thongtha et al. (2014)	<ul style="list-style-type: none"> • This paper focused on autoclaved aerated concrete with sugar sediment waste. • The authors found that at 40°C outside temperature, decrement factor of autoclaved aerated concrete was decreased from 0.418 to 0.032 and time lag was increased from 18 to 68 min when wall thickness increased from 0 to 75mm.
21.	Najim and Fadhil (2015)	<ul style="list-style-type: none"> • The authors studied the thermal performance of reinforced concrete based roofs in Iraq region using the cyclic admittance method.

The building envelopes or enclosures such as walls and roofs should be designed in such a way that internal built environment must be in a comfortable condition, even

when the outside ambient conditions are outside the comfort range. In buildings, the maximum incident heat gain occurs through the roof and the walls. The incident solar radiation is maximum on roofs as compared to the walls (NBC 2005). Hence it is imperative to pay attention on the building roofs to reduce heat gain into the building. Table 2.1.2 shows a review of literature on building roofs.

Table 2.1.2 Literature review on building roofs

No.	Author/Year	Summary
1.	Tang et al. (2003)	<ul style="list-style-type: none"> The authors used finite element model for the comparison of flat and curved roofs. The results of this article confirm that curved roofs are not suitable for areas with higher air temperatures and intense sky diffused radiation typical of hot humid zones. Compared to a flat roof, curved roofs can be more energy efficient under hot arid climatic conditions if they are appropriately designed architectonically (with an opening for natural ventilation near the top) and geometrically.
2.	Tang and Etzion (2004)	<ul style="list-style-type: none"> The authors developed a simulation model to investigate roof pond with gunny bags. Analysis in the paper showed that, irrespective of the type of buildings it is applied to, the Roof pond with gunny bags has a better cooling effect than a roof covered with wetted gunny bags. This has been widely considered to be one of the most efficient roof evaporative cooling techniques in the past. This is mainly due to the creation of thermal stratification within the pond, just as experimentally observed by the present authors in the previous study.
3.	Levinson et al.	<ul style="list-style-type: none"> The authors describe how the application of

	(2007)	reflective roof tile coatings yielded measurable reductions in roof surface temperature, attic air temperature, unconditioned interior air temperature, and ceiling heat flux. The coatings reduced peak roof surface temperature by 5–14K and peak ceiling heat flux by 13–21%.
4.	Alvarado and Martínez (2008)	<ul style="list-style-type: none"> • The lab scaled prototype experimental results demonstrate that the newly designed aluminium–polyurethane insulation system with an optimal orientation reduces the midpoint temperature of a cement based roof significantly in Texas climatic conditions. • The results also indicate that the roof insulation system can reduce the typical thermal load by over 70%.
5.	Alexandri and Jones (2008)	<ul style="list-style-type: none"> • A 2-D prognostic micro model was developed and used. This paper discusses the thermal effect of covering the building envelope with vegetation on the microclimate in the built environment, for various climates and urban canyon geometries. • In this research, it has been shown by the authors that there is an important potential of lowering urban temperatures when the building envelope is covered with vegetation. Air temperature decreases at roof level can reach up to 26°C maximum and 12.8°C day-time average (Riyadh), while inside the canyon decreases reach up to 11.3°C maximum and 9.1°C daytime average, again for hot and arid Riyadh.
6.	Hadavand and Yaghoubi (2008)	<ul style="list-style-type: none"> • It was observed from the simulation studies that the heat flow through the curved surface roof is

		<p>lower than flat surface roof.</p> <ul style="list-style-type: none"> • Authors concluded that the heat flow in North-South faced vaulted roof is significantly lower compared to flat roof.
7.	Halwatura and Jayasinghe (2009)	<ul style="list-style-type: none"> • The simulations were carried out in DERO-LTH simulation tool. It was noticed that polyethylene Insulation of 50 mm thickness give lower air conditioning loads in air conditioned buildings. • Authors concluded that polyethylene Insulation of 25mm thickness give comfortable conditions in free running buildings.
8.	Lee et al. (2009)	<ul style="list-style-type: none"> • In this paper, various materials were used by the authors for the roof panels having ventilated cavities: asphalt shingle, clay and concrete, tile, slate, wood shake and shingle, metal shingles, synthetic products, some metal panel roof systems, and fiber cement products, etc. • Experimental study results showed that the cooling performance of the ventilated roof is better compared to the non-ventilated roof.
9.	Sethi (2009)	<ul style="list-style-type: none"> • The author performed Thermal modelling and experimental validation studies of shape and orientation of green building. The amount of solar radiation available at different latitudes is different for the same greenhouse shape as described in this paper. At 10° N latitude, all the selected shapes receive more radiation in winter but less in summer. Whereas at 31° N, the same greenhouse shapes receive the least amount of solar radiation in winter months but greater in the summer months. This difference further increase

		at 50° N latitude and the solar radiation received in winter months are much less as compared to the quantity received in summer months.
10.	Chel and Tiwari (2009)	<ul style="list-style-type: none"> • The authors explain how the passive house (or mud-house) was found energy efficient and eco-friendly habitat for achieving natural thermal comfort for rural population of India since they cannot afford for window air conditioner or air heater in harsh summer and winter climatic conditions in India. It is a case study.
11.	Kabre (2010)	<ul style="list-style-type: none"> • The new thermal performance index (TPI) is calculated for a number of roofs common in India and Australia. Thermal performance of ten materials is presented by the authors.
12.	Kontoleon and Eumorfopoulou (2010)	<ul style="list-style-type: none"> • The authors explain how the adoption of plant-covered wall designs appears to be suitable for buildings located in the northern Greek region during the cooling period. • It shows how Temperature differences between the exterior and interior surfaces of plant-covered walls in Greek are essentially reduced when compared with the conventional bare walls.
13.	Barrios et al. (2011)	<ul style="list-style-type: none"> • The authors presented 1-D heat transfer model for periodic outdoor conditions. This paper describes that for the air conditioning case the most important physical property of a monolayer wall/roof is the thermal conductivity, which must be as low as possible, and that for the free running case the most important physical property is the thermal diffusivity, which must be as low as possible.

Ventilation replaces the existing air in the room by fresh air. It is essential to provide cooling inside the room by air movement. For comfortable conditions in warm and humid climatic conditions, an indoor air speed of 1.5 – 2.0 m/s can cause comfort in the rooms. Table 2.1.3 presents some of the important literature review of the earlier research carried out on natural ventilation.

Table 2.1.3 Literature review on natural ventilation

No.	Author/Year	Summary
1.	Priyadarsini et al. (2004)	<ul style="list-style-type: none"> The scale model of building with active and passive stack was studied by the authors. This investigation has pointed out that the Even the passive stack fails to improve the ventilation inside the rooms. The objective of enhancing the ventilation is met with the use of active stack.
2.	Mathur and Mathur (2006)	<ul style="list-style-type: none"> This Study shows that optimum inclination at any place varies from 40° to 60° depending upon latitude. The experimental and theoretical validations were presented by the authors. The maximum mass flow rate through an inclined solar chimney in Jaipur (India) 27° N latitude was obtained at an absorber inclination of 45° by authors.
3.	Hirano et al. (2006)	<ul style="list-style-type: none"> This study explores the effects that porous residential buildings have on the natural ventilation performance and, consequently, the cooling load reduction in hot and humid regions. Two residential building models, namely a model with a void ratio of 0% and a “porous” model with a void ratio of 50%, are evaluated using CFD analysis and thermal and airflow network

		analysis.
4.	Bu et al. (2010)	<ul style="list-style-type: none"> In this article the relationships between the ventilation rate and a variety of parameters including wind direction, opening type, plan area of the airway space and building coverage ratio, etc., were investigated by the authors for detached and multi building models .
5.	Fatimah et al. (2010)	<ul style="list-style-type: none"> The physical experimental modelling was compared with the mathematical modelling. The authors of this article explain that solar induced ventilation strategy is able to enhance the stack ventilation in the hot and humid climate. It is able to create air temperature difference of more than the usual air temperature difference attained by Malaysia naturally ventilated buildings.
6.	Gagliano et al. (2012)	<ul style="list-style-type: none"> The paper describes that the performance of the ventilated roof are functions of the position of the thermal insulating layer using Fluent simulation tool. Authors state that the best performances have been obtained placing the thermal insulation under the air layer, near the cold surface.

Laterite stone is a locally available, natural and cost effective ferruginous building material in South-West coast of India. The provisional cost of burnt clay brick in South -West India is around 5 INR per piece and the provisional cost of the laterite stone is 28 INR per piece after finishing. Laterite stone construction is cost effective as the volume of laterite stone (390 mm X 190 mm X 190 mm) is nearly nine times higher than the volume of the burnt clay bricks (190 mm X 90 mm X 90 mm). For the same compressive strength not less than 3.5 N/mm² (as per IS 3620:1979 & IS 1077:1992) and for the same volume covered by a laterite stone, the burnt clay bricks

would cost 45 INR or more. The large size and smooth machine cut of laterite stone can cut down the time taken to complete a structure which in turn saves labor cost. The research work carried out on laterite stone is presented in Table 2.1.4.

Table 2.1.4 Literature review on laterite stone

1.	Kasthurba et al. (2007)	<ul style="list-style-type: none"> • The four different laterite quarry stones available in the Malabar region of South India were investigated by the authors for physical and mechanical properties.
2.	Kasthurba et al. (2008)	<ul style="list-style-type: none"> • The four different laterite stones in South West coastal India were studied for chemical and micro structural analysis. • The authors concluded that the chemical composition in all four different quarry laterite stones is almost same.
3.	Kasthurba et al. (2014)	<ul style="list-style-type: none"> • The Authors summarise the distribution of laterite in various countries. The physical properties of laterite stones in Malabar region were presented in the article.

2.2 MOTIVATION

From the foregoing literature on energy efficient buildings, it can be observed that the proper design of building enclosures or envelopes such as, walls and roofs and the appropriate selection of building and insulating materials for building construction can save lots of energy for reducing cooling loads and help in energy efficient and environment friendly building construction. The present study focuses on providing mathematical models for unsteady heat transfer characteristics of building envelopes of various configurations. These unsteady thermal characteristics of building envelopes are used to study the thermal performance of the buildings.

2.3 OBJECTIVES OF THE PRESENT STUDY

During the present study, the derivation of one dimensional diffusion equation under periodic convective boundary conditions was presented and a computer program was developed for different configurations of the walls and roofs using MATLAB to compute unsteady state thermal characteristics such as thermal admittance, decrement factor, time lag, surface factor, surface factor time lag and thermal heat capacity. On the other hand, thermo physical properties of laterite stone were measured experimentally at different relative humidity and at different temperatures of ambient air. From the foregoing review of literature, the objectives of the current study are as follows,

- To present analytical method (cyclic admittance method) for solving the one dimensional diffusion equation under periodic convective boundary conditions for computing dynamic thermal response characteristics such as thermal admittance, decrement factor, time lag, surface factor, surface factor time lag and areal thermal heat capacity of homogeneous walls/roofs, typical multilayer Walls/Roofs with or without air spaces, hollow bricks and stuffed bricks and also to develop a computer program using MATLAB to compute unsteady thermal characteristics of all configurations of walls, roofs and bricks.
- To measure the thermal properties of local building material, i.e., laterite stone from South West coastal India. The objective also includes the study of the effect of ambient air relative humidity and temperature on dynamic thermal response of laterite walls.
- To study decrement factor and time lag of laterite and concrete buildings in four different climatic regions of India such as hot and dry (Ahmedabad (23.07⁰N, 72.63⁰E)), moderate (Bangalore (12.97⁰N, 77.58⁰E)), composite (Hyderabad (17.45⁰N, 78.47⁰E)) and warm and humid (Mangalore (12.87⁰N, 74.88⁰E)).
- To study thermal performance of various homogeneous building and insulating materials for energy efficient and environmental friendly building construction.

- To investigate the significance of the insulation location within the Walls on unsteady thermal characteristics for energy efficient building enclosure design.
- To study the effect of air space thickness in the Wall on unsteady thermal response heat transfer characteristics.
- To optimize the air space location within the Walls for reducing cooling loads from unsteady thermal response characteristic perspective.
- To optimize the insulation location within building roof for reduced cooling loads from unsteady state thermal characteristics point of view.
- To investigate the thermal performance of hollow and stuffed bricks exposed to the sinusoidal periodic excitation and to compare both types of bricks.
- To study the effect of wind velocity on unsteady state thermal characteristics and to propose the best configuration of composite wall at higher wind velocity regions from optimum dynamic thermal response point of view.

CHAPTER-3

UNSTEADY STATE THERMAL CHARACTERISTICS OF THE WALLS

3.1 INTRODUCTION

There are two levels of dynamic modeling, i.e., Transient and Cyclic. The present study focuses on the cyclic response admittance method since the actual condition matches with this model. The cyclic-response admittance method attempts to consider the effects of dynamic conditions on (i) fabric heat transfer, and (ii) fabric thermal sorption and storage, effectively by determining unsteady-state multiplier factors for application to the steady-state properties of the fabric. Normally, under simplified steady-state conditions, the difference between indoor and outdoor air temperatures is taken to produce a thermal gradient across the thickness of the wall, the profile of which is determined by the thermo-physical properties of the wall material and its corresponding surface resistances. Instead of the outside air temperature the admittance model uses the hypothetical sol-air temperature, as a single point variable to establish this thermal gradient. This represents the rate of heat flow into the external wall surface by convection from the surrounding air plus shortwave solar radiation and radiative exchange to the surroundings (e.g. other buildings, ground and sky). Analogous to sol-air temperature (external), the environmental temperature is a single point hypothetical temperature that represents the rate of heat flow into the internal wall surface by (a) convection from the room and (b) radiation from surrounding objects.

3.2 ADMITTANCE PROCEDURE

The admittance procedure is used to calculate these unsteady state parameters. This method uses matrices to simplify the temperature and energy cycles for a composite building fabric element (wall or roof) that is subjected to sinusoidal temperature variations at the sol-air node. The building walls do not generate any internal heat and

the thermal properties of the wall are same in all three directions. The governing diffusion equation in three dimensions of the wall for the temperature $T(x,y,z,t)$ without internal heat generation and the same thermal properties of the material in three dimensions can be written as Eqs. (3.1).

$$\frac{\partial T}{\partial t} = \frac{k}{\rho C_p} \left(\frac{\partial^2 T}{\partial x^2} + \frac{\partial^2 T}{\partial y^2} + \frac{\partial^2 T}{\partial z^2} \right) \quad (3.1)$$

The building wall has three dimensions, i.e., length, breadth (Thickness) and height. Since the temperature difference along the length and height of the walls are small, the diffusion equation is reduced to one dimensional i.e., through the thickness of the wall. One dimensional heat flow diffusion equation was solved using matrix algebra with periodic boundary conditions at sol-air node. This method is called as admittance method and it is used to calculate unsteady state thermal response characteristics of homogeneous and composite walls. The temperature distribution in a homogeneous wall subjected to one dimensional heat flow is given by the diffusion equation as given in the Eqs. (3.2). And its periodic solution is as follows (Davies 2004),

$$\frac{\partial^2 T(X, t)}{\partial X^2} = \frac{\rho C_p}{k} \frac{\partial T(X, t)}{\partial t} \quad (3.2)$$

Where, T is temperature, X is the thickness of the material (m), ρ is density in kg/m^3 , C_p is specific heat capacity in J/kg K and k is thermal conductivity in W/m K . t is time in s.

The boundary conditions are,

$$k \left(\frac{\partial T}{\partial x} \right)_{x=0} = h_i [T_{x=0}(t) - T_i]$$

$$k \left(\frac{\partial T}{\partial x} \right)_{x=L} = h_e [T_{sa}(t) - T_{x=L}(t)]$$

Where, h_i is brick inner surface heat transfer coefficient, h_e is brick outer surface heat transfer coefficient, T_i is indoor room air temperature and T_{sa} is sol-air temperature. the steady state solution of the problem at $t=0$ was taken as initial condition. In the computations inside temperature of the room is constant at T_i . Figure 3.2.1 shows Schematic diagram of homogeneous wall with boundary conditions.

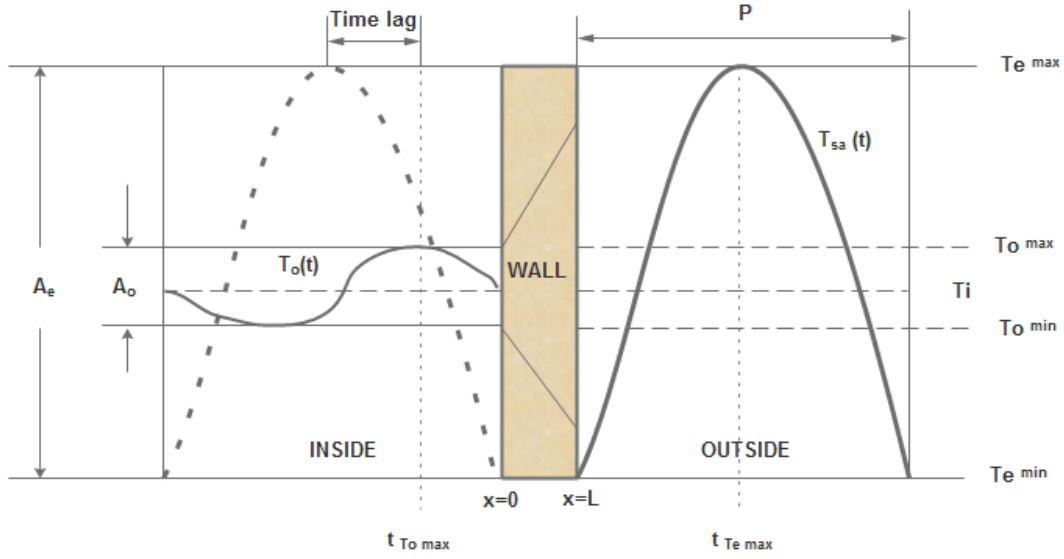


Figure 3.2.1 Schematic diagram of homogeneous wall with boundary conditions

Space/Time independent solution for the above equation is as follows,

$$T(x, t) = A \exp(x/\xi) \exp(t/\zeta) \quad (3.3)$$

Where, ξ and ζ have units of distance and time respectively. The Eqs. (3.3) satisfies the Fourier equation if $\xi^2 = k\zeta$. Wall slab is excited periodically. For periodic heat transfer ζ is an imaginary number and its value is taken as $\zeta = P / (j2\pi)$ then $\xi^2 = k P / (j2\pi)$. Where $j = \sqrt{-1}$ then imposition of the boundary conditions on a finite thickness slab, we obtain a periodic solution with sinusoidal excitation with period P . P is an independent variable and it is a positive value of time, whereas values of z are characteristics of the system. Then

$$\frac{x}{\xi} = \frac{x}{\pm(\kappa P / j2\pi)^{1/2}} = \pm(i + j) \left(\frac{\pi \rho c_p x^2}{\lambda P} \right)^{1/2} = \pm(1 + j)\gamma x \quad (3.4)$$

$$\text{Where, } \gamma = \sqrt{\pi \rho c_p / \lambda P} .$$

The Fourier equation solution can be written as,

$$T(x, t) = [A' \exp(\gamma x + j\gamma x) + B' \exp(-\gamma x - j\gamma x)] \exp(j2\pi t / P) \quad (3.5)$$

$$T(x, t) = [A \sinh(\gamma x + j\gamma x) + B \cosh(\gamma x + j\gamma x)] \exp(j2\pi t / P) \quad (3.6)$$

When the conducting medium finite thickness slab X, temperature and flows at the two surfaces are considered then the above equation can be related as,

$$T_e = T_i \cosh(z + jz) + q_i (\sinh(z + jz))/a$$

$$q_e = T_i (\sinh(z + jz)) \times a + q_i \cosh(z + jz) \text{ Or they can be arranged as,}$$

$$\begin{bmatrix} T_e \\ q_e \end{bmatrix} = \begin{bmatrix} \cosh(z + jz) & (\sinh(z + jz))/a \\ (\sinh(z + jz)) \times a & \cosh(z + jz) \end{bmatrix} \begin{bmatrix} T_i \\ q_i \end{bmatrix} \quad (3.7)$$

Where,

$$\text{Cyclic thickness}(z) = \sqrt{\pi \rho c_p X^2 / \lambda P} = \sqrt{\pi c r / P}$$

$$\text{Characteristic admittance of slab}(a) = \sqrt{j 2 \pi \lambda \rho c_p / P} = \sqrt{j 2 \pi c / r P}.$$

Transmission matrix of single layer can be written as,

$$\begin{bmatrix} A + jB & (C + jD)/a \\ (-D + jC).a & A + jB \end{bmatrix} \quad (3.8)$$

Where,

$$A = \cosh(z) \cos(z),$$

$$B = \sinh(z) \sin(z),$$

$$C = [\cosh(z) \sin(z) + \sinh(z) \cos(z)] / \sqrt{2}$$

$$D = [\cosh(z) \sin(z) - \sinh(z) \cos(z)] / \sqrt{2}.$$

Transmission matrix of surface internal and external film resistances can be written as,

$$E_{si} = \begin{bmatrix} 1 & -R_{si} \\ 0 & 1 \end{bmatrix} \text{ and } E_{se} = \begin{bmatrix} 1 & -R_{se} \\ 0 & 1 \end{bmatrix} \quad (3.9)$$

The building element with outside inside conditions is shown in Figure 3.2.1. The transmission matrix for homogeneous wall can be written as,

$$\begin{bmatrix} T_i \\ q_i \end{bmatrix} = \begin{bmatrix} 1 & -R_{si} \\ 0 & 1 \end{bmatrix} \begin{bmatrix} x_1 & x_2 \\ x_3 & x_1 \end{bmatrix} \begin{bmatrix} 1 & -R_{se} \\ 0 & 1 \end{bmatrix} \begin{bmatrix} T_e \\ q_e \end{bmatrix} \quad (3.10)$$

Transmission matrix for composite wall can be written as,

$$\begin{bmatrix} T_i \\ q_i \end{bmatrix} = \begin{bmatrix} 1 & -R_{si} \\ 0 & 1 \end{bmatrix} \begin{bmatrix} x_1 & x_2 \\ x_3 & x_1 \end{bmatrix} \begin{bmatrix} y_1 & y_2 \\ y_3 & y_1 \end{bmatrix} \cdots \begin{bmatrix} 1 & -R_{se} \\ 0 & 1 \end{bmatrix} \begin{bmatrix} T_e \\ q_e \end{bmatrix} \quad (3.11)$$

Transmission matrix for composite wall with air space can be written as,

$$\begin{bmatrix} T_i \\ q_i \end{bmatrix} = \begin{bmatrix} 1 & -R_{si} \\ 0 & 1 \end{bmatrix} \begin{bmatrix} x_1 & x_2 \\ x_3 & x_1 \end{bmatrix} \begin{bmatrix} y_1 & y_2 \\ y_3 & y_1 \end{bmatrix} \cdots \begin{bmatrix} 1 & -R_a \\ 0 & 1 \end{bmatrix} \begin{bmatrix} 1 & -R_{se} \\ 0 & 1 \end{bmatrix} \begin{bmatrix} T_e \\ q_e \end{bmatrix} \quad (3.12)$$

Where,

x and y represent number of layers of the wall.

The inside and outside surface resistances are determined by the processes of heat transfer which occur at the boundary between a wall/roof and the air. Heat is transferred both by radiation and convective heat transfer at the air and wall surface interface. Figure 3.2.2 shows homogeneous building element with outside and inside conditions.

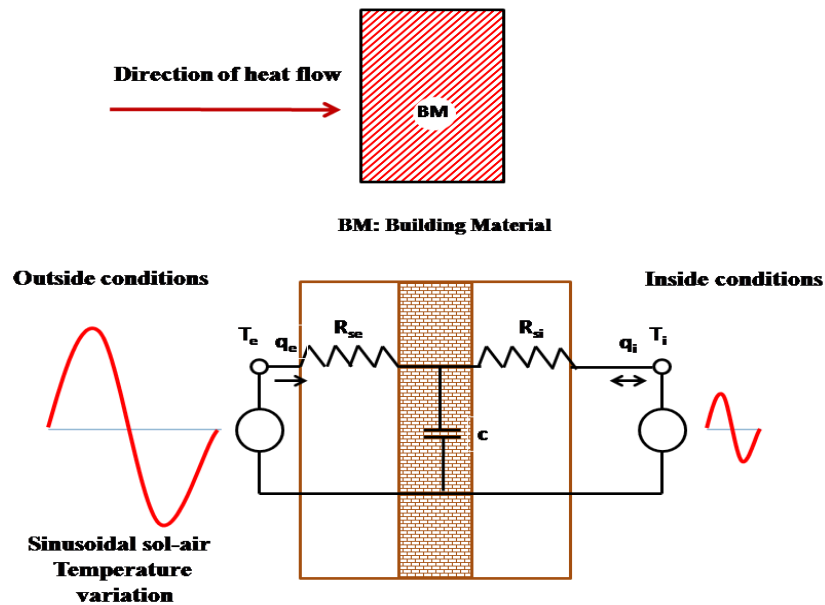


Figure 3.2.2 Homogeneous building element with outside and inside conditions.

$$\text{External surface resistance, } R_{se} = \frac{1}{h_c + Eh_r} \quad (3.13)$$

$$\text{Internal surface resistance, } R_{si} = \frac{1}{(1.2Eh_r + h_c)} \quad (3.14)$$

Convective heat transfer coefficient at external surface as per CIBSE standard,

$$h_c = 5.8 + 4.1C_s \quad (\text{For all wind speeds})$$

$h_c = 16.7 C_s^{0.5}$ (For wind speeds up to 3.5 m/s)

$h_c = 2.5 \text{ W/m}^2 \text{ K}$ (For internal surface resistance)

The radiative heat transfer coefficient depends upon the absolute temperatures of radiating surface and the surface or environment receiving the radiation. It should be considered that, for night time clear skies, the difference between the wall surface temperature and the sky temperature will be very large and causing an underestimation of h_c in these circumstances. This should be incorporated into the calculations.

Radiative heat transfer coefficient, $h_r = 4\sigma T_s^3$ (3.15)

Where,

C_s = Wind speed in m/s

T_s = mean surface absolute temperature in 'K'

σ = Stefan boltzman constant ($5.67 \times 10^{-8} \text{ W/m}^2 \text{ K}^4$)

E = Emissivity factor

The emissivity factor is influenced by the geometry of the room and the wall surface emissivities. For a cubical room with one exposed surface, all the internal surfaces having a high emissivity, E may be written as follows as per CIBSE Standards,

$E = K\varepsilon$

Here, K =geometry constant = 1 and ε = emissivity of surface = 0.9, for most of the building materials.

Air space surface resistance can be written as,

$$R_a = \frac{1}{1.25 + 2.32 \left(1 + \sqrt{\left(1 + \frac{t_a^2}{b_a^2} \right)} - \frac{t_a}{b_a} \right)} \quad (3.16)$$

Where,

t_a is air space thickness and b_a is air space breadth

Table 3.2.1 shows the external, internal and air space surface resistance values for different type of building elements.

Transmission matrix can be further reduced as follows,

$$\begin{bmatrix} T_i \\ q_i \end{bmatrix} = \begin{bmatrix} e_1 & e_2 \\ e_3 & e_4 \end{bmatrix} \begin{bmatrix} T_e \\ q_e \end{bmatrix} \quad (3.17)$$

Here e_1 , e_2 , e_3 and e_4 are the components of matrices.

Unsteady thermal characteristics of the laterite wall at various humidity levels are calculated by the following correlations (CIBSE 2006).

The cyclic transmittance is

$$u = 1/e_2 \quad (3.18)$$

For finite walls and for sinusoidal temperature variations the temperature and energy cycles can be linked by the use of matrix algebra, (CIBSE 2006). For a composite wall, the matrices of each of the layers can be multiplied together to give the relation between inside and outside, (Davies 2004).

Table 3.2.1 The external, internal and air space surface resistances. (CIBSE 2006)

Type of Element	External surface resistance (R_{se}) [m ² K/W]	Internal surface resistance (R_{si}) [m ² K/W]	Airspace resistance (R_a) [m ² K/W]
External walls	0.04	0.13	0.18
Party walls and internal partitions	0.13	0.13	0.18
Roofs:			
Pitched	0.04	0.10	0.16
Flat	0.04	0.10	0.16
Ground floors	0.04	0.17	0.21
Internal floors/ceilings	0.13	0.13	0.18

In nature, variety of climatic conditions produce unsteady state. Diurnal variations produce an approximately repetitive 24-hour cycle of increasing and decreasing temperatures. The effect of this on a building is that in the hot period heat flows from

the environment into the building where some of it is stored and at night during the cool period the heat flow is reversed from the building to the environment. As the cycle is repetitive, it can be described as periodic heat flow. During this periodic flow, thermal characteristics of the wall are unsteady. The following are the unsteady state thermal characteristics of the walls (CIBSE 2006).

3.2.1 Thermal transmittance (U)

This is the steady state heat flow through the element per unit degree of temperature difference between the internal and external environmental temperatures per unit area. Note that this quantity may differ from other U-values quoted as it does not take account of thermal bridging and is sensitive to the values of surface thermal resistances used.

$$U = \frac{1}{R_{se} + \left(\frac{x_1}{k_1}\right) + \left(\frac{x_2}{k_2}\right) + R_a \dots + \dots R_{si}} \quad (3.19)$$

3.2.2 Thermal admittance (Y)

This is the amount of energy leaving the internal surface of the element into the room per unit degree of temperature swing. This is under theoretical conditions where the internal environmental temperature undergoes periodic oscillation and the external environmental temperature is constant.

The thermal admittance (Y) is used to calculate the heat flow into the thermal storage of a wall, whereas thermal transmittance (U) is used to calculate the heat flow through the wall. Both thermal admittance and thermal transmittance have the same units. Thermal transmittance is the reciprocal of thermal resistance, whereas the thermal admittance uses a matrix which includes heat capacity, thermal conductivity, thickness and density of the building material (Hall 2010). The higher the thermal admittance, then the higher is the thermal mass. It can be calculated by,

$$Y = \left| \left(\frac{q_i}{\theta i} \right)_{T_e=0} \right| = |-e_1/e_2| \quad (3.20)$$

3.2.3 Time lead for thermal admittance (ω)

This is the time difference between the timing of the peak heat flow at the internal surface and timing of the peak internal temperature.

$$\omega = \frac{12}{\pi} \arctan \left(\frac{\text{Im}(-e_1/e_2)}{\text{Re}(-e_1/e_2)} \right) \quad (3.21)$$

3.2.4 Decrement factor (f)

In the morning as the outdoor temperature increases, heat starts entering the outer surface of the wall. Each particle in the wall will absorb a certain amount of heat for every degree of rise in the temperature. Depending on the specific heat of the wall material heat to the next particle will only be transmitted after the temperature of the first particle has increased. Thus the corresponding increase of the internal surface temperature will be delayed.

The outdoor temperature will have reached its peak and started decreasing before the inner surface temperature has reached the same level. From this moment the heat stored in the wall will be dissipated partly to the outside and only partly to the inside. As the outdoor air cools, an increasing portion of this stored heat flows outwards. And when the wall temperature falls below the indoor temperature the direction of heat flow is completely reversed. The two quantities characterizing this periodic change are the time lag (or phase shift) and the decrement factor (or amplitude attenuation). Decrement factor is the ratio of the maximum outer and inner surface temperature amplitudes taken from the daily mean.

This is the ratio of the peak heat flow out of the external surface of the element per unit degree of external temperature swing to the steady state heat flow through the element per unit degree of temperature difference between the internal and external environmental temperatures.

The decrement Factor (f) is the attenuation of the rate of heat transfer through a wall due to the thermal heat storage capacity of the wall. Lower the decrement factor, then the higher is the thermal mass. It can be calculated by,

$$f = \left| -\frac{1}{Ue_2} \right| \quad (3.22)$$

3.2.5 Decrement delay (ϕ)

This is the time lag between the timing of the internal temperature peak and the peak heat flow out of the external surface.

The value of 'f' is 1 and the value of 'ϕ' is 0 for thin structures of low thermal capacity values. With increasing thermal capacity of structure materials, 'f' decreases as 'ϕ' increases.

The decrement delay (ϕ) is the time taken for the heat wave to travel from the outermost surface to the innermost surface of the wall (Duffin 1984). It can be calculated by,

$$\phi = \frac{12}{\pi} \arctan \left(\frac{\text{Im}(-\frac{1}{Ue_2})}{\text{Re}(-\frac{1}{Ue_2})} \right) \quad (3.23)$$

3.2.6 Surface factor (F)

This is the ratio of the swing in heat flow from the internal surface of the element to the swing in heat flow received at the internal surface of the element.

The physical process is involved is that short wave radiation is absorbed at the surface, which, after a delay due to thermal storage, causes temperature of that surface to rise. Heat is then transferred to the space in the form of long-wave radiation and convection. The effect is raising the internal heat transfer temperature (i.e. environmental temperature). The response of space to changes in environmental temperature is characterized by the admittance of the surface, which depends on the long-wave emissivity, the surface heat transfer coefficient and the thermal properties of the structure.

The surface factor (F) indicates the responsiveness of the building material surface to the short wave radiation. This relates the admission and absorption of energy to the thermal capacity of a structural element and helps to decide whether the building material is fast responsive or slow responsive to short wave radiation. It is dimensionless.

$$F = | 1 - R_{si}(-e_1/e_2) | \quad (3.24)$$

3.2.7 Time lag for the surface factor (ψ)

This is the time lag between the timing of the peak heat flow entering the surface and peak heat flow leaving the surface into the room.

The surface factor has its associated time lag, it is called surface factor time lag (ψ), it is the time lag between the timing of the peak heat flow entering the wall surface and peak heat flow leaving the wall surface into the room. It is calculated by,

$$\psi = \frac{12}{\pi} \arctan \left(\frac{\text{Im}(1 - R_{si}(-e_1/e_2))}{\text{Re}(1 - R_{si}(-e_1/e_2))} \right) \quad (3.25)$$

Buildings are categorized as fast or slow, with regards to their thermal response to short-wave radiation as follows:

FAST: Surface factor, $F=0.8$, with a delay ψ of 1 hour

SLOW: Surface factor, $F=0.5$, with a delay ψ of 2 hours

3.2.8 Thermal heat capacity (χ)

Thermal heat capacity (χ) is the amount of heat energy stored in the wall during the day time per unit area of building element per unit degree of outside temperature swing. The same stored heat energy is released during the night time. It can be calculated using the following correlation,

$$\chi = \frac{t}{2\pi} \left| \frac{e_4 - 1}{e_2} \right| \quad (3.26)$$

The penetration length, phase velocity and optimum fabric thickness can be calculated as follows (Magyari and Keller 1998),

3.2.9 Penetration length (σ_L)

The thickness of the wall at which the thermal effects are very strong is called penetration length, and the approximate value for this hot region can be calculated by

$$\sigma_L = \sqrt{2\alpha/\omega_v} \quad (3.27)$$

3.2.10 Phase velocity (v)

The phase velocity of thermal heat wave is the velocity of heat wave with which it penetrates into the wall and it can be calculated by

$$v = \sqrt{2\alpha\omega_v} \quad (3.28)$$

Where, $\omega_v = 2\pi/P$

3.2.11 Optimum fabric thickness (d (or) L_{opt})

The optimum fabric thickness is the thickness of the wall at which heat storage capacity is maximum and further can be calculated by

$$d \text{ (or) } L_{opt} = 1.18251\sigma_L \quad (3.29)$$

The computer program was developed using MATLAB to solve one dimensional diffusion equation with convective periodic conditions and to compute dynamic thermal properties of homogeneous and composite building walls of various configurations. For validation purpose, the results of the computer simulation program were compared with the CIBSE standards. The validation has been conducted for a solid brick wall with thickness 0.22 m, thermal conductivity 0.77 W/mK, specific heat capacity 1000 J/kgK and density 1750 kg/m³. The solid brick wall is plastered inside with dense plaster of thickness 0.013 m, thermal conductivity 0.57 W/mK, specific heat capacity 1000 J/kgK and density 1300 kg/m³. The unsteady thermal response characteristics of the composite solid brick wall were compared with CIBSE standard results as shown in Table 3.2.2. The deviation of the present simulation program results from the CIBSE standard results was found to be less than or equal to 2.5% and therefore the program is contemplated to be reliable to use for other external walls.

Table 3.2.2 Comparison of dynamic thermal response characteristics of composite brick wall results with CIBSE results

S.No.	Dynamic properties of composite wall	Present simulation program results	CIBSE Results	Deviation (%)
1	Transmittance (U)	2.09	2.09	0
2	Decrement factor (f)	0.41	0.42	-2.38
3	Time lag (ϕ)	7.56	7.40	2.16
4	Admittance (Y)	4.50	4.49	0.22
5	Surface factor (F)	0.48	0.49	-2.04
6	Surface factor time lag (Ψ)	1.56	1.60	-2.50

CHAPTER-4

DYNAMIC THERMAL RESPONSE CHARACTERISTICS OF LATERITE WALLS

4.1 INTRODUCTION

The most prominent building elements that ensure energy efficiency in buildings are building enclosures. The construction cost of buildings can be drastically reduced by using natural building materials in comparison to conventional building materials. Using natural building materials depreciates negative ecological impact and promotes environmental sustainability. Hence, it is imperative to dedicate attention to the thermal performance of natural and sustainable building materials.

Laterite stone is a locally available, natural, environment friendly and cost effective ferruginous building material in South-West coastal India. Laterite rocks originate in this region due to heavy rainfall, intermittent hot seasons and terrain with hills and valleys. The weather in South-West coastal India is hot and humid. The word Laterite was adopted from the Latin word “Later” meaning brick (Gidigasu 1974). The formation of laterite rocks usually transpires in the tropics and subtropics of India, Ceylon, Brazil, France, Germany, Nigeria, Ghana, Venezuela, East Africa, South Africa, Australia and South America. The formation of laterite rocks occurs in hot and humid regions within 30°N and 30°S of the equator (Kasthurba et al. 2014). The root cause for formation of laterite is prolonged and repetitive wet and dry seasons. The laterite stone is recognized by different names in different countries. They are well designated as Laterite, Cabook, Canga, Carapace, Eisenkruste, Ironstone, Mantle rock, Moco de hierro, Murrum, Ferricrete, Pisolite and plinthite in India, Ceylon, Brazil, France, Germany, Nigeria, Ghana, Venezuela, East Africa, South Africa, Australia and South America, respectively (Aleva 1994). Laterite stones are generally available in dark red, dark brown and yellowish red in color. They possess

compressive strength of 2.5 to 5 Mpa and specific gravity ranging between 1.5-3. The provisional cost of burnt clay brick in South -West India is around 5 INR per piece and the provisional cost of the laterite stone is 28 INR per piece after finishing. Laterite stone construction is cost effective as the volume of laterite stone (390 mm X 190 mm X 190 mm) is nearly nine times higher than the volume of the burnt clay bricks (190 mm X 90 mm X 90 mm). For the same compressive strength not less than 3.5 N/mm^2 (IS: 1077 1992) and for the same volume covered by a laterite stone, the burnt clay bricks would cost 45 INR or more. The large size and smooth machine cut of laterite stone can cut down the time taken to complete a structure which in turn saves labor cost.

From the previous reported literature, and to the best of knowledge, no work has been reported on an analysis of the thermal properties of laterite stones and dynamic thermal performance of laterite stone walls hence, this work was carried out and was reported in this paper.

All building materials, except metals and glasses are porous and therefore able to absorb moisture from the ambient air. The effect of moisture is negligible in high thermal conductivity materials, but it is considerable in low thermal conductivity building materials like laterite rocks. When compared with corresponding dry building materials, thermal properties of moist building materials are drastically altered and the magnitude of these changes depends on the relative humidity of the ambient air. Moisture is significant among the parameters that may affect the thermal performance of building materials. Water and ice have a much higher thermal conductivity than air or other gases in the pores of building materials so a moist material has a higher thermal conductivity than a dry material. The moisture in pores of the building material forms convection currents in the materials. The moisture in the pores will short circuit the insulation or act as parallel resistances, which reduce the thermal resistance. In most cases for building application materials are only hygroscopically moist (Trechsel 2001).

The energy efficient building envelopes can be designed based on the unsteady state thermal characteristics of the wall materials. These unsteady thermal characteristics of any building materials not only depend on the thickness of the materials, but they also depend on their thermo physical properties such as, thermal conductivity, specific

heat, thermal diffusivity and density. These thermo physical properties are greatly influenced by the temperature and relative humidity of the environment. The water vapor permeability and thermal conductivity as a function of temperature and relative humidity in RH controlled chamber was studied earlier (Valovirta and Vinha 2004). The thermo physical properties of moist air as a function of temperature and relative humidity were presented (Tsilingiris 2008). This paper presents the thermo physical properties of laterite stone as a function of temperature and relative humidity.

Thermal conductivity and specific heat of porous building materials display a unique behavior when moisture is present in their structure. This paper presents the experimental investigation of the effect of ambient air humidity and temperature on thermal properties of the laterite rocks used in South-West coastal India. The experimental technique employed was transient plane source method in the saturated salt solution humidity controlled chamber. Experimental results showed an increase of thermal conductivity by 14.7% and specific heat by 9.15% with an increase in the relative humidity of ambient air in the hygroscopic range. A porous and ferruginous matrix of laterite was studied using a scanning electron microscope. Elemental composition and its distribution over a porous laterite surface was studied using energy dispersive x-ray spectroscopy. The effects of relative humidity of the ambient air and temperature on the unsteady state thermal heat transfer characteristics like, transmittance, admittance, decrement factor, time lag, surface factor, surface factor time lag and heat capacity for different thicknesses of the laterite rock walls were investigated analytically. One dimensional heat flow equation under periodic convective boundary conditions is solved using matrix algebra and a computer simulation program was developed to calculate unsteady state thermal characteristics. Results indicate that the decrement factor reduces by 8.35% and time lag increases by 2.88% with an increase in the relative humidity of ambient air compared to the dry state for the Indian standard laterite rock thickness.

This chapter also investigates dynamic thermal characteristics of laterite and concrete building walls in four different orientations of the wall (East, west, north and south) and in four different climatic zones of India. The dynamic thermal characteristics studied includes decrement factor and time lag. The thermal performance of laterite and concrete walls in four climatic zones of India such as hot and dry (Ahmedabad),

temperate (Bangalore), composite (Hyderabad) and warm and humid (Mangalore) was studied. The thermo physical properties of laterite walls such as thermal conductivity, specific heat capacity, thermal diffusivity and density were measured experimentally using the transient plane source method. In order to study the thermal performance of laterite and concrete walls, meteorological data of each region as per Indian Society of Heating Refrigerating and Air-conditioning engineers on peak summer day of the year was applied to the outer surface of the building walls in Energy Plus 8.1.0.009 simulation tool. The meteorological data serves as boundary conditions for building models designed in Design builder 4.3.0.039 version and simulated in Energy plus simulation tool. All the simulations were carried out on peak summer day of concerned region under clear sky conditions. From the results, it is observed that the thermal performance of laterite buildings is better than the concrete buildings. The simulation results showed that for hot and dry climate, the laterite stone wall in the east orientation offers the least decrement factor (0.2722) than the east oriented concrete wall (0.2955). Similarly, the laterite wall offers the highest time lag (7.75 h) than the concrete wall (7.25 h) in the eastern orientation. The results also revealed that the laterite stone walls are more energy efficient than the concrete walls from lower decrement factor and higher time lag perspective in all orientations of the walls and in all four climatic zones of India. The results help in designing energy efficient and sustainable building enclosures for reduced cooling loads.

4.2 THE EFFECT OF AIR RELATIVE HUMIDITY AND TEMPERATURE ON THERMAL PROPERTIES AND DYNAMIC THERMAL RESPONSE CHARACTERISTICS OF LATERITE WALLS

4.2.1 Morphology and chemical composition of laterite rocks

The laterite rocks are ferruginous materials available in dark red to dark brown color, with pores lined with yellowish white clay. They are also available in pink and ochre colors based on iron oxide in various states of hydration. Due to its porous structure lined with yellowish clay, these rocks are able to absorb more moisture when they are exposed to a humid environment. JEOL JSM- 6308LA scanning electron microscope with energy dispersive x-ray spectroscopy was used for the characterization of laterite

stone. The surface of the laterite stone to be examined was coated with sputtered gold using the low vacuum sputtering system for electrical conduction characteristics (Koo 2006). The coated laterite stone surface was scanned by an electron beam and the back scattered beam of electrons were collected and displayed on a cathode tube. This image is photographed to represent laterite surface characteristics. Scanning electron microscopy (SEM) captured significant features of laterite stone with pores as shown in Figure 4.2.1. Elemental composition of laterite stones and its distribution over a porous surface was studied using energy dispersive x-ray spectroscopy (EDS). EDS is included as a part of SEM. With EDS in an electron microscope, one can attain elemental analysis of the laterite stone. It was observed that the laterite stone consists of dark red to dark brown colored hard ferruginous material which absorbs less moisture and soft yellowish white clayey material which absorbs more moisture from the humid air as presented in Figure 4.2.2 (a) and Figure 4.2.2 (b) respectively. The laterite rock pores are lined with yellowish white clay and able to absorb the maximum amount of moisture. Elemental composition of laterite stone is presented in Figure 4.2.3 and it is noticed that laterite rocks are rich in oxides of iron, aluminium, silicon and carbon.

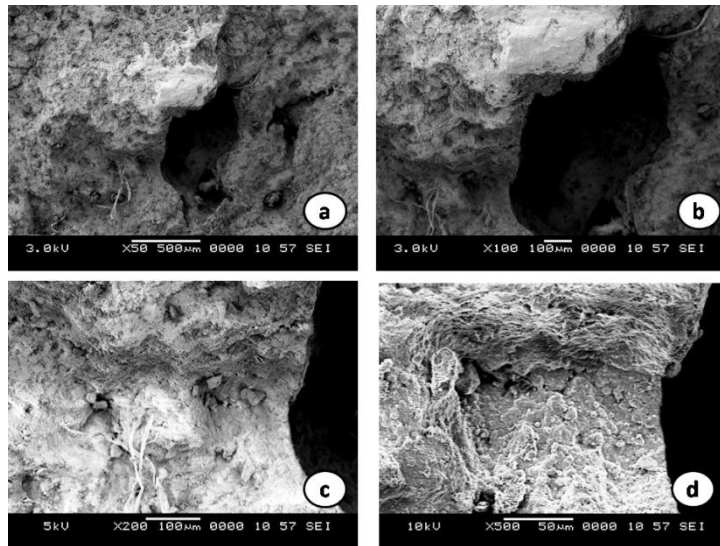


Figure 4.2.1 SEM images of laterite stone: (a) Laterite overview, (b) Porous area in Fe-rich laterite, (c) Details of Fe-rich matrix around a pore of (b), (d) Dark colored Fe-rich aggregates around a pore of (b)

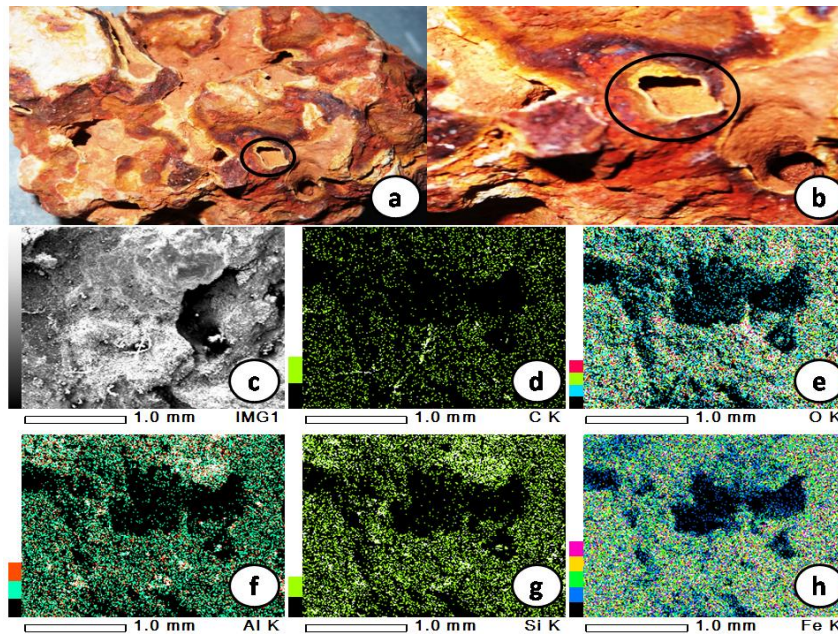


Figure 4.2.2 EDS Mapping of laterite: (a) Pore in Fe-rich matrix of laterite, (b) Pore lined with yellowish white clay, (c) Details of surface for EDS mapping. (d) Carbon distribution over a surface of (c), (e) Oxides distribution over a surface of (c), (f) Al distribution over a surface of (c), (g) Si distribution over a surface of (c), (h) Fe distribution over a surface of (c)

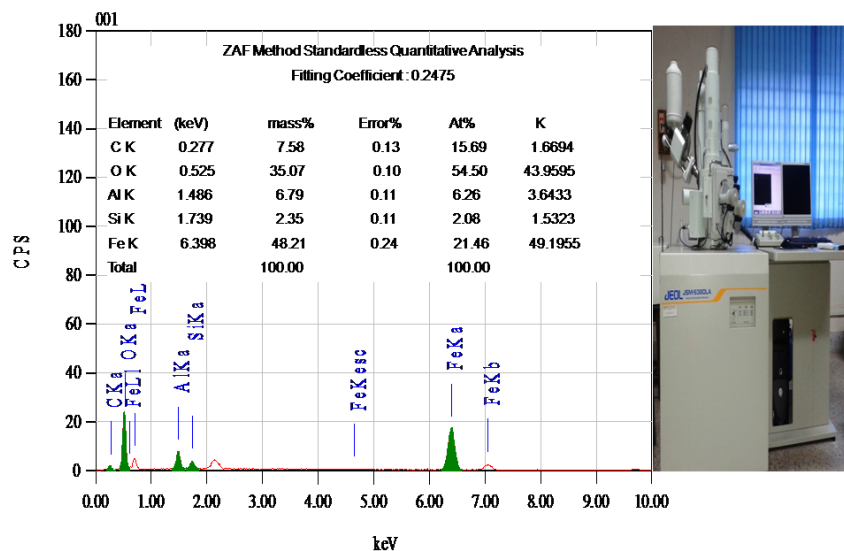


Figure 4.2.3 EDS spectrum of laterite rocks containing oxides of C, Al, Si and Fe

4.2.2 Pore structure and heat transfer through a moist pore of the laterite rocks

The important heat flows due to temperature gradients in moist porous materials are (Treschsel and Bomberg 2009), (1a) Conduction in the solid laterite. (1b) Conduction of humid air in the pores of the laterite. (2) Conduction in the water film bound to the clayey white yellowish pore walls. (3) Evaporation and condensation within a pore of a laterite. The moisture moves one way in the vapor phase and then back again in the liquid phase. This process is caused by temperature differences between the pore walls and takes place even if the moisture gradient is equal to zero. (4) Radiation between the pore walls. (5) Convection in the pores. In most practical cases, this can be neglected. Figure 4.2.4 clearly shows significant heat flows in a moist porous laterite rocks. Moisture absorption of laterite rocks in relation to the relative humidity of ambient air at 23°C were measured experimentally.

The maximum absorption depends on the temperature and the relative moisture content of the ambient air, and is called equilibrium moisture content. Figure 4.2.5 illustrates the equilibrium moisture content of the laterite rock walls in relation to the relative humidity of ambient air at a constant temperature of 23°C. These sorption curves show that the sorption increases with increasing air humidity, but the increase is not linear. Hence, there is a specific curve for each material (Bansal et al. 1994). It is apparent that the laterite stone walls are active in the absorption process when the relative humidity is raised from 50 to 98% in 48 hours of time. During this absorption process, thermal properties of laterite rocks change significantly.

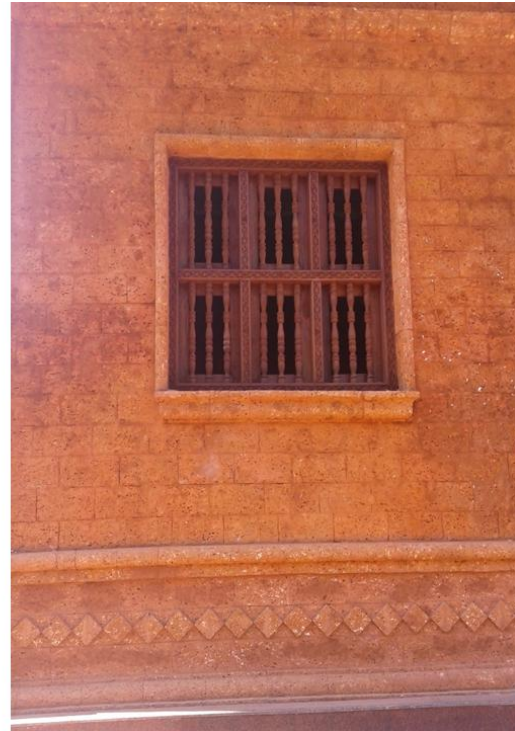
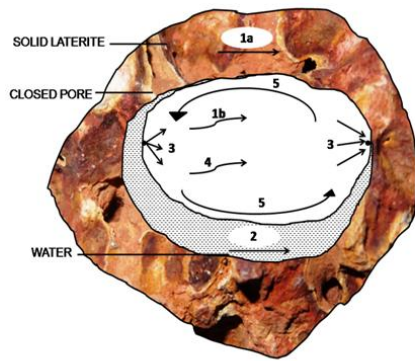


Figure 4.2.4 Heat transfer mechanism in the pore structure of a moist laterite rock walls

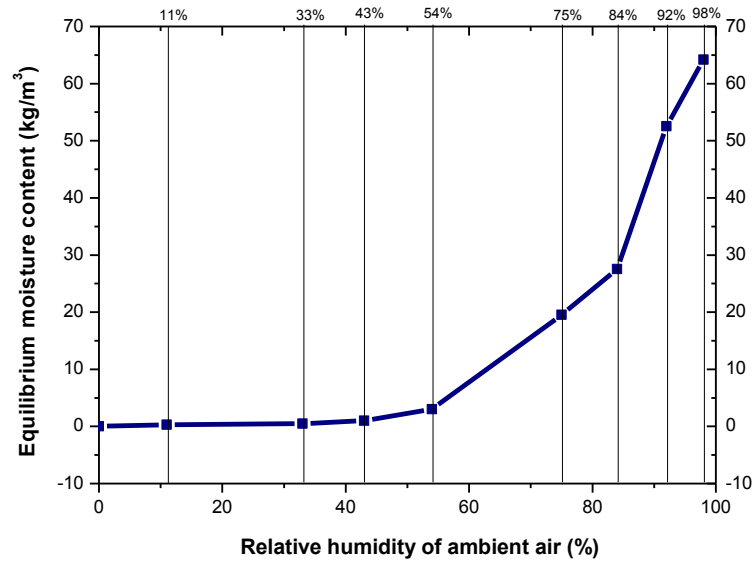


Figure 4.2.5 Equilibrium moisture content of laterite rocks in relation to the relative humidity of ambient air at 23°C

4.2.3 Effect of moisture in ambient air on thermal properties of laterite rocks

A hot disk TPS 2500 instrument as per ISO 22007-2 was used for simultaneous measurement of thermal conductivity, specific heat and thermal diffusivity of the laterite rocks. The double spiral sensor (model 5465 and 3.189mm radius) made of nickel foil with electric insulation on each side was placed in between two pieces of the laterite sample (Log and Gustafsson 1995) and the sample and sensor was placed in an airtight humidity chamber with a transparent window. Inside the chamber a humidity meter was placed. The humidity of the chamber was controlled by placing a petri-dish with saturated salt solutions as shown in Figure 4.2.6. Each salt and its solution have different relative humidity equilibrium with the air in the chamber. Before each measurement, the chamber was left undisturbed for at least 48 hours for the humidity level to reach its equilibrium. In this method TPS element acts as both temperature sensor and heating element. A constant 0.2 W of input power is supplied to the double spiral sensor and increase in the temperature is directly related to the variation in sensor resistance that is simultaneously recorded by the same spiral heating element. The spiral gives the constant heating rate per unit spiral length and records the average temperature of the sensor operating as a resistance thermometer. The average temperature response can be written as (Gustafsson 1991),

$$\Delta T = G + \frac{P_0}{k\pi^{3/2}r} D(\tau) \quad (4.1)$$

Here, temperature increase of the sensor in terms of variable (τ), $\tau = \sqrt{\frac{t-t_{corr}}{\theta}}$, Characteristic time which depend both on sensor parameters and the sample (θ), $\theta = \frac{r^2}{\alpha}$, k is thermal conductivity and G indicates the imperfect thermal contact conditions in a measurement between sensor probe and the laterite surface to remove the effect of any thermal contact effects during analysis, r is the hot disk radius (3.189mm), P_0 is total sensor output power and α is the thermal diffusivity of the material. From this, the thermal conductivity (k) of the laterite can be obtained by plotting the graph between increase in the temperature (ΔT) and Geometric function (D (τ)). The thermal conductivity (k) can be extracted from the slope of the best line fit. An iterative procedure is followed to form the best model fit of Eqn. (1) to the experimental data points for obtaining thermal diffusivity (α) and time correction

(t_{corr}). The humidity meter was used to check that the humidity was stable. Five repetitive measurements were performed at each humidity level. The measurements were performed with 0.2W of input power and 5s measurement time. Relative humidities maintained in the chamber were 0%, 11%, 33%, 54%, 75%, 84%, 92% and 98% using saturated solutions such as phosphorous pentoxide, lithium chloride, magnesium chloride, magnesium nitrate, sodium chloride, potassium chloride, potassium nitrate and potassium sulphate respectively. All the thermal properties were measured in the hygroscopic range of 0 to 98% RH. The experiments were carried out in K-Analys AB, Sweden. Table 4.2.1 shows the thermal properties of laterite stone at various relative humidity levels maintained by saturating salts. The humidity environment chamber was maintained at $23\pm 1^\circ\text{C}$ as per the ASTM standard C-1498 procedure.



Figure 4.2.6 Experimental set up for thermal property measurement at various relative humidity levels

Table 4.2.1 Experimentally measured thermal properties of laterite rocks at various humidity levels and constant temperature

S.NO.	Saturation salt	RH [%]	k of laterite [W/m K]	Mean standard deviation of experiment for k	Cp of laterite [J/kgK]	Mean standard deviation of experiment for Cp
1.	Phosphorus pentoxide	0	1.2475	0.00048461	1695	0.0030515
2.	Lithium Chloride	11	1.2742	0.00041902	1731	0.00040878
3.	Magnesium Chloride	33	1.2945	0.0005688	1759	0.0020962
4.	Magnesium Nitrate	54	1.305	0.0004217	1768	0.002198
5.	Sodium Chloride	75	1.349	0.00088066	1798	0.0016671
6.	Potassium Chloride	84	1.376	0.00038363	1820	0.0021084
7.	Potassium Nitrate	92	1.454	0.00083132	1878	0.0011558
8.	Potassium sulphate	98	1.478	0.0011098	1888	0.0035401

The relative humidity of ambient air adversely affects the thermal properties and the unsteady state thermal characteristics of the building materials, especially in low thermal conductivity materials like laterite rocks. Experimentally measured thermal property values are curve fitted with the best accuracy. Figure 4.2.7 (a) and Figure 4.2.7 (b) show a curve fit for thermal conductivity and specific heat of laterite rocks as a function of relative humidity of ambient air, respectively. It is observed that the thermal conductivity of the laterite rocks increases with the increase in the relative humidity of ambient by 14.73% when the relative humidity of ambient air varies from 0 to 98% RH. This increase in the thermal conductivity with the increase in the relative humidity attributed to the increase of humid air convective currents in the pores of laterite rocks. The specific heat capacity of the laterite rocks increases with the increase in the relative humidity of ambient air by 9.15% when the relative humidity of air varies in the hygroscopic range. Dry laterite has a specific heat

capacity of 1715 J/kgK at 23°C whereas moist laterite at 98% RH has a specific heat capacity of 1888 J/kgK at 23°C. It takes 1.1 times as much energy to heat the moist laterite than the dry laterite. The increase in the specific heat capacity of laterite rocks with the increase in the relative humidity is due to higher specific heat capacities of the humid air present in the pores of the laterite stones. The thermal conductivity and the specific heat capacity of laterite rocks are increased by only 3.45% and 2.42% respectively from 0 to 50% RH but they are more active in the adsorption process from 50 to 98% RH. Hence, thermal conductivity and specific heat capacity are increased by 12.68% and 6.89% respectively during this adsorption process. At higher relative humidity levels laterite rocks are more reddish in color due to the presence of moisture in it. The variation in these thermal properties greatly influences the unsteady state thermal characteristics of laterite rock walls.

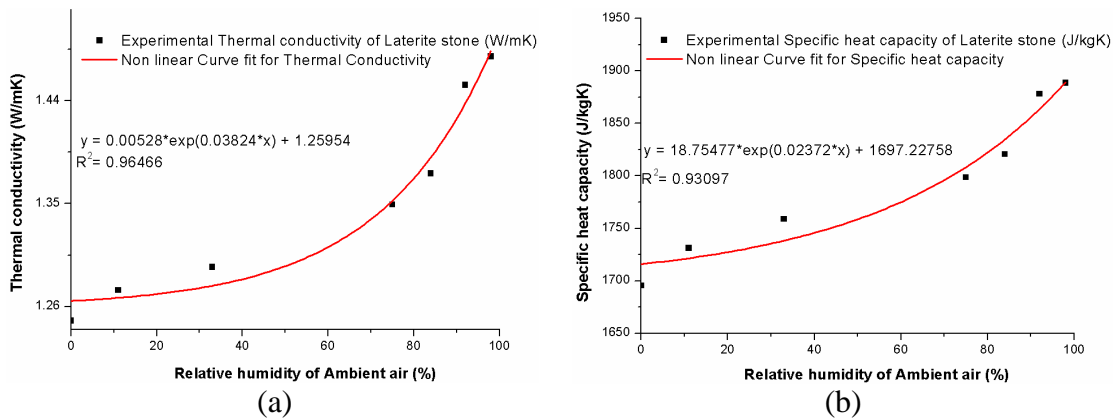


Figure 4.2.7 Thermal properties at constant temperature: (a) Thermal conductivity of laterite rocks as a function of relative humidity of ambient air, (b) Specific heat of laterite rocks as a function of relative humidity of ambient air

4.2.4 Effect of ambient air temperature on thermal properties of laterite rocks

The laterite sample was placed in a holder that fits into an oil bath. The same 3.189 mm radius, sensor was used for measuring thermal properties at various temperatures. The sample was first cooled down to 0°C and then thermal properties at 0°C, 20°C, 40°C and 60°C were measured during heating cycle. Humidity equilibrium was maintained at each step of the sample heating. Table 4.2.2 shows the thermal properties of laterite rocks at various temperatures. The thermal conductivity of laterite rock at 0°C is observed to be the highest among all the considered temperatures. This maximum thermal conductivity is credited to the freezing of humid

air in the pores of the laterite rocks. The thermal conductivity of the laterite stones increases with the increase in the temperature from 20°C to 60°C as accredited to increase in the convective currents in the pores of the laterite stones.

Table 4.2.2 Experimentally measured thermal properties of laterite rocks at various temperatures and constant relative humidity

S.NO.	Temperature [°C]	k [W/m K]	Mean standard deviation of experiment for k	Cp [J/kgK]	Mean standard deviation of experiment for Cp
1.	0	1.332	0.0002	1870	0.0030515
2.	20	1.289	0.0004	1910	0.00040878
3.	40	1.306	0.0015	2040	0.0020962
4.	60	1.307	0.009	2140	0.002198

4.2.5. Effect of moisture and temperature on admittance and transmittance of laterite rocks

Figure 4.2.8 (a) and Figure 4.2.8 (b) depict that for thin cross section walls, the value of admittance is equal to the value of transmittance. At wall thickness 0.01 m, the admittance and transmittance values are nearly equal. At smaller wall thicknesses ranging from 0.01 to 0.1 m, the wall does not have much ability to store heat. Hence the wall transfers most of the heat received at the external wall surface to the internal wall surface. At 0.1 mm wall thickness, the admittance of the wall starts increasing with the increase in the wall thickness. Admittance increases with the thickness of the laterite wall linearly against optimum fabric thickness (d) until a constant value is reached due to increase in the ability of wall to store heat. The optimum fabric thickness is the optimum thickness of the wall where the wall can store the maximum amount of heat within it. This optimum thickness of the laterite wall lies in between 0.1 m and 0.28 m (End of the uptrend line). As per CIBSE standards, the optimum thickness occurs for wall thicknesses greater than 0.1 m. It was also suggested that the optimum fabric thickness can be achieved at the wall thicknesses nearer to 0.2 m (Rees et al. 2000). The transmittance value goes on decreasing with the increase in the laterite wall thickness. The effect of relative humidity of ambient air on admittance and the transmittance of laterite rocks is clearly noticeable. Both the admittance and the transmittance increase with the increase in the relative humidity of the ambient air.

High thermal admittance values are advantageous from a thermal mass perspective, whereas low thermal transmittance values are desirable for low transmission loads through walls or good thermal insulation. Thermal admittance is a dynamic property. As the thermal heat capacity increases, the thermal admittance value increases. Thermal transmittance is a steady state property and it doesn't depend upon the specific heat capacity of the material and it depends only on the thickness, thermal conductivity and outside and inside surface resistances. The admittance value of laterite rocks increases with an increase in the temperature and due to the increase of specific heat of the laterite stone with an increase in the temperature. The transmittance remains almost constant at the temperatures 0°C, 20°C, 40°C and 60°C. From these results it is understood that, relative humidity of the ambient air affects both the transmittance and admittance whereas the temperature affects only admittance values. High admittance values are useful from a thermal mass perspective and low thermal transmittance will minimize heat loss.

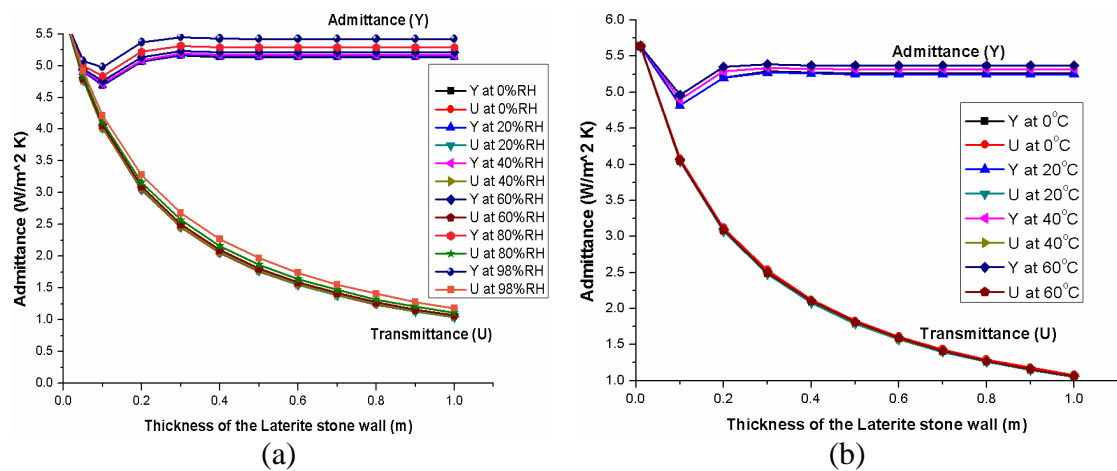


Figure 4.2.8 Admittance and Transmittance: (a) Admittance and transmittance of laterite rocks as a function of relative humidity of ambient air and thickness at constant temperature, (b) Admittance and transmittance of laterite rocks as a function of temperature and thickness at constant relative humidity

4.2.6. Effect of moisture and temperature on thermal heat capacity of laterite rocks

Higher thermal heat capacity or higher thermal mass stores maximum heat energy while heating in day time and slowly releases heat energy to the environment during

the cooling at night time. With the varying thermal mass decrement factor and time lags of the walls can be altered. Figure 4.2.9 (a) and Figure 4.2.9 (b) illustrate the thermal heat capacity of laterite rocks as a function of relative humidity and temperature of ambient air, respectively. From the results, it is inferred that the thermal heat capacity of the laterite walls increases with the increase in the relative humidity of ambient air from 0 to 98% RH. For the same thickness, a moist laterite wall has more thermal heat capacity than the dry laterite walls. Optimum fabric thickness value varies from material to material. Thermal heat capacity of laterite rocks increases with the increase in thickness of the wall until it reaches the optimum fabric thickness. Maintaining wall thickness greater than the optimum fabric thickness does not give more energy storage, but it rather reduces energy storage. Optimum energy storage of 8.048×10^4 (J/m²K) occurs at an optimum fabric thickness ($d_{0\% \text{ RH}}$) of 0.28m in dry state, whereas optimum energy storage of 8.472×10^4 (J/m²K) occurs at an optimum fabric thickness ($d_{98\% \text{ RH}}$) of 0.274m in the 98% RH ambient air. The values of d_1 , d_2 , d_3 and d_4 represent the optimum fabric thicknesses of the laterite rock walls at 0°C, 20°C, 40°C and 60°C respectively. The observed optimum fabric thickness values are 0.27m, 0.265m, 0.255m and 0.25m at 0°C, 20°C, 40°C and 60°C temperatures respectively. It is clear from the results that the both moisture and temperature affect the optimum thickness of the walls.

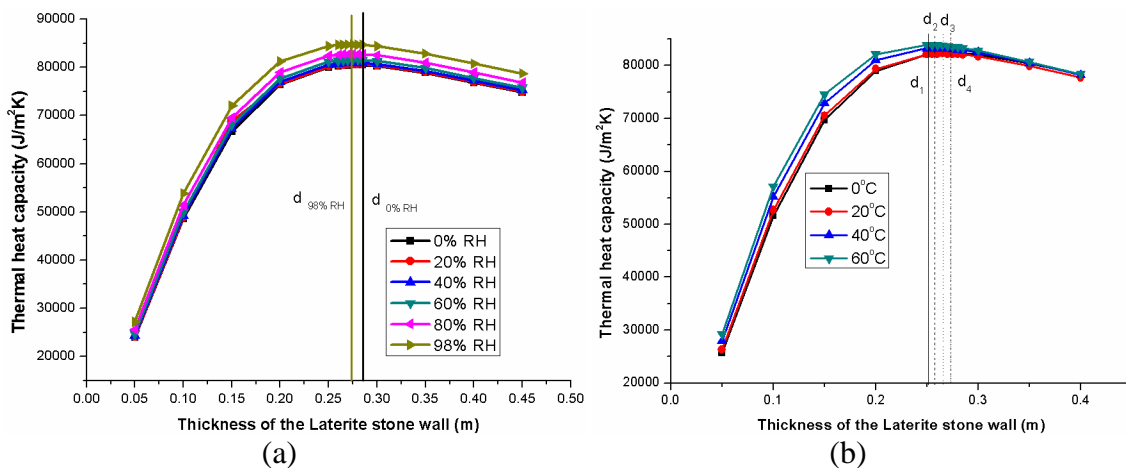


Figure 4.2.9 Thermal heat capacity: (a) Thermal heat capacity of laterite rocks as a function of relative humidity of ambient air and thickness at constant temperature, (b) Thermal heat capacity of laterite rocks as a function of temperature and thickness at constant relative humidity

4.2.7. Effect of moisture and temperature on decrement factor and time lag of laterite rocks

The decrement factor and its time lag are significant thermal characteristics, to analyze the thermal mass or thermal heat capacity of any material. During the daytime, the process of heat transfer from the outside surface to inside surface is periodic. The amplitude of heat wave propagating from the outside surface to the inside surface of the wall is based on solar radiation and convection between outside wall surface and air. The decrement factor of the wall should be as low as possible to reduce the magnitude of heat transfer through the wall and its time lag due to thermal mass should be as high as possible for reducing cooling loads into the building. These decrement factor and time lag are functions of outside temperatures, inside temperatures and material thermal properties of the wall layers. Thermal properties such as, thermal conductivity, specific heat and thermal diffusivity are functions of temperature and relative humidity of the ambient air. For the laterite rock walls, decrement factor reduces with the increase in the relative humidity of the ambient air and the time lag increases with the increase in the relative humidity of the ambient air from 0 to 98% RH as shown in Figure 4.2.10 (a) and Figure 4.2.10 (b). The results show that the dry laterite rocks have higher decrement factors and least time lags and moist laterite walls have lower decrement factors and higher time lags. It can also be observed that the decrement factor decreases and time lag increases with the increase in the laterite wall thickness. Figure 4.2.11 (a) and Figure 4.2.11 (b) show the decrement factor and its time lag as a function of temperature and thickness. From this, it is evident that decrement factor of laterite rocks decreases and its time lag increases with the increase in the temperature. This decrease in decrement factors and increase in the time lag values is due to the increase in the specific heat of the material with increase in the relative humidity and temperature. The increase in the specific heat of the material increases the thermal heat capacity of the wall or thermal mass. Enhanced thermal mass is responsible for the reduced decrement factors and improved time lag values.

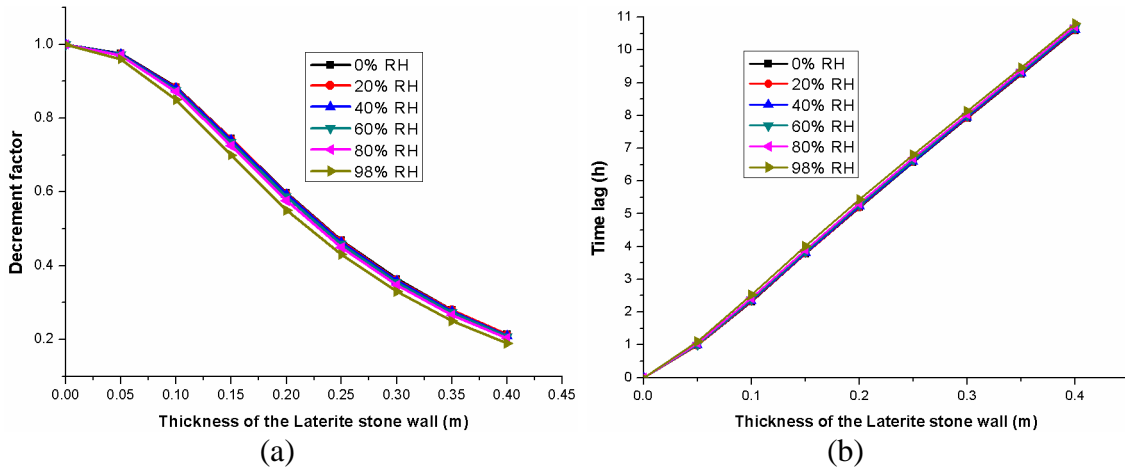


Figure 4.2.10 Decrement factor and it's time lag at constant temperature: (a) Decrement factor of laterite rocks as a function of relative humidity and thickness, (b) Time lag of laterite rocks as a function of relative humidity and thickness

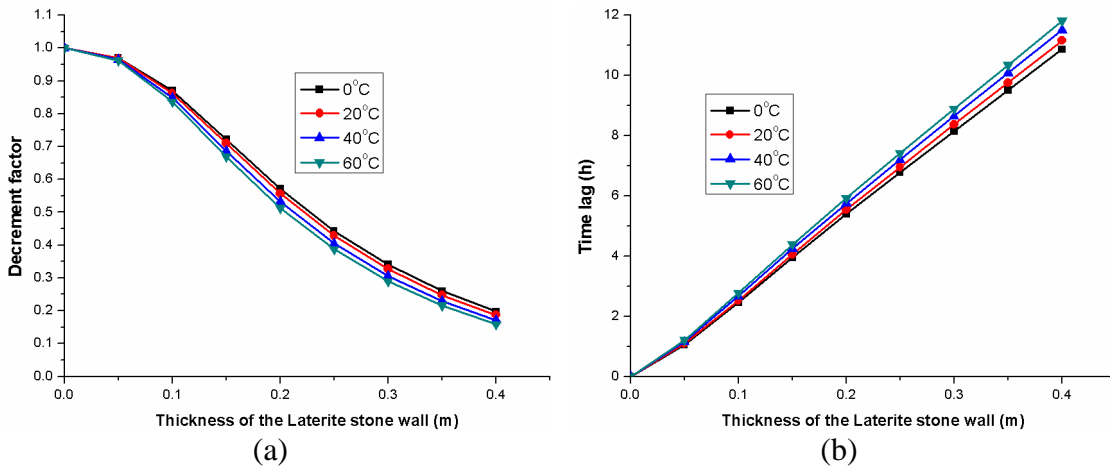


Figure 4.2.11 Decrement factor and it's time lag at constant relative humidity: (a) Decrement factor of laterite rocks as a function of temperature and thickness, (b) Time lag of laterite rocks as a function of temperature and thickness

4.2.8. Effect of moisture and temperature on surface factor and surface factor time lags

The amplitude of surface factor increases with the decrease of thermal conductivity or decrease of moisture in the building material. Building materials with high thermal conductivity or high moisture have lower surface factors and high surface factor time

lag. The Surface factor should be as low as possible and surface factor time lag should be as high as possible for the slow responsiveness of the wall to the short wave radiation.

Figure 4.2.12 (a) and Figure 4.2.12 (b) show the surface factor and surface factor time lags of laterite rocks as a function of relative humidity and thickness. The surface factor of the laterite rocks decreases with the increase in the moisture content of the ambient air and the surface factor time lag increases with the increase in the relative humidity of the ambient air due to increase in the thermal conductivity of laterite rocks with relative humidity. The laterite walls are slow responsive to short wave radiation at 98% RH due to their lower surface factors (0.36) and higher surface factor time lags (1.99) whereas the laterite walls are fast responsive to short wave radiation at 0% RH due to their higher surface factors (0.41) and lower surface factor time lags (1.87). The surface factor and it's time lag of laterite rocks as a function of temperature and thickness is shown in Figure 4.2.13 (a) and Figure 4.2.13 (b). The fluctuation of surface factor and it's time lag at temperatures 0°C, 20°C, 40°C and 60°C is due to the fluctuation of the thermal conductivities of laterite walls at those temperatures. From this, it is observed that the surface factor and surface factor time lag depend only upon thermal conductivity and do not depend upon the thickness of the laterite wall.

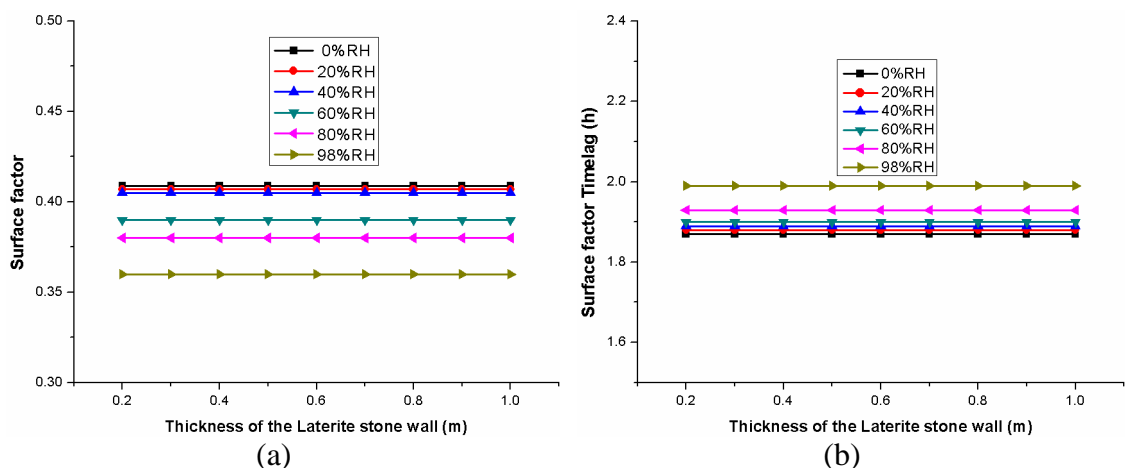


Figure 4.2.12 Surface factor and it's time lag at constant temperature: (a) Surface factor of laterite rocks as a function of humidity and thickness, (b) Surface factor time lag of laterite rocks as a function of humidity and thickness

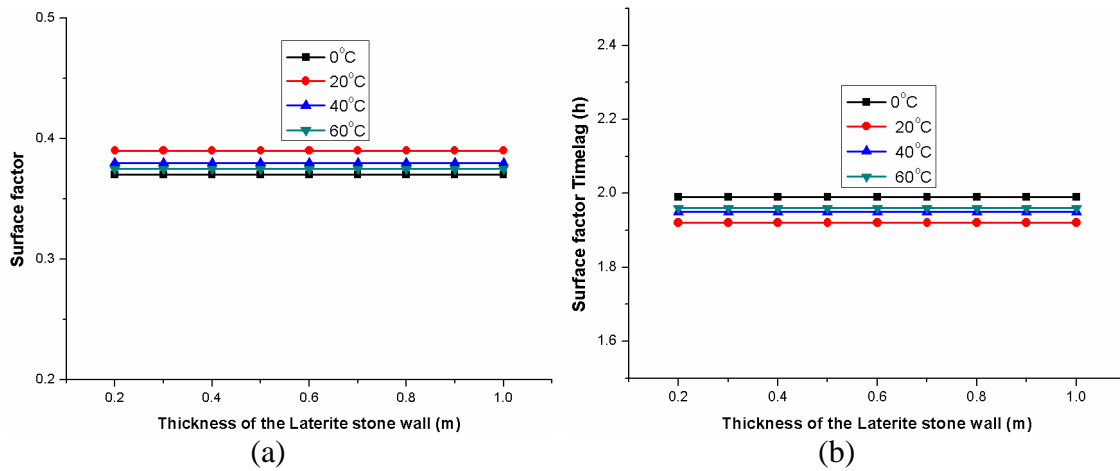


Figure 4.2.13 Surface factor and its time lag at constant relative humidity: (a) Surface factor of laterite rocks as a function of temperature and thickness, (b) Surface factor time lag of laterite rocks as a function of temperature and thickness

4.2.9. Effect of moisture, temperature and outside convective heat transfer coefficient on decrement factor and decrement time lags

Figure 4.2.14 (a) and Figure 4.2.14 (b) show the variation of decrement factor and time lag with varying outside convective heat transfer coefficient (h_o) for laterite rock walls at different relative humidity levels. It can be clearly observed that, there is a considerable influence of outside convective heat transfer coefficient on decrement factor and time lag. The decrement factor increases and the time lag decreases with the increase in the outside convective heat transfer coefficient. From this it is clear that the decrement factor and time lag not only depend upon the thermal properties and thickness, but they also depend upon outside convective heat transfer coefficients. Decrement factor and its time lag of laterite rocks as a function of temperature and heat transfer coefficient are shown in Figure 4.2.15 (a) and Figure 4.2.15 (b) respectively.

The results show that the unsteady state thermal characteristics of Indian standard thickness laterite (0.29m) rocks vary drastically with increase in relative humidity of ambient air from 0 to 98%. Transmittance increases by 8.47%, admittance increases by 5.28%, decrement factor decreases by 8.35%, time lag increases by 2.88%, surface factor decreases by 10.24%, surface factor time lag increases by 5.27% and thermal heat capacity increases by 4.96%. The increase in the temperature from 0°C to 60°C

causes the following changes in the thermal parameters of laterite wall, the admittance increases by 1.9%, decrement factor reduces by 14.5%, decrement factor time lag increases by 8.3% and thermal heat capacity increases by 1.1%.

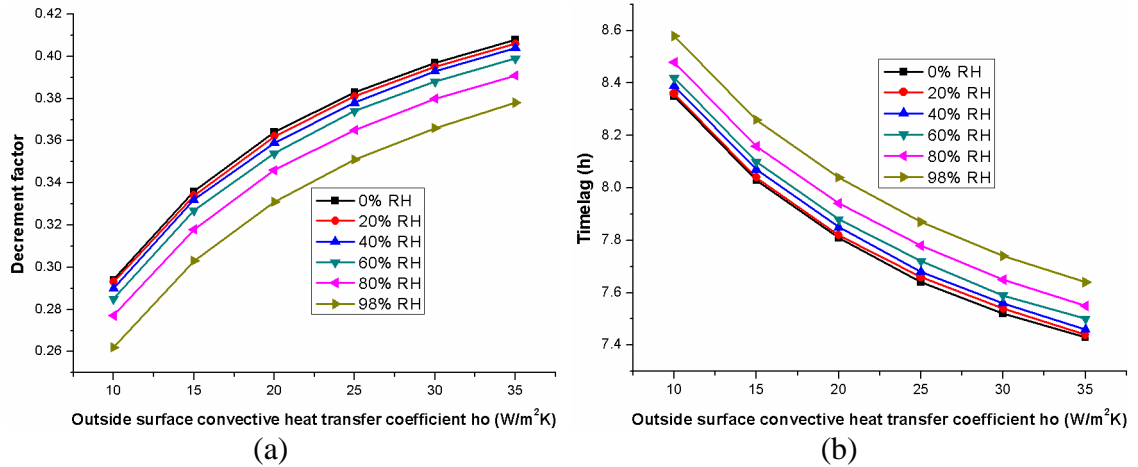


Figure 4.2.14 Decrement factor and it's time lag at constant temperature: (a)

Decrement factor of laterite rocks as a function of humidity and heat transfer coefficient, (b) Time lag of laterite rocks as a function of humidity and heat transfer coefficient

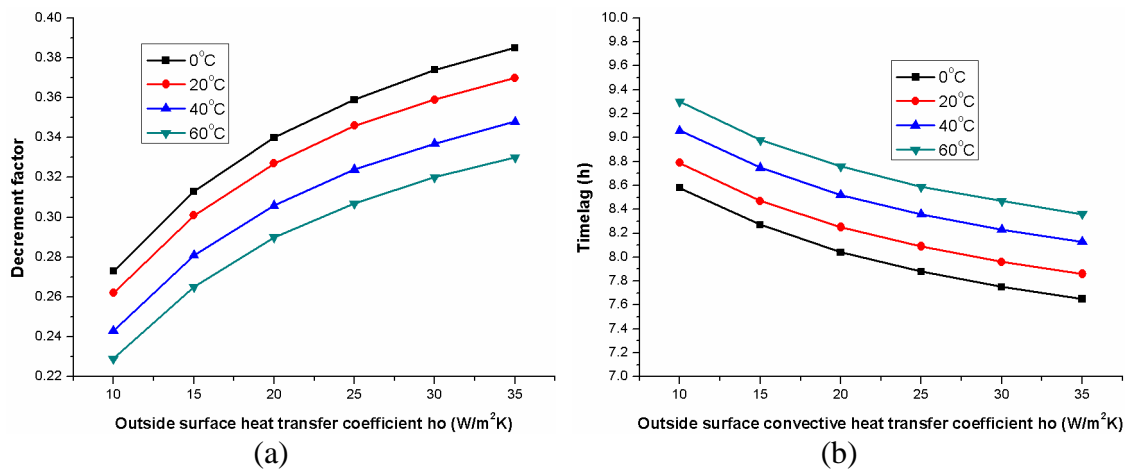


Figure 4.2.15 Decrement factor and it's time lag at constant relative humidity: (a)

Decrement factor of laterite rocks as a function of temperature and heat transfer coefficient, (b) Time lag of laterite rocks as a function of temperature and heat transfer coefficient

4.3 THE DECREMENT FACTOR AND TIME LAG OF LATERITE AND CONCRETE BUILDINGS IN FOUR DIFFERENT CLIMATIC ZONES OF INDIA

4.3.1 Thermal properties and methodology

The building models with different building materials were designed in Design builder version 4.3.0.039. The dimensions of the building models are 3.5 m X 3.5 m X 3.5 m with 0.2286 m external wall thickness. The building materials for wall materials used are laterite stone and dense concrete. The floor was designed with dense concrete with 0.14 m thickness and plastered on the top side of the floor with 0.01 m cement plaster. The roof was designed with reinforced cement concrete of 0.13 m thickness and it was plastered at the top and bottom side of the roof with 0.01 m cement plaster.

The thermal analysis of the building models with the above building dimensions and materials were carried out using licensed Energy plus 8.1 simulation software in different climatic zones of India. The major city is selected in the each climate zone. The four climatic zones of India such as hot and dry (Ahmedabad (23.07⁰N, 72.63⁰E)), moderate (Bangalore (12.97⁰N, 77.58⁰E)), composite (Hyderabad (17.45⁰N, 78.47⁰E)) and warm and humid (Mangalore (12.87⁰N, 74.88⁰E)). The heat gain in buildings of four different cities on the peak summer day was computed. Thermal analysis was carried out for climatic regions of Ahmedabad (Peak summer day May 15th), Bangalore (Peak summer day April 15th), Hyderabad (Peak summer day May 15th) and Mangalore (Peak summer day April 15th) on peak summer days of the year as per the Indian standards Table 4.1. shows the thermo physical properties of building materials. Thermo physical properties of building materials are as per the Indian standards. Thermo physical properties of laterite stone were measured experimentally. Figure 4.3.1 shows sun path diagram of four climatic regions of India on peak summer days. The Sun path diagram is a graphical illustration of sun paths in the sky for various days in the year. Figure 4.3.2 shows outside and inside eastern laterite wall surface temperatures in four different climatic regions. Figure 4.3.3 shows outside and inside western laterite wall surface temperatures in four different

climatic regions. Figure 4.3.4 shows outside and inside northern laterite wall surface temperatures in four different climatic regions. Figure 4.3.5 shows outside and inside southern laterite wall surface temperatures in four different climatic regions. The decrement factor and time lag values can be computed using equations 4.2 and 4.3.

$$\text{Decrement factor } f = \frac{T_{i \max} - T_{i \min}}{T_{e \max} - T_{e \min}} \quad (4.2)$$

$$\text{Time lags } \phi_{\min} = t_{T_{i \min}} - t_{T_{e \min}} \text{ and } \phi_{\max} = t_{T_{i \max}} - t_{T_{e \max}} \quad (4.3)$$

Where, T_e and T_i are wall external and internal surface temperature; t = Time.

Table 4.3.1 Thermo physical properties of building materials

Building material	k [W/mK]	ρ [kg/m ³]	Cp [J/kgK]
Laterite stone	1.3698	1000	1926.1
Dense concrete	1.74	2410	880
Reinforced cement concrete	1.58	2288	880
Cement plaster	0.721	1762	840

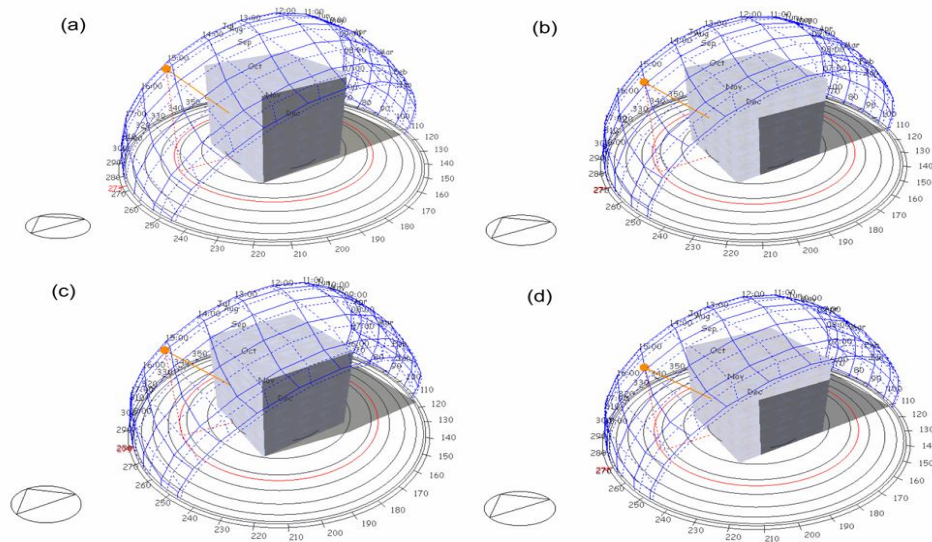
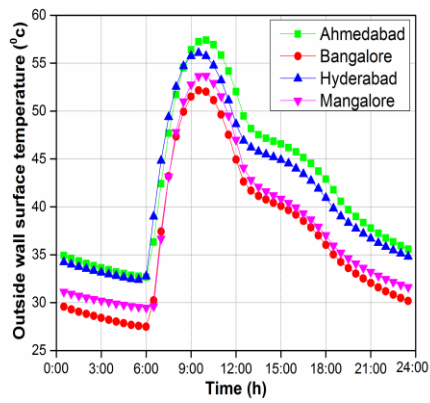
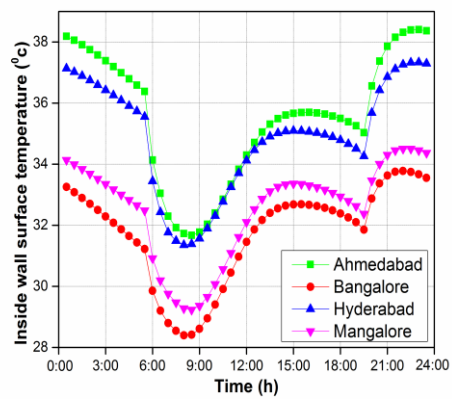


Figure 4.3.1 Sun path diagrams on peak summer day: (a) Ahmedabad climatic region, (b) Bangalore climatic region, (c) Hyderabad climatic region, (d) Mangalore climatic region

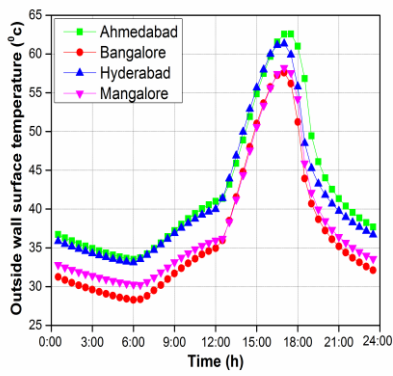


(a)

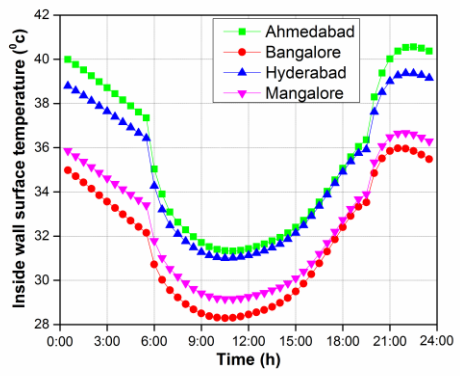


(b)

Figure 4.3.2 Surface temperatures of Eastern laterite wall: (a) Outside wall surface temperatures, (b) Inside wall surface temperatures



(a)



(b)

Figure 4.3.3 Surface temperatures of Western laterite wall: (a) Outside wall surface temperatures, (b) Inside wall surface temperatures

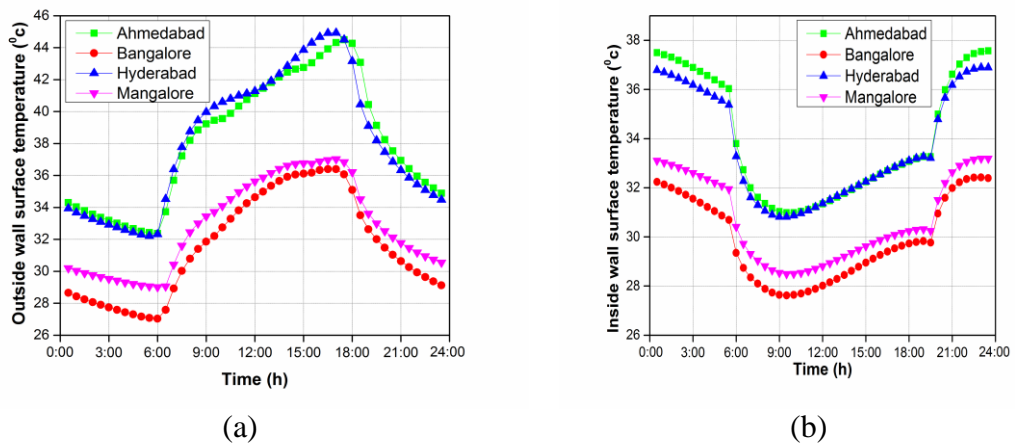


Figure 4.3.4 Surface temperatures of Northern laterite wall: (a) Outside wall surface temperatures, (b) Inside wall surface temperatures

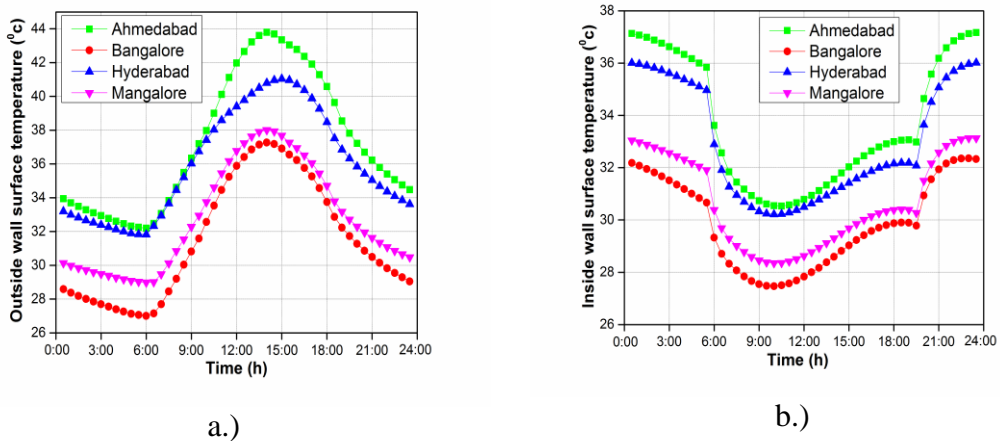


Figure 4.3.5 Surface temperatures of Southern laterite wall: (a) Outside wall surface temperatures, (b) Inside wall surface temperatures

4.3.2 Decrement factor and time lag of buildings in hot and dry climatic zones (ahmedabad) of india

The decrement factor (f) is the attenuation of temperature amplitude during the heat wave penetration through building walls. Figure 4.3.6 shows the decrement factor of laterite and dense concrete building walls in hot and dry climatic zones (Ahmedabad) of India.

The average decrement factor for laterite walls in the Ahmedabad climatic region is 0.426. The average decrement factor for concrete walls was observed to be 0.458. From the results, it is observed that the laterite walls are better than concrete wall from low decrement factor perspective.

Figure 4.3.7 shows the Time lag of laterite and dense concrete building walls in hot and dry climatic zones (Ahmedabad) of India. The time required by the heat wave of period 24 h to propagate through a building wall from the outside surface to inside surface is called the time lag (ϕ). The ϕ_{\max} is equal to the ϕ_{\min} when the outside surface temperature is periodic and sinusoidal. The boundary conditions are periodic and non sinusoidal when ϕ_{\max} is not equal to the ϕ_{\min} .

The laterite walls oriented to east, north and south have different ϕ_{\max} and ϕ_{\min} values and hence, the outside temperature variations are periodic non sinusoidal. The laterite wall oriented to west has the same ϕ_{\max} and ϕ_{\min} values and hence, the outside temperature variations are periodic and sinusoidal. The laterite wall ϕ_{\max} values are 13h, 5h, 6h and 9.5h, respectively, for eastern, western, northern and southern wall orientations. The laterite wall ϕ_{\min} values are 2.5 h, 5h, 3.5h and 4.5h, respectively, for eastern, western, northern and southern wall orientations. The average ϕ_{\max} value for laterite wall in the Ahmedabad climatic region is 8.375h. The average ϕ_{\min} value for laterite wall in the Ahmedabad climatic region is 3.875 h. In summer climates, the higher ϕ_{\min} values are recommended for reducing cooling loads. The concrete walls oriented to east, north and south have different ϕ_{\max} and ϕ_{\min} values and hence, the outside temperature variations are periodic non sinusoidal. The concrete wall oriented to west has the same ϕ_{\max} and ϕ_{\min} values and hence, the outside temperature variations are periodic and sinusoidal. The concrete wall ϕ_{\max} values are 12.5h, 4.5h, 5.5h and 9.5h, respectively, for eastern, western, northern and southern wall orientations. The concrete wall ϕ_{\min} values are 2h, 4.5h, 3.5h and 4h, respectively, for eastern, western, northern and southern wall orientations. The average ϕ_{\max} value for concrete wall in the Ahmedabad climatic region is 8 h. The average ϕ_{\min} value for concrete wall in the Ahmedabad climatic region is 3.5 h. In summer climates, the higher ϕ_{\min} values are recommended for reducing cooling loads. The laterite walls have higher ϕ_{\min} values than the concrete walls. Hence, the laterite walls are energy

efficient than the concrete walls in the Ahmedabad climatic regions. The average values of decrement factor and the time lag for laterite and dense concrete buildings in the Ahmedabad climatic region were shown in Table 4.3.2 and 4.3.3.

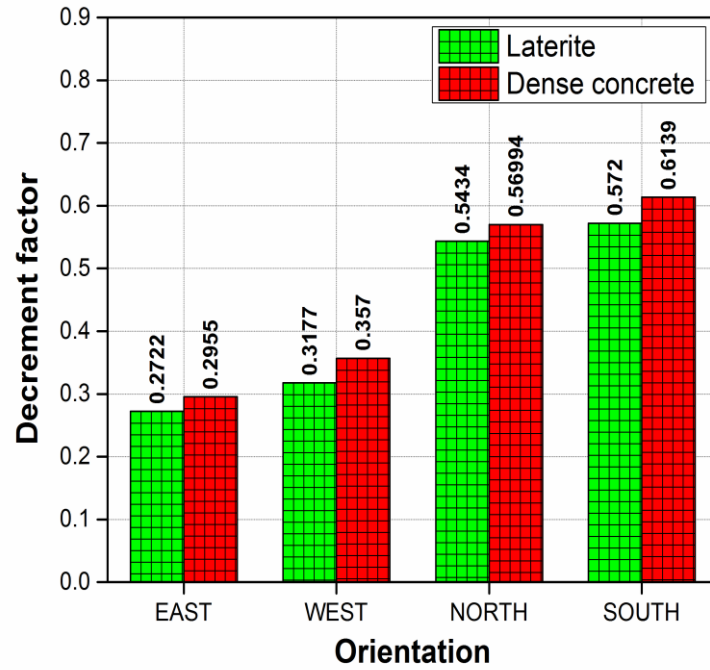


Figure 4.3.6 Decrement factor of laterite and dense concrete building walls in hot and dry climatic zones (Ahmedabad) of India

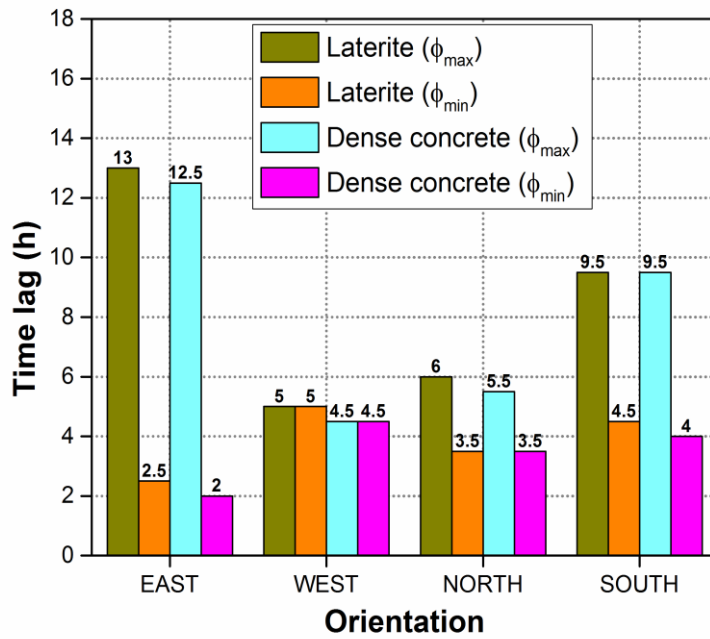


Figure 4.3.7 Time lag of laterite and dense concrete building walls in hot and dry climatic zones (Ahmedabad) of India

Table 4.3.2 Decrement factor and time lag of laterite buildings in Ahmedabad climatic region

Laterite buildings (Ahmedabad climatic region)			
Wall orientation	ϕ_{max} [h]	ϕ_{min} [h]	f
East	13	2.5	0.2722
West	5	5	0.3177
North	6	3.5	0.5434
South	9.5	4.5	0.5721
Average	8.375	3.875	0.42635

Table 4.3.3 Decrement factor and time lag of dense concrete buildings in Ahmedabad climatic region

Dense concrete buildings (Ahmedabad climatic region)			
orientation	ϕ_{\max} [h]	ϕ_{\min} [h]	f
East	12.5	2	0.2955
West	4.5	4.5	0.357
North	5.5	3.5	0.569
South	9.5	4	0.613
Average	8	3.5	0.458

4.3.3 Decrement factor and time lag of buildings in moderate climatic zones (bangalore) of india

Figure 4.3.8 shows the decrement factor of laterite and dense concrete building walls in moderate climatic zones (Bangalore) of India.

The average decrement factor for laterite walls in the Bangalore climatic region is 0.367. The average decrement factor for concrete walls was observed to be 0.399. From the results, it is observed that the laterite walls are better than concrete wall from low decrement factor perspective in Bangalore climatic regions.

Figure 4.3.9 shows the time lag of laterite and dense concrete building walls in moderate climatic zones (Bangalore) of India. The laterite walls oriented to east, north and south have different ϕ_{\max} and ϕ_{\min} values and hence, the outside temperature variations are periodic non sinusoidal. The laterite wall oriented to west has the same ϕ_{\max} and ϕ_{\min} values and hence, the outside temperature variations are periodic and sinusoidal. The laterite wall ϕ_{\max} values are 12.5h, 4.5h, 6.5h and 9h, respectively, for eastern, western, northern and southern wall orientations. The laterite wall ϕ_{\min} values are 2 h, 4.5h, 3.5h and 4h, respectively, for eastern, western, northern and southern wall orientations. The average ϕ_{\max} value for laterite wall in the Bangalore climatic region is 8.125h. The average ϕ_{\min} value for laterite wall in the Bangalore climatic

region is 3.5 h. In summer climates, the higher ϕ_{\min} values are recommended for reducing cooling loads.

The concrete walls oriented to east, north and south have different ϕ_{\max} and ϕ_{\min} values and hence, the outside temperature variations are periodic non sinusoidal. The concrete wall oriented to west has the same ϕ_{\max} and ϕ_{\min} values and hence, the outside temperature variations are periodic and sinusoidal. The concrete wall ϕ_{\max} values are 12h, 4h, 5.5h and 8.5h, respectively, for eastern, western, northern and southern wall orientations. The concrete wall ϕ_{\min} values are 2 h, 4h, 3h and 3.5h, respectively, for eastern, western, northern and southern wall orientations. The average ϕ_{\max} value for concrete wall in the Bangalore climatic region is 7.5 h. The average ϕ_{\min} value for concrete wall in the Bangalore climatic region is 3.125 h. In summer climates, the higher ϕ_{\min} values are recommended for reducing cooling loads. The laterite walls have higher ϕ_{\min} values than the concrete walls. Hence, the laterite walls are more energy efficient than the concrete walls in the Bangalore climatic regions as well. The average values of decrement factor and the time lag for laterite and dense concrete buildings in Bangalore climatic region were shown in Table 4.3.4 and 4.3.5.

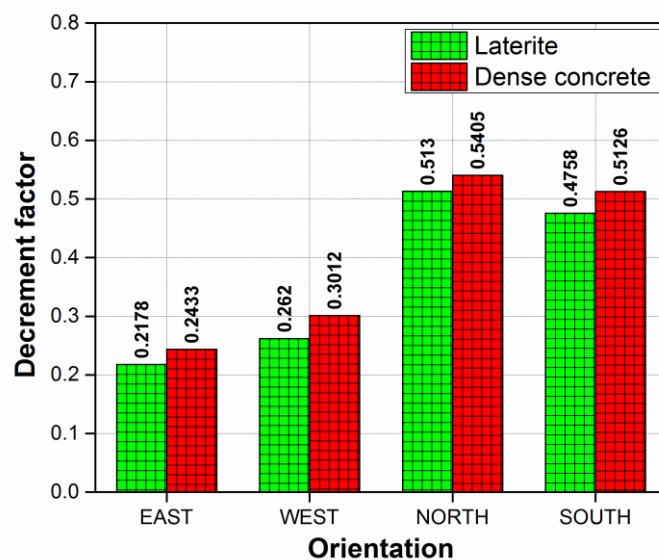


Figure 4.3.8 Decrement factor of laterite and dense concrete building walls in moderate climatic zones (Bangalore) of India

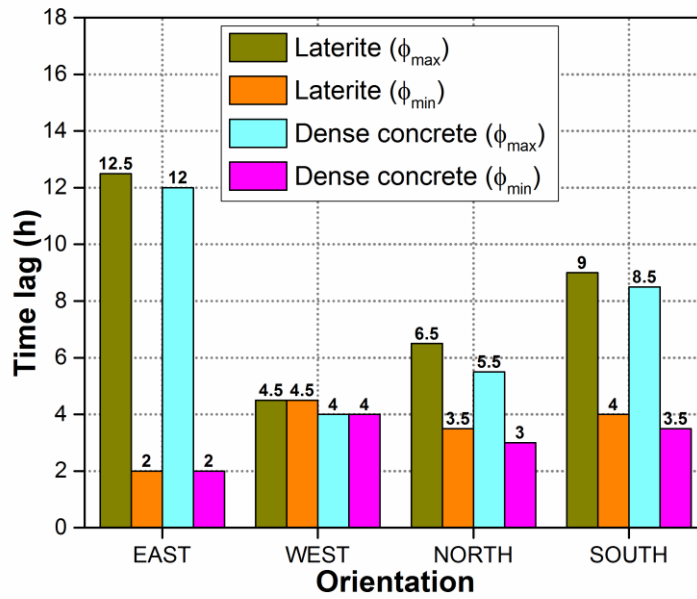


Figure 4.3.9 Time lag of laterite and dense concrete building walls in moderate climatic zones (Bangalore) of India

Table 4.3.4 Decrement factor and time lag of laterite buildings Bangalore climatic region

Laterite buildings (Bangalore climatic region)			
Wall orientation	ϕ_{max} [h]	ϕ_{min} [h]	f
East	12.5	2	0.2178
West	4.5	4.5	0.2620
North	6.5	3.5	0.5130
South	9	4	0.4758
Average	8.125	3.5	0.367

Table 4.3.5 Decrement factor and time lag of dense concrete buildings
Bangalore climatic region

Dense concrete buildings (Bangalore climatic region)			
orientation	ϕ_{\max} [h]	ϕ_{\min} [h]	f
East	12	2	0.2433
West	4	4	0.3012
North	5.5	3	0.5405
South	8.5	3.5	0.5126
Average	7.5	3.125	0.399

4.3.4 Decrement factor and time lag of buildings in composite climatic zones (Hyderabad) of India

Figure 4.3.10 shows the decrement factor of laterite and dense concrete building walls in composite climatic zones (Hyderabad) of India.

The average decrement factor for laterite walls in the Hyderabad climatic region is 0.413. The average decrement factor for concrete walls was observed to be 0.441. From the results, it is observed that the laterite walls are better than concrete wall from low decrement factor perspective in the Hyderabad climatic regions.

Figure 4.3.11 shows the time lag of laterite and dense concrete building walls in composite climatic zones (Hyderabad) of India. The laterite walls oriented to east, west, north and south have different ϕ_{\max} and ϕ_{\min} values and hence, the outside temperature variations are periodic non sinusoidal. The laterite wall ϕ_{\max} values are 13.5h, 5h, 6h and 8.5h, respectively, for eastern, western, northern and southern wall orientations. The laterite wall ϕ_{\min} values are 2.5 h, 4.5h, 4h and 4h, respectively, for eastern, western, northern and southern wall orientations. The average ϕ_{\max} value for laterite wall in the Hyderabad climatic region is 8.25h. The average ϕ_{\min} value for laterite wall in the Hyderabad climatic region is 3.75 h.

The concrete walls oriented to east, north and south have different ϕ_{\max} and ϕ_{\min} values and hence, the outside temperature variations are periodic non sinusoidal. The concrete wall oriented to west has not much difference between ϕ_{\max} and ϕ_{\min} values and hence, the outside temperature variations are periodic and nearly sinusoidal. The concrete wall ϕ_{\max} values are 12.5h, 4.5h, 5.5h and 8.5h, respectively, for eastern, western, northern and southern wall orientations. The concrete wall ϕ_{\min} values are 2.5h, 4.5h, 3.5h and 4h, respectively, for eastern, western, northern and southern wall orientations. The average ϕ_{\max} value for concrete wall in the Hyderabad climatic region is 7.75 h. The average ϕ_{\min} value for concrete wall in the Hyderabad climatic region is 3.625 h. In summer climates, the higher ϕ_{\min} values are recommended for reducing cooling loads. The laterite walls have higher ϕ_{\min} values than the concrete walls. Hence, the laterite walls are recommended for energy efficient building construction than the concrete walls in the Hyderabad climatic regions as well. The average values of decrement factor and the time lag for laterite and dense concrete buildings in the Hyderabad climatic region were shown in Table 4.3.6 and 4.3.7.

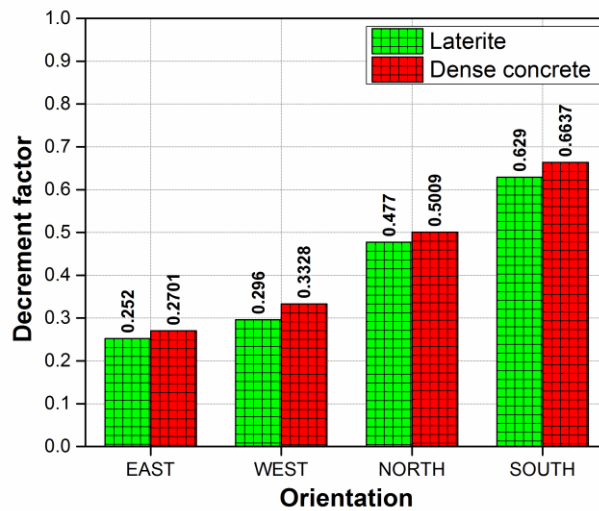


Figure 4.3.10 Decrement factor of laterite and dense concrete building walls in composite climatic zones (Hyderabad) of India

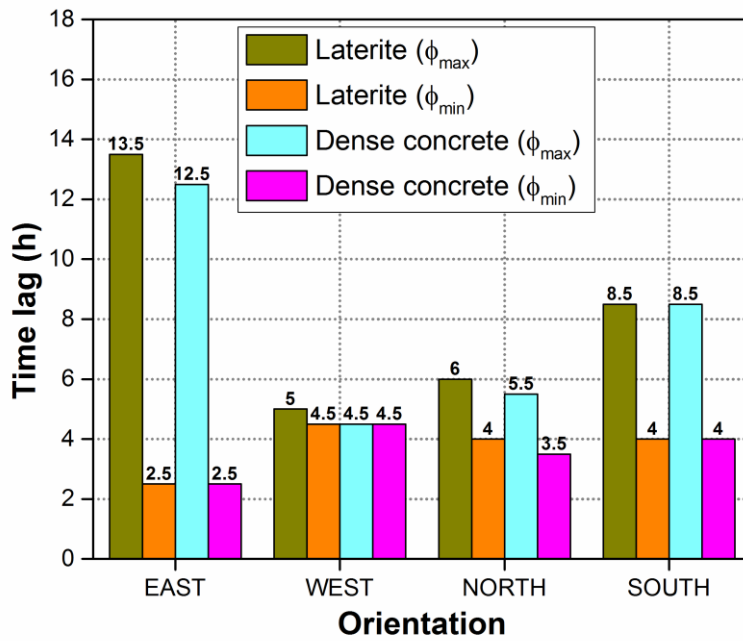


Figure 4.3.11 Time lag of laterite and dense concrete building walls in composite climatic zones (Hyderabad) of India

Table 4.3.6 Decrement factor and time lag of laterite buildings in Hyderabad climatic region

Laterite buildings (Hyderabad climatic region)			
Wall orientation	ϕ_{max} [h]	ϕ_{min} [h]	f
East	13.5	2.5	0.252
West	5	4.5	0.296
North	6	4	0.477
South	8.5	4	0.629
Average	8.25	3.75	0.413

Table 4.3.7 Decrement factor and time lag of dense concrete buildings in Hyderabad climatic region

Dense concrete buildings (Hyderabad climatic region)			
orientation	ϕ_{\max} [h]	ϕ_{\min} [h]	f
East	12.5	2.5	0.2701
West	4.5	4.5	0.3328
North	5.5	3.5	0.5009
South	8.5	4	0.6637
Average	7.75	3.625	0.441

4.3.5 Decrement factor and time lag of buildings in warm and humid climatic zones (Mangalore) of India

Figure 4.3.12 shows the decrement factor of laterite and dense concrete building walls in warm and humid climatic zones (Mangalore) of India.

The average decrement factor for laterite walls in the Mangalore climatic region is 0.401. The average decrement factor for concrete walls was observed to be 0.429. From the results, it is observed that the laterite walls are better than concrete wall from a low decrement factor perspective in Mangalore climatic regions.

Figure 4.3.13 shows the time lag of laterite and dense concrete building walls in warm and humid climatic zones (Mangalore) of India. The laterite walls oriented to east, west, north and south have different ϕ_{\max} and ϕ_{\min} values and hence, the outside temperature variations are periodic and non sinusoidal. The laterite wall ϕ_{\max} values are 12h, 4.5h, 6h and 9.5h, respectively, for eastern, western, northern and southern wall orientations. The laterite wall ϕ_{\min} values are 2.5 h, 4h, 3.5h and 4h, respectively, for eastern, western, northern and southern wall orientations. The average ϕ_{\max} value for laterite wall in the Mangalore climatic region is 8h. The average ϕ_{\min} value for laterite wall in the Mangalore climatic region is 3.5 h.

The concrete walls oriented to east, west, north and south have different ϕ_{\max} and ϕ_{\min} values and hence, the outside temperature variations are periodic and non sinusoidal. The concrete wall ϕ_{\max} values are 11.5h, 4.5h, 6h and 9h, respectively, for eastern, western, northern and southern wall orientations. The concrete wall ϕ_{\min} values are 2h, 4h, 3.5h and 4h, respectively, for eastern, western, northern and southern wall orientations. The average ϕ_{\max} value for concrete wall in the Mangalore climatic region is 7.75 h. The average ϕ_{\min} value for concrete wall in the Mangalore climatic region is 3.375 h. In summer climates, the higher ϕ_{\min} values are recommended for reducing cooling loads. The laterite walls have higher ϕ_{\min} values than the concrete walls. Hence, the laterite walls are recommended for energy efficient building construction than the concrete walls in Mangalore climatic regions. The average values of decrement factor and time lag for laterite and dense concrete buildings in the Mangalore climatic region were shown in Table 4.3.8 and 4.3.9.

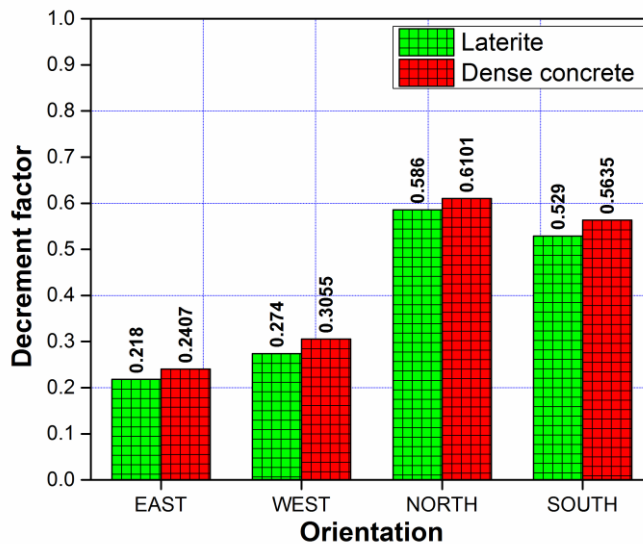


Figure 4.3.12 Decrement factor of laterite and dense concrete building walls in warm and humid climatic zones (Mangalore) of India

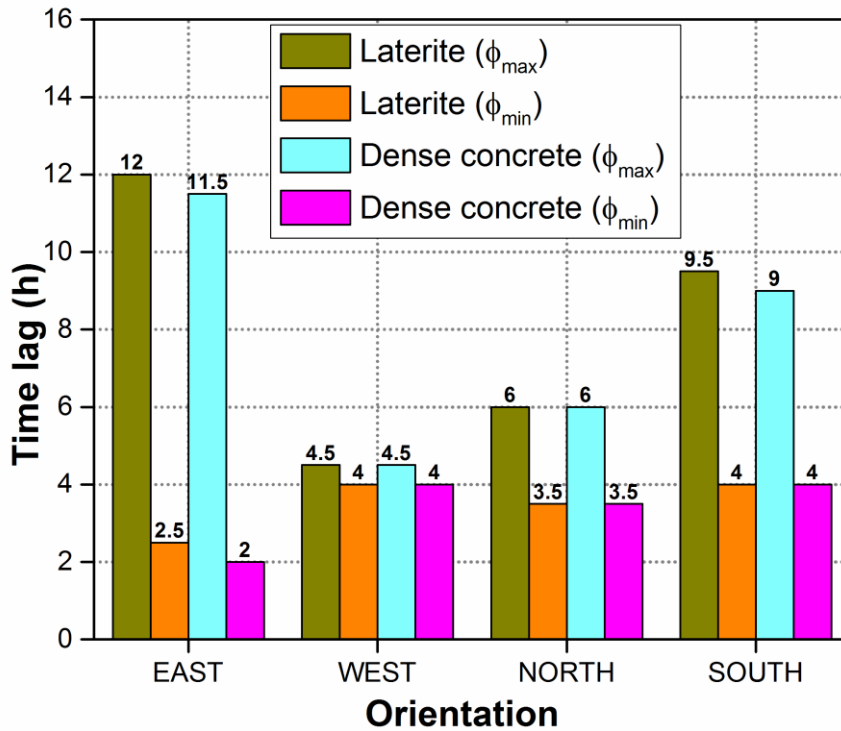


Figure 4.3.13 Time lag of laterite and dense concrete building walls in warm and humid climatic zones (Mangalore) of India

Table 4.3.8 Decrement factor and time lag of laterite buildings in Mangalore climatic region

Laterite buildings (Mangalore climatic region)			
Wall orientation	ϕ_{max} [h]	ϕ_{min} [h]	f
East	12	2.5	0.218
West	4.5	4	0.274
North	6	3.5	0.586
South	9.5	4	0.529
Average	8	3.5	0.401

Table 4.3.9 Decrement factor and time lag of dense concrete buildings in Mangalore climatic region

Dense concrete buildings (Mangalore climatic region)			
orientation	ϕ_{\max} [h]	ϕ_{\min} [h]	f
East	11.5	2	0.2407
West	4.5	4	0.3055
North	6	3.5	0.6101
South	9	4	0.5635
Average	7.75	3.375	0.429

4.4 SUMMARY

The changes in the laterite stone thermal properties due to relative humidity and temperature have to be considered in designing energy efficient laterite stone buildings, as they are exposed to different humidity and temperature environments in practice.

- Moisture absorption of laterite rocks increases with the increase in the relative humidity from 50 to 98% RH. This sudden rise in moisture absorption causes the thermal conductivity and specific heat capacity of laterite to increase. The thermal conductivity and the specific heat capacity of laterite rocks increase by 14.73% and by 9.15%, respectively, with relative humidity of ambient air compared with the dry laterite rocks.
- Both relative humidity and temperature affect the decrement factor and its time lag values. The increase in the relative humidity from 0% RH to 98% RH decreases the decrement factor by 8.35% and increases the time lag by 2.88%, whereas, the increase in the temperature from 0°C to 60°C decreases the decrement factor by 14.5% and increases the time lag by 8.3%.
- Laterite rock walls are slow responsive to short wave radiation at higher relative humidity levels due to their lower surface factors (0.36) and higher surface factor time lags (1.99) whereas dry laterite walls are fast responsive to short wave radiation due

to their higher surface factors (0.41) and lower surface factor time lags (1.87). From this it is concluded that the responsiveness of the laterite walls to the short wave radiation is reduced with an increase in the relative humidity.

- Optimum fabric thickness of the laterite wall decreases with the increase in the relative humidity and temperature of ambient air. Optimum thickness of the laterite rocks to be maintained in highly humid coastal regions is found to be 0.274m (at 98% RH) from humidity point of view and optimum thickness of the laterite rocks to be maintained in hot regions is found to be 0.255 m (at 40°C) from a temperature point of view.
- Thermal admittance and thermal transmittance of the laterite rocks increase with the increase in the relative humidity of ambient air, whereas an increase in the temperature increases the thermal admittance and keeps thermal transmittance almost constant.
- The average decrement factor for laterite buildings in Ahmedabad, Bangalore, Hyderabad and Mangalore climatic regions is less than that of the average decrement factor of concrete buildings in all climatic regions. The average decrement factor of the laterite building walls in the Mangalore climatic region is 6.526% less than that of the average decrement factor of the dense concrete building walls in the Mangalore climatic region. Hence, the laterite walls are recommended over concrete walls from a low decrement factor point of view.
- In summer climates, the higher ϕ_{\min} values are recommended for reducing cooling loads. The laterite building walls have higher ϕ_{\min} values than the concrete building walls. The average time lag (ϕ_{\min}) of the laterite building walls in the Mangalore climatic region is 3.57% higher than that of the average time lag (ϕ_{\min}) of the dense concrete building walls in the Mangalore climatic region. Hence, the laterite walls are recommended for energy efficient building construction than the concrete walls from higher average time lag perspective.
- The results of the study help in selection of energy efficient building materials from lower decrement factor and higher time lag perspective.

CHAPTER-5

EFFECT OF THERMAL PROPERTIES OF BUILDING MATERIALS, INSULATION LOCATION, AIR SPACE THICKNESS AND AIR SPACE LOCATION WITHIN WALL ON DYNAMIC THERMAL PROPERTIES OF WALLS

5.1 INTRODUCTION

Climate responsive building design involves the study of the thermal response of building and insulating materials exposed to periodic changes of environmental conditions. In this study, ten homogeneous building materials (Laterite stone, Madras black clay, Indore black clay, Slate, Burnt brick, Mud brick, Reinforced brick, Brick tile, Mud phuska and Cinder concrete) and ten homogeneous insulating materials (Saw dust, Rice husk, Coir board, Jute felt, Jute fiber, Coconut pitch, Straw board, Asbestos fiber, Wall board and Chip board) are investigated. Unsteady thermal response characteristics and Optimum wall thicknesses of building and insulating materials were calculated.

Passive cooling is one of the methods to keep the building cool and to reduce the load on air conditioner. Passive cooling demands the study of the thermal characteristics like admittance, transmittance, decrement factor, time lag, surface factor and surface factor time lags. These characteristics were determined for both homogeneous and composite walls. In this study, five building materials such as, Laterite stone, Burnt brick, Mud brick, Reinforced brick and Fly ash bricks were selected as homogeneous building materials. Five local Insulating materials such as Saw dust, Rice husk, Coir board, Jute felt and Jute fiber were selected to form the composite wall along with building materials. The composite walls were framed using the combination of building and insulation materials. Total hundred combinations of composite walls, without insulation and with insulation material located at the inner side, at mid plane and at outer side of the composite walls were studied. To study the thermal

characteristics of such configurations of composite wall, one dimensional heat flow diffusion equation was solved using matrix algebra under periodic convection boundary conditions. The penetration length, the phase velocity of the heat waves in the wall and optimum fabric thickness of the selected building and insulating materials were calculated.

This paper also presents the comprehensive investigation of the effect divided air space thickness within the wall on unsteady heat transfer characteristics such as, thermal transmittance, thermal admittance, decrement factor and time lag of five building material walls for energy efficient building enclosure design. The five building material composite walls such as laterite stone, mud brick, cellular concrete, dense concrete and cinder concrete with total thirty configurations were studied. A computer simulation program was developed to compute unsteady heat transfer characteristics using the cyclic admittance procedure. From the results, it is observed that the decrement factor decreases with the increase in the divided air space thickness within the composite wall for all building materials. Dense concrete (DC) was observed to be the energy efficient from the lowest decrement factor point of view among five studied building materials. Dense concrete decrement factor decreases by 23.67% for 0.02 m air space thickness compared to the conventional composite wall without air space. It is also noticed that the time lag increases with the increase in the divided air space thickness within the composite wall for all building materials. Cellular concrete (CLC) was observed to be the energy efficient from highest time lag perspective among five studied building materials. Cellular concrete time lag increases by 6.23% for 0.02 m air space thickness compared to the conventional composite wall without air space. Both thermal insulation and thermal mass can be enhanced with the air spaces within the wall structure.

This chapter also aims to present the optimum location of vertical air space within composite walls to be maintained based on thermal response characteristics such as admittance, transmittance, decrement factor, time lag, surface factor and surface factor time lags. In this study, six building materials: Laterite stone, burnt brick, mud brick, reinforced brick, fly ash brick and concrete block were selected and computations were made for forty two configurations of the composite walls with seven configurations for each building material (without air space, air space at the

outer side, air space at mid center plane, air space at the inner side, air space at the outer and the inner sides, air space at the outer side and mid center plane and air space at mid center plane and the inner side).

5.2 EFFECT OF THERMAL PROPERTIES OF BUILDING AND INSULATING MATERIALS ON DYNAMIC THERMAL PROPERTIES OF WALLS

5.2.1 Thermal properties and unsteady thermal response characteristics of building and insulating materials

Table 5.2.1 shows the thermo-physical properties of Building materials and Table 5.2.2 shows the thermo-physical properties of Insulating materials considered for the study (SP: 41 1987). Ten building and ten insulation materials were selected for the study. The computer program was developed and used to calculate the unsteady state thermal characteristics of homogeneous and composite walls. The building materials are coded as shown in Table 5.2.1. The insulating materials are coded as shown in Table 5.2.2 Plaster was represented by code P. Thermal properties of Laterite stone (LS) and plaster (P) were calculated experimentally in K-Analys, AB Sweden.

Table 5.2.3 and Table 5.2.4 show the unsteady state thermal characteristics of building and insulating materials, respectively. The nominal thickness of the homogeneous wall was taken as 0.2 m. One dimensional diffusion equation was solved under periodic boundary conditions using matrix algebra. In the present study, the walls are considered as external walls, therefore external and internal surface resistances selected are $0.04 \text{ m}^2 \text{ K/W}$ and $0.13 \text{ m}^2 \text{ K/W}$, respectively. Among all the studied insulating materials, coconut pitch insulation (CPI) is found to be energy efficient from lowest decrement factor (0.22) and highest time lag (11.80 h) point of view. Hence this insulation is used to frame the composite walls with the most commonly used building materials in South India. Five composite walls are coded from C-A₁ to C-A₅.

Table 5.2.1 Thermo physical properties of building materials

Building material	Code	k [W/mK]	ρ [kg/m ³]	Cp [J/kgK]	$\alpha \times 10^{-7}$ [m ² /s]
Laterite Stone	LS	1.3698	1000	1926.1	7.11
Madras Black clay	MBC	0.735	1899	880	4.39
Indore Black clay	IBC	0.606	1683	880	4.09
Slate	SL	1.72	2750	840	7.44
Burnt brick	BB	0.811	1820	880	5.06
Mud brick	MB	0.75	1731	880	4.92
Reinforced brick	RB	1.10	1920	840	6.82
Brick tile	BT	0.798	1892	880	4.79
Mud phuska	MP	0.519	1622	880	3.63
Cinder concrete	CNC	0.686	1406	840	5.80
Plaster	P	0.57	1300	1000	4.38

Table 5.2.2 Thermo physical properties of insulating materials

Insulating material	Code	k [W/mK]	ρ [kg/m ³]	Cp [J/kgK]	$\alpha \times 10^{-7}$ [m ² /s]
Saw dust	SD	0.051	188	1000	2.71
Rice husk	RH	0.051	120	1000	4.25
Coir board	CB	0.038	97	1000	3.91
Jute felt	JF	0.042	291	880	1.64
Jute fiber	JFB	0.067	329	1090	1.86
Coconut pitch insulation	CPI	0.06	520	1090	1.05
Straw board	SB	0.057	310	1300	1.41
Asbestos fiber	AF	0.06	640	840	1.11
Wall board	WB	0.047	262	1260	1.42
Chip board	CHB	0.067	432	1260	1.23

Figure 5.2.1 shows the configuration of composite wall. Table 5.2.5 shows the configuration of composite walls with thicknesses of plaster, building materials and Insulation materials. Table 5.2.6 shows the unsteady state thermal characteristics of composite walls.

Table 5.2.3 Unsteady state thermal characteristics of building materials

Code	U [W/m ² K]	f	φ [h]	Y [W/m ² K]	ω [h]	F	Ψ [h]
LS	3.16	0.56	5.44	5.26	1.12	0.38	1.94
MBC	2.26	0.51	6.39	4.58	1.39	0.48	1.66
IBC	2.00	0.52	6.43	4.26	1.52	0.52	1.53
SL	3.49	0.52	5.63	5.63	0.97	0.33	2.09
BB	2.40	0.54	5.95	4.61	1.38	0.47	1.68
MB	2.29	0.55	5.95	4.48	1.43	0.49	1.63
RB	2.84	0.60	5.26	4.87	1.27	0.43	1.80
BT	2.37	0.52	6.15	4.65	1.37	0.47	1.69
MP	1.80	0.50	6.74	4.07	1.58	0.55	1.46
CNC	2.16	0.64	5.17	4.07	1.59	0.54	1.49

Table 5.2.4 Unsteady state thermal characteristics of insulating materials

Code	U [W/m ² K]	f	φ [h]	Y [W/m ² K]	ω [h]	F	Ψ [h]
SD	0.24	0.61	6.17	0.77	2.79	0.92	0.27
RH	0.24	0.77	4.30	0.60	2.88	0.94	0.22
CB	0.18	0.76	4.53	0.48	2.93	0.95	0.17
JF	0.20	0.40	8.75	0.81	2.71	0.92	0.28
JFB	0.31	0.43	8.20	1.17	2.59	0.88	0.41
CPI	0.28	0.22	11.80	1.36	2.51	0.86	0.47
SB	0.27	0.33	9.78	1.15	2.59	0.88	0.40
AF	0.28	0.24	11.41	1.33	2.52	0.87	0.46
WB	0.22	0.33	9.66	0.96	2.65	0.90	0.33
CHB	0.31	0.27	10.79	1.40	2.50	0.86	0.49

Table 5.2.5 Configuration of composite walls

Configuration	Thickness [m]
C-A ₁	0.015 P + 0.1 LS + 0.02 CPI + 0.1 LS + 0.015 P
C-A ₂	0.015 P + 0.1 BB + 0.02 CPI + 0.1 BB + 0.015 P
C-A ₃	0.015 P + 0.1 MB + 0.02 CPI + 0.1 MB + 0.015 P
C-A ₄	0.015 P + 0.1 RB + 0.02 CPI + 0.1 RB + 0.015 P
C-A ₅	0.015 P + 0.1 CNC + 0.02 CPI + 0.1 CNC + 0.015 P

Table 5.2.6 Unsteady state thermal characteristics of composite walls.

Code	U [W/m ² K]	f	ϕ [h]	Y [W/m ² K]	ω [h]	F	Ψ [h]
C-A ₁	1.42	0.30	8.87	5.11	1.36	0.44	2.10
C-A ₂	1.24	0.32	9.10	4.66	1.55	0.50	1.89
C-A ₃	1.21	0.33	9.05	4.57	1.60	0.51	1.86
C-A ₄	1.35	0.35	8.50	4.85	1.52	0.48	2.02
C-A ₅	1.18	0.42	8.09	4.30	1.83	0.56	1.81

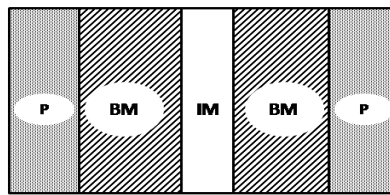


Figure 5.2.1 Configuration of composite wall. (BM: Building material, IM: Insulating material, P: Plaster)

5.2.2 Optimum fabric thickness of building and insulating materials

Wall thickness greater than optimum does not give any additional energy storage benefits rather it reduces energy storage. The physical explanation given is, that as heat stored in the fabric from previous days tries to escape, it meets with the current heat flow attempting to enter the fabric. Also, as d increases, after the peak Y value has been achieved, the thermal transmittance, U and volumetric heat capacity, continue to increase. Optimum wall thicknesses for building and insulating materials were calculated using Eq. (3.24). (Magyari et al. 1998).

Figure 5.2.2 (a) and Figure 5.2.2 (b) show the variation of admittance and transmittance of the building materials with thickness. From figures, it is observed that for thin cross section fabrics admittance is equal to the transmittance. The values of $a_1, b_1, c_1, d_1, e_1, f_1, g_1, h_1, i_1$ and j_1 represent the optimum fabric thicknesses of ten building materials.

Figure 5.2.3 (a) and Figure 5.2.3 (b) show the variation of admittance and transmittance of the insulating materials with thickness. The values of $a_2, b_2, c_2, d_2, e_2, f_2, g_2, h_2, i_2$ and j_2 represent the optimum fabric thickness of ten insulating materials. The results show that among all the ten building materials studied, Mud phuska (MP) has least optimum fabric thickness value i_1 (0.118 m) and slate (SL) has higher

optimum fabric thickness value d_1 (0.169 m). It can also be observed that among all the ten insulating materials studied, Coconut pitch insulation (CPI) material has least optimum fabric thickness value f_1 (0.064 m) and rice husk (RH) has higher optimum fabric thickness value b_2 (0.127m). At an optimum fabric thickness all the building and insulating materials have the maximum thermal heat capacity.

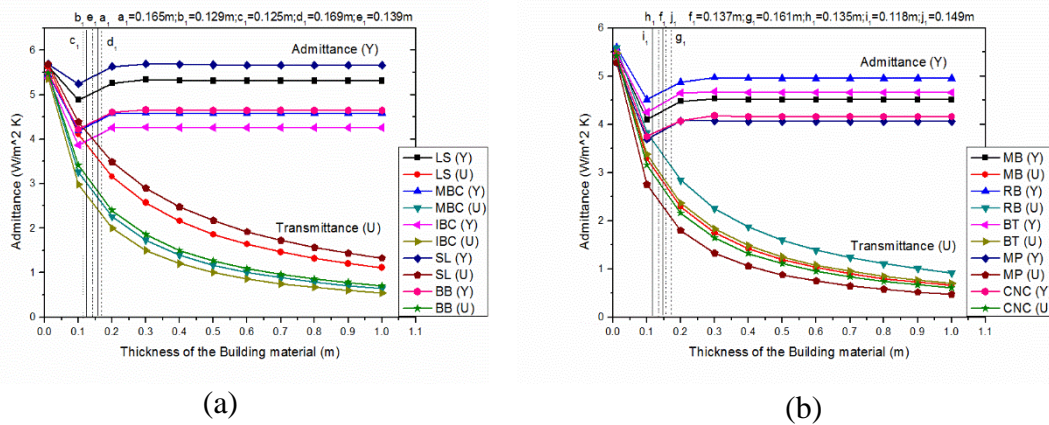


Figure 5.2.2 (a) Optimum wall thickness of Building materials, (LS, MBC, IBC, SL and BB) (b) Optimum wall thickness of Building materials (MB, RB, BT, MP and CNC)

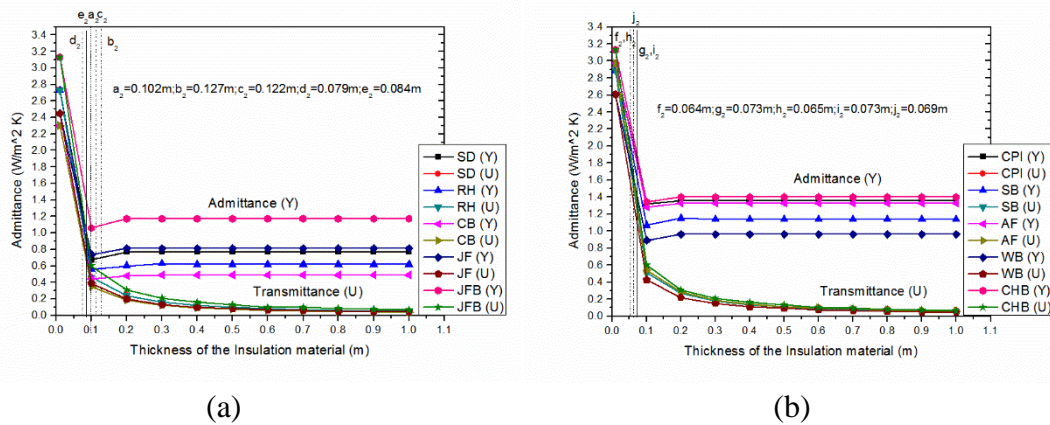


Figure 5.2.3 (a) Optimum wall thickness of Insulation materials, (SD, RH, CRB, JF and JFB) (b) Optimum wall thickness of Insulation materials (CPI, SB, AF, WB and CHB)

5.2.3. Decrement factor and it's time lag of building and insulating materials

Figure 5.2.4 (a) and Figure 5.2.4 (b) show the effects of wall thickness of the homogeneous building materials on the decrement factor and it's time lag. Figure 5.2.5 (a) and Figure 5.2.5 (b) show the effects of wall thickness of the homogeneous insulating materials on the decrement factor and it's time lag. The decrement factor of the building material decreases with an increase in the wall thickness. The smaller the decrement factor the more effective the wall at suppressing temperature swings. The time lag of building materials increases with an increase in the wall thickness. The larger the time lags, the more effective the wall at suppressing temperature swings.

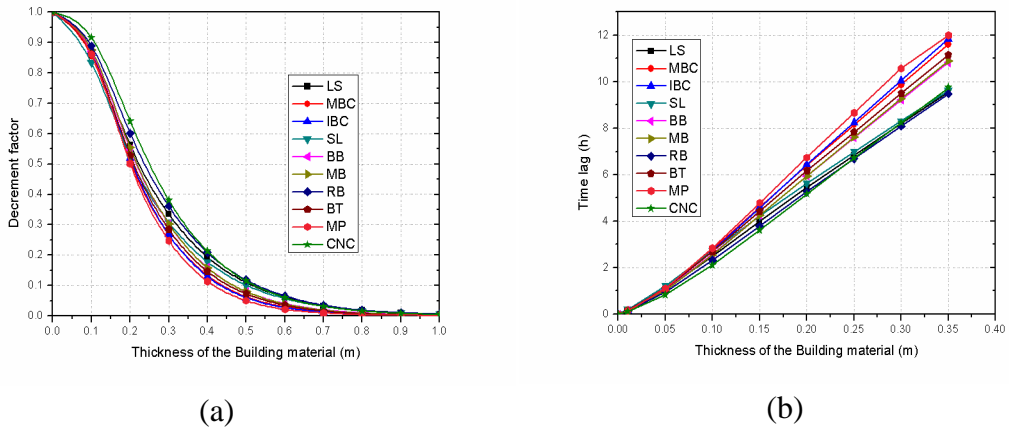


Figure 5.2.4 (a) Decrement factor of Building materials, (b) Time lag of Building materials

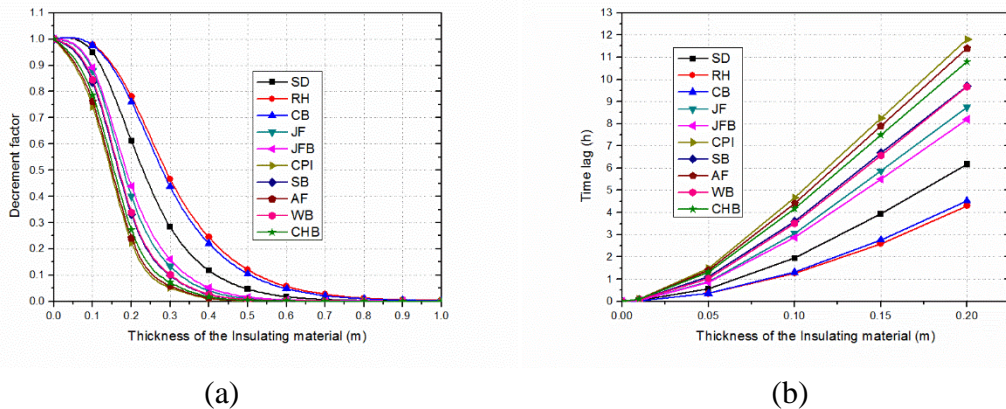


Figure 5.2.5 (a) Decrement factor of Insulation materials, (b) Time lag of Insulation materials

From Figure 5.2.4, it is observed that mud phuska (MP) has least decrement factor and higher decrement time lags whereas cinder concrete (CNC) has higher decrement factors and lower time lags among ten building materials studied. From Figure 5.2.5, it was observed that coconut pitch insulation (CPI) has least decrement factor and higher decrement time lags whereas rice husk insulation (RH) has higher decrement factors and lower time lags among ten insulating materials studied.

5.2.4 Surface factor and it's time lag of building and insulating materials

Buildings with surface factor 0.8 with time delay of one hour are fast responsive to short wave radiation, whereas buildings with surface factor 0.5 with time delay of two hours are slow responsive to short wave radiation. From Figure 5.2.6, it can be observed that among ten studied building materials, slate (SL) is slow responsive to short wave radiation due to its lowest surface factor (0.33) and highest surface factor time lags (2.09 h) whereas mud phuska (MP) is fast responsive to short wave radiation due to its higher surface factor (0.55) and lower surface factor time lags (1.46).

From Figure 5.2.7, it is observed that among ten insulating materials studied, chip board insulation (CHB) is slow responsive to short wave radiation due to its low surface factor (0.86) and high surface factor time lags (0.49 h) whereas coir board (CB) is fast responsive to short wave radiation due to its higher surface factor (0.95) and lower surface factor time lags (0.17 h). From Figure 5.2.6 and Figure 5.2.7, it was observed that surface factor and it's time lag do not depend on the thickness of the wall, but they depend only on thermal conductivity of the building or insulating material. It is clear from the Figures 5.2.6 and 5.2.7 that the insulating materials are fast responsive to short wave radiation than the building materials due to their higher surface factors and lower surface factor time lags.

5.2.5 Decrement factor and it's time lag of composite walls

In practice, building walls are composite, i.e., they are constructed with the combination of two or more homogeneous materials. Hence the best insulation material (coconut pitch (CPI)) among ten studied insulating materials was used as insulation material to frame composite walls with the most commonly used building materials (among ten building materials), Laterite stone (LS), burnt bricks (BB), mud bricks (MB), reinforced brick (RB) cinder concrete (CNC) and plaster (P). The

insulation material was placed at the center of the composite wall as shown in Figure 5.2.1. From Table 5.2.6, it is observed that burnt brick composite walls (C-A₂) with Coconut pitch insulation (CPI) give lowest decrement factor values (0.32) and highest decrement time lags (9.1 h) whereas cinder concrete composite walls (C-A₅) with coconut pitch insulation give highest decrement factor (0.42) and lowest decrement time lags (8.09 h). Figure 5.2.8 shows the decrement factor and its time lag of composite walls.

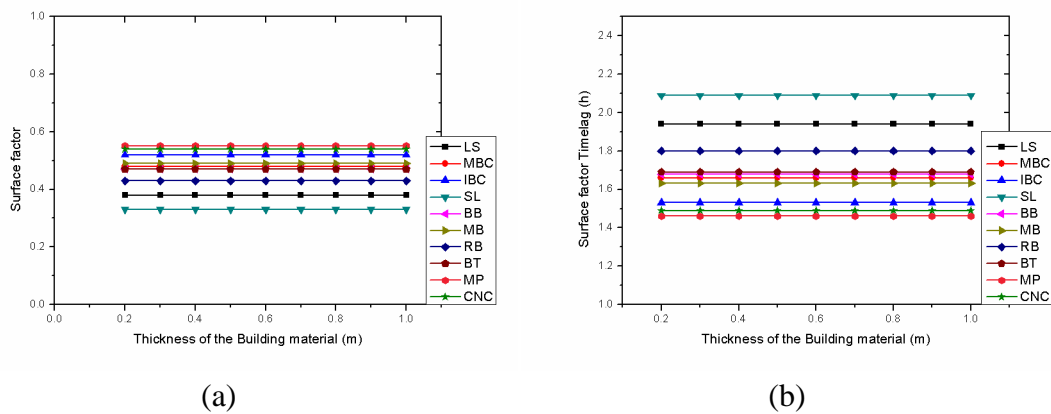


Figure 5.2.6 (a) Surface factor of Building materials, (b) Surface factor Time lag of Building materials

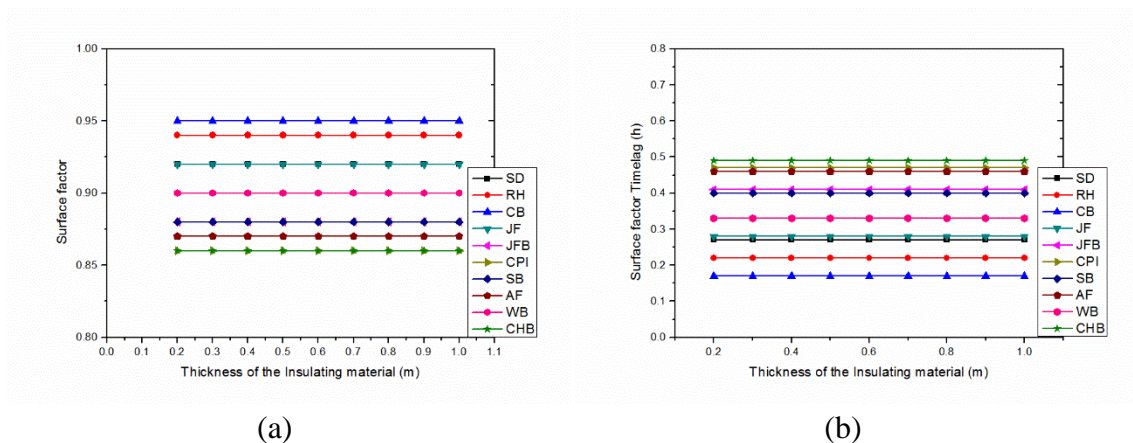


Figure 5.2.7 (a) Surface factor of Insulation materials, (b) Surface factor Time lag of Insulation materials

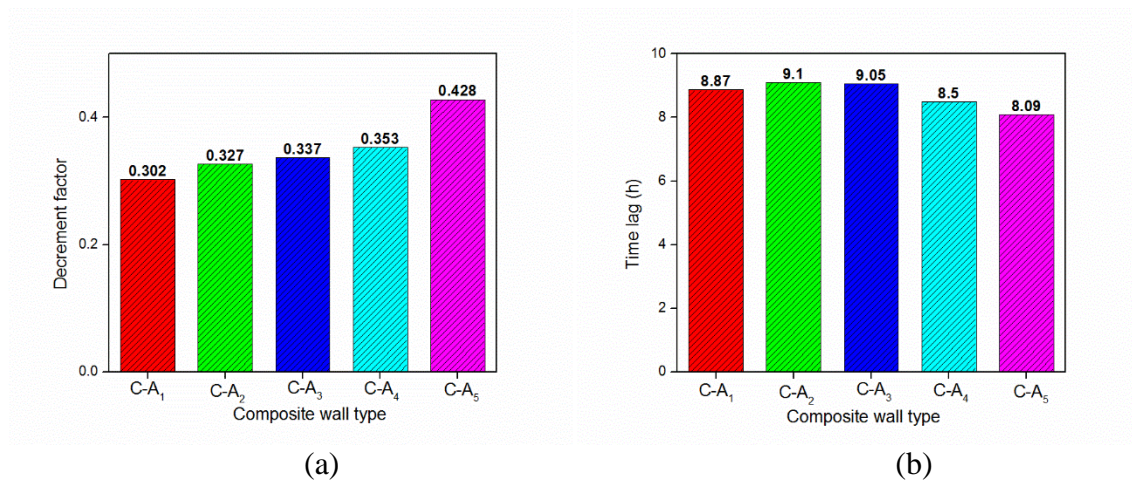


Figure 5.2.8 (a) Decrement factor of composite walls, (b) Time lag of composite walls

5.3 EFFECT OF INSULATION LOCATION WITHIN WALL ON DYNAMIC THERMAL PROPERTIES OF WALLS

5.3.1 Unsteady state thermal characteristics of building and insulating materials

Table 5.3.1 shows the thermal properties, penetration length, phase velocity and optimum fabric thickness of the Indian Building and Insulating materials considered for the study (SP: 41 1987). Five building and five insulation materials were selected for the study. The computer program was used to calculate the unsteady state thermal characteristics of homogeneous and composite wall materials. The building and insulating materials are coded as shown in Table 5.3.1. Plaster was represented by code P. The unsteady state thermal characteristics for all building and insulating materials were calculated and shown in Table 5.3.3. In this study, nominal thickness of the homogeneous wall was taken as 0.2m. In the present study, external and internal surface resistances selected are $0.04 \text{ m}^2 \text{ K/W}$ and $0.13 \text{ m}^2 \text{ K/W}$ respectively. Transient plane source technique (Gustafsson, 1991) was employed to calculate thermal properties of laterite stone and fly ash bricks.

Table 5.3.1 Thermal properties and Optimum thickness values of Building and Insulating materials

S.No.	Building material	Code	k [W/mK]	ρ [kg/m ³]	Cp [J/kgK]	$\alpha \times 10^{-7}$ [m ² /s]	$V \times 10^{-6}$ [m/s]	d [m]
1.	Laterite Stone	LS	1.369	1000	1926.1	7.11	0.1016	0.165
2.	Burnt brick	BB	0.811	1820	880	5.06	8.578	0.139
3.	Mud brick	MB	0.75	1731	880	4.92	8.459	0.137
4.	Reinforced brick	RB	1.10	1920	840	6.82	9.959	0.161
5.	Fly ash brick	FAB	0.360	1700	857	2.47	5.993	0.097
6.	Saw dust	SD	0.051	188	1000	2.71	6.278	0.102
7.	Rice husk	RH	0.051	120	1000	4.25	7.862	0.127
8.	Coir board	CB	0.038	97	1000	3.91	7.541	0.122
9.	Jute felt	JF	0.042	291	880	1.64	4.883	0.079
10.	Jute fibre	JFB	0.067	329	1090	1.86	5.201	0.084
11.	Cement plaster	P	0.721	1762	840	4.87	-	-

The penetration length is the minimum thickness of the wall to be maintained for heat storage. The phase velocity is the velocity of the heat wave passing through the wall. The optimum fabric thickness is the thickness at which maximum heat storage occurs. Wall thickness greater than optimum gives no additional energy storage benefit and can actually reduce energy storage. The physical explanation given is that as heat stored in the fabric from previous days tries to escape, it meets with the current heat flow attempting to enter the fabric.

Table 5.3.2 Composite wall configuration and Thickness

S.No.	Configuration	Thickness of the wall from outside to inside [m]
1.	C-B ₁	0.015P+0.2BM+0.015P
2.	C-B ₂	0.015P+0.02IM+0.2BM+0.015P
3.	C-B ₃	0.015P+0.1BM+0.02IM+0.1BM+0.015P
4.	C-B ₄	0.015P+0.2BM+0.02IM+0.015P

Figure 5.3.1 shows the configurations of the composite walls selected for this analysis. Four configurations were selected to study the effect of the insulation location on time lag and the decrement factor of the composite walls. Table 5.3.2 shows the configuration and thickness of the composite walls used for the study.

Table 5.3.3 Unsteady state thermal characteristics of Building and Insulating materials

CODE	U [W/m ² K]	f	φ [h]	Y [W/m ² K]	ω [h]	F	Ψ [h]	χ [J/m ² K]
LS	3.165	0.563	5.44	5.26	1.12	0.398	1.99	79818
BB	2.401	0.549	5.95	4.61	1.38	0.488	1.72	71789
MB	2.29	0.554	5.95	4.48	1.43	0.505	1.67	69884
RB	2.84	0.601	5.26	4.87	1.27	0.452	1.82	74096
FAB	1.37	0.401	8.15	3.72	1.69	0.599	1.34	57782
SD	0.244	0.610	6.17	0.774	2.79	0.927	0.276	12172
RH	0.244	0.779	4.30	0.605	2.88	0.944	0.218	9465
CB	0.184	0.760	4.53	0.48	2.93	0.956	0.173	7539
JF	0.202	0.400	8.75	0.819	2.71	0.922	0.288	12372
JFB	0.316	0.438	8.20	1.178	2.59	0.886	0.415	18030

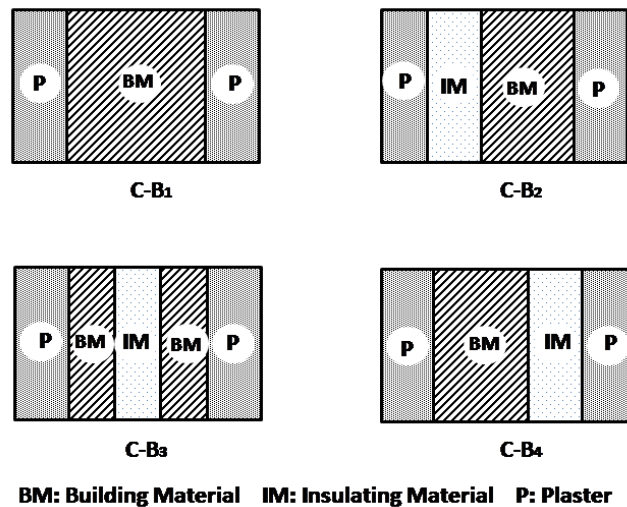


Figure 5.3.1 Configurations of Composite walls

5.3.2 Optimum fabric energy storage of building and insulating materials

The fluctuating component of the conduction through the building fabric, caused by cyclic variation in the sol–air temperature, is treated by using a modified heat flow for all external surfaces which is effectively the thermal transmittance (U) multiplied by the decrement factor, (f). The second and most important point to consider is the rate of transfer of heat energy between the internal surface of the fabric and the environmental node. The rate of flow of this heat energy, for each degree of deviation about the mean environmental temperature value, is known as the thermal admittance. It is this unsteady state parameter that positively indicates the ability of the fabric to absorb (and store) heat energy from the environmental node, i.e. fabric energy storage or ‘thermal mass’. The associated time dependency of this heat transfer is referred to as the lead time. Figure 5.3.2 shows the variation of admittance and transmittance of the building and insulating materials with thickness. From figures it can be observed that for thin cross section fabrics admittance is equal to the transmittance. The values of a_3 , b_3 , c_3 , d_3 and e_3 represent the optimum fabric thicknesses of the five building materials as shown in Figure 5.3.2 (a) and the values of a_4 , b_4 , c_4 , d_4 and e_4 represent the optimum fabric thickness of the five insulating materials as shown in Figure 5.3.2 (b). From the results, It was observed that among all the five building materials studied, fly ash bricks have least optimum fabric thickness value e_3 (0.097 m) and laterite stones from the south west coast of India have higher optimum fabric thickness value a_3 (0.165 m). It can also be observed that among all the five insulating

materials studied, jute felt insulation material has least optimum fabric thickness value d_4 (0.079m) and rice husk has higher optimum fabric thickness value b_4 (0.127m). At an optimum fabric thickness all the building and insulating materials have maximum thermal heat capacity values. Penetration length, phase velocity and optimum fabric thickness values of all the building and insulating materials were shown in the Table 5.3.1.

5.3.3 Effect of thickness on time lag and decrement factor of building and insulating materials

The effect of wall thickness of the building materials on the decrement factor and time lag was shown in Figure 5.3.3. The thickness of the homogeneous walls considered for the study is 0 to 1m. The decrement factor of the building material decreases and its time lag increases with an increase in the wall thickness. The smaller the decrement factor the more effective the wall at suppressing temperature swings. Figure 5.3.3 (a) and Figure 5.3.3 (b) show the decrement factor and its time lag of the building materials used in the study. From these figures, it was observed that the fly ash bricks have lower decrement factor values (0.401) and higher time lags (8.15h) whereas reinforced bricks have higher decrement factor values (0.601) and lower time lags (5.26 h). Figure 5.3.4 (a) and Figure 5.3.4 (b) show the decrement factor and its time lag of the insulating materials used. From the figures, it was observed that among all the studied insulating materials, jute felt has lower decrement factor values (0.4) and higher time lags (8.75 h) whereas rice husk has higher decrement factor values (0.77) and lower time lags (4.3 h).

5.3.4 Effect of thickness on surface factor and its time lag of building and insulating materials

Figure 5.3.5 (a) and 5.3.5 (b) show the surface factor and its time lag of building and insulating materials. Surface factor and its time lag of the homogeneous walls is independent of the wall thickness. The surface factor and its time lag value increases with increasing thermal conductivity and remain virtually independent of the material thickness. From the results, it was observed that among all the building materials studied, fly ash bricks have higher surface factors (0.599) and lower surface factor

time lags (1.34 h), whereas laterite stones have lower surface factors (0.398) and higher surface factor time lags (1.99 h). Among insulating materials studied, it was observed that the coir board has higher surface factors (0.956) and lower surface factor time lags (0.173 h) whereas jute fiber has lower surface factors (0.886) and higher surface factor time lags (0.415 h).

5.3.5 Effect of insulation location on decrement factor and it's time lag of composite walls

Figure 5.3.6 (a) and 5.3.6 (b) show the effect of the insulation location on decrement factor and it's time lags of laterite stone (LS). Laterite stone with Configuration B₁ without insulation gives the higher decrement factor (0.461) and lower time lags (6.37h). Laterite stone with five insulation materials placed in three different configurations was studied. From the results, it was observed that the laterite stone (LS) with the coir board insulation (CB) located at the outer surface (Configuration B₂) gives the least decrement factor (0.21) and laterite stone with the saw dust insulation (SD) located at the inner surface (Configuration B₄) gives the highest decrement factor (0.3438). Laterite stone with the jute felt insulation (JF) located at the mid plane of the wall (Configuration B₃) gives the highest time lag (8.9h) and laterite stone with the jute fiber insulation (JFB) located at the inner surface gives the least time lag (7.4h).

Figure 5.3.7 (a) and 5.3.7 (b) show the effect of the insulation location on decrement factor and it's time lags of Burnt brick (BB). Burnt brick with Configuration B₁ without insulation gives the higher decrement factor (0.459) and lower time lags (6.93h). From the results, it was observed that the burnt brick (BB) with the coir board insulation (CB) located at the outer surface (Configuration B₂) gives the least decrement factor (0.22) and burnt brick with the jute fiber (JFB) located at the inner and at the mid plane (Configuration B₃& B₄) gives the highest decrement factor (0.34). Burnt brick with the jute felt insulation (JF) located at the center of the wall (Configuration B₃) gives the highest time lag (9.15h) and burnt brick with the jute fiber insulation (JFB) located at the inner surface gives the least time lag (8.13h).

Figure 5.3.7 (c) and 5.3.7 (d) show the effect of the insulation location on decrement factor and it's time lags of mud brick (MB). Mud brick with Configuration B₁ without

insulation gives the higher decrement factor (0.466) and lower time lags (6.95h). From the results, it was observed that the mud brick (MB) with the coir board insulation (CB) located at the outer surface (Configuration B₂) gives the least decrement factor (0.23) and mud brick with the jute fiber insulation (JFB) located at the center and at the inner surface (Configuration B₃&B₄) gives the highest decrement factor (0.359 & 0.345). Mud brick with the jute felt insulation (JF) located at the center of the wall (Configuration B₃) gives the highest time lag (9.1h) and mud brick with the jute fiber insulation (JFB) located at the inner surface gives the least time lag (8.1h).

Figure 5.3.7 (e) and 5.3.7 (f) show the effect of the insulation location on decrement factor and it's time lags of reinforced brick (RB). Reinforced brick with Configuration B₁ without insulation gives the higher decrement factor (0.501) and lower time lags (6.23h). From the results, it was observed that the reinforced brick (RB) with the coir board insulation (CB) located at the outer surface (Configuration B₂) gives the least decrement factor (0.24) and reinforced brick with the jute fiber insulation (JFB) located at the inner surface (Configuration B₄) gives the highest decrement factor (0.384). Reinforced brick with the jute felt insulation (JF) located at the mid plane of the wall (Configuration B₃) gives the highest time lag (8.6h) and reinforced brick with the jute fiber insulation (JFB) and rice husk (RH) located at the inner surface gives the least time lag (7.4h & 7.37h).

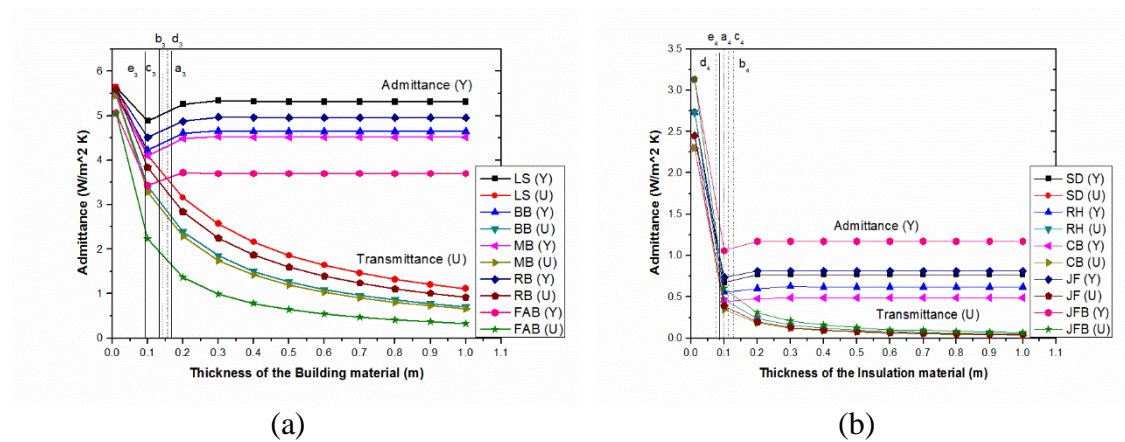
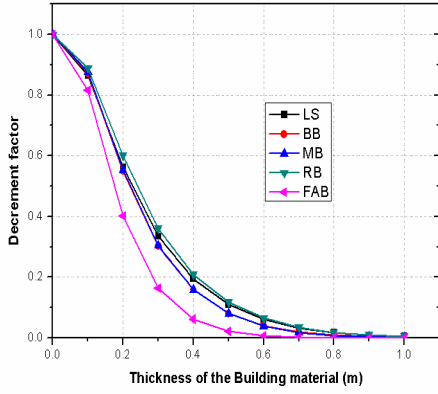
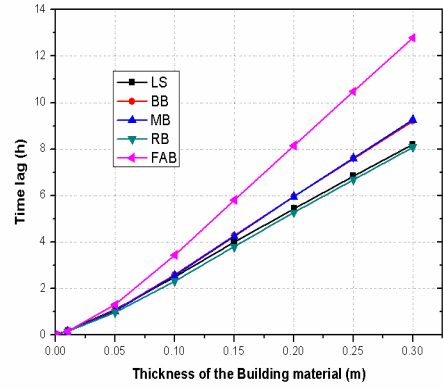


Figure 5.3.2 (a) Optimum fabric energy storage thickness of Building materials, (b) Optimum fabric energy storage thickness of insulating materials

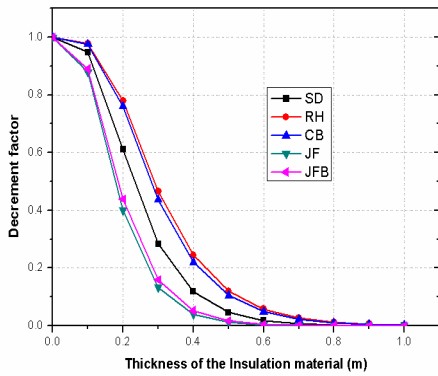


(a)

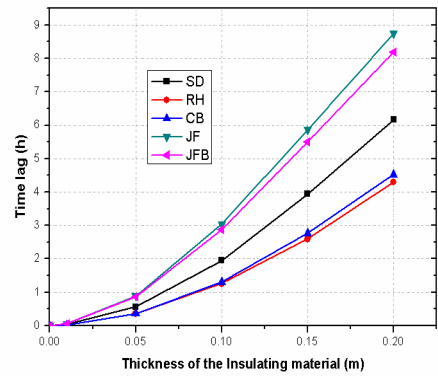


(b)

Figure 5.3.3 (a) Decrement factor of Building materials, (b) Time lag of Building materials

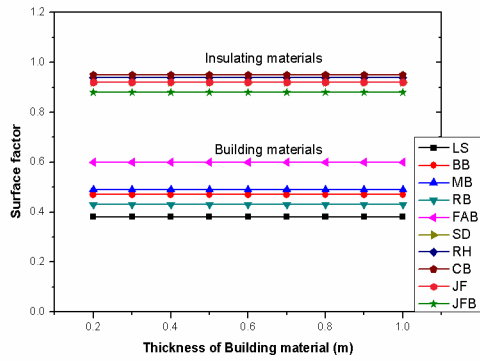


(a)

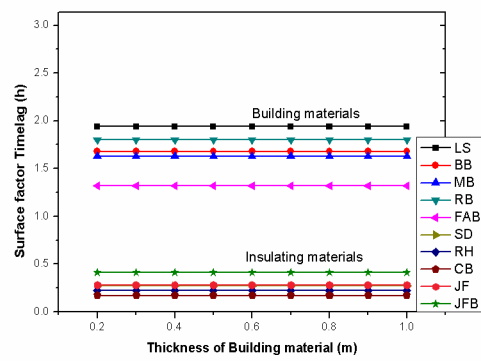


(b)

Figure 5.3.4 (a) Decrement factor of Insulating materials, (b) Time lag of Insulating materials

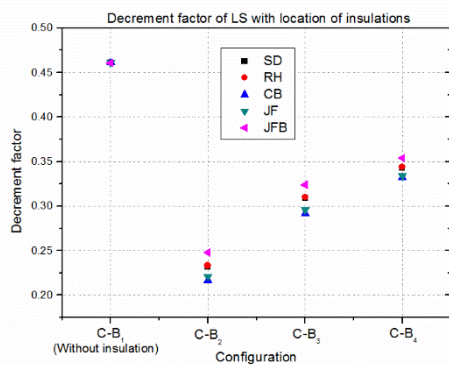


(a)

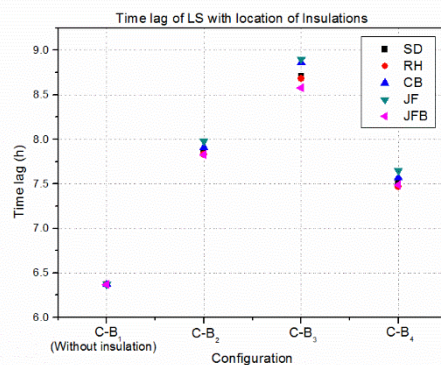


(b)

Figure 5.3.5 (a) Surface factor of Building and insulating materials, (b) Surface factor time lag of Building and insulating materials



(a)

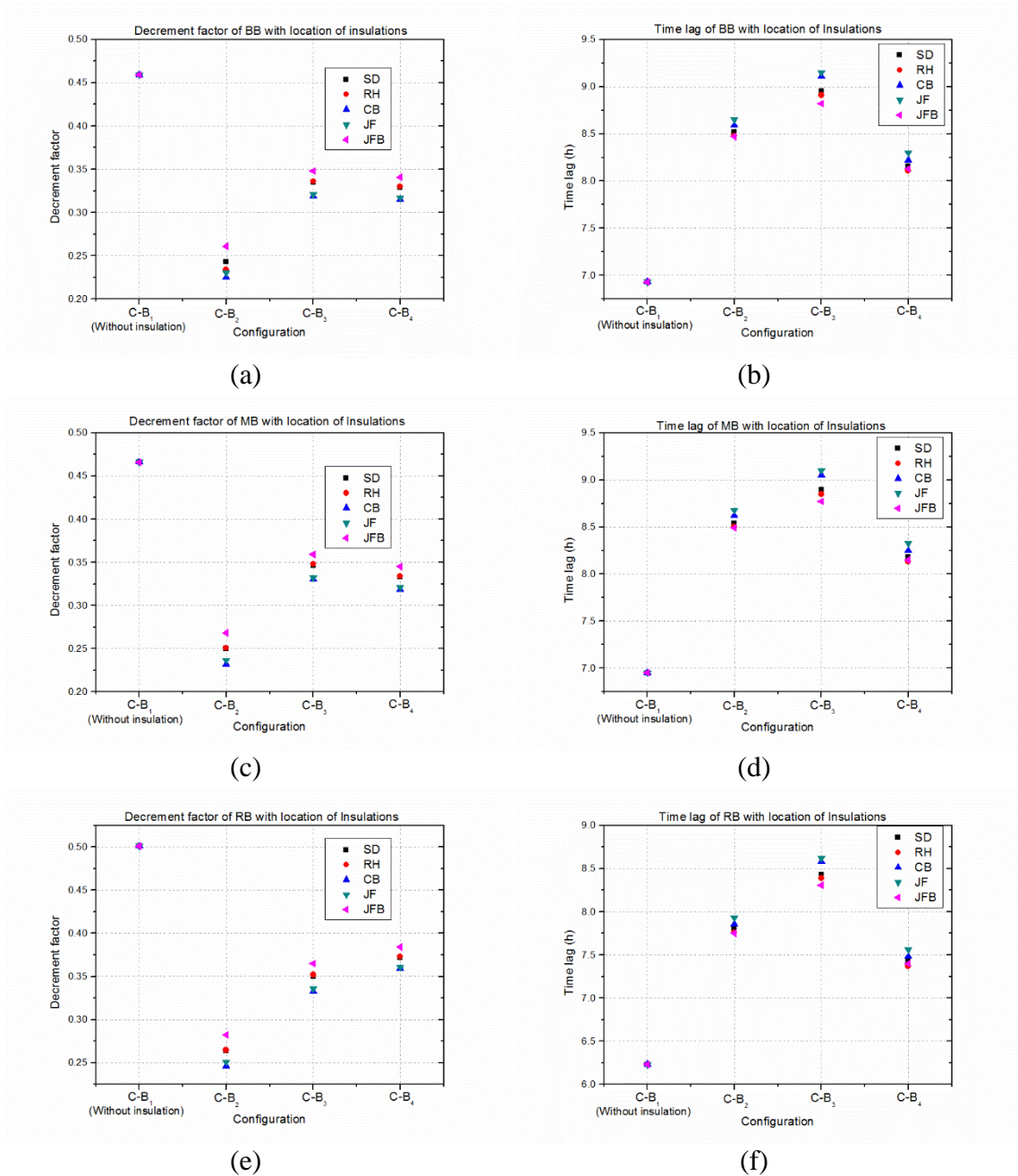


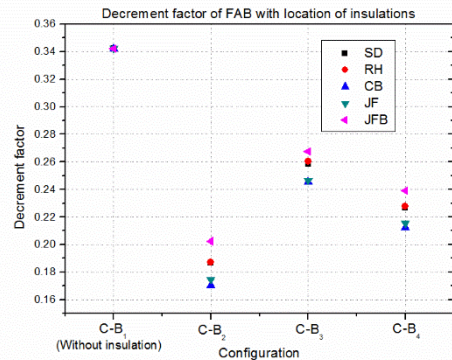
(b)

Figure 5.3.6 (a) Effect of insulation location on decrement factor of LS, (b) Effect of insulation location on time lag of LS

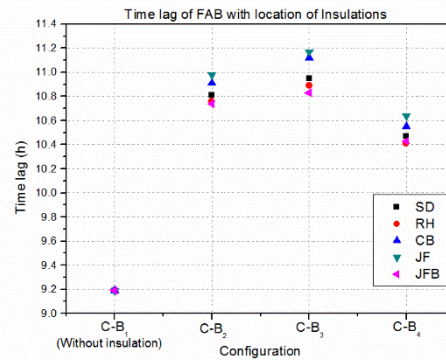
Figure 5.3.7 (g) and 5.3.7 (h) show the effect of the insulation location on decrement factor and its time lags of fly ash brick (FAB). Reinforced brick with Configuration B₁ without insulation gives the higher decrement factor (0.342) and lower time lags (9.19h). Fly ash brick with five insulation materials placed in three different configurations was studied. From the results, it was observed that the fly ash brick (FAB) with the coir board insulation (CB) located at the outer surface (Configuration B₂) gives the least decrement factor (0.17) and fly ash brick with the jute fiber insulation (JFB) located at the mid plane of the wall (Configuration B₃) gives the

highest decrement factor (0.26). Fly ash brick with the jute felt insulation (JF) located at the mid center plane of the wall (Configuration B₃) gives the highest time lag (11.17h) and fly ash brick with the jute fiber insulation (JFB) and rice husk (RH) located at the inner surface gives the least time lag (10.43h & 10.41h).





(g)



(h)

Figure 5.3.7 Effect of Insulation location on Decrement factor and its time lag for different configurations

5.4 EFFECT OF AIR SPACE THICKNESS WITHIN WALL ON DYNAMIC THERMAL PROPERTIES OF WALLS

5.4.1 Building material thermal properties and their unsteady thermal response characteristics

Table 5.4.1 shows the thermal properties of the building materials at 50°C considered for the study. The thermal properties of building materials such as, Mud brick, Cellular concrete, Dense concrete, Cinder concrete and Cement plaster were taken from the Indian standard guide for heat insulation of non-industrial buildings as per IS code 3792-1978. In this code guarded hot plate method and ASTM heat flow methods are used to calculate thermal properties of building materials (IS: 3792 1978). Thermal properties of laterite stone were measured using the transient plane source method experimentally at K- Analys, Sweden. Five building materials were selected for the study. The computer simulation program has been developed to calculate the unsteady state thermal characteristics of homogeneous and composite wall materials. The five building materials are coded from LS to CNC. The cement plaster was represented by code P. In this study walls are considered as external walls and external and internal surface resistances considered are 0.04 m² K/W and 0.13 m² K/W, respectively for external walls as per CIBSE standards. Table 5.4.2 shows the six composite wall configurations with different airspace thicknesses.

Figure 5.4.1 shows the configurations of six composite walls without and with different divide air space thicknesses.

Table 5.4.1 Thermo physical properties of building materials

S.No.	Wall material	Code	k [W/mK]	ρ [kg/m ³]	Cp [J/kgK]	α [m ² /s] X 10 ⁻⁷
1.	Laterite stone*	LS	1.369	1000	1926	7.112
2.	Mud brick	MB	0.75	1731	880	4.92
3.	Cellular concrete	CLC	0.188	704	1050	2.543
4.	Dense concrete	DC	1.74	2410	880	8.204
5.	Cinder concrete	CNC	0.686	1406	840	5.808
6.	Cement plaster	P	0.721	1762	840	4.871

*Experimentally measured thermal property values.

Table 5.4.2 Composite wall configuration with different air space thicknesses

S.No.	Configuration	Thickness of the wall from outside to inside [m]
1.	C-C ₁	0.015 P + 0.2 BM + 0.015 P
2.	C-C ₂	0.015 P + 0.1 BM + 0.005 A + 0.1 BM + 0.015 P
3.	C-C ₃	0.015 P + 0.1 BM + 0.01 A + 0.1 BM + 0.015 P
4.	C-C ₄	0.015 P + 0.1 BM + 0.015 A + 0.1 BM + 0.015 P
5.	C-C ₅	0.015 P + 0.1 BM + 0.02 A + 0.1 BM + 0.015 P
6.	C-C ₆	0.015 P + 0.1 BM + 0.025 A + 0.1 BM + 0.015 P

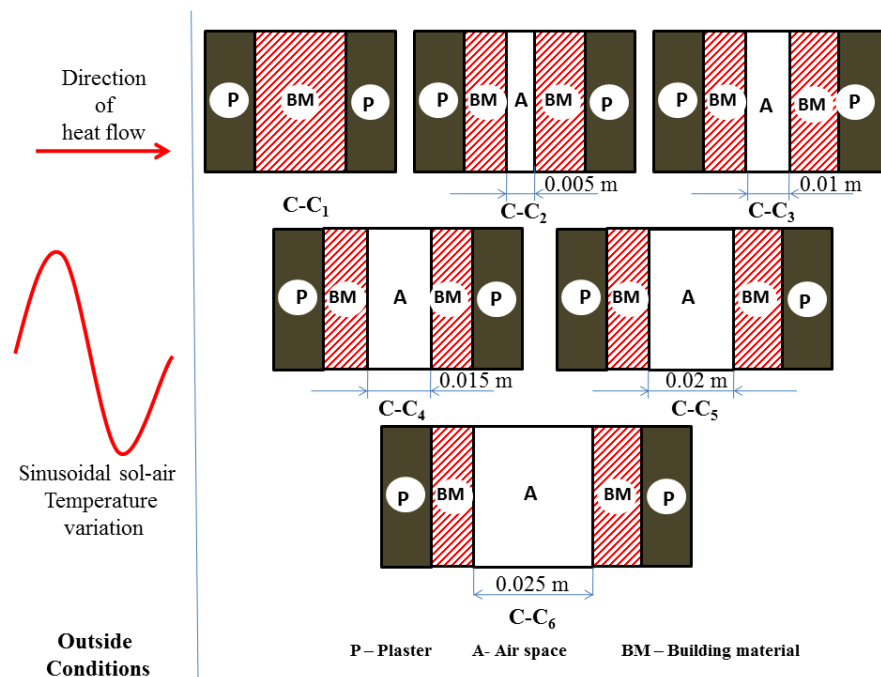


Figure 5.4.1 Configuration of composite walls with different air spaces

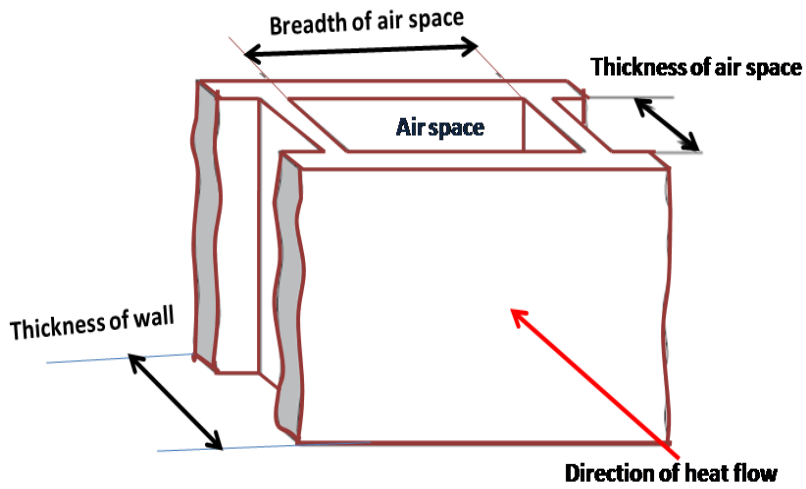


Figure 5.4.2 Wall structure with divided air space.

Table 5.4.3 Divided airspace resistances for horizontal heat flow (CIBSE 2006)

S.No.	Air space thickness t_a [m]	Air space breadth b_a [m]	Air space resistance R_a [$m^2 K/W$]
1.	0.005	≥ 0.2	0.11
2.	0.01	≥ 0.2	0.15
3.	0.015	≥ 0.2	0.17
4.	0.02	≥ 0.2	0.18
5.	0.025	≥ 0.2	0.18

Table 5.4.4 Effect of air space thickness on unsteady thermal characteristics of Laterite walls

Laterite stone (LS)					
S.No.	Configuration	U [W/m^2K]	Y [W/m^2K]	f	ϕ [h]
1.	C-C ₁	2.790	5.030	0.461	6.372
2.	C-C ₂	2.138	5.103	0.397	7.601
3.	C-C ₃	1.970	5.144	0.378	7.855
4.	C-C ₄	1.895	5.163	0.370	7.960
5.	C-C ₅	1.860	5.171	0.366	8.008
6.	C-C ₆	1.860	5.171	0.366	8.008

Table 5.4.5 Effect of air space thickness on unsteady thermal characteristics of Mud brick walls

Mud brick (MB)					
S.No.	Configuration	U [W/m ² K]	Y [W/m ² K]	f	φ [h]
1.	C-C ₁	2.090	4.500	0.466	6.950
2.	C-C ₂	1.700	4.582	0.422	7.836
3.	C-C ₃	1.592	4.614	0.408	8.049
4.	C-C ₄	1.542	4.630	0.401	8.141
5.	C-C ₅	1.519	4.637	0.398	8.183
6.	C-C ₆	1.519	4.637	0.398	8.183

The walls are exposed to periodic cyclic variations in temperatures and the heat flow through the wall is in the horizontal direction. The air spaces considered in the present study are divided air spaces as shown in Figure 5.4.2. Table 5.4.3 shows the divided air space resistances of different air space thicknesses in horizontal direction as per CIBSE standards.

Table 5.4.6 Effect of air space thickness on unsteady thermal characteristics of Cellular concrete walls

Cellular concrete (CLC)					
S.No.	Configuration	U [W/m ² K]	Y [W/m ² K]	f	φ [h]
1.	C-C ₁	0.780	3.105	0.447	8.397
2.	C-C ₂	0.721	3.135	0.430	8.762
3.	C-C ₃	0.701	3.145	0.425	8.876
4.	C-C ₄	0.691	3.150	0.423	8.929
5.	C-C ₅	0.687	3.152	0.421	8.955
6.	C-C ₆	0.687	3.152	0.421	8.955

Table 5.4.7 Effect of air space thickness on unsteady thermal characteristics of Dense concrete walls

Dense concrete (DC)					
S.No.	Configuration	U [W/m ² K]	Y [W/m ² K]	f	φ [h]
1.	C-C ₁	3.060	5.228	0.452	6.207
2.	C-C ₂	2.291	5.289	0.378	7.602
3.	C-C ₃	2.099	5.332	0.358	7.872
4.	C-C ₄	2.014	5.351	0.349	7.981
5.	C-C ₅	1.947	5.361	0.345	8.030
6.	C-C ₆	1.947	5.361	0.345	8.030

Table 5.4.4, Table 5.4.5, Table 5.4.6, Table 5.4.7 and Table 5.4.8 show the effect of divided air space thickness within the wall on unsteady state thermal characteristics of laterite stone, mud brick, cellular concrete, dense concrete and cinder concrete, respectively.

Table 5.4.8 Effect of air space thickness on unsteady thermal characteristics of Cinder concrete walls

Cinder concrete (CNC)					
S.No.	Configuration	U [W/m ² K]	Y [W/m ² K]	f	ϕ [h]
1.	C-C ₁	1.988	4.242	0.549	6.209
2.	C-C ₂	1.631	4.303	0.513	6.931
3.	C-C ₃	1.531	4.331	0.501	7.114
4.	C-C ₄	1.485	4.345	0.495	7.195
5.	C-C ₅	1.464	4.352	0.492	7.232
6.	C-C ₆	1.464	4.352	0.492	7.232

5.4.2 Thermal transmittance and admittance of homogeneous building materials

Thermal transmittance is a measure of thermal insulation of the wall. It gives the heat loss through a given thickness of the wall. Thermal transmittance consists of conduction, convection and radiation elements. The lower thermal transmittance value signifies the better thermal performance. Thermal admittance is a measure of the thermal mass of the wall. Thermal mass slows down the heat transfer processes from outside of the wall to the inside of the wall by storing excess heat within the material for several hours. The higher thermal admittance signifies the better thermal mass. From Figure 5.4.3, it is observed that cellular concrete (CLC) is the best from the lowest thermal transmittance perspective and dense concrete (DC) is the best from the highest thermal admittance perspective for all thicknesses of the walls among five building materials studied. At smaller thicknesses of the walls transmittance is equal to the admittance values. The optimum fabric thickness signifies the optimum thickness of the wall where the maximum amount of heat is stored within the material. Figure 5.4.3 shows the optimum fabric thickness values 0.139 m (a₅), 0.137 m (b₅), 0.083 m (c₅), 0.106 m (d₅) and 0.126 m (e₅) for the building materials, laterite stone, mud brick, cellular concrete, dense concrete and cinder concrete, respectively. From the results, it is observed that cellular concrete has the least optimum fabric

thickness (0.083 m) and the laterite stone has the highest fabric thickness (0.139 m) among five studied building materials.

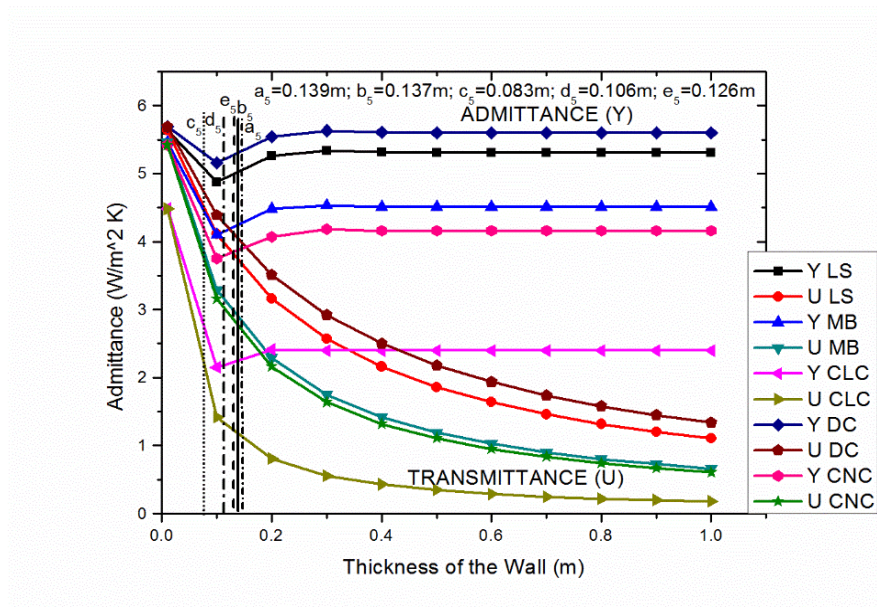


Figure 5.4.3 Thermal transmittance and admittance of building materials as a function of thickness

5.4.3 Decrement factor and time lag of building materials

The thermal heat capacity of the wall slows down the heat transfer from outside to inside of the wall. The thermal heat storage capacity of the building material can be determined by the decrement factor and its time lag. The attenuation of inside wall surface cyclic temperature compared to the outside wall surface cyclic temperature is called as decrement factor. The delay in propagation of heat wave from outside of the wall to the inside wall due to thermal heat capacity or thermal storage capacity of the wall is called as time lag. Figure 5.4.4 (a) shows the decrement factor of homogeneous building materials and Figure 5.4.4 (b) shows the time lag of homogeneous building materials studied. From the results it is observed that at 0.2 m wall thickness building materials, laterite stone (LS), Mud brick (MB), Cellular concrete (CLC), Dense concrete (DC) and Cinder concrete (CNC) have decrement factors, 0.563, 0.554, 0.497, 0.559 and 0.641, respectively. Time lags are 5.44 h, 5.95 h, 7.28 h, 5.31 h and 5.17 h, respectively, for LS, MB, CLC, DC and CNC. Among five building materials studied, cellular homogeneous building materials (CLC) are the best materials from lowest decrement factor (0.497 at 0.2 m) and highest time lag

(5.31 h at 0.2m) perspective. CLC is the best from lower decrement factor and higher time lag perspective for all wall thicknesses.

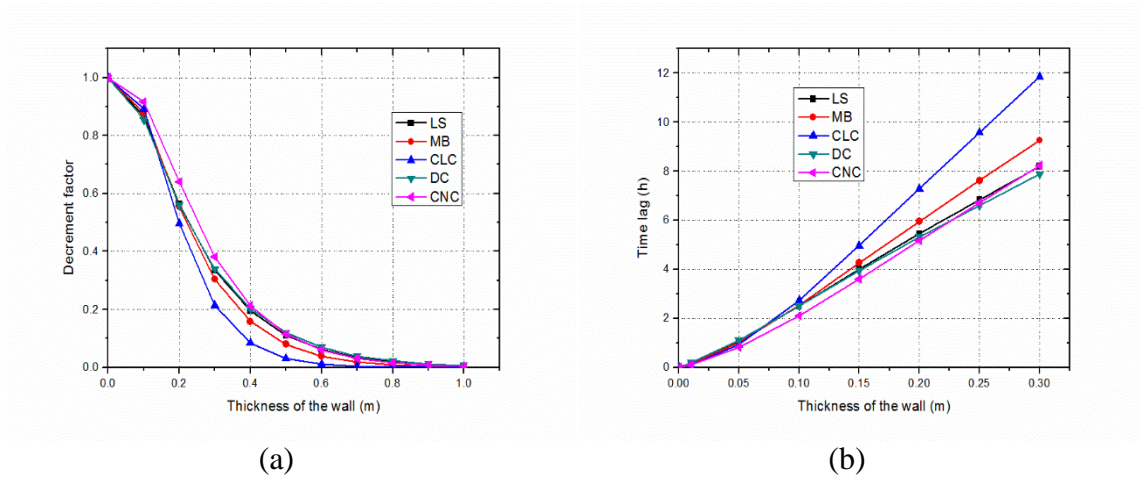


Figure 5.4.4 (a) Decrement factor of building materials, (b) Time lag of building materials as a function of thickness

5.4.4 Effect of air space thickness on thermal transmittance and thermal admittance

Figure 5.4.5 shows the effect of air space thickness on thermal transmittance and admittance of composite walls. From the results it is obvious that thermal transmittance decreases and thermal admittance increases with the increase in the divided air space thickness up to 0.02 m of the air space thickness afterwards thermal transmittance and thermal admittance remain constant. This is because of constant air gap resistance of the air space after 0.02m. From the results, it is clear that among five materials studied, dense concrete (DC) has the highest admittance value at all divided air space thicknesses and recommended for high thermal mass. Cellular concrete (CLC) has the least thermal transmittance value at all divided air space thicknesses among five studied building materials and recommended for high thermal insulation.

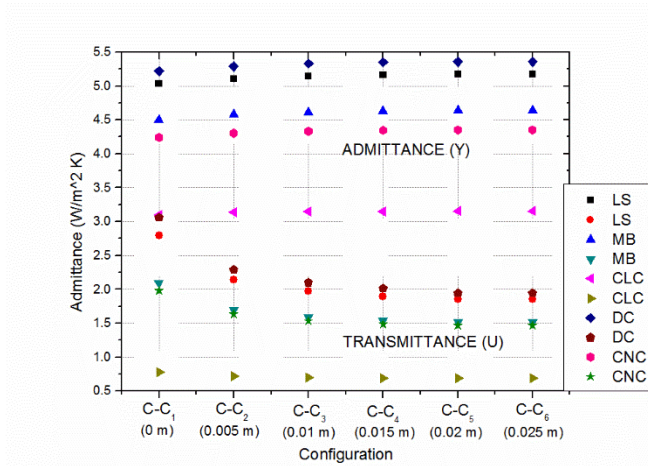


Figure 5.4.5 Effect of air space thickness on thermal transmittance and admittance of composite

5.4.5 Effect of air space thickness on decrement factor and time lag

Figure 5.4.6 (a) shows the effect of divided air space thickness on the decrement factor of composite walls. From the results, it is observed that decrement factor decreases with the increase in the air space thickness within the wall up to 0.02 m and afterwards it remains constant for all materials. This is because of the constant air gap resistance of $0.18 \text{ m}^2 \text{ K/W}$ after 0.02 m thickness of the air space. The decrement factor of building materials; laterite stone (LS), Mud brick (MB), Cellular concrete (CLC), Dense concrete (DC) and Cinder concrete (CNC) decrease 20.60%, 14.59%, 5.81%, 23.67% and 10.38%, respectively, from without air space configuration (C-C₁) to 0.02 m air space thickness configuration (C-C₅), beyond this limit they remain almost constant. From the results, it is observed that dense concrete (DC) has the least decrement factor for all air space thicknesses; hence it is recommended from the lowest decrement factor perspective among five studied building materials with air spaces.

Figure 5.4.6 (b) shows the effect of divided air space thickness on time lag of composite walls. From the results, it is observed that time lag increases with the increase in the air space thickness within the wall up to 0.02 m and afterwards it remains constant for all materials. The time lag of building materials; laterite stone (LS), Mud brick (MB), Cellular concrete (CLC), Dense concrete (DC) and Cinder concrete (CNC) increase by 20.42%, 15.06%, 6.23%, 22.70% and 14.14%, respectively, from without air space configuration (C-C₁) to 0.02 m air space

thickness configuration (C-C₅), beyond this limit they remain almost constant. From the results, it is observed that Cellular concrete (CLC) has the highest time lag for all air space thicknesses; hence it is recommended from highest time lag perspective among five studied building materials with air spaces.

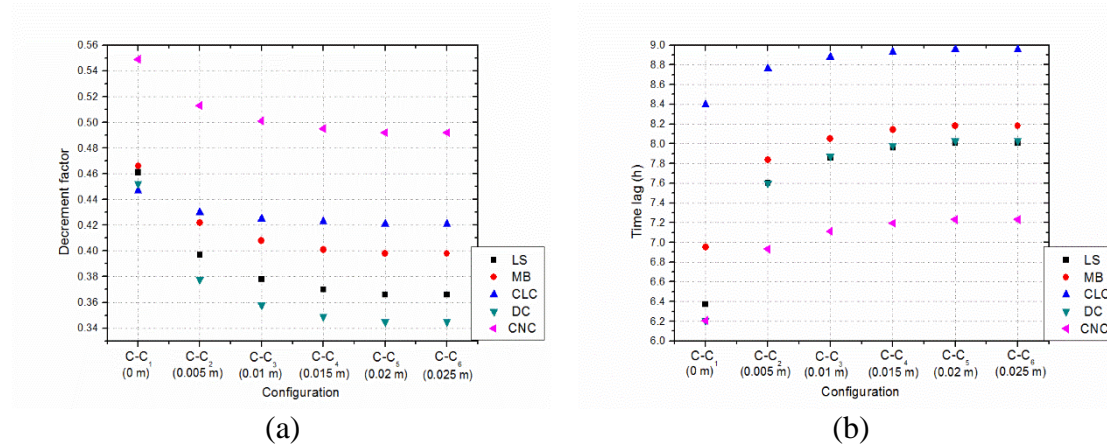


Figure 5.4.6 (a) Effect of air space thickness on decrement factor, (b) Effect of air space thickness on time lag

5.5 EFFECT OF AIR SPACE LOCATION WITHIN WALL ON DYNAMIC THERMAL PROPERTIES OF WALLS

5.5.1 Thermal properties and unsteady thermal characteristics of building materials

Table 5.5.1 shows the thermo-physical properties of the building materials considered for the study (SP: 41 1987). Five building materials were selected for the study. The computer program has been developed to calculate the unsteady state thermal characteristics of homogeneous and composite wall materials. The computer program solves one dimensional diffusion equation under convective periodic boundary conditions using matrix algebra and calculates unsteady thermal responsive characteristics. The building materials are coded from LS to CNCB. Plaster board was represented by code P.

Table 5.5.1 Thermo physical properties of building materials

S.No.	Building material	Code	k [W/mK]	ρ [kg/m ³]	Cp [J/kgK]	α [m ² /s]
1.	Laterite Stone*	LS	1.3698	1000	1926.1	7.11×10^{-7}
2.	Burnt brick	BB	0.811	1820	880	5.06×10^{-7}
3.	Mud brick	MB	0.75	1731	880	4.92×10^{-7}
4.	Reinforced brick	RB	1.10	1920	840	6.82×10^{-7}
5.	Fly ash brick*	FAB	0.360	1700	857	2.47×10^{-7}
6.	Concrete block	CNCB	1.31	2240	840	6.96×10^{-7}
7.	Plaster board	P	0.21	700	1000	3.0×10^{-7}

*Experimentally measured thermal property values.

Table 5.5.2 Unsteady thermal response characteristics of laterite stone composite walls

Laterite stone composite walls							
CODE	U [W/m ² K]	f	ϕ [h]	Y [W/m ² K]	ω [h]	F	Ψ [h]
C-D ₁	2.29	0.37	6.69	4.18	0.88	0.48	0.99
C-D ₂	1.62	0.25	7.42	4.23	0.85	0.47	0.98
C-D ₃	1.62	0.29	8.49	4.25	1.16	0.50	1.28
C-D ₄	1.62	0.31	7.15	2.46	0.84	0.69	0.39
C-D ₅	1.25	0.18	7.87	2.48	0.81	0.68	0.38
C-D ₆	1.25	0.18	9.46	4.24	1.14	0.50	1.26
C-D ₇	1.25	0.22	9.08	2.51	0.99	0.68	0.46

Table 5.5.3 Unsteady thermal response characteristics of burnt brick composite walls

Burnt brick composite walls							
CODE	U [W/m ² K]	F	ϕ [h]	Y [W/m ² K]	ω [h]	F	Ψ [h]
C-D ₁	1.86	0.39	7.20	3.81	1.13	0.54	1.02
C-D ₂	1.39	0.27	7.98	3.84	1.09	0.54	1.00
C-D ₃	1.39	0.32	8.61	3.89	1.34	0.55	1.22
C-D ₄	1.39	0.31	7.70	2.36	1.03	0.70	0.44
C-D ₅	1.11	0.20	8.48	2.36	1.00	0.70	0.43
C-D ₆	1.11	0.21	9.58	3.89	1.33	0.55	1.21
C-D ₇	1.11	0.24	9.22	2.41	1.15	0.70	0.50

Table 5.5.4 Unsteady thermal response characteristics of mud brick composite walls

Mud brick composite walls							
CODE	U [W/m ² K]	f	φ [h]	Y [W/m ² K]	ω [h]	F	Ψ [h]
C-D ₁	1.79	0.39	7.19	3.74	1.18	0.55	1.03
C-D ₂	1.35	0.27	7.99	3.76	1.14	0.55	1.01
C-D ₃	1.35	0.33	8.54	3.82	1.39	0.56	1.22
C-D ₄	1.35	0.32	7.71	2.33	1.07	0.71	0.45
C-D ₅	1.09	0.21	8.50	2.34	1.04	0.71	0.44
C-D ₆	1.09	0.22	9.51	3.81	1.37	0.56	1.20
C-D ₇	1.09	0.25	9.15	2.38	1.18	0.71	0.51

Table 5.5.5 Unsteady thermal response characteristics of reinforced brick composite walls

Reinforced brick composite walls							
CODE	U [W/m ² K]	f	φ [h]	Y [W/m ² K]	ω [h]	F	Ψ [h]
C-D ₁	2.12	0.42	6.53	3.98	1.03	0.52	1.02
C-D ₂	1.53	0.28	7.31	4.04	0.99	0.51	1.02
C-D ₃	1.53	0.34	8.07	4.04	1.31	0.53	1.28
C-D ₄	1.53	0.34	7.02	2.41	0.95	0.70	0.42
C-D ₅	1.20	0.21	7.79	2.42	0.92	0.69	0.41
C-D ₆	1.20	0.22	9.07	4.04	1.28	0.53	1.26
C-D ₇	1.20	0.26	8.68	2.45	1.10	0.69	0.49

Table 5.5.6 Unsteady thermal response characteristics of fly ash brick composite walls

Fly ash brick composite walls							
CODE	U [W/m ² K]	f	φ [h]	Y [W/m ² K]	ω [h]	F	Ψ [h]
C-D ₁	1.18	0.29	9.34	3.26	1.49	0.62	0.99
C-D ₂	0.97	0.21	10.15	3.25	1.48	0.62	0.98
C-D ₃	0.97	0.25	10.39	3.33	1.56	0.62	1.06
C-D ₄	0.97	0.23	9.89	2.17	1.34	0.74	0.50
C-D ₅	0.83	0.16	10.69	2.17	1.34	0.74	0.50
C-D ₆	0.83	0.17	11.28	3.33	1.56	0.62	1.06
C-D ₇	0.83	0.19	10.98	2.21	1.37	0.73	0.52

Table 5.5.7 Unsteady thermal response characteristics of concrete block composite walls

Concrete block composite walls							
CODE	U [W/m ² K]	f	φ [h]	Y [W/m ² K]	ω [h]	F	Ψ [h]
C-D ₁	2.26	0.38	6.70	4.15	0.91	0.49	0.99
C-D ₂	1.60	0.25	7.44	4.20	0.87	0.48	0.98
C-D ₃	1.60	0.29	8.46	4.22	1.18	0.50	1.28
C-D ₄	1.60	0.31	7.16	2.45	0.86	0.69	0.39
C-D ₅	1.24	0.19	7.89	2.47	0.83	0.69	0.38
C-D ₆	1.24	0.18	9.44	4.21	1.16	0.50	1.26
C-D ₇	1.24	0.22	9.05	2.50	1.00	0.69	0.47

In the present study, external and internal surface resistances taken are 0.04 m² K/W and 0.13 m² K/W respectively for external walls as per CIBSE standards. The air space resistance considered for 25 mm and 50 mm air space thickness is 0.18 m² K/W as per CIBSE environmental design guide.

Table 5.5.2, Table 5.5.3, Table 5.5.4, Table 5.5.5, Table 5.5.6 and Table 5.5.7 show unsteady thermal response characteristics of laterite stone, burnt brick, mud brick, reinforced brick, fly ash brick and concrete block composite walls, respectively. Table 5.5.8 shows the configuration of composite walls with thicknesses.

Table 5.5.8 Composite wall configuration and thickness

S.No	Configuration	Thickness of the wall from outside to inside [m]
1.	C-D ₁	0.0125 P + 0.2 BM + 0.0125 P
2.	C-D ₂	0.0125 P + 0.05 A + 0.2 BM + 0.0125 P
3.	C-D ₃	0.0125 P + 0.1 BM + 0.05 A + 0.1 BM + 0.0125 P
4.	C-D ₄	0.0125 P + 0.2 BM + 0.05 A + 0.0125 P
5.	C-D ₅	0.0125 P + 0.025 A + 0.2 BM + 0.025 A + 0.0125 P
6.	C-D ₆	0.0125 P + 0.025 A + 0.1 BM + 0.025 A + 0.1 BM + 0.0125 P
7.	C-D ₇	0.0125 P + 0.1 BM + 0.025 A + 0.1 BM + 0.025 A + 0.0125 P

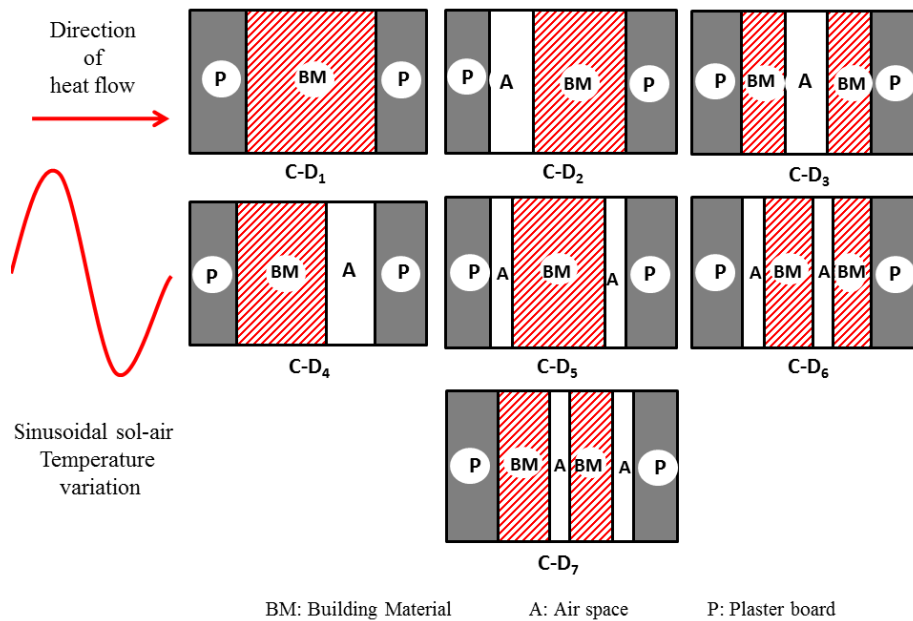


Figure 5.5.1 Configurations of Composite walls

Figure 5.5.1 shows the configurations of the composite walls selected for this research work. Seven configurations were selected to study the effect of continuous unventilated air space location on transmittance, admittance, admittance time lead, decrement factor, decrement factor time lag, surface factor and surface factor time lag of the composite walls. Configuration D₁ is a composite wall without air space.

5.5.2 Optimum wall thicknesses of the building materials

From Figure 5.5.2, it was observed that for thin cross section walls, admittance is equal to the transmittance. The values of a_6 , b_6 , c_6 , d_6 , e_6 and f_6 represent the optimum fabric thicknesses of the building materials from LS to CNCB respectively. The optimum values of building materials are found to be 0.165 m, 0.139m, 0.137 m, 0.161 m, 0.097m and 0.163 m for building materials LS, BB, MB, RB, FAB and CNCB respectively. From the results, It is observed that among all the six building materials studied, fly ash bricks have least optimum fabric thickness value e_6 (0.097m) and laterite stones have higher optimum fabric thickness value a_6 (0.165m). At an optimum wall thickness, all the building materials have maximum thermal heat capacity values.

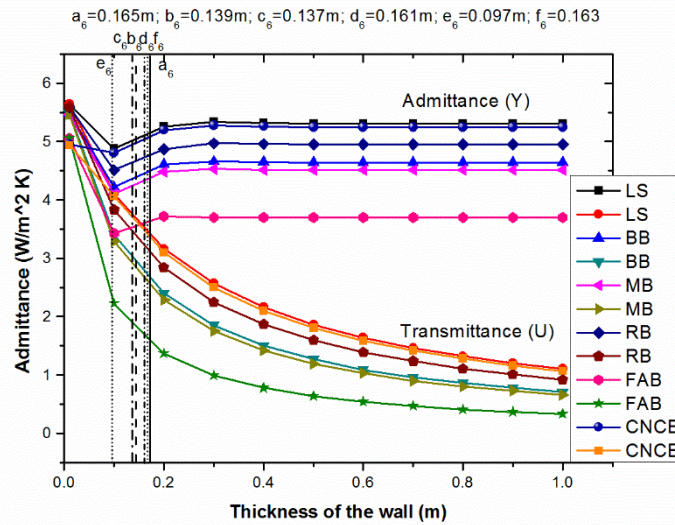


Figure 5.5.2 Optimum fabric thickness of Building materials

5.5.3 Effect of wall thickness on decrement factor and its time lag of building materials

The effect of wall thickness of the building materials on the decrement factor and the time lag is shown in Figures 5.5.3 and 5.5.4 respectively. The thickness of the homogeneous walls considered for the study is 0 to 1m. The decrement factor of the building material decreases and its time lag increases with an increase in the wall thickness. The smaller the decrement factor, the more effective the wall at suppressing temperature swings. Figure 5.5.3 shows decrement factor of the building materials and Figure 5.5.4 shows the time lag of the building materials used in the study. The homogeneous wall with thickness 0.2 m has the decrement factors 0.563, 0.549, 0.554, 0.601, 0.401 and 0.566 for building materials LS, BB, MB, RB, FAB and CNCB respectively. And the time lag is found to be 5.44 h, 5.95 h, 5.95 h, 5.26 h, 8.15 h and 5.45 h for building materials LS to CNCB respectively. From the results, it is observed that fly ash bricks have lower decrement factor values (0.401) and higher time lags (8.15h) whereas reinforced bricks have higher decrement factor values (0.601) and lower time lags (5.26h).

5.5.4 Effect of wall thickness on surface factor and it's time lag of building materials

Figures 5.5.5 and 5.5.6 show the effects of wall thickness of the homogeneous wall on the surface factor and it's time lags respectively. The thickness of the homogeneous walls considered for the study is 0 to 1m. For all thicknesses of homogeneous wall, the surface factor is found to be 0.38, 0.47, 0.49, 0.43, 0.6 and 0.39 for building materials LS to CNCB respectively, and their corresponding surface factor time lags are 1.94h, 1.68h, 1.63h, 1.8h, 1.32h and 1.92h, respectively. From the results it is clear that surface factor and it's time lag of the homogeneous walls are independent of the wall thickness. From the results, it is observed that among all the building materials considered for the study, fly ash bricks have higher surface factors (0.6) and lower surface factor time lags (1.32h) hence they are fast responsive to short wave radiation, whereas laterite stones have lower surface factors (0.38) and higher surface factor time lags (1.94h) hence laterite stones are slow responsive to short wave radiation.

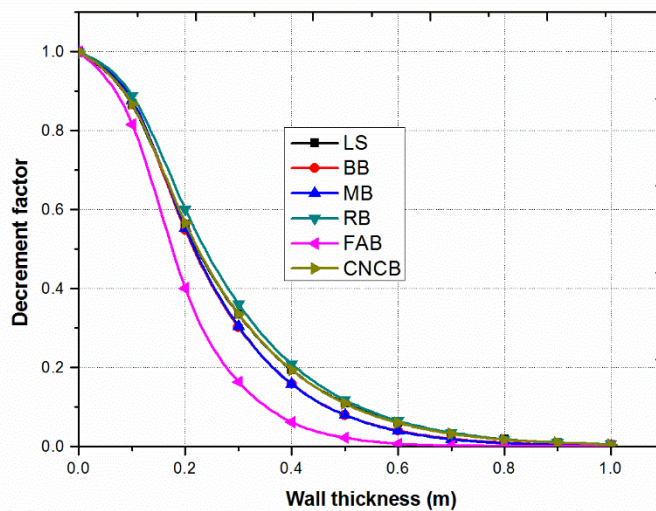


Figure 5.5.3 Decrement factor of Building materials

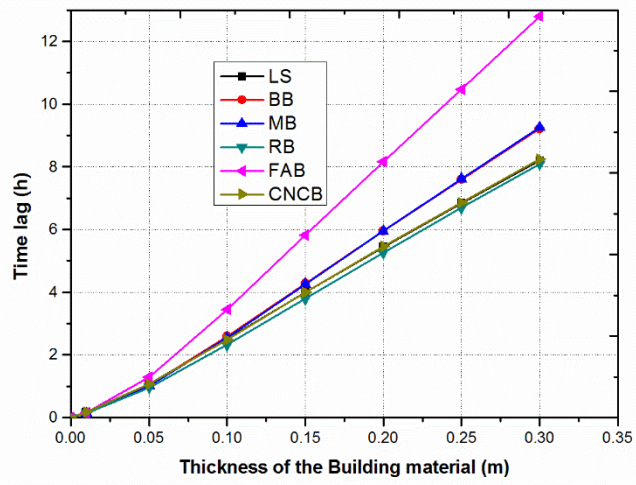


Figure 5.5.4 Time lag of Building materials

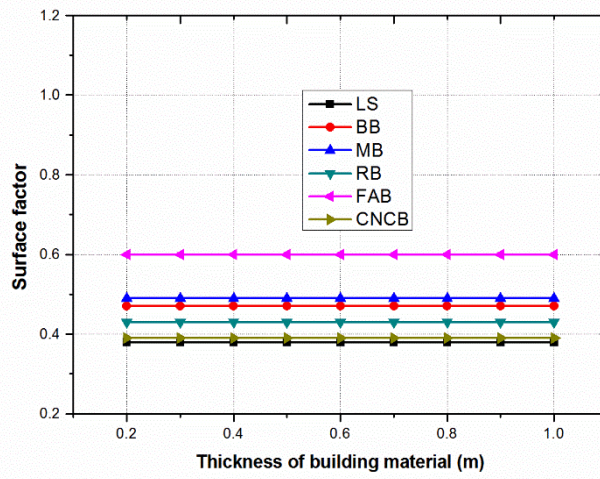


Figure 5.5.5 Surface factor of Building materials

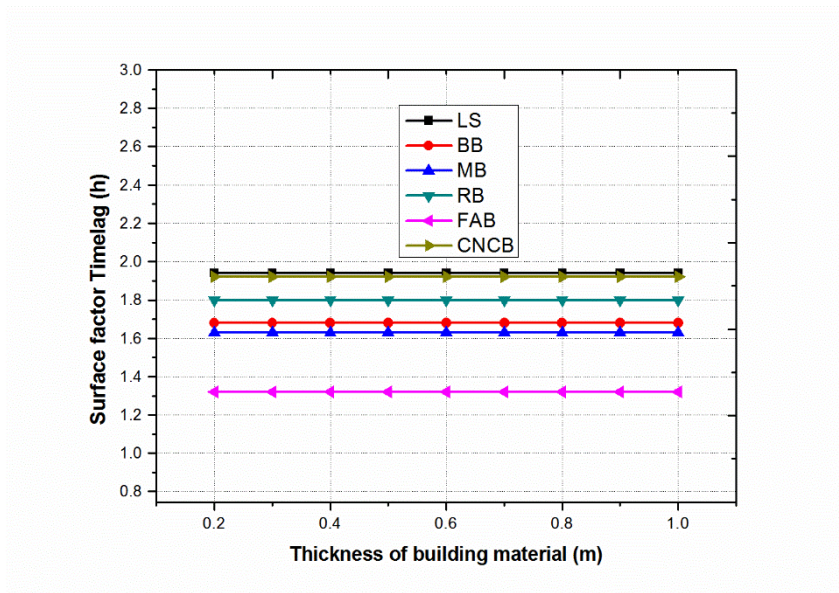
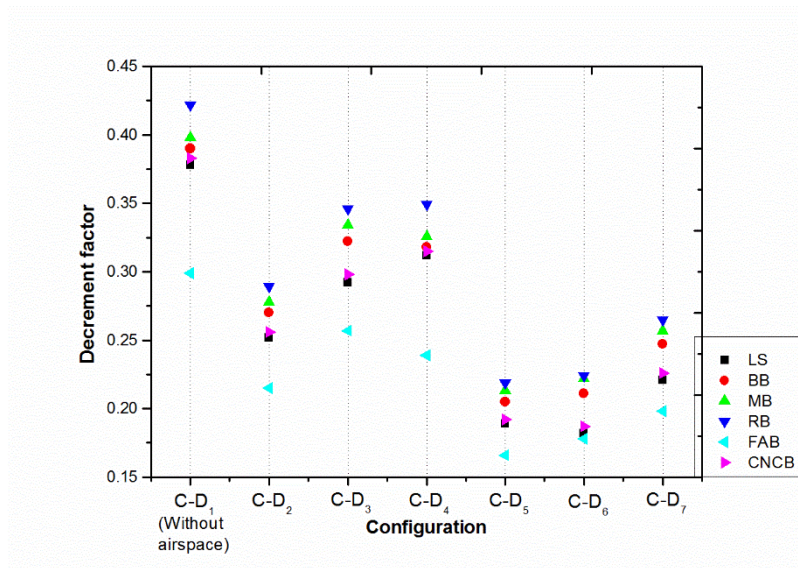


Figure 5.5.6 Surface factor time lag of Building materials

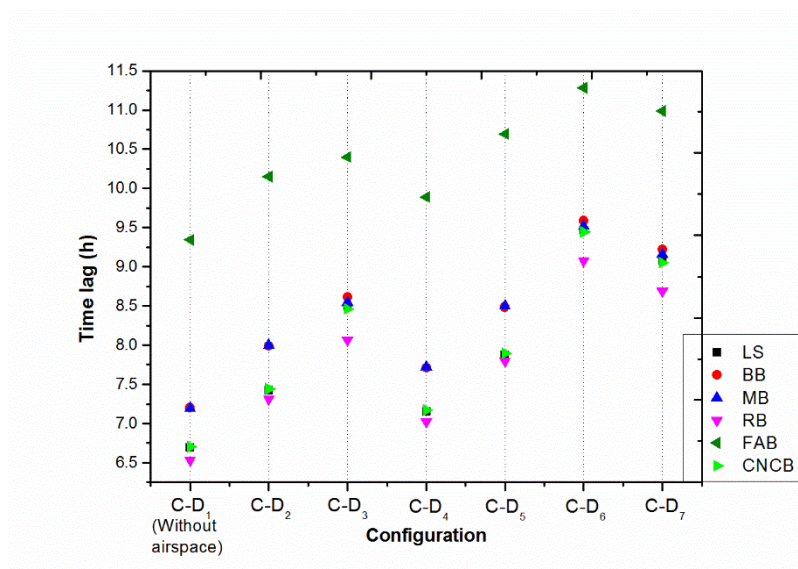
5.5.5 Effect of air space location in the wall on decrement factor and it's time lag of composite walls

Figures 5.5.7 (a) and 5.5.7 (b) show the effect of continuous unventilated air space location on decrement factor and it's time lags of composite walls. Configuration D_1 without air space gives the higher decrement factors of 0.378, 0.390, 0.398, 0.422, 0.299 and 0.383 and lower time lags of 6.69h, 7.2h, 7.19h, 6.53h, 9.34h and 6.7h with composite walls of building materials LS, BB, MB, RB, FAB and CNCB respectively. For reduced cooling loads of the buildings, the decrement factor should be as low as possible and time lag should be as high as possible. An air space location within the wall acts as insulation to reduce decrement factor and to increase time lag values without causing any extra construction cost. From the results, it is observed that the laterite stone (LS) with the air space located at the outer surface and mid center plane (C- D_6) gives the least decrement factor (0.1823) and highest time lag (9.46h) among all the configurations of laterite stone composite walls. It is noted from the results that burnt brick (BB) with the air space located at outer surface and inner surface (C- D_5) gives the lowest decrement factor (0.205) and burnt brick (BB) with the air space located at the outer surface and mid center plane (C- D_6) gives the highest time lag (9.58h) among all the composite walls of burnt brick. It is seen from the results that mud brick (MB) with the air space located at outer surface and inner

surface (C-D₅) gives the lowest decrement factor (0.33) and mud brick (MB) with the air space located at the outer surface and mid center plane (C-D₆) gives the highest time lag (9.51h) among all the configurations of mud brick composite walls. It is inferred from the results that reinforced brick (RB) with the air space located at the outer surface and inner surface (C-D₅) gives the lowest decrement factor (0.21) and reinforced brick (RB) with the air space located at the outer surface and mid center plane (C-D₆) gives the highest time lag (9.07h) among all the configurations of reinforced brick composite walls. It is also observed that fly ash brick (FAB) with the air space located at the outer surface and inner surface (C-D₅) gives the lowest decrement factor (0.16) and fly ash brick (FAB) with the air space located at the outer surface and mid center plane (C-D₆) gives the highest time lag (11.28h) among all the configurations of all considered building material composite walls. It can also be observed from the results that concrete block (CNCB) with the air space located at the outer surface and mid center plane (C-D₆) gives the least decrement factor (0.187) and highest time lag (9.44h) among all the configurations of concrete block composite walls. C-D₄ is the worst placing of the air space within the wall for laterite (LS), reinforced brick (RB) and concrete block (CNCB) composite walls from the lowest decrement factor point of view. C-D₃ is the worst placing of the air space within the wall for burnt brick (BB), mud brick (MB) and fly ash brick (FAB) composite walls from the lowest decrement factor point of view. C-D₄ is observed to be the worst placing of the air space within the wall from higher time lag point of view for all considered building material composite walls. Among single air spaced configurations studied, C-D₃ is highly recommended from highest time lag point of view and C-D₂ is highly recommended from the lowest decrement factor point of view for all the composite walls studied.



(a)



(b)

Figure 5.5.7 (a) Decrement factor of composite walls, (b) Time lag of composite walls

5.6 SUMMARY

- From 5.2, it is observed that the burnt brick composite wall with Coconut pitch insulation is the best composite wall for reduced cooling loads due to smaller decrement factors (0.32) and higher time lag values (9.1h) among all the studied composite walls.
- Mud phuska and coconut pitch have the least optimum fabric thicknesses (0.118m and 0.064m) among all the building and insulating materials studied respectively.

Using these materials in construction, energy can be saved with smaller thicknesses of the walls.

- Mud phuska and coconut pitch are the best homogeneous building and insulation materials respectively, from the least decrement factor and the highest time lag point of view. Hence, these are recommended for energy efficient building construction among studied materials.
- From 5.3, it is noticed that the composite wall with insulation placed at the mid center plane of the wall (C-B₃) gives higher time lags and the composite wall with insulation placed at the outer surface (C-B₂) gives the least value of decrement factors. Placing half of the insulation at the mid center plane and another half of the insulation at the outer surface give higher time lags and lower decrement factors.
- The insulation located at the inner surface of the composite wall (C-B₄) gives the lower time lags and higher decrement factors. This is the worst case of placing the insulation in the wall among all studied configurations.
- Fly ash brick with the jute felt insulation located at the mid center plane of the wall gives the highest time lag (11.17h) and fly ash brick with the coir board insulation located at the outer surface gives the least decrement factor (0.17) among all the composite wall configurations studied with hundred different combinations.
- Decrement factors of the fly ash brick (0.4) and jute felt (0.4) are the least among all the studied building and insulating materials, respectively. Time lags of the fly ash bricks (8.15h) and jute felt (8.75h) are the highest among all the studied building and insulating materials. Hence, these two materials are more effective at suppressing temperature swings.
- From the results, it was observed that building materials are slow responsive to short wave radiation due to their lower surface factors and higher surface factor time lags whereas insulating materials are fast responsive to short wave radiation due to their higher surface factors and lower surface factor time lags. Hence the insulating materials should not be exposed to radiation.
- Among all the studied building and insulating materials, Fly ash bricks have less limiting value of ' e_3 ' (0.097m) and jute felt insulation material has least optimum fabric thickness value of ' d_4 ' (0.079m). With these building and insulating materials both energy and material saving is possible in building construction.

- From 5.4, it is observed that the decrement factor of laterite stone (LS), Mud brick (MB), Cellular concrete (CLC), Dense concrete (DC) and Cinder concrete (CNC) decrease 20.60%, 14.59%, 5.81%, 23.67% and 10.38%, respectively, from without air space configuration (C-C₁) to 0.02 m air space thickness configuration (C-C₅) and the time lag of laterite stone (LS), Mud brick (MB), Cellular concrete (CLC), Dense concrete (DC) and Cinder concrete (CNC) increase by 20.42%, 15.06%, 6.23%, 22.70% and 14.14%, respectively, from without air space configuration (C-C₁) to 0.02 m air space thickness configuration (C-C₅), beyond 0.02m air gap thickness both decrement factor and time lag remain almost constant.
- Decrement factor decreases with the increase in the divided air space thickness within the composite wall for all building materials. Dense concrete (DC) was observed to be the energy efficient from the lowest decrement factor point of view among five studied building materials. Dense concrete decrement factor decreases by 23.67 % for 0.02 m air space thickness as compared to the conventional composite wall without air space.
- Time lag increases with the increase in the divided air space thickness within the composite wall for all building materials. Cellular concrete (CLC) was observed to be the energy efficient from the highest time lag perspective among five studied building materials. Cellular concrete time lag increases by 6.23% for 0.02 m air space thickness as compared to the conventional composite wall without air space.
- Admittance values increase and transmittance values decrease with the increase in the air space thickness from 0.005 m to 0.02 m. With these air spaces both thermal insulation and thermal mass of the wall can be increased.
- From the results, it is observed that cellular concrete has the least optimum fabric thickness (0.083 m) and they are the best materials from lowest decrement factor (0.497 at 0.2 m) and highest time lag (5.31 h at 0.2m) perspective among five studied homogeneous building materials.
- From 5.5, it is clear that the unventilated continuous air space within the composite wall adversely affects the time lag and decrement factor of composite walls along with thickness and thermal properties of the wall. The composite wall with insulation placed at the outer surface (C-D₂) gives the least value of decrement factors and the

composite wall with air space located at the mid center plane (C-D₃) of the wall give higher time lags among all the single air spaced composite walls studied.

- The composite wall with unventilated continuous air space located at outer and mid center plane of the composite wall (C-D₆) is highly recommended configuration of the composite wall for all building materials studied from highest time lag point of view. The composite wall with air space located at the inner and outer side of the composite wall (C-D₅) is recommended for burnt brick, mud brick, reinforced brick and fly ash brick composite walls from the lowest decrement factor point of view. The composite wall with air space located at outer and mid center plane of the composite wall (C-D₆) is recommended for laterite and concrete block composite walls. The configuration C-D₆ is collectively the best configuration from lower decrement factor and higher time lag for all building materials.
- Fly ash brick (FAB) with the air space located at the outer surface and inner surface (C-D₅) gives the lowest decrement factor (0.16) and fly ash brick (FAB) with the air space located at the outer surface and mid center plane (C-D₆) gives the highest time lag (11.28h) among all the configurations of all considered building material composite walls. Hence, these building material composite walls are recommended among all the studied composite walls from lowest decrement factor and highest time lag point of view.
- Optimum wall thickness values are computed for Laterite stone, Burnt bricks, Mud bricks, Reinforced bricks, Fly ash bricks and Concrete blocks. From the results, it is observed that Fly ash bricks have less limiting value of 'e₆' (0.097m) among all studied homogeneous building materials due to their low thermal diffusivity. Hence Fly ash bricks store maximum amount of energy during the first half cycle at lower wall thickness and therefore saves energy and material.
- From the results, it is concluded that the homogeneous fly ash brick walls have the lowest decrement factor (0.401) and the highest time lags (8.15h) among all studied building materials. Hence, these bricks are recommended for environment friendly and energy efficient building construction.

CHAPTER-6

EFFECT OF INSULATION LOCATION WITHIN ROOF ON DYNAMIC THERMAL PROPERTIES OF THE ROOFS

6.1 INTRODUCTION

Building roofs are responsible for the huge heat gain into the buildings. The present work presents a thorough analytical analysis of the influence of the insulation location inside the flat roof exposed directly to sun radiation to reduce heat gain into the buildings. The unsteady thermal response parameters of the building roof such as admittance, transmittance, decrement factor and time lags have been investigated by solving one dimensional diffusion equation under convective periodic boundary conditions. The results reveal that the roof with insulation placed at the outer side and at the mid center plane of the roof is the most energy efficient from the lower decrement factor point of view and the roof with the insulation placed at the mid center plane and the inner side of the roof is the best from highest time lag point of view among seven studied configurations. The composite roof with expanded polystyrene insulation located at the outer side and at the mid center plane of the roof is found to be the best roof from the lowest decrement factor (0.130) point of view and the composite roof with resin bonded mineral wool insulation located at the mid center plane and at the inner side of the roof is found to be the energy efficient from the highest time lag point (9.33h) of view among the seven configurations with five different insulation materials studied. The optimum fabric energy storage thickness of reinforced cement concrete, expanded polystyrene, foam glass, rock wool, rice husk, resin bonded mineral wool and cement plaster were computed. From the results, it is concluded that rock wool has the least optimum fabric energy storage thickness (0.114 m) among seven studied building roof materials.

6.2 THERMAL PROPERTIES AND UNSTEADY THERMAL RESPONSE PARAMETERS OF ROOF MATERIALS

Table 6.2.1 shows the thermal properties of materials used for the roof construction. Thermal properties of all the roofing and insulating materials are taken from Indian standard code: 3792-1978 (IS: 3792 1978 and SP: 41 1987). Thermal properties in the code are measured using guarded hot plate method and ASTM heat flow methods. The values k , ρ , C_p and α indicate the values of thermal conductivity, density, specific heat capacity and thermal diffusivity, respectively. Reinforced cement concrete along with cement plaster was used as roofing material.

Table 6.2.1 Thermal properties of materials at 50°C

Building material	Code	k [W/mk]	ρ [kg/m ³]	C_p [J/kgK]	$\alpha \times 10^{-7}$ [m ² /s]	L_{opt} [m]
Reinforced cement concrete	RCC	1.58	2288	880	7.84	0.173
Cement plaster	P	0.721	1762	840	4.87	0.136
Expanded polystyrene	EP	0.035	34	1340	7.68	0.171
Foam glass	FG	0.055	160	750	4.58	0.132
Rockwool	RW	0.043	150	840	3.41	0.114
Rice husk	RH	0.051	120	1000	4.25	0.127
Resin bonded mineral wool	RBMW	0.036	99	1000	3.63	0.118

Table 6.2.2 Unsteady thermal response parameters of homogeneous materials at 0.15 m thickness

Code	U [W/m ² K]	f	ϕ [h]	Y [W/m ² K]	ω [h]	F	Ψ [h]
RCC	4.25	0.74	3.74	6.17	1.23	0.42	1.82
P	2.87	0.75	4.02	4.81	1.66	0.57	1.40
EP	0.22	0.97	1.42	0.29	2.11	0.97	0.09
FG	0.34	0.92	2.42	0.58	2.63	0.95	0.17
RW	0.27	0.87	3.13	0.55	2.84	0.95	0.16
RH	0.32	0.91	2.58	0.57	2.70	0.95	0.17
RBMW	0.23	0.89	2.92	0.44	2.83	0.96	0.13

Five insulation materials such as, expanded polystyrene, foam glass, rock wool, rice husk and resin bonded mineral wool were selected and their unsteady thermal response parameters have been computed using a computer program.

Table 6.2.3 Configurations of the composite roof with thicknesses

S.No.	Configuration of the roof	Thickness of the roof from outside to inside [m]
1.	C-E ₁	0.03 P + 0.15 RCC + 0.03 P
2.	C-E ₂	0.01 P + 0.04 IM + 0.15 RCC + 0.01 P
3.	C-E ₃	0.01 P + 0.075 RCC + 0.04 IM + 0.075 RCC + 0.01 P
4.	C-E ₄	0.01 P + 0.15 RCC + 0.04 IM + 0.01 P
5.	C-E ₅	0.01 P + 0.02 IM + 0.075 RCC + 0.02 IM + 0.075 RCC + 0.01 P
6.	C-E ₆	0.01 P + 0.075 RCC + 0.02 IM + 0.075 RCC + 0.02 IM + 0.01 P
7.	C-E ₇	0.01 P + 0.02 IM + 0.15 RCC + 0.02 IM + 0.01 P

The insulation materials in this study are coded from EP to RBMW. Table 6.2.2 shows unsteady thermal response parameters of homogeneous materials at 0.15m material thickness. Table 6.2.3 shows the configurations of the composite roofs with thicknesses. Figure 6.2.1 shows the configurations of the composite roofs studied. Total seven configurations with five insulation materials have been studied for optimum insulation position inside the roof. The outside and inside surface resistances are taken as 0.04 m² K/W and 0.10 m² K/W respectively for roofs as per CIBSE standards.

Configuration E₁ is a composite roof with reinforced cement concrete covered by inside and outer side cement plaster and without any insulation material. Configuration E₂ is a composite roof with insulation placed at the outer side of the roof. Configuration E₃ is a composite roof with insulation placed at the mid center plane of the roof. Configuration E₄ is a composite roof with insulation placed at the inside of the roof. Configuration E₅ is a composite roof with half of the insulation placed at the outer side and another half of the insulation placed at the mid center plane of the roof. Configuration E₆ is a composite roof with half of the insulation placed at the mid center plane of the roof and another half of the insulation placed at the inner side. Configuration E₇ is a composite roof with half of the insulation placed at the outer side of the roof and another half of the insulation placed at the inner side

of the roof. Figure 6.2.2 shows the images of roofing and insulating materials used in this study.

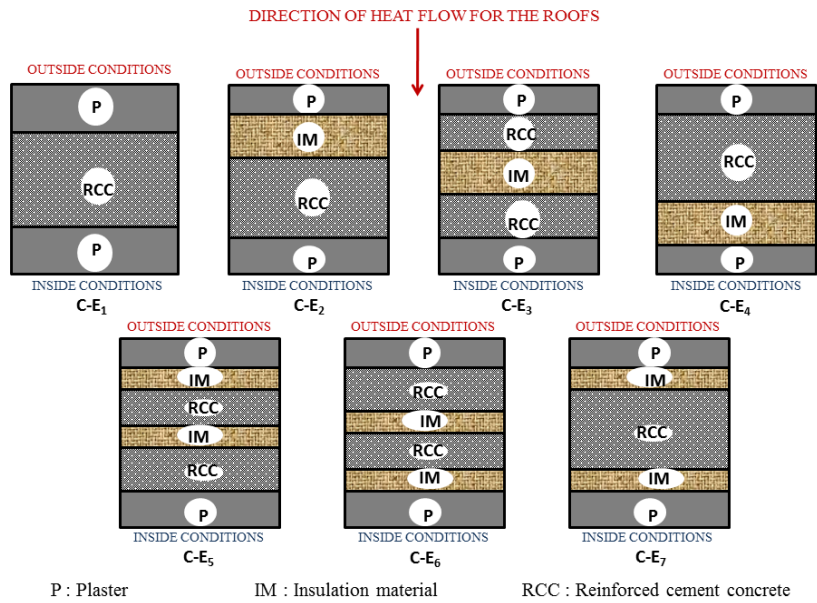


Figure 6.2.1 Configurations of Composite roofs



Figure 6.2.2 Images of roofing and insulation materials

6.3 OPTIMUM FABRIC ENERGY STORAGE THICKNESS

Thermal mass plays very important role in the design of energy efficient buildings. Thermal mass is the ability of a building wall or roof to absorb and store excess heat for several hours. The thermal capacity of roof materials, delays the heat transfer from outside to inside of the wall. There is a misconception that the more is the thermal mass the more is the energy efficient the building for cooling. If the fabric energy storage thickness is large then it absorbs more and more heat. The absorbed heat will be added to the next day heat and hence increases the cooling loads. If the fabric energy storage thickness is small then absorbed heat will be immediately released into the building. Therefore, if the mass more than optimum is provided, then it will not be utilized. The thickness of the fabric at which it absorbs the maximum amount of heat is called the optimum fabric energy storage thickness. From Figure 6.3.1, it is observed that at smaller thicknesses of the materials admittance is equal to the transmittance. The values of a_7 and b_7 represent the optimum fabric thicknesses of the reinforced cement concrete and cement plaster respectively. From Figure 6.3.1 (a), it is observed that cement plaster (P) has the least optimum fabric thickness value of 0.136 m and Reinforced cement concrete (RCC) has the highest optimum fabric thickness value of 0.173 m among two roofing materials studied. The values of a_8 , b_8 , c_8 , d_8 and e_8 represent the optimum fabric thickness values of the insulation materials, expanded polystyrene, foam glass, rock wool, rice husk and resin bonded mineral wool, respectively. It is clearly observed from Figure 6.3.1 (b) that rock wool has the least optimum fabric thickness value of 0.114 m and the expanded polystyrene has the highest optimum fabric thickness value of 0.171 m among five studied insulation materials. The thermal performance of the roofs can be measured by two parameters one is thermal insulation and another one is thermal mass. The thermal transmittance is a steady state property and it is the measure of thermal insulation. Thermal transmittance is a measure of heat loss by conduction, convection and radiation through a thickness of the wall or roof. Thermal transmittance is the reciprocal of thermal resistance of wall or roof material. The thermal admittance is the measure of thermal mass. For reduced cooling loads, thermal transmittance should be as low as possible and thermal admittance should be as high as possible.

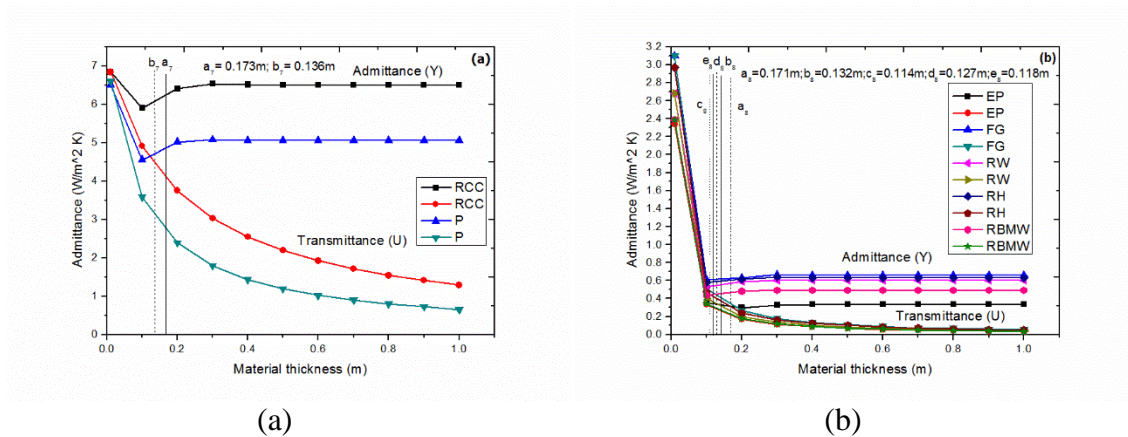


Figure 6.3.1 Optimum fabric thickness: (a) Roofing materials, (b) Insulation materials

6.4 DECREMENT FACTOR AND TIME LAG OF ROOFING AND INSULATING MATERIALS

Decrement factor and time lag are the most important unsteady heat transfer characteristics for determining thermal mass or thermal heat storage of any wall or roof materials. The attenuation of outside sinusoidal heat wave as it progresses through the wall or roof is called as the decrement factor. The time taken by the outside sinusoidal heat wave to travel outside surface to inside surface is called as the time lag. Figure 6.4.1 (a) and Figure 6.4.1 (b) show the decrement factor and its time lag respectively, for roofing and insulating materials. The decrement factor of the building material decreases with an increase in the wall thickness. The smaller the decrement factor the more effective the roof at suppressing temperature swings. The time lag of the heat wave should be as high as possible to delay an outside sinusoidal heat wave to enter into the room through the wall or roof. The decrement factor reduces and the time lag increases with an increase in the material thickness. From figures, it is clear that at 0.15 m material thickness, reinforced cement concrete has the lowest decrement factor (0.74) and the cement plaster has the highest time lag (4.02 h) among all the studied roofing and insulating materials. The cement plaster has the highest time lag at all the thicknesses among all the seven materials studied and the expanded polystyrene has the highest decrement factor and the lowest time lag values at all the thicknesses among all the seven materials studied.

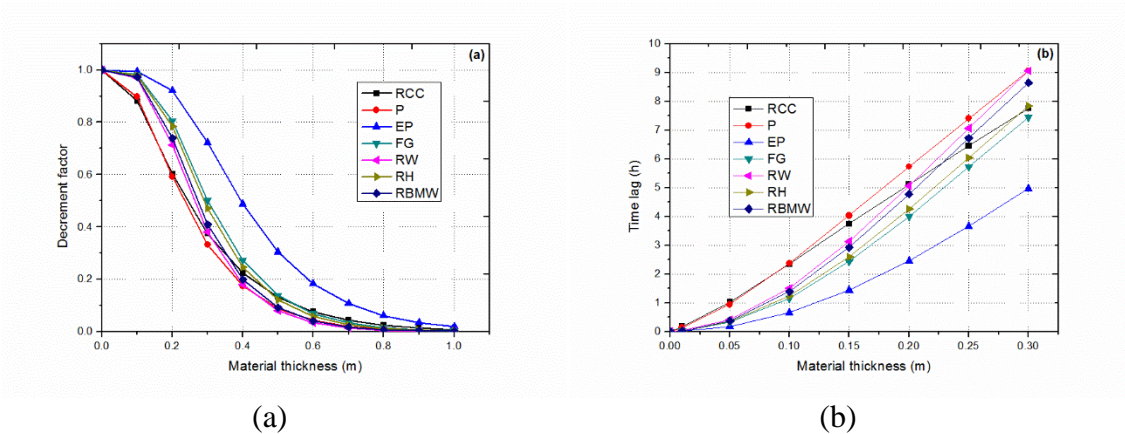


Figure 6.4.1 Decrement factor and time lag of homogeneous materials: (a) Decrement factor of roofing and insulating materials, (b) Time lag of roofing and insulating materials

6.5 SURFACE FACTOR AND SURFACE FACTOR TIME LAG OF ROOFING AND INSULATING MATERIALS

Buildings with surface factor 0.8 with time delay of one hour are fast responsive to short wave radiation, whereas buildings with surface factor 0.5 with time delay of two hours are slowly responsive to short wave radiation. Figure 6.5.1 (a) and Figure 6.5.1 (b) show the surface factor and its time lag respectively, for roofing and insulating materials. Among all the seven roofing and insulating materials studied, the reinforced cement concrete has the lowest surface factor (0.42) and highest surface factor time lag (1.82). Hence RCC is slow responsive to short wave radiation as compared to the other materials studied.

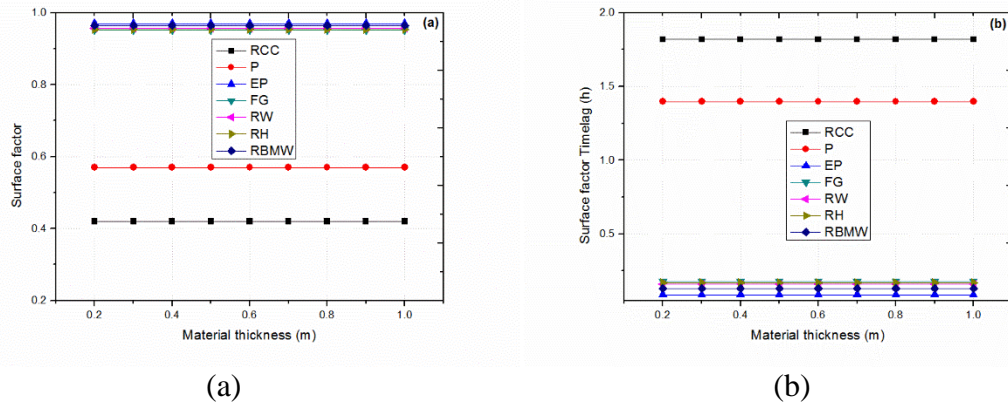


Figure 6.5.1 Surface factor and surface factor time lag of homogeneous materials: (a) Surface factor of roofing and insulating materials, (b) Surface factor time lag of roofing and insulating materials

6.6 EFFECT OF INSULATION POSITION IN THE COMPOSITE ROOF ON DECREMENT FACTOR AND TIME LAG

Figure 6.6.1 (a) and Figure 6.6.1 (b) show the effect of the insulation location in the composite roof on decrement factor and its time lag respectively. It is observed from the results that the composite roof without insulation (Configuration E_1) has the highest decrement factor (0.526) and the lowest time lag values (5.62) among seven studied configurations with five insulation materials. Reinforced cement concrete (RCC) with expanded polystyrene insulation (EP) combination gives decrement factors 0.319, 0.467, 0.476, 0.1308, 0.1585 and 0.204 in configurations E_2 , E_3 , E_4 , E_5 , E_6 and E_7 respectively. Reinforced cement concrete with expanded polystyrene insulation gives the least decrement factor (0.1308) in configuration E_5 and it gives the highest decrement factor (0.476) in configuration E_4 . Reinforced cement concrete (RCC) with expanded polystyrene insulation (EP) combination gives time lags 6.32h, 6.91h, 5.76h, 7.36h, 9.29h and 8.46h in configurations E_2 , E_3 , E_4 , E_5 , E_6 and E_7 respectively. Reinforced cement concrete with expanded polystyrene insulation gives the least time lag (5.76h) in configuration E_4 and it gives the highest time lag (9.29h) in configuration E_6 . Hence, for reinforced cement concrete with extended polystyrene insulation, configuration E_5 is optimum from lowest decrement factor (0.1308) point of view and Configuration E_6 is optimum from highest time lag (9.29h) point of view.

Reinforced cement concrete (RCC) with foam glass insulation (FG) combination gives decrement factors 0.337, 0.483, 0.489, 0.187, 0.226 and 0.283 in configurations E₂, E₃, E₄, E₅, E₆ and E₇, respectively. Reinforced cement concrete (RCC) with foam glass insulation (FG) combination gives time lags 6.33h, 6.85h, 5.78h, 7.15h, 8.72h and 7.98h in configurations E₂, E₃, E₄, E₅, E₆ and E₇, respectively. For reinforced cement concrete with glass foam insulation combination, configuration E₅ is optimum from lowest decrement factor (0.187) point of view and configuration E₆ is optimum from highest time lag (8.72h) point of view.

Reinforced cement concrete (RCC) with rock wool insulation (RW) combination gives decrement factors 0.325, 0.471, 0.480, 0.154, 0.186 and 0.237 in configurations E₂, E₃, E₄, E₅, E₆ and E₇ respectively. Reinforced cement concrete (RCC) with rock wool insulation (RW) combination gives time lags 6.44h, 7.0h, 5.89h, 7.34h, 9.11h and 8.32h in configurations E₂, E₃, E₄, E₅, E₆ and E₇, respectively. For reinforced cement concrete with rock wool insulation combination, configuration E is optimum from lowest decrement factor (0.154) point of view and configuration F is optimum from highest time lag (9.11h) point of view.

Reinforced cement concrete (RCC) with rice husk insulation (RH) combination gives decrement factors 0.333, 0.479, 0.486, 0.176, 0.214 and 0.269 in configurations E₂, E₃, E₄, E₅, E₆ and E₇, respectively. Reinforced cement concrete (RCC) with rice husk insulation (RH) combination gives time lags 6.36h, 6.89h, 5.81h, 7.21h, 8.84h and 8.09h in configurations E₂, E₃, E₄, E₅, E₆ and E₇, respectively. For reinforced cement concrete with rice husk insulation combination, configuration E₅ is optimum from lowest decrement factor (0.176) point of view and configuration E₆ is optimum from highest time lag (8.84h) point of view.

Reinforced cement concrete (RCC) with resin bonded mineral wool insulation (RBMW) combination gives decrement factors 0.319, 0.465, 0.475, 0.133, 0.161 and 0.207 in configurations E₂, E₃, E₄, E₅, E₆ and E₇ respectively. Reinforced cement concrete (RCC) with resin bonded mineral wool insulation (RBMW) combination gives time lags 6.44h, 7.03h, 5.89h, 7.42h, 9.33h and 8.51h in configurations E₂, E₃, E₄, E₅, E₆ and E₇, respectively. For reinforced cement concrete with resin bonded mineral wool insulation combination, configuration E₅ is optimum from lowest

decrement factor (0.133) point of view and configuration E_6 is optimum from highest time lag (9.33h) point of view.

Among seven configurations with five insulation materials studied, configuration E_5 is found to be the best optimum insulation location from the lowest decrement point of view and configuration E_6 is found to be the best optimum location from highest time lag point of view.

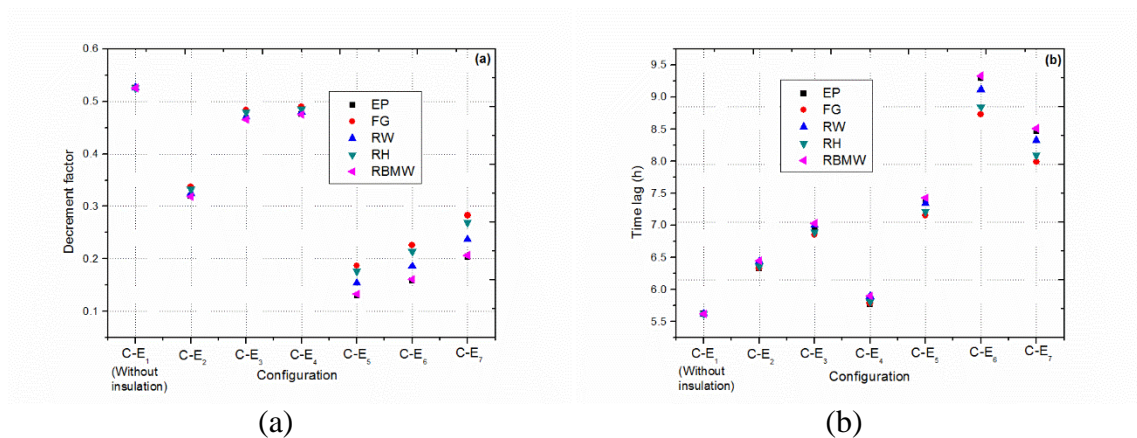


Figure 6.6.1 Decrement factor and time lag of composite roofs: (a) Effect of insulation location on decrement factor, (b) Effect of insulation location on time lag

6.7 SUMMARY

- The composite roof with insulation placed at the outer side of the roof (C-E₂) is the optimum position from the lowest decrement point of view and the composite roof with insulation placed at the mid center plane of the roof (C-E₃) is optimum from highest time lag point of view for all the materials studied among single insulation configurations E₂, E₃ and E₄.
- The composite roof with half of the insulation placed at the outer side and another half of the insulation placed at the mid center plane of the roof (C-E₅) is the optimum location from the lowest decrement factor point of view for all the insulation materials studied among all the configurations.
- The composite roof with half of the insulation placed at the mid center plane of the roof and another half of the insulation placed at the inner side of the roof (C-E₆) is the optimum location from highest time lag point of view for all the insulation materials studied among seven configurations.

- Reinforced cement concrete (RCC) with expanded polystyrene insulation (EP) placed at the outer side and at the mid center plane of the roof (C-E₅) is the best combination from the lowest decrement factor (0.130) point of view among seven studied configurations with five insulation materials.
- Reinforced cement concrete (RCC) with resin bonded mineral wool insulation (RBMW) placed at the mid center plane and at the inner side of the roof (C-E₆) is the best combination from highest time lag point (9.33h) of view among seven studied configurations with five insulation materials.
- The configuration C-E₆ is observed to be the second best configuration after C-E₅ from the lower decrement factor point of view for all the insulation materials studied among seven configurations. The configuration C-E₆ is the best from both lower decrement factor and higher time lag perspective.
- Reinforced cement concrete (RCC) with expanded polystyrene insulation (EP) placed at the mid center plane and at the inner side of the roof (C-E₆) gives 69.86% less decrement factor and 39.50% higher time lag values than the common roof configuration (C-E₁).
- The results of the study aid in designing energy efficient composite roofs for reduced cooling loads.

CHAPTER-7

DYNAMIC THERMAL PERFORMANCE OF HOLLOW AND STUFFED BRICKS

7.1 INTRODUCTION

The space cooling systems account for nearly 30% of energy consumption in India. The objective of this chapter is to investigate the unsteady thermal response characteristics of hollow bricks with different materials and varying air gap in hollow bricks for reducing heat gain in buildings. Five air gap configurations of hollow bricks with five different materials are considered for the study keeping the overall brick thickness same in all the cases. Case I (C-F₁) indicates solid brick, Case II (C-F₂) indicates only one air gap, case III (C-F₃) with two air gaps, case IV (C-F₄) with three air gaps, case V (C-F₅) with four air gaps and case VI (C-F₆) with five air gaps. Five brick materials considered are Concrete, burnt brick, mud brick, cinder concrete and cellular concrete. In order to obtain the unsteady thermal characteristics such as, admittance, transmittance, decrement factor, time lag, surface factor, surface factor time lag and areal thermal heat capacity of hollow bricks, a computer simulation program was developed which employs a cyclic admittance method. From the results it is observed that thermal admittance, surface factor time lag, decrement factor time lag and areal thermal heat capacity values increase with the increase in the number of air gaps in hollow bricks, whereas thermal transmittance and decrement factor reduces with the increase in the number of air gaps in the hollow bricks. Considering the unsteady thermal properties studied, it is observed that among the twenty five combinations concrete block with five air gaps is the best and the most energy efficient. It possesses highest admittance (5.84), lowest decrement factor (0.64), highest time lag (5.84h), highest areal thermal heat capacity (58885 J/m²K) and highest surface factor time lag (1.37h) among twenty five combinations of hollow

brick air gap configurations and five brick materials studied. Also it is observed that five air gap configuration hollow bricks are having better unsteady thermal properties compared to all other air gaps. These results are useful in designing energy efficient passive building construction.

The highly insulated external walls are essential prerequisites for low energy consumption of buildings. Filling shell of the brick with insulation material is one of the methods to reduce cooling loads in buildings. This chapter also aims to investigate the dynamic thermal parameters of various insulation filled bricks. The dynamic thermal parameters of stuffed bricks highlighted include thermal transmittance, admittance, decrement factor, time lag and areal thermal heat capacity. The four brick materials such as mud bricks, burnt bricks, concrete blocks and fly ash bricks were selected. The insulation materials used for filling shells of the brick are foam glass and asbestos fiber. The total, forty eight stuffed bricks were investigated. The shell of the brick is filled by the insulation and the each layer of insulation is separated by a brick web. The shell and web thickness of the brick were maintained as per the Indian standards. The six configurations of the stuffed bricks were investigated (1. Solid brick, 2. Bricks with the shell of the brick filled with single layer of insulation, 3. Bricks with the shell of the brick filled with two layers of insulation with each insulation layer separated with a brick web, 4. Bricks with the shell of the brick filled with three layers of insulation with each insulation layer separated by a brick web, 5. Bricks with the shell of the brick filled with four layers of insulation with each insulation layer separated by a brick web and 6. Bricks with the shell of the brick filled with five layers of insulation with each insulation layer separated by a brick web). From the results, it is observed that the stuffed bricks significantly improve time lag values as compared to the conventional solid bricks. The decrement factor decreases, admittance increases and areal thermal heat capacity increases with the increase in the no. of insulation layers in the bricks. The concrete blocks with the shell of the bricks filled with five layers of asbestos fiber insulation offer the highest admittance ($3.11\text{Wm}^2\text{K}$), the lowest decrement factor (0.435), the highest time lag values (8.26 h) and the highest areal thermal heat capacity ($57366\text{ J/m}^2\text{K}$) among all insulation filled bricks studied. The results of the paper help in designing energy efficient stuffed bricks for reducing cooling loads in buildings.

7.2 DYNAMIC THERMAL PERFORMANCE OF HOLLOW BRICKS

7.2.1 Dynamic thermal response of solid and hollow bricks

Table 7.2.1 shows the thermo-physical properties of the brick materials considered for the study. In the Table k , ρ , C_p and α represent the values of thermal conductivity, density, specific heat capacity and thermal diffusivity, respectively. Thermo-physical properties of bricks are taken from Indian standard code IS 3792:1978 and their characterization is as per the code (IS: 3792 1978). Figure 7.2.1 shows the configuration of six different types of solid and hollow bricks taken for the study. The external dimensions of the brick are 0.29m X 0.14m X 0.09m, as per the Indian standard code IS 3952:1988. The web thickness for all the hollow bricks studied is not less than 0.008m as per the IS code (IS: 3952 1988). Table 7.2.2 shows the air space dimensions and their resistances. Air space resistance of brick hollow depends mainly on its thickness and breadth. The bricks are considered as external bricks therefore internal surface resistance R_{si} is taken as $0.13 \text{ m}^2 \text{ K/W}$ and external surface resistance R_{se} is taken as $0.04 \text{ m}^2 \text{ K/W}$ as per CIBSE standards for computations of external solid and hollow bricks. The computer simulation program was developed to calculate all the unsteady thermal response characteristics of solid and hollow bricks. The results of the simulation program are confirming to CIBSE standards. The unsteady state thermal characteristics were measured for all the bricks considered for the study. Table 7.2.3, Table 7.2.4, Table 7.2.5, Table 7.2.6 and Table 7.2.7 show unsteady thermal response characteristics of both solid and hollow bricks made of concrete, burnt brick, mud brick, cinder concrete and cellular concrete respectively.

Table 7.2.1 Thermo physical properties of brick materials

Brick material	Code	k [W/mK]	ρ [kg/m ³]	C_p [J/kgK]	$\alpha \times 10^{-7}$ [m ² /s]
Dense concrete block	DC	1.74	2410	880	8.204
Burnt brick	BB	0.811	1820	880	5.063
Mud brick	MB	0.75	1731	880	4.923
Cinder Concrete	CNC	0.686	1406	840	5.808
Cellular concrete block	CLC	0.188	704	1050	2.543

Table 7.2.2 Composite wall configuration with different air space thicknesses

S.No.	Air space thickness t_a [m]	Air space breadth b_a [m]	Air space resistance R_a [m ² K/W]
1.	0.11	0.29	0.193
2.	0.05	0.29	0.181
3.	0.03	0.29	0.176
4.	0.02	0.29	0.174
5.	0.014	0.29	0.173

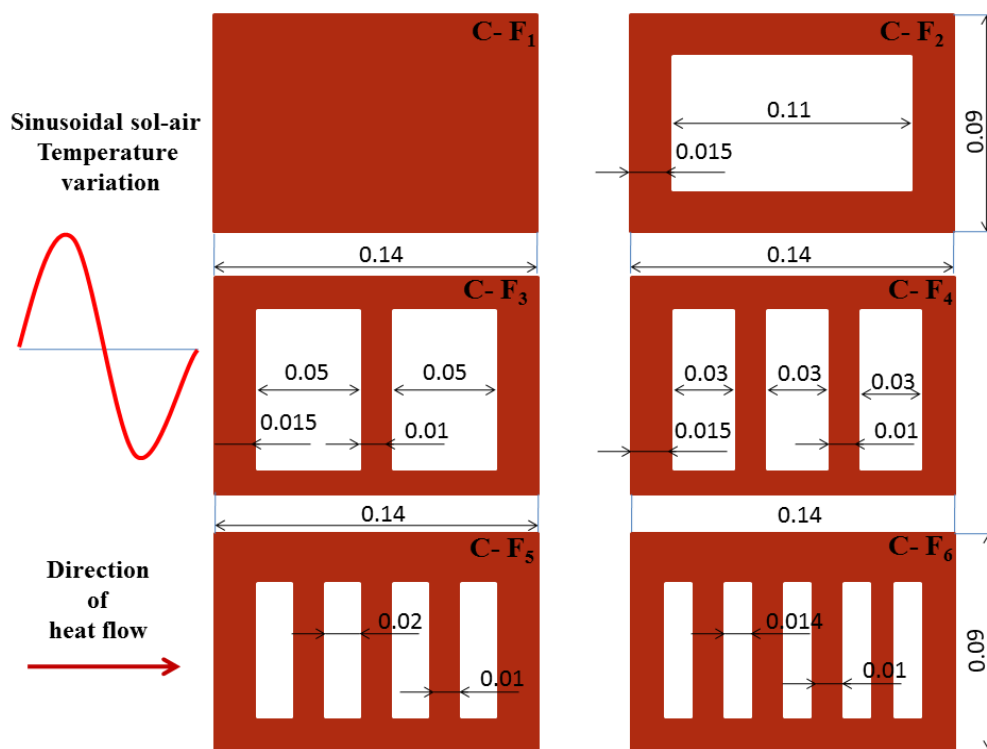


Figure 7.2.1 Configurations of the bricks. (All dimensions are in “m”)

Table 7.2.3 Unsteady thermal response characteristics of Dense concrete blocks

DC Configuration	U [W/m ² K]	f	ϕ [h]	Y [W/m ² K]	ω [h]	F	Ψ [h]	χ [J/m ² K]
C-F ₁	3.994	0.736	3.672	5.335	0.983	0.374	1.875	70521
C-F ₂	2.630	0.976	1.100	2.986	1.247	0.644	0.742	38711
C-F ₃	1.802	0.938	2.005	2.692	2.198	0.731	1.004	47231
C-F ₄	1.376	0.868	3.143	2.813	2.661	0.757	1.202	53999
C-F ₅	1.110	0.764	4.452	2.973	2.780	0.756	1.323	57862
C-F ₆	0.930	0.641	5.842	3.605	2.758	0.749	1.371	58885

Table 7.2.4 Unsteady thermal response characteristics of burnt bricks

BB Configuration	U [W/m ² K]	f	φ [h]	Y [W/m ² K]	ω [h]	F	Ψ [h]	χ ₂ [J/m ² K]
C-F ₁	2.919	0.746	3.935	4.404	1.364	0.505	1.554	62491
C-F ₂	2.500	0.985	0.886	2.726	1.064	0.666	0.560	29126
C-F ₃	1.720	0.960	1.612	2.314	2.002	0.755	0.766	35981
C-F ₄	1.316	0.913	2.541	2.337	2.591	0.787	0.933	41953
C-F ₅	1.064	0.836	3.640	2.464	2.832	0.793	1.053	46180
C-F ₆	0.891	0.735	4.842	2.571	2.872	0.789	1.119	48322

Table 7.2.5 Unsteady thermal response characteristics of mud bricks

MB Configuration	U [W/m ² K]	f	φ [h]	Y [W/m ² K]	ω [h]	F	Ψ [h]	χ ₂ [J/m ² K]
C-F ₁	2.804	0.753	3.911	4.273	1.411	0.522	1.504	60797
C-F ₂	2.482	0.986	0.851	2.689	1.030	0.669	0.532	27687
C-F ₃	1.708	0.964	1.547	2.258	1.960	0.758	0.729	34264
C-F ₄	1.308	0.919	2.441	2.264	2.568	0.791	0.892	40069
C-F ₅	1.057	0.847	3.503	2.383	2.832	0.799	1.010	44300
C-F ₆	0.886	0.750	4.671	2.490	2.887	0.796	1.078	46588

Table 7.2.6 Unsteady thermal response characteristics of cinder concrete

CC Configuration	U [W/m ² K]	f	φ [h]	Y [W/m ² K]	ω [h]	F	Ψ [h]	χ ₂ [J/m ² K]
C-F ₁	2.674	0.819	0.303	3.844	1.466	0.568	1.279	51909
C-F ₂	2.459	0.991	0.668	2.589	0.837	0.675	0.414	21506
C-F ₃	1.694	0.977	1.217	2.053	1.691	0.767	0.570	26790
C-F ₄	1.297	0.949	1.932	1.959	2.376	0.807	0.706	31734
C-F ₅	1.049	0.899	2.798	2.023	2.770	0.822	0.816	35815
C-F ₆	0.879	0.827	3.778	2.120	2.927	0.824	0.893	38655

Table 7.2.7 Unsteady thermal response characteristics of cellular concrete blocks

CCB Configuration	U [W/m ² K]	f	φ [h]	Y [W/m ² K]	ω [h]	F	Ψ [h]	χ [J/m ² K]
C-F ₁	1.093	0.745	4.503	2.313	2.248	0.768	0.835	35740
C-F ₂	1.914	0.995	0.553	1.986	0.747	0.748	0.256	12947
C-F ₃	1.342	0.986	0.989	1.537	1.486	0.818	0.354	16397
C-F ₄	1.037	0.968	1.558	1.406	2.167	0.851	0.441	19702
C-F ₅	0.843	0.935	2.253	1.410	2.647	0.867	0.517	22634
C-F ₆	0.710	0.885	3.053	1.464	2.906	0.872	0.576	24987

7.2.2 Decrement factor and time lag of solid bricks

Decrement factor decreases and decrement time lag increases with the increase in the thickness of the solid bricks. Figure 7.2.2 (a) and 7.2.2 (b) show the decrement factor and its time lag as a function of thickness. Lower the decrement factor the higher is the wall effectiveness at suppressing temperature swings. The time lag of decrement factor should be as high as possible. From the results it is observed that Dense concrete block (DC) up to 0.1 m offers lower decrement factor, whereas cellular concrete block (CLC) offers lower decrement factor for all its thicknesses over 0.1m among five brick materials studied. The cellular concrete blocks (CLC) give the highest time lag value at all the thicknesses of the bricks among five studied brick materials.

7.2.3 Admittance and transmittance of solid bricks

High thermal admittance values are advantageous from a thermal mass perspective, whereas low thermal transmittance values are desirable for low energy transfer through walls. Thermal transmittance is steady state property and thermal admittance is a dynamic property of brick material. Figure 7.2.3 shows admittance and the transmittance of solid bricks as a function of thickness. From the results, it is noted that dense concrete block (DC) has the highest thermal mass due to higher thermal admittance values and cinder concrete (CNC) has the lowest thermal mass due to lower thermal admittance values at all the brick thicknesses among five brick materials studied. Cellular concrete block (CLC) has the lowest thermal transmittance values at all brick thicknesses among five brick materials investigated therefore they serve as the best insulation materials.

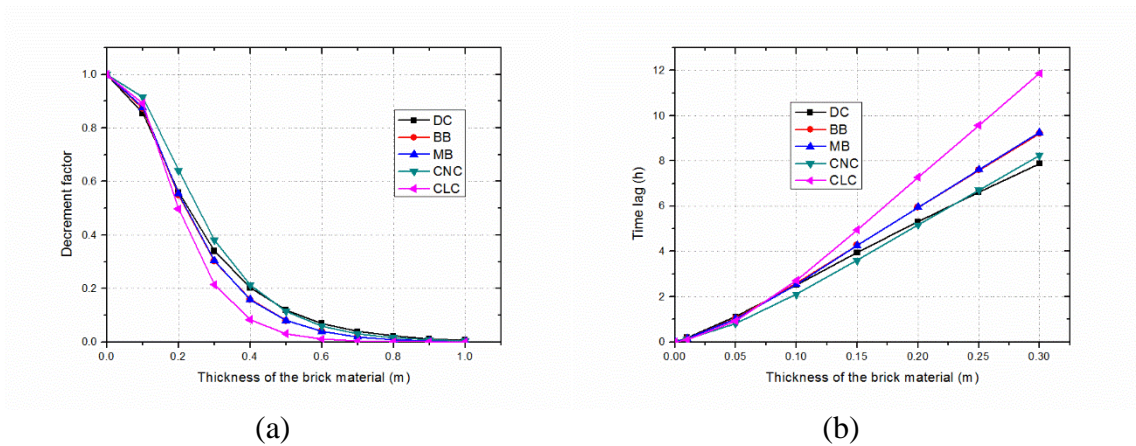


Figure 7.2.2(a) Decrement factor of solid brick as a function of thickness, (b) Time lag of solid brick as a function of thickness

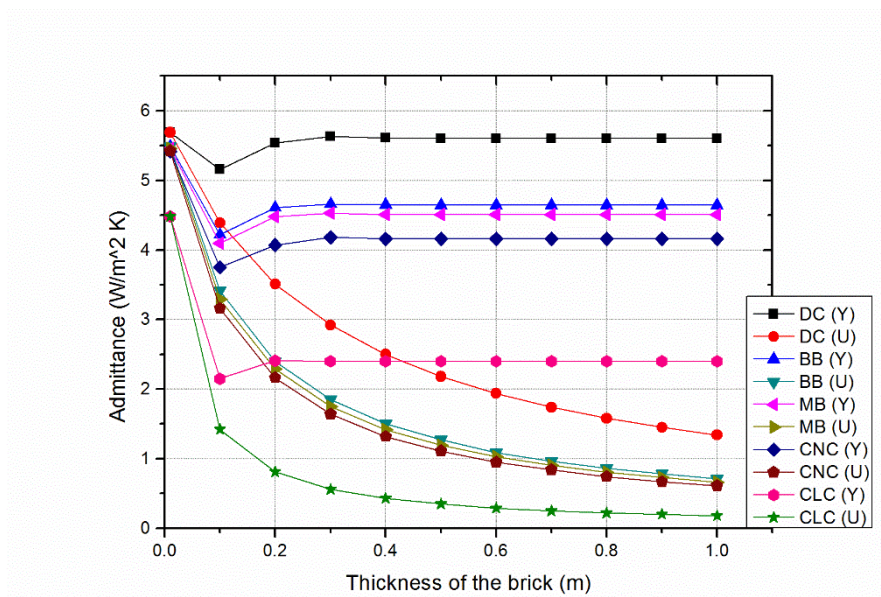


Figure 7.2.3 Admittance and transmittance of solid brick as a function of thickness

7.2.4 Admittance and transmittance of hollow bricks

Figure 7.2.4 shows the admittance and transmittance of hollow bricks of five different brick materials. From the results, it is observed that thermal transmittance decreases with the increase in the number of air gaps in the brick. For reduced cooling loads in the buildings, admittance should be as high as possible and thermal transmittance should be as low as possible. Brick with five air gaps (C-F₆) offers the maximum thermal admittance values at minimum thermal transmittance among all studied configurations with five brick materials. Among all the studied hollow brick

configurations (From C-F₂ to C-F₆), dense concrete block bricks (DC) with five air gaps (C-F₆) offer highest admittance values (3.06 W/m²K) therefore concrete block bricks can store maximum energy (58885 J/m²K) among all studied configurations with five brick materials. Cellular concrete blocks (CLC) offer lowest thermal transmittance for all the configurations among five brick materials studied hence, they are good insulators. It is observed that solid bricks have high thermal admittance with high thermal transmittance values, whereas hollow bricks have good admittance values at reduced thermal transmittance values.

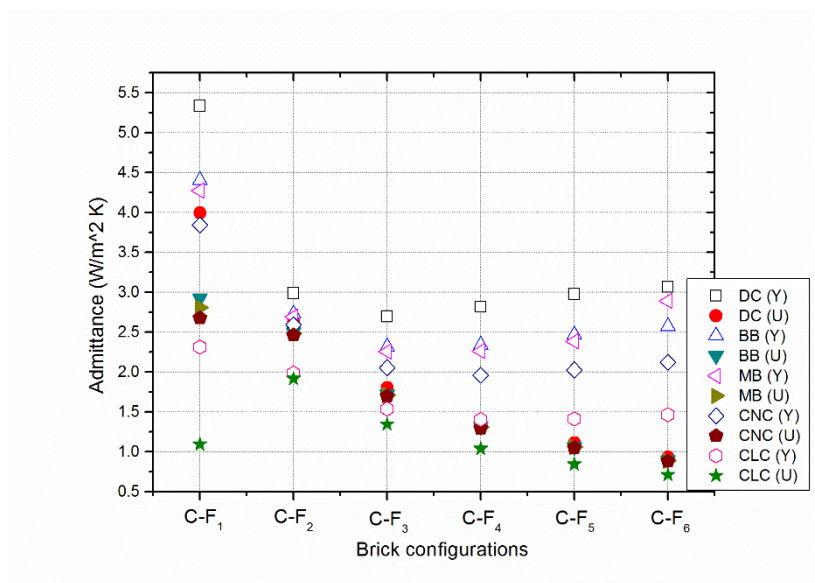


Figure 7.2.4 Admittance and transmittance of hollow bricks

7.2.5 Surface factor and it's time lag of hollow bricks

Figure 7.2.5 shows the surface factor and it's time lag of hollow bricks of five different brick materials. Surface factor should be as low as possible and surface factor time lag should be as high as possible. Responsiveness of the bricks to the short wave radiation decreases with the increase in the number of air gaps in the bricks. From the results, it is observed that bricks with five air gaps (C-F₆) have higher surface factor time lags compared to the other hollow brick configurations. Dense concrete blocks (DC) with five air gaps offer highest surface factor time lags (1.37) among all the studied hollow brick configurations (C-F₂ to C-F₆). Hence, they are slow responsive to short wave radiation than any other studied hollow brick configurations with five brick materials.

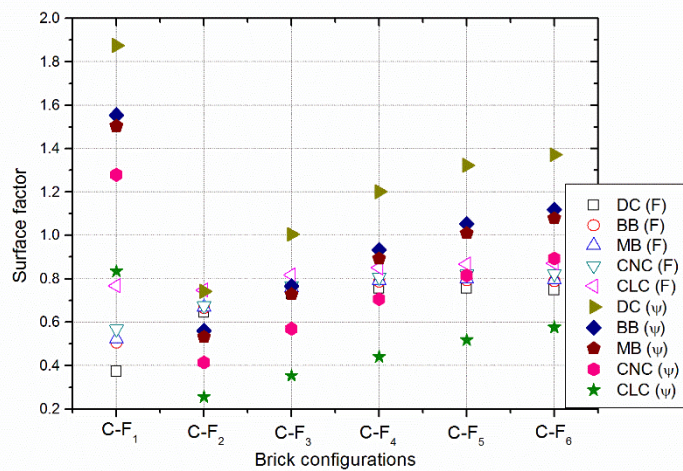


Figure 7.2.5 Surface factor and it's time lag of hollow bricks

7.2.6 Decrement factor and it's time lag of hollow bricks

Figure 7.2.6 (a) and 7.2.6 (b) show the decrement factor and it's time lag of hollow bricks of five different brick materials respectively. Hollow effect is significant on decrement factor and time lag values. The decrement factor decreases and time lag value increase with the increase in the number of air gaps in the bricks. Bricks with four air gaps offer the lowest decrement factor and the highest time lag values among all the studied hollow bricks. From the results, it is observed that dense concrete block (DC) with five air gaps offer the least decrement factor (0.64) and highest time lag (5.84) values among all the studied configurations with five brick materials. Hence increasing the number of air gaps in the bricks is the best from lower decrement factor and higher time lag perspective.

7.2.7 Areal thermal heat capacity of hollow bricks

Figure 7.2.7 shows the areal thermal heat capacity of the hollow bricks. This gives the clear picture of the amount of energy stored in the brick during daytime. The same amount of energy will be released during night time. From the results, it is noticed that areal thermal heat capacity increases with the increase in the number of air gaps in the bricks. Dense concrete block is observed to be efficient for storing maximum energy among all the configurations of five brick materials studied, whereas cellular concrete blocks are observed to be poor in storage among all the configurations studied with five brick materials. Dense concrete block (DC) with five air gaps (C-F₆)

stores maximum energy (58885 J/m²K) among all the hollow brick configurations studied with five brick materials.

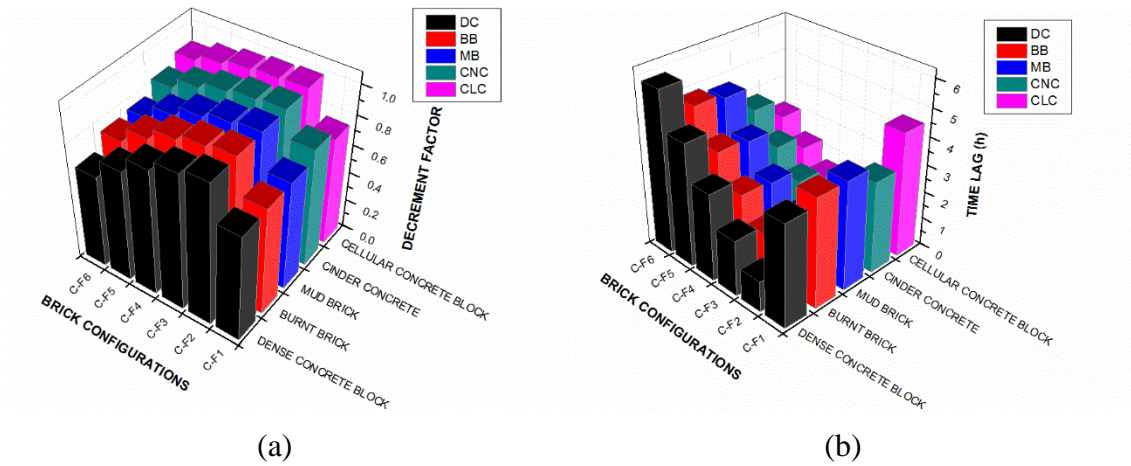


Figure 7.2.6 (a) Decrement factor of hollow bricks, (b) Time lag of hollow bricks

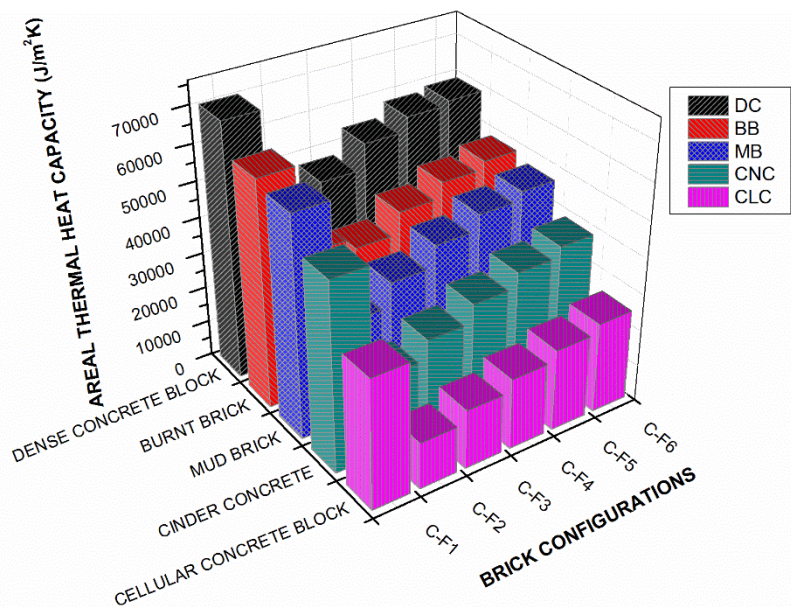


Figure 7.2.7 Areal thermal heat capacity of hollow bricks

7.3. DYNAMIC THERMAL PERFORMANCE OF STUFFED BRICKS

7.3.1 Thermal properties and dynamic thermal parameters of bricks

Table 7.3.1 shows the thermal properties of brick and insulation materials considered for this study. The thermal properties of the brick and insulation materials are as per the Indian standards (SP: 41, 1987). Four brick materials such as mud brick, burnt brick, concrete block and fly ash bricks were selected and two insulation materials such as foam glass and asbestos fiber were selected as filling materials in the shell of the bricks. Figure 7.3.1 shows configurations of the bricks. The various configuration of the bricks are solid brick (C-G₁), bricks with the shell of the brick filled with single layer of insulation (C-G₂), bricks with the shell of the brick filled with two layers of insulation with each insulation layer separated by a brick web (C-G₃), bricks with the shell of the brick filled with three layers of insulation with each insulation layer separated by a brick web (C-G₄), bricks with the shell of the brick filled with four layers of insulation with each insulation layer separated by a brick web (C-G₅) and bricks with the shell of the brick filled with five layers of insulation with each insulation layer separated by a brick web (C-G₆). Table 7.3.2 shows the brick configurations with thicknesses. The nominal thickness of brick configurations is considered as 0.14 m and the web thickness is maintained 0.01 m (not less than 0.008 m) as per the Indian standards. The dynamic thermal parameters of bricks include thermal transmittance, thermal admittance, decrement factor, time lag and areal thermal heat capacity. The computer simulation program was developed and used to compute dynamic thermal parameters of various brick configurations. The accuracy of the computer simulation results was validated with the CIBSE standard values and its accuracy is confirming to CIBSE standards. The outside and inside surface resistances of the bricks considered for the study is 0.04 m² K/W and 0.13 m² K/W respectively as per the CIBSE standards. Table 7.3.3 shows the dynamic thermal parameters of mud bricks filled with foam glass insulation. Table 7.3.4 shows the dynamic thermal parameters of mud bricks filled with asbestos fiber insulation. Table 7.3.5 shows the dynamic thermal parameters of burnt bricks filled with foam glass insulation. Table 7.3.6 shows the dynamic thermal parameters of burnt bricks filled with asbestos fiber insulation. Table 7.3.7 shows the dynamic thermal parameters of

concrete blocks filled with foam glass insulation. Table 7.3.8 shows the dynamic thermal parameters of concrete blocks filled with asbestos fiber insulation. Table 7.3.9 shows the dynamic thermal parameters of fly ash bricks filled with foam glass insulation. Table 7.3.10 shows the dynamic thermal parameters of fly ash bricks filled with asbestos fiber insulation.

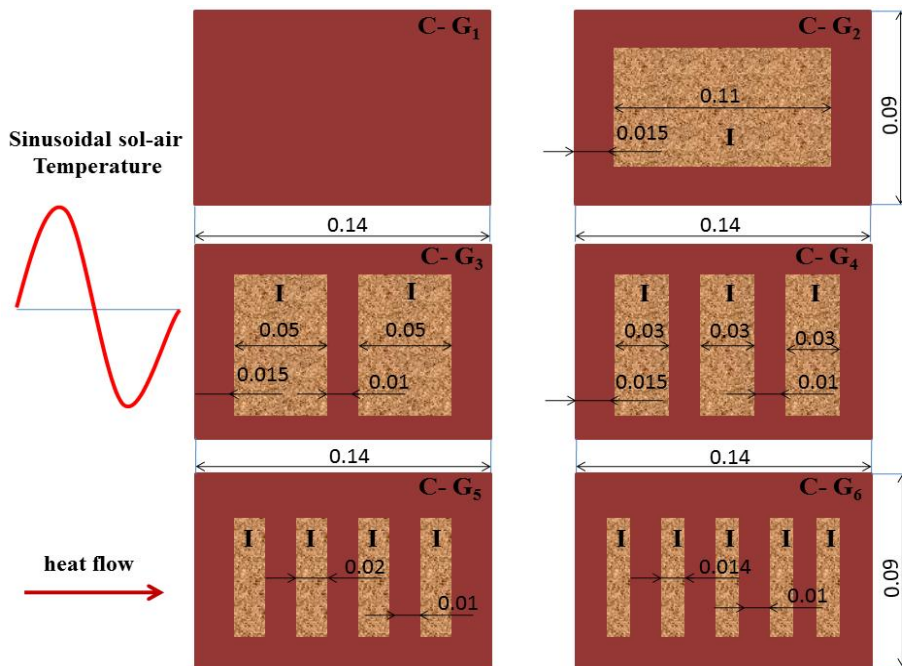


Figure 7.3.1 Configurations of bricks

Table 7.3.1 Thermal properties of brick and insulation materials

Brick and insulation materials	Code	k	ρ	Cp
Mud brick (B)	MB	0.75	1731	880
Burnt brick (B)	BB	0.811	1820	880
Dense concrete block (B)	DC	1.74	2410	880
Fly ash brick (B)	FAB	0.360	1700	857
Foam glass (I)	FG	0.055	160	750
Asbestos fiber (I)	AF	0.06	640	840

Table 7.3.2 Brick configurations and Thickness

S.No.	Configuration	Thickness of the brick from outside to inside (m)
1.	C-G ₁	0.14B
2.	C-G ₂	0.015B+0.11I+0.015B
3.	C-G ₃	0.015B+0.05I+0.01B+0.05I+0.015B
4.	C-G ₄	0.015B+0.03I+0.01B+0.03I+0.01B+0.03I+0.015B
5.	C-G ₅	0.015B+0.02I+0.01B+0.02I+0.01B+0.02I+0.01B+0.02I+0.015B
6.	C-G ₆	0.015B+0.014I+0.01B+0.014I+0.01B+0.014I+0.01B+0.014I+0.01B+0.014I+0.015B

Table 7.3.3 Dynamic thermal parameters of mud bricks filled with foam glass insulation

MB with FG Configuration	U (W/m ² K)	f	φ (h)	Y (W/m ² K)	ω (h)	χ (J/m ² K)
C-G ₁	2.8048	0.75336	3.9118	4.2737	1.4119	60797
C-G ₂	0.4525	0.9386	2.5657	1.8469	4.0568	29867
C-G ₃	0.4899	0.7764	4.0927	1.9555	3.7253	33034
C-G ₄	0.5339	0.7019	5.0626	2.1046	3.4474	36459
C-G ₅	0.5867	0.6519	5.7125	2.2575	3.2165	39883
C-G ₆	0.6511	0.6184	6.1351	2.4142	3.0153	43478

Table 7.3.4 Dynamic thermal parameters of mud bricks filled with asbestos fiber insulation

MB with AF Configuration	U (W/m ² K)	f	φ (h)	Y (W/m ² K)	ω (h)	χ (J/m ² K)
C-G ₁	2.8048	0.75336	3.9118	4.2737	1.4119	60797
C-G ₂	0.4894	0.6513	6.3317	2.4181	3.3967	41956
C-G ₃	0.5291	0.5658	6.7176	2.3838	3.2561	41452
C-G ₄	0.5759	0.5377	7.0252	2.4437	3.0710	43079
C-G ₅	0.6316	0.5270	7.1740	2.5391	2.9136	45498
C-G ₆	0.6994	0.5255	7.1997	2.6534	2.7718	48446

Table 7.3.5 Dynamic thermal parameters of burnt bricks filled with foam glass insulation

BB with FG Configuration	U (W/m ² K)	f	φ (h)	Y (W/m ² K)	ω (h)	χ (J/m ² K)
C-G ₁	2.9197	0.74693	3.9355	4.4045	1.3641	62491
C-G ₂	0.4531	0.9362	2.6091	1.9177	4.0603	31051
C-G ₃	0.4908	0.7644	4.2029	2.0250	3.7233	34235
C-G ₄	0.5354	0.6865	5.2147	2.1742	3.4395	37688
C-G ₅	0.5888	0.6349	5.8896	2.3278	3.2043	41151
C-G ₆	0.6541	0.6006	6.3261	2.4858	2.9999	44809

Table 7.3.6 Dynamic thermal parameters of burnt bricks filled with asbestos fiber insulation

BB with AF Configuration	U (W/m ² K)	f	φ (h)	Y (W/m ² K)	ω (h)	χ (J/m ² K)
C-G ₁	2.9197	0.7469	3.9355	4.4045	1.3641	62491.44
C-G ₂	0.4901	0.6504	6.3650	2.4806	3.4052	43053
C-G ₃	0.5303	0.5584	6.7915	2.4429	3.2632	42468
C-G ₄	0.5775	0.5275	7.1358	2.5027	3.0729	44115
C-G ₅	0.6340	0.5150	7.3104	2.5999	2.9103	46599
C-G ₆	0.7028	0.5123	7.3535	2.7168	2.7639	49643

Table 7.3.7 Dynamic thermal parameters of dense concrete blocks filled with foam glass insulation

DC with FG Configuration	U (W/m ² K)	f	φ (h)	Y (W/m ² K)	ω (h)	χ (J/m ² K)
C-G ₁	3.9947	0.73609	3.6727	5.3355	0.98347	70521
C-G ₂	0.4572	0.9196	2.8710	2.3803	4.0335	38878
C-G ₃	0.4973	0.6877	4.8589	2.4692	3.6794	41928
C-G ₄	0.5450	0.5921	6.1191	2.6108	3.3733	45397
C-G ₅	0.6028	0.5342	6.9372	2.7634	3.1219	49033
C-G ₆	0.6744	0.4987	7.4480	2.9257	2.9038	53053

Table 7.3.8 Dynamic thermal parameters of concrete blocks filled with asbestos fiber insulation

DC with AF Configuration	U (W/m ² K)	f	φ (h)	Y (W/m ² K)	ω (h)	χ ₂ (J/m ² K)
C-G ₁	3.9947	0.73609	3.6727	5.3355	0.98347	70521
C-G ₂	0.4949	0.6435	6.5613	2.8919	3.4254	50411
C-G ₃	0.5378	0.5123	7.2328	2.8303	3.2819	49238
C-G ₄	0.5887	0.4653	7.8014	2.8848	3.0674	50929
C-G ₅	0.6503	0.4441	8.1286	2.9887	2.8795	53766
C-G ₆	0.7263	0.4359	8.2666	3.1181	2.7090	57366

Table 7.3.9 Dynamic thermal parameters of fly ash bricks filled with foam glass insulation

FAB with FG Configuration	U (W/m ² K)	f	φ (h)	Y (W/m ² K)	ω (h)	χ ₂ (J/m ² K)
C-G ₁	1.7897	0.64005	5.34	3.6448	1.764	56658
C-G ₂	0.4438	0.9344	2.6821	1.7703	4.0152	28722
C-G ₃	0.4764	0.7760	4.1785	1.8725	3.6895	31644
C-G ₄	0.5141	0.6990	5.1548	2.0099	3.4177	34747
C-G ₅	0.5583	0.6448	5.8348	2.1480	3.1928	37764
C-G ₆	0.6109	0.6060	6.3065	2.2865	2.9984	40839

Table 7.3.10 Dynamic thermal parameters of fly ash bricks filled with asbestos fiber insulation

FAB with AF Configuration	U (W/m ² K)	f	φ (h)	Y (W/m ² K)	ω (h)	χ ₂ (J/m ² K)
C-G ₁	1.7897	0.6400	5.34	3.6448	1.764	56658
C-G ₂	0.4793	0.6341	6.5313	2.3147	3.3238	40125
C-G ₃	0.5134	0.5548	6.9026	2.2827	3.1949	39608
C-G ₄	0.5529	0.5257	7.2138	2.3331	3.0231	40934
C-G ₅	0.5988	0.5119	7.3887	2.4137	2.8770	42917
C-G ₆	0.6532	0.5060	7.4591	2.5093	2.7461	45296

7.3.2 Thermal transmittance and admittance of insulation filled bricks

Thermal admittance and thermal transmittance have the same units. Thermal admittance is the ability of a brick to admit, absorb and emit heat. Thermal admittance mainly depends upon thermal properties of inner side of the brick. For thin bricks, thermal transmittance and thermal admittance are the same. Thermal admittance

becomes constant for bricks more than 0.2 m thick. Figure 7.3.2 shows the thermal transmittance and admittance of bricks filled with foam glass insulation. From the results, it is observed that the thermal transmittance of the stuffed bricks is less than the conventional solid bricks and hence the stuffed bricks have more thermal resistance than the solid bricks. It is also noticed from the results that the thermal admittance of the stuffed bricks increases with the increasing number of insulation layers in the brick. The Bricks with the shell of the brick filled with five layers of insulation with each insulation layer separated by a brick web have more thermal mass than the Bricks with the shell of the brick filled with single layer of insulation. From Figure 7.3.2, it is observed that the concrete blocks with the shell of the brick filled with five foam glass layers of insulation with each insulation layer separated by a brick web have the highest admittance value ($2.9257 \text{ W/m}^2\text{K}$) among all the studied bricks filled with foam glass insulation. It is also clear from the results that the fly ash bricks with the shell of the brick filled with five foam glass layers of insulation with each insulation layer separated by a brick web have the lowest admittance value ($2.2865 \text{ W/m}^2\text{K}$) among all the studied bricks filled with foam glass insulation. Figure 7.3.3 shows the thermal transmittance and admittance of bricks filled with asbestos fiber insulation. From the results, it is noticed that the concrete blocks with the shell of the brick filled with five asbestos fiber layers of insulation with each insulation layer separated by a brick web have the highest admittance value ($3.1181 \text{ W/m}^2\text{K}$) among all the studied bricks filled with asbestos fiber insulation. It is also clear from the results that the fly ash bricks with the shell of the brick filled with five asbestos layers of insulation with each insulation layer separated by a brick web have the lowest admittance value ($2.5093 \text{ W/m}^2\text{K}$) among all the studied bricks filled with asbestos fiber insulation.

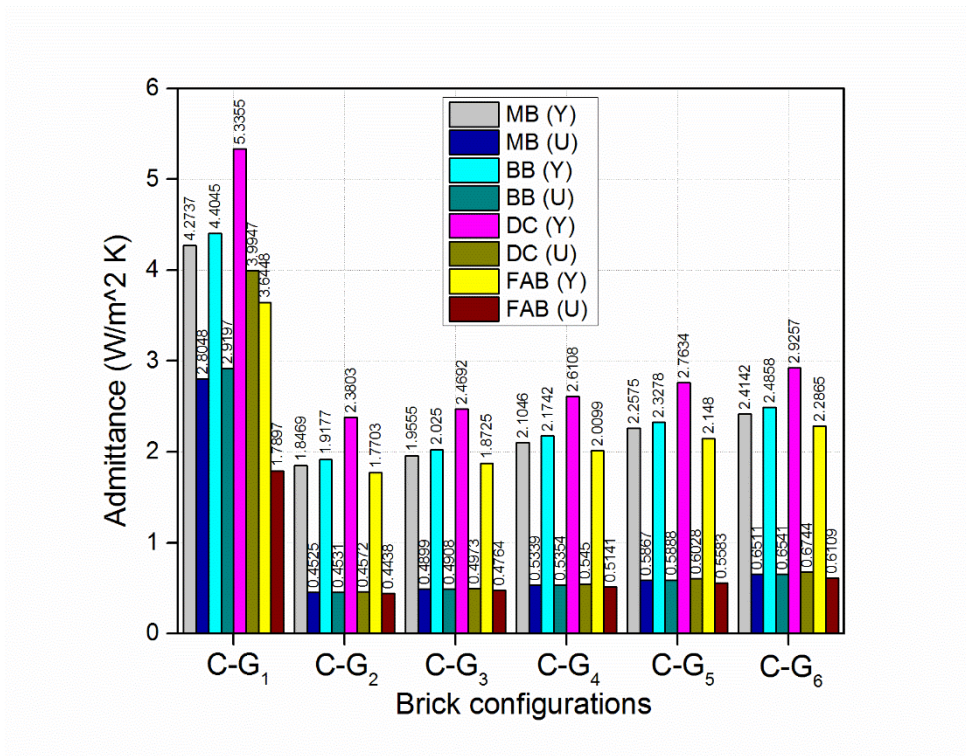


Figure 7.3.2 Thermal transmittance and admittance of bricks filled with foam glass insulation

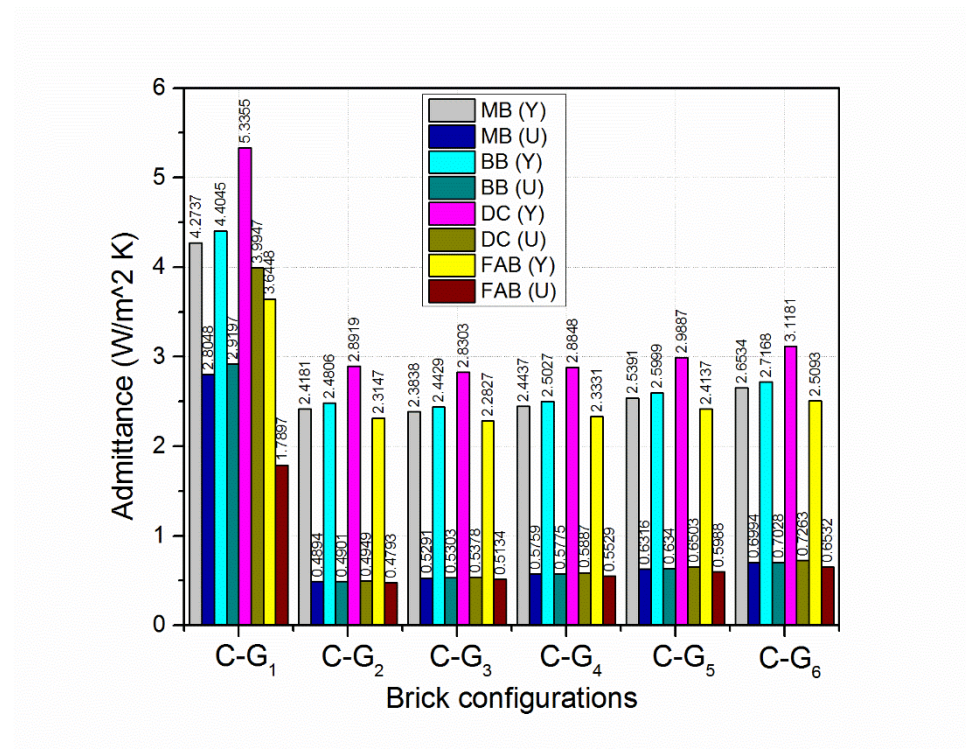


Figure 7.3.3 Thermal transmittance and admittance of bricks filled with asbestos fibre insulation

7.3.3 Decrement factor and time lag of insulation filled bricks

The dampening of the outside sinusoidal heat wave as it passes through the brick (Decrement factor) should be as low as possible to reduce the outside heat wave effect on indoor comfort conditions. The time taken by heat wave to pass from outer side of the brick to the inner side of the brick (Time lag) should be as high as possible. The decrement factor and time lag are the measures of thermal mass. Figure 7.3.4 (a) shows the decrement factor of bricks filled with foam glass insulation. From the results, it is observed that the decrement factor decreases and time lag increases with the increasing number of insulation layers in the brick. It is also observed that the mud bricks with the shell of the brick filled with five foam glass layers of insulation with each insulation layer separated by a brick web have the highest decrement factor value (0.6184) among all the studied bricks filled with foam glass insulation. It is also clear from the results that the concrete blocks with the shell of the brick filled with five foam glass layers of insulation with each insulation layer separated by a brick web have the lowest decrement value (0.4987) among all the studied bricks filled with foam glass insulation. Figure 7.3.4 (b) shows the time lag of bricks filled with foam glass insulation. From the results, it is observed that the concrete blocks with the shell of the brick filled with five foam glass layers of insulation with each insulation layer separated by a brick web have the highest time lag value (7.448 h) among all the studied bricks filled with foam glass insulation. It is also clear from the results that the mud bricks with the shell of the brick filled with five foam glass layers of insulation with each insulation layer separated by a brick web have the lowest time lag value (6.1351 h) among all the studied bricks filled with foam glass insulation. Figure 7.3.5 (a) shows the decrement factor of bricks filled with asbestos fiber insulation. From the results, it is noticed that the mud bricks with the shell of the brick filled with five asbestos fiber layers of insulation with each insulation layer separated by a brick web have the highest decrement factor value (0.5255) among all the studied bricks filled with asbestos fiber insulation. It is also clear from the results that the concrete blocks with the shell of the brick filled with five asbestos fiber layers of insulation with each insulation layer separated by a brick web have the lowest decrement value (0.4359) among all the studied bricks filled with foam glass insulation. Figure 7.3.5 (b) shows

the time lag of bricks filled with asbestos insulation. From the results, it is observed that the concrete blocks with the shell of the brick filled with five asbestos fiber layers of insulation with each insulation layer separated by a brick web have the highest time lag value (8.266 h) among all the studied bricks filled with asbestos fiber insulation. It is also clear from the results that the mud bricks with the shell of the brick filled with five asbestos fiber layers of insulation with each insulation layer separated by a brick web have the lowest time lag value (7.199 h) among all the studied bricks filled with asbestos fiber insulation.

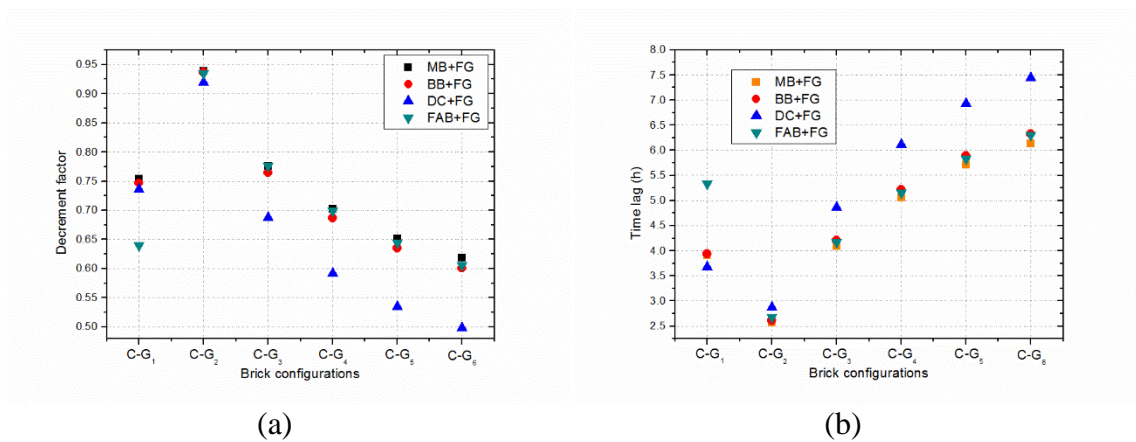


Figure 7.3.4 Decrement factor and time lag of bricks filled with foam glass Insulation

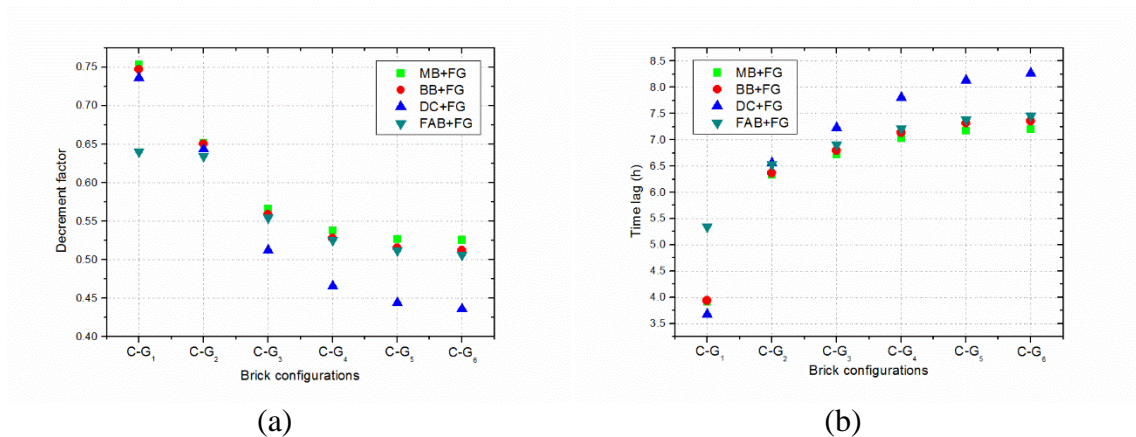


Figure 7.3.5 Decrement factor and time lag of bricks filled with asbestos fibre Insulation

7.3.4 Areal thermal heat capacity of insulation filled bricks

The areal thermal heat capacity of the brick is the amount of heat stored in the brick over the first half period of the heat flow swing per unit area of brick element per unit degree of temperature swing. This gives the information about thermal mass of the brick. Figure 7.3.6 shows areal thermal heat capacity of bricks filled with foam glass insulation. From the results, it is noticed that the concrete blocks with the shell of the brick filled with five foam glass layers of insulation with each insulation layer separated by a brick web have the highest areal thermal heat capacity ($53053 \text{ J/m}^2\text{K}$) among all the studied bricks filled with foam glass insulation. It is also clear from the results that the fly ash bricks with the shell of the brick filled with five foam glass layers of insulation with each insulation layer separated by a brick web have the lowest areal thermal heat capacity value ($40839 \text{ J/m}^2\text{K}$) among all the studied bricks filled with foam glass insulation. Figure 7.3.7 shows the areal thermal heat capacity of bricks filled with asbestos fiber insulation. From the results, it is noticed that the concrete blocks with the shell of the brick filled with five asbestos fiber layers of insulation with each insulation layer separated by a brick web have the highest areal thermal heat capacity ($57366 \text{ J/m}^2\text{K}$) among all the studied bricks filled with asbestos fiber insulation. It is also observed from the results that the fly ash bricks with the shell of the brick filled with five asbestos fiber layers of insulation with each insulation layer separated by a brick web have the lowest areal thermal heat capacity value ($45296 \text{ J/m}^2\text{K}$) among all the studied bricks filled with asbestos fiber insulation.

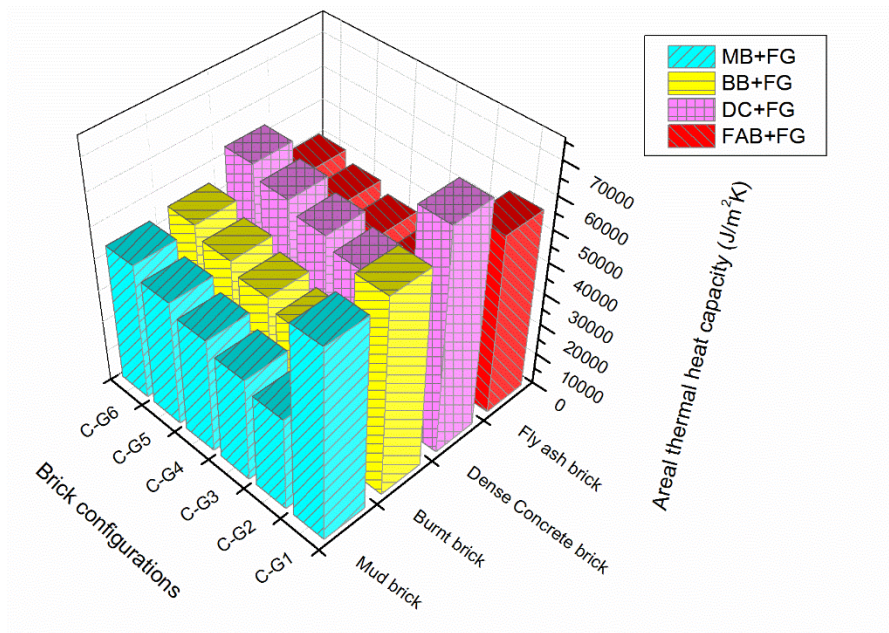


Figure 7.3.6 Areal thermal heat capacity of bricks filled with foam glass insulation

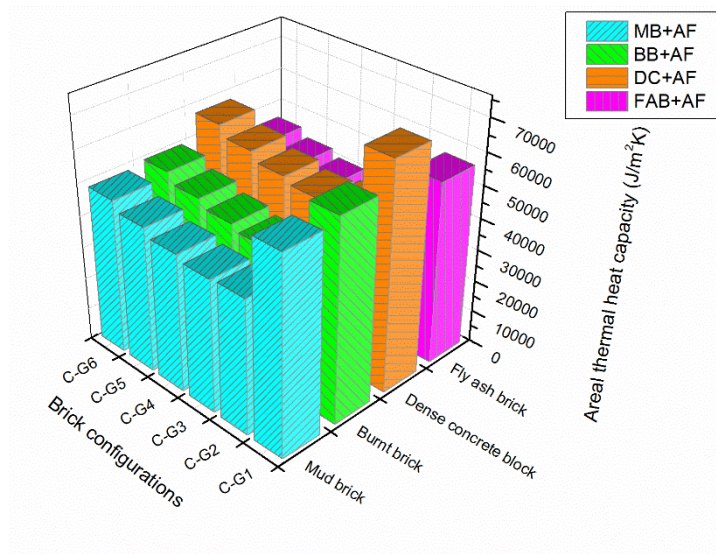


Figure 7.3.7 Areal thermal heat capacity of bricks filled with asbestos fiber insulation

7.4 SUMMARY

- From 7.2, it is noticed that the thermal admittance, decrement time lag, surface factor time lag and areal thermal heat capacity of the bricks increase with the increase in the number of air gaps within the brick due to improved thermal mass and thermal insulation. These enhanced unsteady state properties make the hollow bricks more energy efficient than the solid bricks.

- Thermal transmittance and decrement factor of the hollow bricks decrease with the increase in the number of air gaps in the bricks. This behavior of the bricks helps in reducing cooling loads of the buildings.
- Dense concrete block (DC) with five air gaps offers the highest admittance (5.84) at minimum thermal transmittance, lowest decrement factor (0.64), highest time lag (5.84h), highest areal thermal heat capacity (58885 J/m²K) and highest surface factor time lag (1.37h) values among twenty five hollow brick configurations with five brick materials. Hence, these hollow bricks are recommended for energy efficient building construction among five brick materials.
- Increase in the air gaps in the bricks increases the thermal insulation (decreases the thermal transmittance) and increases the thermal mass. These are essential parameters for energy efficient hollow bricks.
- Hollow bricks with five air spaces (C-F₆) decrease decrement factor of dense concrete bricks, burnt bricks, mud bricks, cinder concrete bricks and cellular concrete bricks by 34.32%, 25.38%, 24.27%, 16.54% and 11.05%, respectively as compared to the hollow brick with single air space (C-F₂).
- Hollow bricks with five air spaces (C-F₆) increase the time lag of dense concrete bricks, burnt bricks, mud bricks, cinder concrete bricks and cellular concrete bricks by 81.17%, 81.70%, 81.78%, 82.31% and 81.88%, respectively as compared to the hollow brick with single air space (C-F₂).
- From 7.3, it is observed that the thermal admittance, decrement time lag and areal thermal heat capacity of the insulation filled bricks increase with the increase in the number of insulation layers in the bricks due to improved thermal mass. These enhanced dynamic parameters make the stuffed bricks more energy efficient than the ordinary solid bricks.
- The decrement factor of the insulation filled bricks decreases with the increase in the number of insulation layers in the bricks. The lower decrement factor values are essential to reduce the effect of outdoor climatic changes on indoor conditions.
- The concrete blocks with the shell of the bricks filled with five layers of asbestos fiber insulation offer the highest admittance (3.11W/m²K), the lowest decrement factor

(0.435), the highest time lag values (8.26 h) and the highest areal thermal heat capacity ($57366 \text{ J/m}^2\text{K}$) among all insulation filled bricks studied.

- Stuffed bricks with five foam glass insulation layers (C-G₆) decrease the decrement factor of mud bricks, burnt bricks, dense concrete bricks and fly ash bricks by 17.91%, 35.84%, 45.76% and 35.14%, respectively as compared to the stuffed bricks with single foam glass insulation layer (C-G₂).
- Stuffed bricks with five foam glass insulation layers (C-G₆) increase the time lag of mud bricks, burnt bricks, dense concrete bricks and fly ash bricks by 36.23%, 58.75%, 61.45% and 57.47%, respectively as compared to the stuffed bricks with single foam glass insulation layer (C-G₂).
- In hot regions, the wall thermal transmittance should be as low as possible and the wall admittance should be as high as possible. In cold regions, the wall thermal transmittance should be as high as possible and the wall admittance should be as low as possible. For reducing cooling loads, the stuffed bricks are recommended and for reducing heating loads, the hollow bricks are recommended.
- The results of the paper help in designing energy efficient hollow and stuffed bricks for reducing cooling loads in buildings.

CHAPTER-8

EFFECTS OF WIND VELOCITY ON DYNAMIC THERMAL CHARACTERISTICS OF OUTER BUILDING ENCLOSURES

8.1 INTRODUCTION

This chapter presents the effect of wind velocity on dynamic thermal characteristics of outer building walls. The dynamic thermal characteristics studied include transmittance, admittance, decrement factor, time lag surface factor, surface factor time lag and areal thermal heat capacity. The building wall materials investigated include burnt bricks, mud bricks, laterite stone and cinder concrete. The various configurations of composite walls studied are the composite wall without insulation, composite wall with insulation located at outer side of the wall, composite wall with insulation located at the mid center of the wall, composite wall with insulation located at inner side of the wall, composite wall with one half of the insulation located at the outer and another half of the insulation located at the inner side of the wall, composite wall with one half of the insulation located at the outer side and another half of the insulation located at the mid center of the wall, composite wall with one half of the insulation located at mid center of the wall and another half of the insulation located at the inner side of the wall. The thermal performance of the homogeneous and composite walls was investigated from wind velocity ranging from 0 to 10 m/s. The total two hundred and fifty six building walls were studied. From the results, it is observed that the admittance, decrement factor and areal thermal heat capacity of the homogeneous building materials decrease with the increase in the external wind velocity. It is also observed that thermal transmittance and surface factor of the homogeneous walls increase with the increase in the external wind velocity. The building wall with half of the insulation placed at the outside of the wall and another half of the insulation placed at the inner side of the wall is observed to be the best

configuration from the low decrement factor at all wind velocities. The building wall with half of the insulation placed at the outside of the wall and another half of the insulation placed at the mid center of the wall is observed to be the best configuration from higher time lag values at all wind velocities.

8.2 BUILDING MATERIAL THERMAL PROPERTIES AND THEIR UNSTEADY THERMAL RESPONSE CHARACTERISTICS

Table 8.2.1 shows the thermo physical properties of the building materials considered for the study. The properties of burnt bricks, mud bricks, cinder concrete and expanded polystyrene were taken as per the Indian standard guide for heat insulation of non-industrial buildings as per IS code 3792-1978. In this code guarded hot plate method and ASTM heat flow methods are used to calculate thermal properties of building materials (IS: 3792 1978). Thermal properties of laterite stone were measured using the transient plane source method experimentally at K- Analys, Sweden. The computer program was developed to compute the dynamic thermal characteristics of homogeneous and composite walls exposed to various wind velocities. In this study, walls are considered as outer enclosures of the building and hence external and internal surface resistances taken are $0.04 \text{ m}^2 \text{ K/W}$ and $0.13 \text{ m}^2 \text{ K/W}$, respectively as per CIBSE standards. Figure 8.2.1 shows images of building and insulating materials. Figure 8.2.2 Configuration of composite walls with expanded polystyrene insulation. The various configurations of composite walls studied are the composite wall without insulation (C-H₁), composite wall with insulation located at outer side of the wall (C-H₂), composite wall with insulation located at the mid center of the wall (C-H₃), composite wall with insulation located at inner side of the wall (C-H₄), composite wall with one half of the insulation located at the outer and another half of the insulation located at the inner side of the wall (C-H₅), composite wall with one half of the insulation located at the outer side and another half of the insulation located at the mid center of the wall (C-H₆), composite wall with one half of the insulation located at mid center of the wall and another half of the insulation located at the inner side of the wall (C-H₇). Table 8.2.2 shows the effect of wind velocity on dynamic thermal characteristics of homogeneous burnt brick walls. Table 8.2.3 shows the effect of wind velocity on dynamic thermal characteristics of homogeneous mud

brick walls. Table 8.2.4 shows the effect of wind velocity on dynamic thermal characteristics of homogeneous laterite stone walls. Table 8.2.5 shows the effect of wind velocity on dynamic thermal characteristics of homogeneous cinder concrete walls.

Table 8.2.1 Thermo physical properties of building materials

S.No.	Building material	Code	k [W/mK]	ρ [kg/m ³]	C _p [J/kgK]
1.	Burnt brick	BB	0.811	1820	880
2.	Mud brick	MB	0.75	1731	880
3.	Laterite stone	LS	1.369	1000	1926
4.	Cinder concrete	CNC	0.686	1406	840
5.	Expanded polystyrene	EP	0.038	16	1340
6.	Cement plaster	P	0.721	1762	840

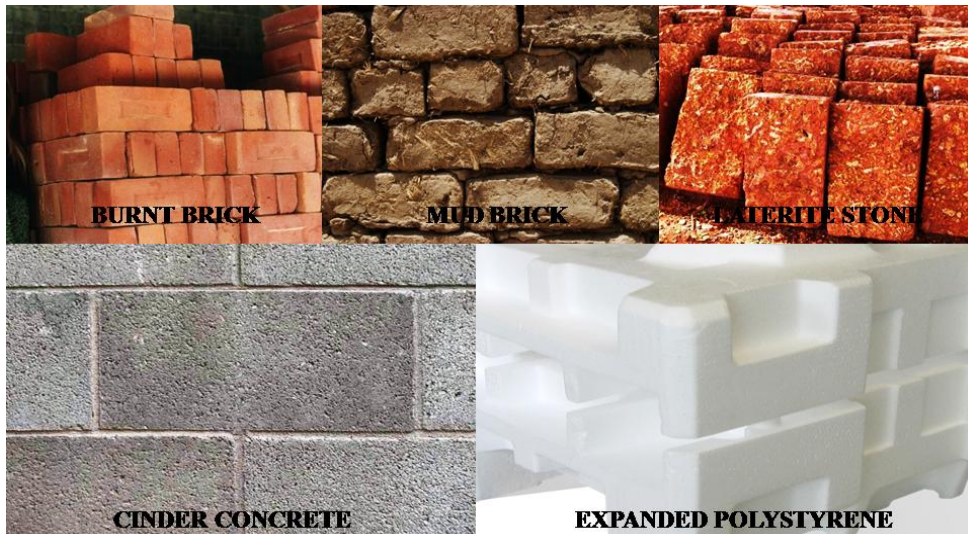


Figure 8.2.1 Building and insulation materials

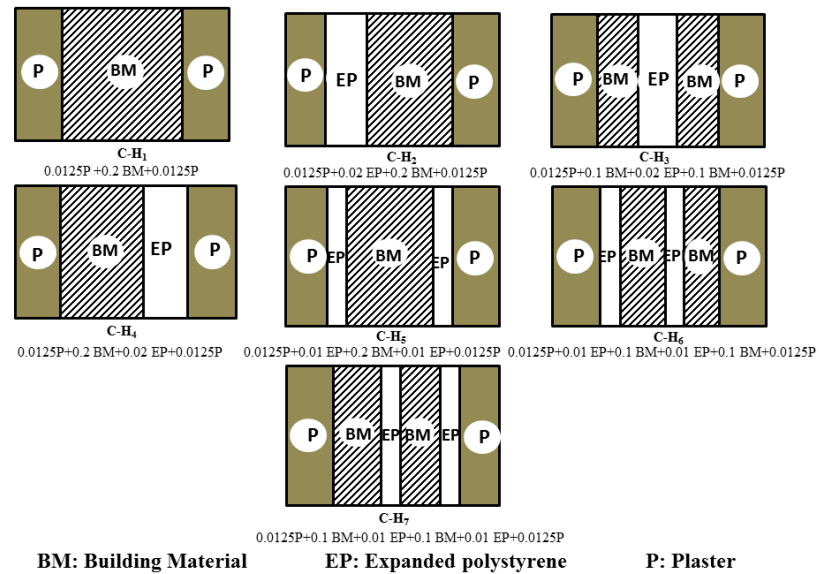


Figure 8.2.2 Configuration of composite walls with expanded polystyrene insulation

Table 8.2.2 Effect of wind velocity on dynamic thermal characteristics of homogeneous burnt brick walls

Burnt brick								
Velocity (m/s)	U (W/m ² K)	f	φ (h)	Y (W/m ² K)	ω (h)	F	Ψ (h)	χ ₂ (J/m ² K)
0	1.9749	0.41445	6.8586	4.6998	1.3445	0.47608	1.7488	71391
0.5	2.2754	0.5043	6.2763	4.65	1.3757	0.48414	1.7385	71994
0.7	2.3121	0.51699	6.1877	4.6415	1.3793	0.48531	1.7353	71976
2	2.4011	0.54908	5.9543	4.6182	1.3874	0.48831	1.7249	71789
4	2.4126	0.55337	5.9219	4.6149	1.3884	0.48872	1.7232	71748
6	2.4662	0.57364	5.7647	4.5985	1.3923	0.49062	1.7145	71490
8	2.4846	0.5807	5.7081	4.5926	1.3934	0.49128	1.7111	71376
10	2.5286	0.59774	5.5671	4.5775	1.3956	0.49288	1.7019	71039

Table 8.2.3 Effect of wind velocity on dynamic thermal characteristics of homogeneous mud brick walls

Mud brick								
Velocity (m/s)	U (W/m ² K)	f	φ (h)	Y (W/m ² K)	ω (h)	F	Ψ (h)	χ ₂ (J/m ² K)
0	1.8997	0.42393	6.8465	4.5656	1.3961	0.49402	1.6934	69526
0.5	2.176	0.51174	6.2681	4.518	1.427	0.50172	1.6844	70079
0.7	2.2097	0.52392	6.1815	4.5101	1.4306	0.50283	1.6816	70060
2	2.2908	0.5545	5.9549	4.4885	1.4386	0.50564	1.6725	69884
4	2.3013	0.55857	5.9237	4.4854	1.4396	0.50602	1.6711	69846
6	2.35	0.57771	5.7726	4.4704	1.4435	0.50779	1.6635	69611
8	2.3667	0.58435	5.7185	4.4649	1.4447	0.50841	1.6605	69508
10	2.4065	0.60032	5.584	4.4512	1.447	0.50989	1.6526	69207

Table 8.2.4 Effect of wind velocity on dynamic thermal characteristics of homogeneous laterite stone walls

Laterite stone								
Velocity (m/s)	U (W/m ² K)	f	φ (h)	Y (W/m ² K)	ω (h)	F	Ψ (h)	χ ₂ (J/m ² K)
0	2.4641	0.39892	6.4128	5.4159	1.098	0.38172	2.0995	80652
0.5	2.9501	0.50425	5.817	5.3241	1.1219	0.39297	2.0415	80667
0.7	3.0122	0.52063	5.718	5.3081	1.1239	0.39465	2.029	80504
2	3.1649	0.56387	5.4456	5.2633	1.1263	0.39893	1.991	79814
4	3.185	0.56985	5.4064	5.2569	1.1263	0.3995	1.9851	79686
6	3.2791	0.59873	5.2116	5.2249	1.1247	0.40216	1.9546	78942
8	3.311	0.60903	5.1394	5.2131	1.1235	0.40307	1.9427	78622
10	3.3903	0.63436	4.955	5.1834	1.119	0.40519	1.9113	77695

Table 8.2.5 Effect of wind velocity on dynamic thermal characteristics of homogeneous cinder concrete walls

Cinder concrete								
Velocity (m/s)	U (W/m ² K)	f	φ (h)	Y (W/m ² K)	ω (h)	F	Ψ (h)	χ ₂ (J/m ² K)
0	1.8139	0.51467	6.0398	4.193	1.5688	0.5459	1.5647	63988
0.5	2.0643	0.60192	5.4686	4.1186	1.5889	0.55458	1.5292	63469
0.7	2.0945	0.61336	5.3868	4.1075	1.5901	0.55569	1.5227	63302
2	2.1672	0.64143	5.1767	4.0789	1.5911	0.55835	1.505	62766
4	2.1766	0.64509	5.1482	4.075	1.5911	0.55869	1.5024	62681
6	2.2202	0.66211	5.0118	4.0565	1.5899	0.56024	1.4898	62240
8	2.2351	0.66794	4.9634	4.05	1.5892	0.56076	1.4851	62069
10	2.2706	0.6818	4.8447	4.034	1.5868	0.56196	1.4734	61615

The homogeneous and composite walls are exposed to periodic cyclic variations in temperatures and the heat flow through the wall is in one direction and i.e. horizontal.

8.3 EFFECT OF WIND VELOCITY ON TRANSMITTANCE AND ADMITTANCE OF HOMOGENEOUS WALLS

The admittance signifies the thermal mass of the wall and thermal transmittance indicates thermal insulation of the wall. The higher the admittance value, the higher is the thermal mass. The lower is the thermal transmittance value, the higher is the thermal insulation value. Figure 8.3.1 shows the effect of wind velocity on transmittance and admittance of homogeneous walls. From the results, it is observed that the thermal transmittance decreases and thermal admittance increases with the increase in the wind velocity. Increase in the outside wind velocity increases the convection coefficient at the external surface which in turn reduces the external surface resistance. Thermal transmittance increases with the increase in the convection coefficient at the external surface and thermal admittance decreases with the increase in the convection coefficient at the external surface. The laterite stone is observed to have higher thermal admittance values as compared to the other studied

building material at all external wind velocities. The expanded polystyrene is observed to have the least thermal transmittance and admittance among studied homogeneous building and insulating materials at all external wind velocities.

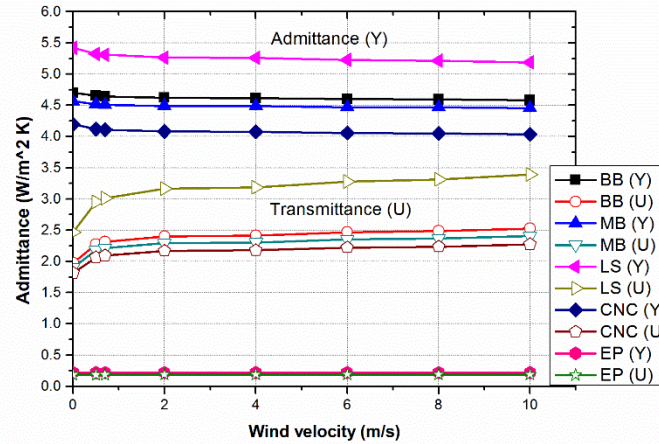


Figure 8.3.1 Effect of wind velocity on transmittance and admittance of homogeneous walls

8.4 EFFECT OF WIND VELOCITY ON DECREMENT FACTOR AND TIME LAG OF HOMOGENEOUS WALLS

Figure 8.4.1 shows the effect of wind velocity on decrement factor and time lag of homogeneous walls. From the results, it is noticed that the decrement factor of the building material increases with the increase in the external wind velocity and the time lag decreases with the increase in the external wind velocity. Increase in external convection coefficient due to increase in external wind velocity increases decrement factor and decreases time lag values. Mud brick has the lowest decrement factor values at all external wind velocities and expanded polystyrene has the highest decrement factor at all external wind velocities among studied materials. It is also noticed that the mud brick has the highest time lag and expanded polystyrene has the least time lag values at all wind velocities among studied building materials.

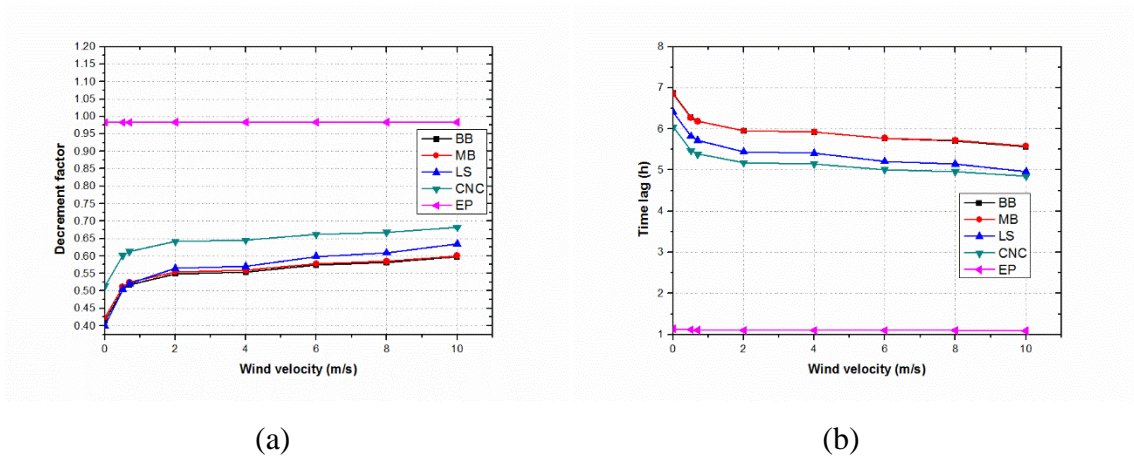


Figure 8.4.1 Effect of wind velocity on: (a) Decrement factor of homogeneous walls, (b) Time lag of homogeneous walls

8.5 EFFECT OF WIND VELOCITY ON SURFACE FACTOR AND SURFACE FACTOR TIME LAG OF HOMOGENEOUS WALLS

Figure 8.5.1 shows the Effect of wind velocity on surface factor and surface factor time lag of homogeneous walls. From the results, it is observed that the surface factor increases and surface factor time lag decreases with the increase in the external wind velocity. The increased external convection coefficient increases the surface factor and decreases the surface factor time lag. The laterite stone has the lowest surface factor and expanded polystyrene has the highest surface factor among studied materials at all external wind velocities. The laterite stone has the highest surface factor time lag and the expanded polystyrene has the lowest surface factor time lag values.

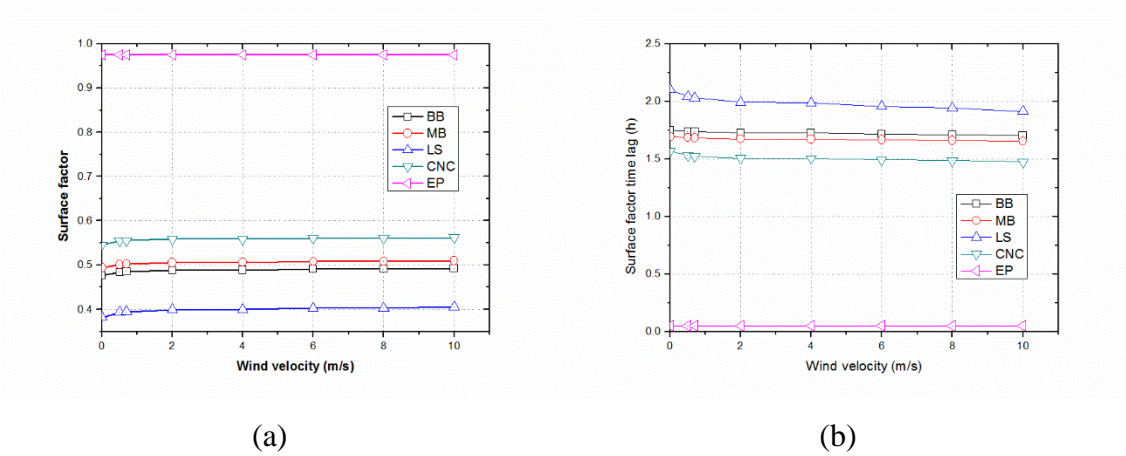


Figure 8.5.1 Effect of wind velocity on: (a) Surface factor of homogeneous walls, (b) Surface factor time lag of homogeneous walls

8.6 EFFECT OF WIND VELOCITY ON AREAL THERMAL HEAT CAPACITY OF HOMOGENEOUS WALLS

Figure 8.6.1 shows the Effect of wind velocity on areal thermal heat capacity of homogeneous walls. The areal thermal heat capacity of building materials decreases with the increase in the external wind velocity. From the results, it is obvious that the laterite stone has the highest areal thermal heat capacity than any other studied building material at all external wind velocities. The expanded polystyrene was observed to have the least areal thermal heat capacity at all external wind velocities among studied building materials.

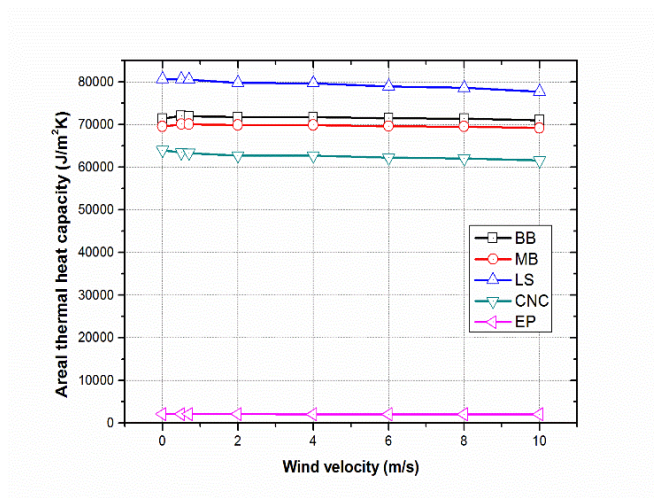


Figure 8.6.1 Effect of wind velocity on areal thermal heat capacity of homogeneous walls

8.7 EFFECT OF WIND VELOCITY ON TRANSMITTANCE AND ADMITTANCE OF COMPOSITE WALLS

Figure 8.7.1 shows the effect of wind velocity on transmittance and admittance of composite burnt brick walls. The burnt brick composite wall with expanded polystyrene insulation located at the mid center of the burnt brick wall (C-H₃) and the burnt brick composite wall with one half of the expanded polystyrene insulation located at the outer side and another half of the insulation located at the mid center of the burnt brick wall (C-H₆) were observed to be energy efficient configurations from higher admittance (At lower transmittance) perspective among seven studied configurations at all external wind velocities. At 10 m/s external wind velocity, the burnt brick composite wall with expanded polystyrene insulation located at the mid center of the burnt brick wall (C-H₃) has 4.898 W/m²K admittance value and 1.0455 W/m²K transmittance value. At 10 m/s external wind velocity, the burnt brick composite wall with one half of the expanded polystyrene insulation located at the outer side and another half of the insulation located at the mid center of the burnt brick wall (C-H₆) has 4.779 W/m²K admittance value and 1.0455 W/m²K transmittance value. The burnt brick composite wall without insulation (C-H₁) has 4.5744 W/m²K admittance value and 2.3247 W/m²K transmittance value. Higher thermal admittance indicates higher thermal mass and lower thermal transmittance indicates higher thermal insulation. Among studied seven configurations at all wind speeds C-H₃ and C-H₆ are preferable due to higher admittance values at lower transmittance.

Figure 8.7.2 shows the effect of wind velocity on transmittance and admittance of composite mud brick walls. The mud brick composite wall with expanded polystyrene insulation located at the mid center of the mud brick wall (C-H₃) and the mud brick composite wall with one half of the expanded polystyrene insulation located at the outer side and another half of the insulation located at the mid center of the mud brick wall (C-H₆) were observed to be energy efficient configurations from higher admittance (At lower transmittance) perspective among seven studied configurations at all external wind velocities. At 10 m/s external wind velocity, the mud brick composite wall with expanded polystyrene insulation located at the mid center of the mud brick wall (C-H₃) has 4.7989 W/m²K admittance value and 1.0240 W/m²K

transmittance value. At 10 m/s external wind velocity, the mud brick composite wall with one half of the expanded polystyrene insulation located at the outer side and another half of the insulation located at the mid center of the mud brick wall (C-H₆) has 4.6798 W/m²K admittance value and 1.024 W/m²K transmittance value. The mud brick composite wall without insulation (C-H₁) has 4.4832 W/m²K admittance value and 2.212 W/m²K transmittance value.

Figure 8.7.3 shows the effect of wind velocity on transmittance and admittance of composite laterite walls. The laterite composite wall with expanded polystyrene insulation located at the mid center of the laterite wall (C-H₃) and the laterite composite wall with one half of the expanded polystyrene insulation located at the outer side and another half of the insulation located at the mid center of the laterite wall (C-H₆) were observed to be energy efficient configurations from higher admittance (At lower transmittance) perspective among seven studied configurations at all external wind velocities. At 10 m/s external wind velocity, the laterite composite wall with expanded polystyrene insulation located at the mid center of the laterite wall (C-H₃) has 5.3902 W/m²K admittance value and 1.1683 W/m²K transmittance value. At 10 m/s external wind velocity, the laterite composite wall with one half of the expanded polystyrene insulation located at the outer side and another half of the insulation located at the mid center of the laterite wall (C-H₆) has 5.2664 W/m²K admittance value and 1.1683 W/m²K transmittance value. The laterite composite wall without insulation (C-H₁) has 5.0247 W/m²K admittance value and 3.0336 W/m²K transmittance value.

Figure 8.7.4 shows the effect of wind velocity on transmittance and admittance of composite cinder concrete walls. The cinder concrete composite wall with expanded polystyrene insulation located at the mid center of the cinder concrete wall (C-H₃) and the cinder concrete composite wall with one half of the expanded polystyrene insulation located at the outer side and another half of the insulation located at the mid center of the cinder concrete wall (C-H₆) were observed to be energy efficient configurations from higher admittance (At lower transmittance) perspective among seven studied configurations at all external wind velocities. At 10 m/s external wind velocity, the cinder concrete composite wall with expanded polystyrene insulation located at the mid center of the cinder concrete wall (C-H₃) has 4.4929 W/m²K

admittance value and 0.9986 W/m²K transmittance value. At 10 m/s external wind velocity, the cinder concrete composite wall with one half of the expanded polystyrene insulation located at the outer side and another half of the insulation located at the mid center of the cinder concrete wall (C-H₆) has 4.3812 W/m²K admittance value and 0.9986 W/m²K transmittance value. The cinder concrete composite wall without insulation (C-H₁) has 4.1905 W/m²K admittance value and 2.1049 W/m²K transmittance value.

Higher thermal admittance indicates higher thermal mass and lower thermal transmittance indicates higher thermal insulation. Among studied seven configurations at all wind speeds C-H₃ and C-H₆ are preferable due to higher admittance values at lower transmittance.

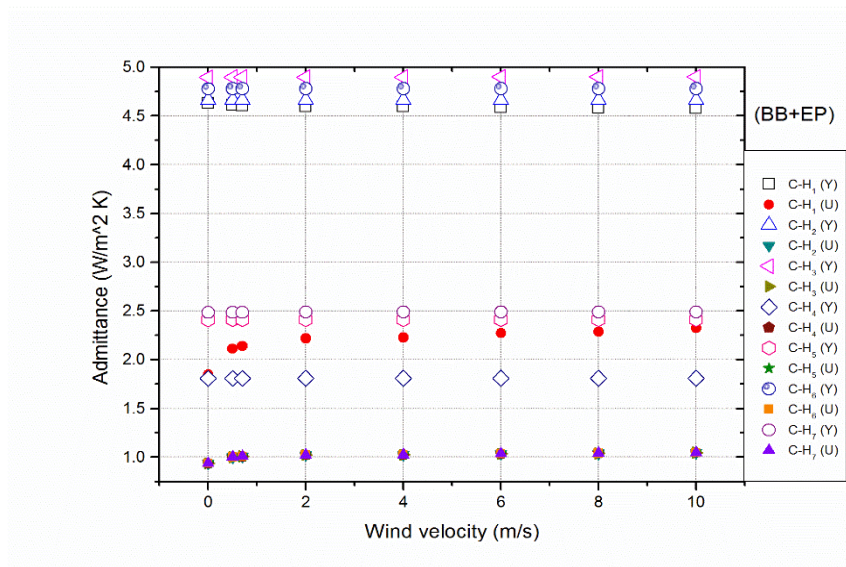


Figure 8.7.1 Effect of wind velocity on transmittance and admittance of composite burnt brick walls

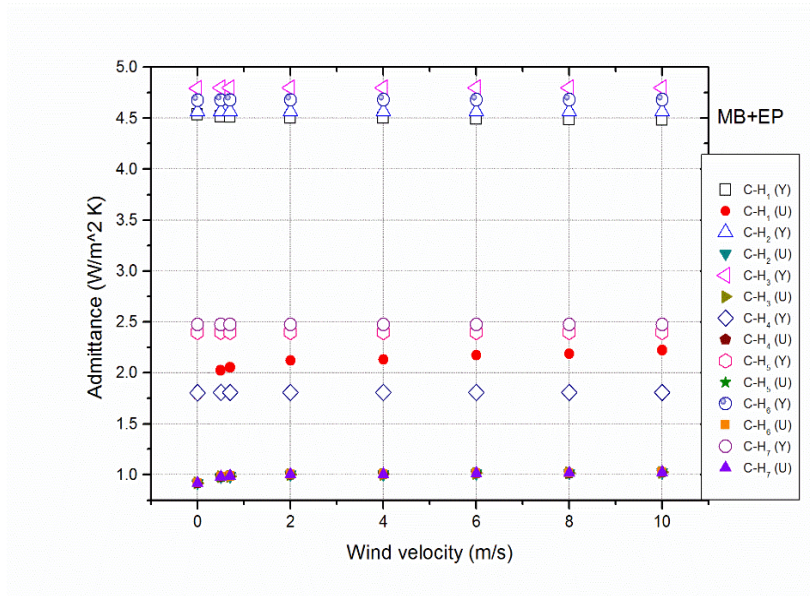


Figure 8.7.2 Effect of wind velocity on transmittance and admittance of composite mud brick walls

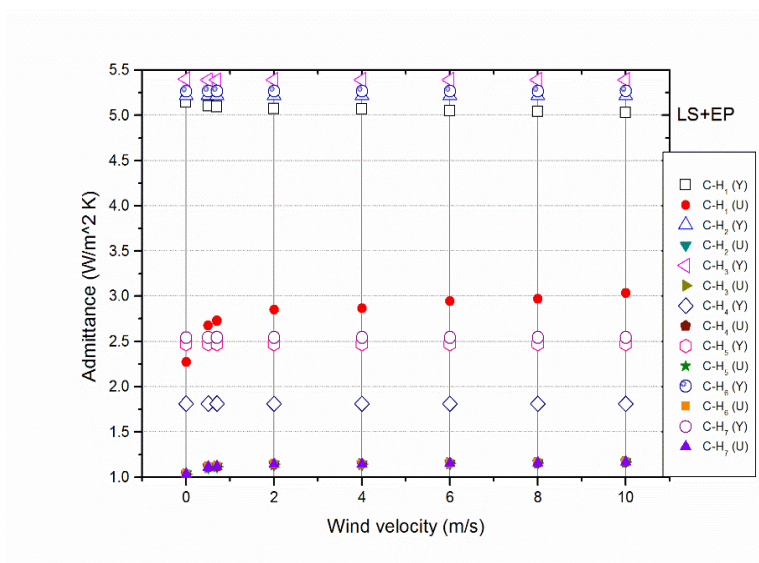


Figure 8.7.3 Effect of wind velocity on transmittance and admittance of composite laterite walls

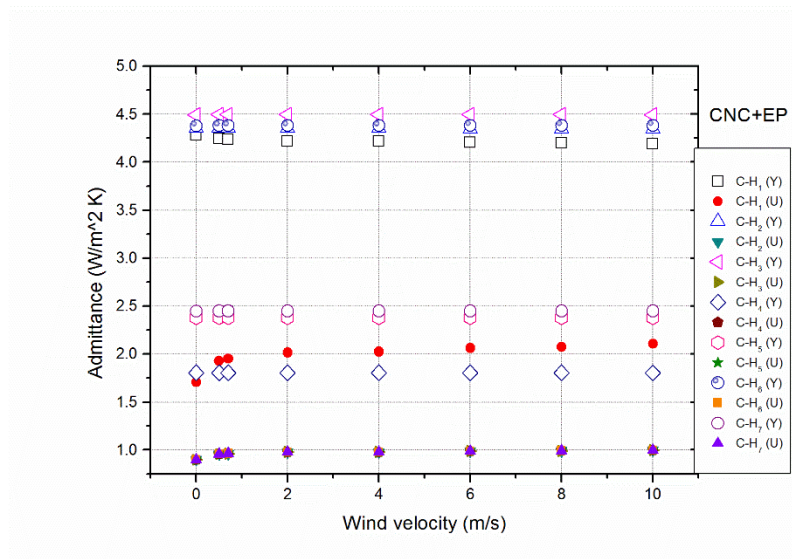


Figure 8.7.4 Effect of wind velocity on transmittance and admittance of composite cinder concrete walls

8.8 EFFECT OF WIND VELOCITY ON DECREMENT FACTOR AND TIME LAG OF COMPOSITE WALLS

Figure 8.8.1 shows the effect of wind velocity on the decrement factor of composite burnt brick walls. From the results, it is observed that the burnt brick composite wall with one half of the expanded polystyrene insulation located at the outer and another half of the expanded polystyrene insulation located at the inner side of the burnt brick wall (C-H₅) and the composite burnt brick wall with one half of the expanded polystyrene insulation located at the outer side and another half of the expanded polystyrene insulation located at the mid center of the burnt brick wall (C-H₆) are found to be energy efficient from lower decrement factor point of view among seven studied configurations at all external wind velocities. At 10 m/s external wind velocity, the burnt brick composite wall with one half of the expanded polystyrene insulation located at the outer and another half of the expanded polystyrene insulation located at the inner side of the burnt brick wall (C-H₅) has the least decrement factor of 0.1896 and the composite burnt brick wall with one half of the expanded polystyrene insulation located at the outer side and another half of the expanded polystyrene insulation located at the mid center of the burnt brick wall (C-H₆) has low decrement factor of 0.2041. The burnt brick composite wall without insulation (C-H₁) has the highest decrement factor value of 0.5172.

Figure 8.8.2 shows the effect of wind velocity on time lag of composite burnt brick walls. From the results, it is observed that the composite burnt brick wall with one half of the expanded polystyrene insulation located at the outer side and another half of the expanded polystyrene insulation located at the mid center of the burnt brick wall (C-H₆) and the composite burnt brick wall with one half of the expanded polystyrene insulation located at mid center of the wall and another half of the expanded polystyrene insulation located at the inner side of the wall (C-H₇) are found to be energy efficient from higher time lag perspective among seven studied configurations at all external wind velocities. At 10 m/s external wind velocity, the composite burnt brick wall with one half of the expanded polystyrene insulation located at the outer side and another half of the expanded polystyrene insulation located at the mid center of the burnt brick wall (C-H₆) has the highest time lag of 9.9059 h and the composite burnt brick wall with one half of the expanded polystyrene insulation located at mid center of the burnt brick wall and another half of the expanded polystyrene insulation located at the inner side of the burnt brick wall (C-H₇) has the high time lag of 8.9944 h. The burnt brick composite wall without insulation (C-H₁) has the least time lag value of 6.4079 h.

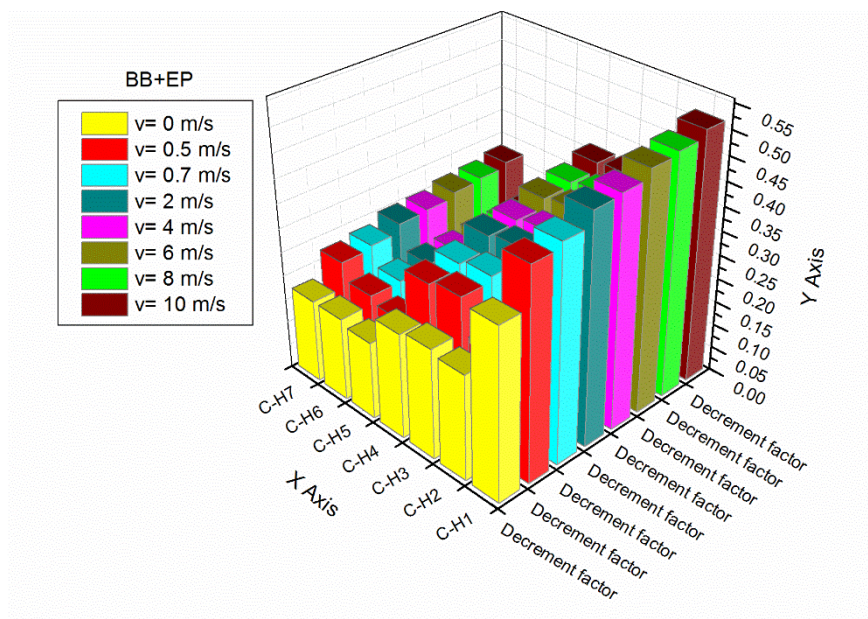


Figure 8.8.1 Effect of wind velocity on decrement factor of composite burnt brick walls

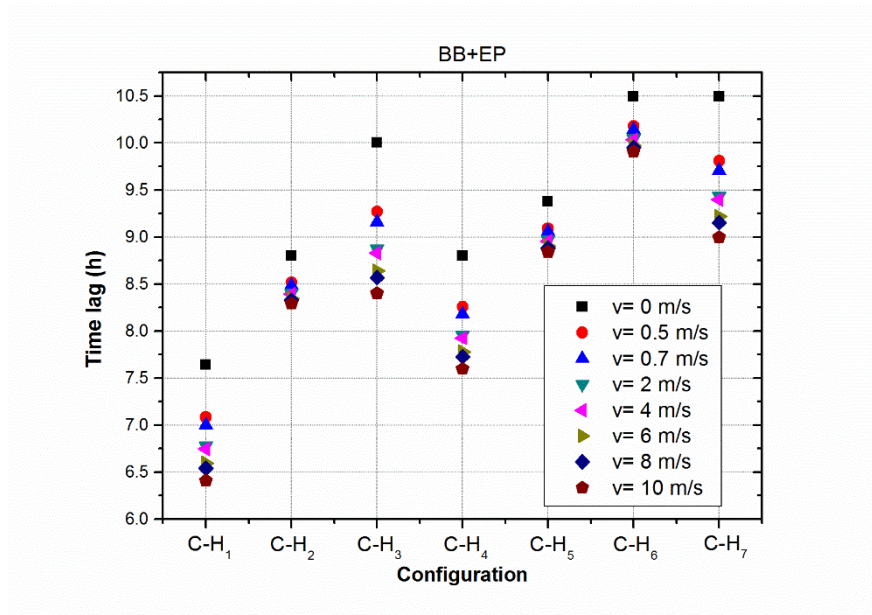


Figure 8.8.2 Effect of wind velocity on time lag of composite burnt brick walls

Figure 8.8.3 shows the effect of wind velocity on decrement factor of composite mud brick walls. From the results, it is observed that the mud brick composite wall with one half of the expanded polystyrene insulation located at the outer and another half of the expanded polystyrene insulation located at the inner side of the mud brick wall (C-H₅) and the composite mud brick wall with one half of the expanded polystyrene insulation located at the outer side and another half of the expanded polystyrene insulation located at the mid center of the mud brick wall (C-H₆) are found to be energy efficient from lower decrement factor point of view among seven studied configurations at all external wind velocities. At 10 m/s external wind velocity, the mud brick composite wall with one half of the expanded polystyrene insulation located at the outer and another half of the expanded polystyrene insulation located at the inner side of the mud brick wall (C-H₅) has the least decrement factor of 0.1965 and the composite mud brick wall with one half of the expanded polystyrene insulation located at the outer side and another half of the expanded polystyrene insulation located at the mid center of the mud brick wall (C-H₆) has low decrement factor of 0.2147. The mud brick composite wall without insulation (C-H₁) has the highest decrement factor value of 0.5219.

Figure 8.8.4 shows the effect of wind velocity on time lag of composite mud brick walls. From the results, it is observed that the composite mud brick wall with one half

of the expanded polystyrene insulation located at the outer side and another half of the expanded polystyrene insulation located at the mid center of the mud brick wall (C-H₆) and the composite mud brick wall with one half of the expanded polystyrene insulation located at mid center of the mud brick wall and another half of the expanded polystyrene insulation located at the inner side of the mud brick wall (C-H₇) are found to be energy efficient from higher time lag perspective among seven studied configurations at all external wind velocities. At 10 m/s external wind velocity, the composite mud brick wall with one half of the expanded polystyrene insulation located at the outer side and another half of the expanded polystyrene insulation located at the mid center of the mud brick wall (C-H₆) has the highest time lag of 9.8365 h and the composite mud brick wall with one half of the expanded polystyrene insulation located at mid center of the mud brick wall and another half of the expanded polystyrene insulation located at the inner side of the mud brick wall (C-H₇) has the high time lag of 8.955 h. The mud brick composite wall without insulation (C-H₁) has the least time lag value of 6.4245 h.

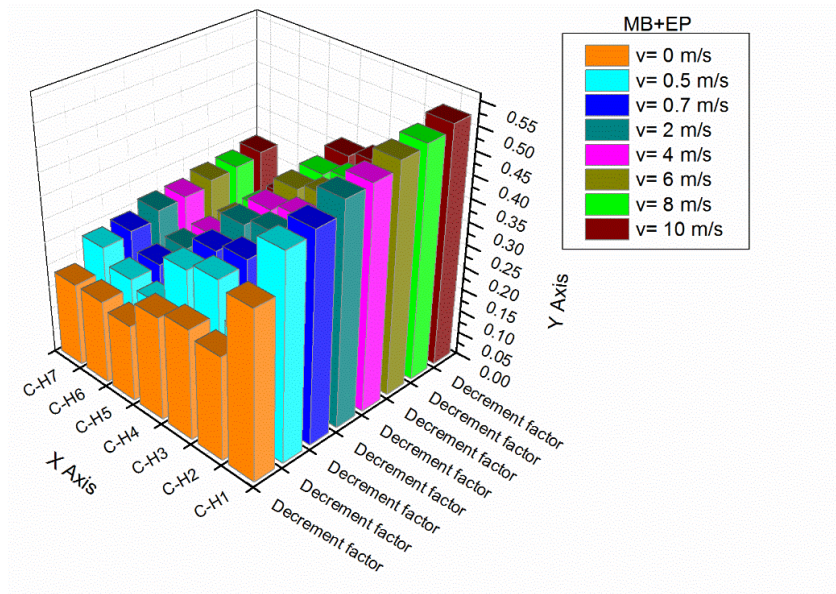


Figure 8.8.3 Effect of wind velocity on decrement factor of composite mud brick walls

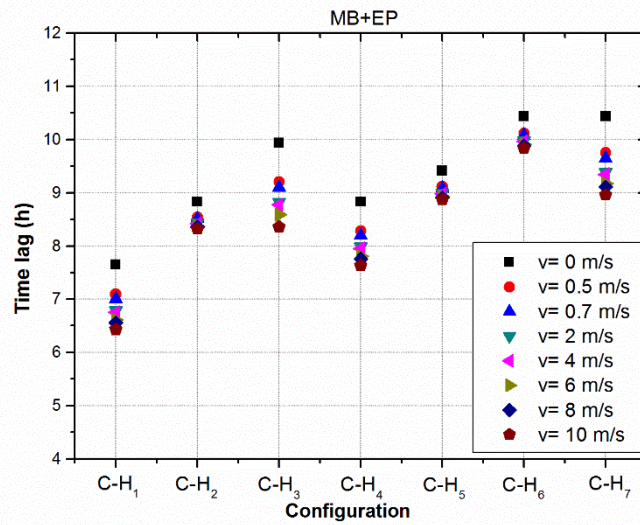


Figure 8.8.4 Effect of wind velocity on time lag of composite mud brick walls

Figure 8.8.5 shows the effect of wind velocity on decrement factor of composite laterite walls. From the results, it is observed that the laterite composite wall with one half of the expanded polystyrene insulation located at the outer and another half of the expanded polystyrene insulation located at the inner side of the laterite wall (C-H₅) and the composite laterite wall with one half of the expanded polystyrene insulation located at the outer side and another half of the expanded polystyrene insulation located at the mid center of the laterite wall (C-H₆) are found to be energy efficient from lower decrement factor point of view among seven studied configurations at all external wind velocities. At 10 m/s external wind velocity, the laterite composite wall with one half of the expanded polystyrene insulation located at the outer and another half of the expanded polystyrene insulation located at the inner side of the laterite wall (C-H₅) has the least decrement factor of 0.1737 and the composite laterite wall with one half of the expanded polystyrene insulation located at the outer side and another half of the expanded polystyrene insulation located at the mid center of the laterite wall (C-H₆) has low decrement factor of 0.1738. The laterite composite wall without insulation (C-H₁) has the highest decrement factor value of 0.5364.

Figure 8.8.6 shows the effect of wind velocity on time lag of composite laterite walls. From the results, it is observed that the composite laterite wall with one half of the

expanded polystyrene insulation located at the outer side and another half of the expanded polystyrene insulation located at the mid center of the laterite wall (C-H₆) and the composite laterite wall with one half of the expanded polystyrene insulation located at mid center of the laterite wall and another half of the expanded polystyrene insulation located at the inner side of the laterite wall (C-H₇) are found to be energy efficient from higher time lag perspective among seven studied configurations at all external wind velocities. At 10 m/s external wind velocity, the composite laterite wall with one half of the expanded polystyrene insulation located at the outer side and another half of the expanded polystyrene insulation located at the mid center of the laterite wall (C-H₆) has the highest time lag of 9.7889 h and the composite laterite wall with one half of the expanded polystyrene insulation located at mid center of the laterite wall and another half of the expanded polystyrene insulation located at the inner side of the laterite wall (C-H₇) has the high time lag of 8.7059 h. The laterite composite wall without insulation (C-H₁) has the least time lag value of 5.8129 h.

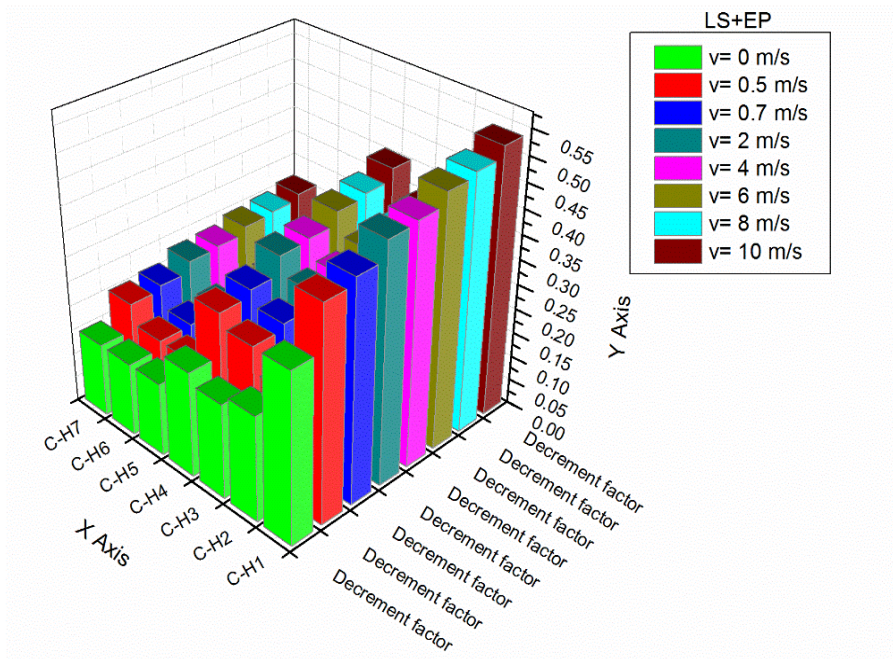


Figure 8.8.5 Effect of wind velocity on decrement factor of composite laterite walls

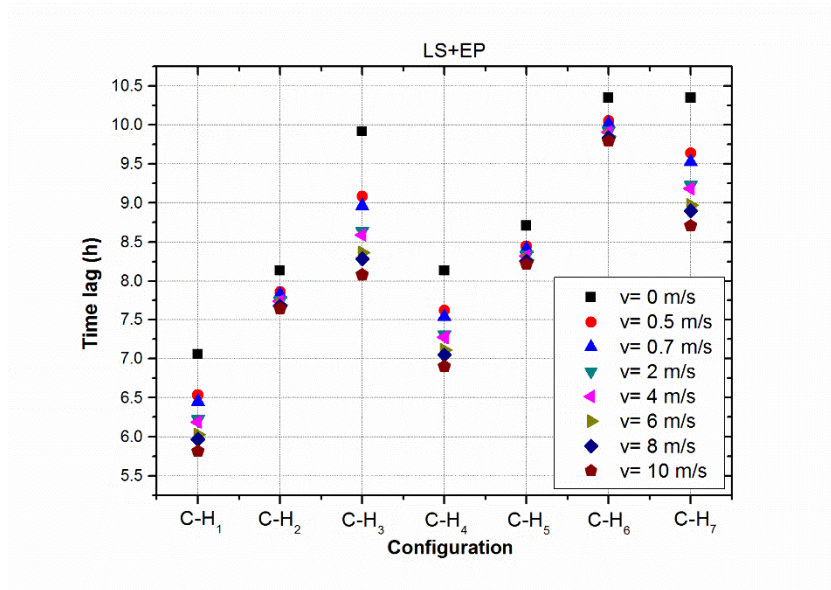


Figure 8.8.6 Effect of wind velocity on time lag of composite laterite walls

Figure 8.8.7 shows the effect of wind velocity on decrement factor of composite cinder concrete walls. From the results, it is observed that the cinder concrete composite wall with one half of the expanded polystyrene insulation located at the outer and another half of the expanded polystyrene insulation located at the inner side of the cinder concrete wall (C-H₅) and the composite cinder concrete wall with one half of the expanded polystyrene insulation located at the outer side and another half of the expanded polystyrene insulation located at the mid center of the cinder concrete wall (C-H₆) are found to be energy efficient from lower decrement factor point of view among seven studied configurations at all external wind velocities. At 10 m/s external wind velocity, the cinder concrete composite wall with one half of the expanded polystyrene insulation located at the outer and another half of the expanded polystyrene insulation located at the inner side of the cinder concrete wall (C-H₅) has the least decrement factor of 0.2544 and the composite cinder concrete wall with one half of the expanded polystyrene insulation located at the outer side and another half of the expanded polystyrene insulation located at the mid center of the cinder concrete wall (C-H₆) has low decrement factor of 0.2941. The cinder concrete composite wall without insulation (C-H₁) has the highest decrement factor value of 0.6044.

Figure 8.8.8 shows the effect of wind velocity on time lag of composite cinder concrete walls. From the results, it is observed that the composite cinder concrete wall with one half of the expanded polystyrene insulation located at the outer side and another half of the expanded polystyrene insulation located at the mid center of the cinder concrete wall (C-H₆) and the composite cinder concrete wall with one half of the expanded polystyrene insulation located at mid center of the laterite wall and another half of the expanded polystyrene insulation located at the inner side of the cinder concrete wall (C-H₇) are found to be energy efficient from higher time lag perspective among seven studied configurations at all external wind velocities. At 10 m/s external wind velocity, the composite cinder concrete wall with one half of the expanded polystyrene insulation located at the outer side and another half of the expanded polystyrene insulation located at the mid center of the cinder concrete wall (C-H₆) has the highest time lag of 8.857 h and the composite cinder concrete wall with one half of the expanded polystyrene insulation located at mid center of the cinder concrete wall and another half of the expanded polystyrene insulation located at the inner side of the cinder concrete wall (C-H₇) has the high time lag of 8.0459 h. The cinder concrete composite wall without insulation (C-H₁) has the least time lag value of 5.6926 h.

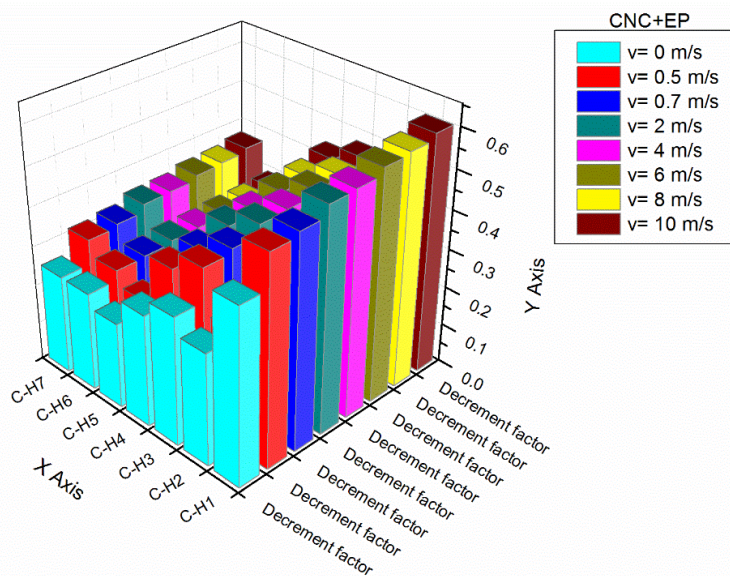


Figure 8.8.7 Effect of wind velocity on decrement factor of composite cinder concrete walls

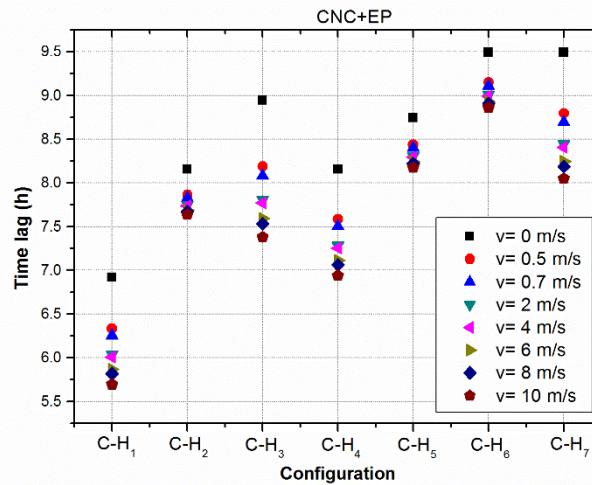


Figure 8.8.8 Effect of wind velocity on time lag of composite cinder concrete walls

8.9 SUMMARY

- Thermal admittance, decrement factor and areal thermal heat capacity of homogeneous building materials decrease with the increase in the external wind velocity.
- Thermal transmittance and surface factor of the homogeneous building materials increase with the increase in the external wind velocity.
- Building material with half of the insulation placed at the outside of the wall and another half of the insulation placed at the inner side of the wall (C-H₅) is the best configuration from the lower decrement factor at all wind velocities among seven studied configurations. Building material with half of the insulation placed at the outside of the wall and another half of the insulation placed at the mid center of the wall (C-H₆) is also found to be the next best configuration from lower decrement factor perspective.
- Building material with half of the insulation placed at the outside of the wall and another half of the insulation placed at the mid center of the wall (C-H₆) is the best configuration from higher time lag values at all wind velocities among seven studied configurations.

- Building material with half of the insulation placed at the outside of the wall and another half of the insulation placed at the mid center of the wall (C-H₆) is the most recommended configuration from the lower decrement factor as well as the higher time lag values at all wind velocities among seven studied configurations.
- At 10 m/s wind velocity, the configuration with half of the insulation placed at the outside of the wall and another half of the insulation placed at the mid center of the wall (C-H₆) increases the time lag of burnt brick, mud brick, laterite stone and cinder concrete composite walls by 35.31%, 34.68%, 40.61% and 35.72%, respectively as compared to the common configuration of the wall (C-H₁).
- At 10 m/s wind velocity, the configuration with half of the insulation placed at the outside of the wall and another half of the insulation placed at the mid center of the wall (C-H₆) decreases the decrement factor of burnt brick, mud brick, laterite stone and cinder concrete composite walls by 60.53%, 58.86%, 67.59% and 51.34%, respectively as compared to the common configuration of the wall (C-H₁).
- The burnt brick composite walls are observed to be energy efficient among four building materials studied from lower decrement factor and higher time lag perspective.
- The results of the study help in selecting energy efficient building wall configurations at higher wind velocities.

CHAPTER-9

CONCLUSIONS AND SCOPE FOR FUTURE WORK

- A computer program which employs an admittance method was developed using MATLAB to compute unsteady thermal state characteristics of homogeneous walls/roofs, typical multilayer Walls/Roofs with or without air spaces, hollow bricks and stuffed bricks.
- Thermal properties of laterite stone were measured and it is observed that the relative humidity and temperature affect the decrement factor and its time lag values of laterite rocks. The increase in the relative humidity from 0% RH to 98% RH decreases the decrement factor by 8.35% and increases the time lag by 2.88%, whereas, the increase in the temperature from 0°C to 60°C decreases the decrement factor by 14.5% and increases the time lag by 8.3%.
- The average decrement factor for laterite buildings in Ahmedabad, Bangalore, Hyderabad and Mangalore climatic regions is less than that of the average decrement factor of concrete building walls in all climatic regions. The average decrement factor of the laterite building walls in the Mangalore climatic region is 6.526% less than that of the average decrement factor of the dense concrete building walls in the Mangalore climatic region. In summer climates, the higher ϕ_{\min} values are recommended for reducing cooling loads. The laterite building walls have higher ϕ_{\min} values than the concrete building walls. The average time lag (ϕ_{\min}) of the laterite building walls in the Mangalore climatic region is 3.57% higher than that of the average time lag (ϕ_{\min}) of the dense concrete building walls in the Mangalore climatic region. Hence, the laterite walls are recommended for energy efficient building construction than the concrete walls from lower decrement factor and higher average time lag perspective.
- The unsteady thermal characteristics of ten building and ten insulating materials were studied and it is observed that the insulating materials are fast responsive to short wave radiation than the building materials due to their higher surface factors and

lower surface factor time lags. Hence insulating materials should not be exposed to direct solar radiation.

- The significant location of insulation within wall was found from lower decrement factor and higher time lag point of view. It is noticed that the composite wall with insulation placed at the mid center plane of the wall (C-B₃) gives higher time lags and the composite wall with insulation placed at the outer surface (C-B₂) gives the least value of decrement factors. Placing half of the insulation at the mid center plane and another half of the insulation at the outer surface give higher time lags and lower decrement factors.
- The effects of air space thickness on unsteady thermal state characteristics were studied. It is observed that the decrement factor of laterite stone (LS), Mud brick (MB), Cellular concrete (CLC), Dense concrete (DC) and Cinder concrete (CNC) decrease 20.60%, 14.59%, 5.81%, 23.67% and 10.38%, respectively, from without air space configuration (C-C₁) to 0.02 m air space thickness configuration (C-C₅) and the time lag of laterite stone (LS), Mud brick (MB), Cellular concrete (CLC), Dense concrete (DC) and Cinder concrete (CNC) increase by 20.42%, 15.06%, 6.23%, 22.70% and 14.14%, respectively, from without air space configuration (C-C₁) to 0.02 m air space thickness configuration (C-C₅), beyond 0.02m air gap thickness both decrement factor and time lag remain almost constant.
- The optimum location of air space within the wall was found. It is clear from the results that the composite wall with unventilated continuous air space located at outer and mid center plane of the composite wall (C-D₆) is highly recommended configuration of the composite wall for all building materials studied from highest time lag point of view. The composite wall with air space located at the inner and outer side of the composite wall (C-D₅) is recommended for burnt brick, mud brick, reinforced brick and fly ash brick composite walls from the lowest decrement factor point of view. The composite wall with air space located at outer and mid center plane of the composite wall (C-D₆) is recommended for laterite and concrete block composite walls. The configuration C-D₆ is collectively the best configuration from lower decrement factor and higher time lag for all building materials.
- The optimum location of insulation within the building roof was found. It is observed that the roof configuration C-E₆ is observed to be the second best configuration after

C-E₅ from the lower decrement factor point of view for all the insulation materials studied among seven configurations. The roof configuration C-E₆ is the best from both lower decrement factor and higher time lag perspective. Reinforced cement concrete (RCC) roof with expanded polystyrene insulation (EP) placed at the mid center plane and at the inner side of the roof (C-E₆) gives 69.86% less decrement factor and 39.50% higher time lag values than the common roof configuration (C-E₁).

- Thermal performance of hollow and stuffed bricks was investigated. It is noticed that the thermal admittance, decrement time lag, surface factor time lag and areal thermal heat capacity of the hollow bricks increase with the increase in the number of air gaps within the brick due to improved thermal mass and thermal insulation. These enhanced unsteady state properties make the hollow bricks more energy efficient than the solid bricks. Hollow bricks with five air spaces (C-F₆) decrease decrement factor of dense concrete bricks, burnt bricks, mud bricks, cinder concrete bricks and cellular concrete bricks by 34.32%, 25.38%, 24.27%, 16.54% and 11.05%, respectively as compared to the hollow brick with single air space (C-F₂). Hollow bricks with five air spaces (C-F₆) increase the time lag of dense concrete bricks, burnt bricks, mud bricks, cinder concrete bricks and cellular concrete bricks by 81.17%, 81.70%, 81.78%, 82.31% and 81.88%, respectively as compared to the hollow brick with single air space (C-F₂). The stuffed bricks with five foam glass insulation layers (C-G₆) decrease the decrement factor of mud bricks, burnt bricks, dense concrete bricks and fly ash bricks by 17.91%, 35.84%, 45.76% and 35.14%, respectively as compared to the stuffed bricks with single foam glass insulation layer (C-G₂). Stuffed bricks with five foam glass insulation layers (C-G₆) increase the time lag of mud bricks, burnt bricks, dense concrete bricks and fly ash bricks by 36.23%, 58.75%, 61.45% and 57.47%, respectively as compared to the stuffed bricks with single foam glass insulation layer (C-G₂). In hot regions, the wall thermal transmittance should be as low as possible and the wall admittance should be as high as possible. In cold regions, the wall thermal transmittance should be as high as possible and the wall admittance should be as low as possible. The stuffed bricks are recommended in hot and humid regions whereas the hollow bricks are recommended in composite climates.
- The effect of wind velocity on thermal performance of various building wall configurations was studied. It is observed that the building material with half of the

insulation placed at the outside of the wall and another half of the insulation placed at the mid center of the wall (C-H₆) is the most recommended configuration from the lower decrement factor as well as the higher time lag values at all wind velocities among seven studied configurations. At 10 m/s wind velocity, the configuration with half of the insulation placed at the outside of the wall and another half of the insulation placed at the mid center of the wall (C-H₆) increases the time lag of burnt brick, mud brick, laterite stone and cinder concrete composite walls by 35.31%, 34.68%, 40.61% and 35.72%, respectively as compared to the common configuration of the wall (C-H₁). At 10 m/s wind velocity, the configuration with half of the insulation placed at the outside of the wall and another half of the insulation placed at the mid center of the wall (C-H₆) decreases the decrement factor of burnt brick, mud brick, laterite stone and cinder concrete composite walls by 60.53%, 58.86%, 67.59% and 51.34%, respectively as compared to the common configuration of the wall (C-H₁).

SCOPE FOR FUTURE WORK

The admittance model can be adopted for different new building and insulation materials. The mathematical admittance model can be further enhanced by incorporating coupled heat and mass transfer in porous building materials. In addition, the experimental investigations on the proposed wall, roof and brick configurations are still attractive for more research and innovation in the field.

REFERENCES

Journal References:

- Alavez-Ramirez, R., Chiñas-Castillo, F., Morales-Dominguez, V., Ortiz-Guzman, M. and Lara-Romero, J. (2014). “Thermal lag and decrement factor of a coconut-ferrocement roofing system.” *Constr Build Mater.*, 55, 246–256. <http://doi.org/10.1016/j.conbuildmat.2014.01.048>
- Alexandri, E. and Jones, P. (2008). “Temperature decreases in an urban canyon due to green walls and green roofs in diverse climates.” *Build Environ.*, 43(4), 480–493. <http://doi.org/10.1016/j.buildenv.2006.10.055>
- Alvarado, J. L. and Martínez, E. (2008). “Passive cooling of cement-based roofs in tropical climates.” *Energy Build.*, 40(3), 358–364. <http://doi.org/10.1016/j.enbuild.2007.03.003>
- Asan, H. (1998). “Effects of wall’s insulation thickness and position on time lag and decrement factor.” *Energy Build.*, 28(3), 299–305. [http://doi.org/10.1016/S0378-7788\(98\)00030-9](http://doi.org/10.1016/S0378-7788(98)00030-9)
- Asan, H. and San, Y. S. (1998). “Effects of Wall ’s thermo physical properties on time lag and decrement factor.” *Energy Build.*, 28, 159–166. [http://doi.org/10.1016/S0378-7788\(98\)00007-3](http://doi.org/10.1016/S0378-7788(98)00007-3)
- Asan, H. (2000). “Investigation of wall’s optimum insulation position from maximum time lag and minimum decrement factor point of view.” *Energy Build.*, 32(2), 197–203. [http://doi.org/10.1016/S0378-7788\(00\)00044-X](http://doi.org/10.1016/S0378-7788(00)00044-X)
- Asan, H. (2006). “Numerical computation of time lags and decrement factors for different building materials.” *Build Environ.*, 41(5), 615–620. <http://doi.org/10.1016/j.buildenv.2005.02.020>
- Barrios, G., Huelsz, G., Rechtman, R. and Rojas, J. (2011). “Wall/roof thermal performance differences between air-conditioned and non air-conditioned rooms.” *Energy Build.*, 43(1), 219–223. <http://doi.org/10.1016/j.enbuild.2010.09.015>
- Bu, Z., Kato, S. and Takahashi, T. (2010). “Wind tunnel experiments on wind-induced natural ventilation rate in residential basements with areaway space.” *Build Environ.*, 45(10), 2263–2272. <http://doi.org/10.1016/j.buildenv.2010.04.009>

- Chel, A. and Tiwari, G. N. (2009). "Thermal performance and embodied energy analysis of a passive house - Case study of vault roof mud-house in India." *Appl. Energy.*, 86(10), 1956–1969. <http://doi.org/10.1016/j.apenergy.2008.12.033>
- Duffin, R.J. (1984). "A passive wall design to minimize building temperature swings." *Sol Energy.*, 33(3/4), 337-342.
- Evola, G. and Marletta, L. (2013). "A dynamic parameter to describe the thermal response of buildings to radiant heat gains." *Energy Build.*, 65, 448–457. <http://doi.org/10.1016/j.enbuild.2013.06.026>
- Fatimah, W., Yusoff, M., Salleh, E., Mariah, N. and Razak, A. (2010). "Enhancement of stack ventilation in hot and humid climate using a combination of roof solar collector and vertical stack." *Build Environ.*, 45(10), 2296–2308. <http://doi.org/10.1016/j.buildenv.2010.04.018>
- Gagliano, A., Patania, F., Nocera, F., Ferlito, A. and Galesi, A. (2012). "Thermal performance of ventilated roofs during summer period." *Energy Build.*, <http://doi.org/10.1016/j.enbuild.2012.03.007>
- Gidigas, M. D. (1974). "Degree of weathering in the identification of laterite materials for engineering purposes - A Review.", *Eng. Geol.*, 8, 213-266.
- Gustafsson, S.E. (1991). "Transient plane source technique for thermal conductivity and thermal diffusivity measurements of solid materials." *Rev. Sci. Instrum.*, 62, 797-804.
- Hadavand, M. and Yaghoubi, M. (2008). "Thermal behavior of curved roof buildings exposed to solar radiation and wind flow for various orientations." *Appl. Energy.*, 85(8), 663–679. <http://doi.org/10.1016/j.apenergy.2008.01.002>
- Hall, M. and Allinson, D. (2008). "Assessing the moisture-content-dependent parameters of stabilised earth materials using the cyclic-response admittance method." *Energy Build.*, 40(11), 2044–2051. <http://doi.org/10.1016/j.enbuild.2008.05.009>
- Halwatura, R. U. and Jayasinghe, M. T. R. (2009). "Influence of insulated roof slabs on air conditioned spaces in tropical climatic conditions-A life cycle cost approach." *Energy Build.*, 41(6), 678–686. <http://doi.org/10.1016/j.enbuild.2009.01.005>
- Hirano, T., Kato, S., Murakami, S., Ikaga, T. and Shiraishi, Y. (2006). "A study on a porous residential building model in hot and humid regions : Part 1 — the natural

- ventilation performance and the cooling load reduction effect of the building model.” *Build Environ.*, 41, 21–32. <http://doi.org/10.1016/j.buildenv.2005.01.018>
- Jin, X., Zhang, X., Cao, Y. and Wang, G. (2012). “Thermal performance evaluation of the wall using heat flux time lag and decrement factor.” *Energy Build.*, 47, 369–374. <http://doi.org/10.1016/j.enbuild.2011.12.010>
- Kabre, C. (2010). “A new thermal performance index for dwelling roofs in the warm humid tropics.” *Build Environ.*, 45(3), 727–738. <http://doi.org/10.1016/j.buildenv.2009.08.017>
- Kasthurba, A. K., Reddy, K. R., and Reddy, D. V. (2014). “Use of Laterite as a Sustainable Building Material in Developing Countries.”, *Int. J. Earth Sci. Eng.* 7(4), 1251-1258.
- Kasthurba, A. K., Santhanam, M. and Mathews, M.S. (2007). “Investigation of laterite stones for building purpose from Malabar region, Kerala state, SW India – Part 1: Field studies and profile characterisation.” *Constr Build Mater.*, 21, 73-82. [doi:10.1016/j.conbuildmat.2005.07.006](http://doi.org/10.1016/j.conbuildmat.2005.07.006)
- Kasthurba, A. K., Santhanam, M. and Achyuthan, H. (2008). “Investigation of laterite stones for building purpose from Malabar region, Kerala, SW India - Chemical analysis and microstructure studies.” *Constr Build Mater.*, 22(12), 2400–2408. <http://doi.org/10.1016/j.conbuildmat.2006.12.003>
- Knowles, T.R. (1983). “Proportioning composites for efficient thermal storage walls.” *Sol Energy.*, 31(3), 319-326.
- Kontoleon, K. J. and Bikas, D. K. (2007). “The effect of south wall’s outdoor absorption coefficient on time lag, decrement factor and temperature variations.” *Energy Build.*, 39(9), 1011–1018. <http://doi.org/10.1016/j.enbuild.2006.11.006>
- Kontoleon, K. J. and Eumorfopoulou, E. A. (2008). “The influence of wall orientation and exterior surface solar absorptivity on time lag and decrement factor in the Greek region.” *Renew. Energy.*, 33(7), 1652–1664. <http://doi.org/10.1016/j.renene.2007.09.008>
- Kontoleon, K. J. and Eumorfopoulou, E. A. (2010). “The effect of the orientation and proportion of a plant-covered wall layer on the thermal performance of a building zone.” *Build Environ.*, 45(5), 1287–1303. <http://doi.org/10.1016/j.buildenv.2009.11.013>

- Kontoleon, K. J., Theodosiou, T. G. and Tsikaloudaki, K. G. (2013). “The influence of concrete density and conductivity on walls’ thermal inertia parameters under a variety of masonry and insulation placements.” *Appl. Energy.*, 112, 325–337. <http://doi.org/10.1016/j.apenergy.2013.06.029>
- Lee, S., Park, S. H., Yeo, M. S. and Kim, K. W. (2009). “An experimental study on airflow in the cavity of a ventilated roof.” *Build Environ.*, 44(7), 1431–1439. <http://doi.org/10.1016/j.buildenv.2008.09.009>
- Levinson, R., Akbari, H. and Reilly, J. C. (2007). “Cooler tile-roofed buildings with near-infrared-reflective non-white coatings.” *Build Environ.*, 42(7), 2591–2605. <http://doi.org/10.1016/j.buildenv.2006.06.005>
- Log, T. and Gustafsson, S. E. (1995). “Transient plane source (TPS) technique for measuring thermal transport properties of building materials.” *Fire Materi.*, 19, 43–49.
- Magyari, E. and Keller, B. (1998). “The storage capacity of a harmonically heated slab revisited”. *Int J Heat Mass Tran.*, 41(10), 1199–1204.
- Mathur, J. and Mathur, S. (2006). “Summer-performance of inclined roof solar chimney for natural ventilation.” *Energy Build.*, 38, 1156–1163. <http://doi.org/10.1016/j.enbuild.2006.01.006>
- Mavromatidis, L. E., Mankibi, M., Michel, P. and Santamouris, M. (2012). “Numerical estimation of time lags and decrement factors for wall complexes including Multilayer Thermal Insulation, in two different climatic zones.” *Appl. Energy.*, 92, 480–491. <http://doi.org/10.1016/j.apenergy.2011.10.007>
- Najim, K. B. (2014). “External load-bearing walls configuration of residential buildings in Iraq and their thermal performance and dynamic thermal behaviour.” *Energy Build.*, 84, 169–181. <http://doi.org/10.1016/j.enbuild.2014.07.064>
- Najim, K. B. and Fadhil, O. T. (2015). “Assessing and improving the thermal performance of reinforced concrete-based roofing systems in Iraq.” *Energy Build.*, 89, 213–221. <http://doi.org/10.1016/j.enbuild.2014.12.049>
- Ozel, M. and Pihtili, K. (2007). “Optimum location and distribution of insulation layers on building walls with various orientations.” *Build Environ.*, 42(8), 3051–3059. <http://doi.org/10.1016/j.buildenv.2006.07.025>

- Priyadarsini, R., Cheong, K. W. and Wong, N. H. (2004). "Enhancement of natural ventilation in high-rise residential buildings using stack system." *Energy Build.*, 36, 61–71. [http://doi.org/10.1016/S0378-7788\(03\)00076-8](http://doi.org/10.1016/S0378-7788(03)00076-8)
- Rees, S. J., Spitler, J. D., Davies, M. G. and Haves, P. H. (2000). "Qualitative comparison of North American and UK cooling load calculation methods.", *International Journal of HVAC & R. Research* 6 (1), 75–99.
- Ruivo, C. R., Ferreira, P. M. and Vaz, D. C. (2013). "On the error of calculation of heat gains through walls by methods using constant decrement factor and time lag values." *Energy Build.*, 60, 252–261. <http://doi.org/10.1016/j.enbuild.2013.02.001>
- Sethi, V. P. (2009). "On the selection of shape and orientation of a greenhouse: Thermal modeling and experimental validation." *Sol Energy.*, 83(1), 21–38. <http://doi.org/10.1016/j.solener.2008.05.018>
- Soon-ching, Ng., Low, K. S. and Tioh, N. H. (2011). "Thermal inertia of newspaper sandwiched aerated lightweight concrete wall panels: Experimental study." *Energy Build.*, 43(10), 2956–2960. <http://doi.org/10.1016/j.enbuild.2011.06.022>
- Sun, C., Shu, S., Ding, G., Zhang, X. and Hu, X. (2013). "Investigation of time lags and decrement factors for different building outside temperatures." *Energy Build.*, 61, 1–7. <http://doi.org/10.1016/j.enbuild.2013.02.003>
- Tang, R., Meir, I. a. and Etzion, Y. (2003). "Thermal behavior of buildings with curved roofs as compared with flat roofs." *Sol Energy.*, 74(4), 273–286. [http://doi.org/10.1016/S0038-092X\(03\)00193-2](http://doi.org/10.1016/S0038-092X(03)00193-2)
- Tang, R. and Etzion, Y. (2004). "On thermal performance of an improved roof pond for cooling buildings." *Build Environ.*, 39(2), 201–209. <http://doi.org/10.1016/j.buildenv.2003.09.005>
- Thongtha, A., Maneewan, S., Punlek, C. and Ungkoon, Y. (2014). "Investigation of the compressive strength, time lags and decrement factors of AAC-lightweight concrete containing sugar sediment waste." *Energy Build.*, 84, 516–525. <http://doi.org/10.1016/j.enbuild.2014.08.026>
- Tsilingiris, P. T. (2008). "Thermo physical and transport properties of humid air at temperature range between 0 and 100°C." *Energ convers Manage.*, 49, 1098-1110.

Ulgen, K. (2002). “Experimental and theoretical investigation of effects of wall’s thermo physical properties on time lag and decrement factor.” *Energy Build.*, 34(3), 273–278. [http://doi.org/10.1016/S0378-7788\(01\)00087-1](http://doi.org/10.1016/S0378-7788(01)00087-1)

Zhang, Y., Du, K., He, J., Yang, L., Li, Y. and Li, S. (2014). “Impact factors analysis on the thermal performance of hollow block wall.” *Energy Build.*, 75, 330–341. <http://doi.org/10.1016/j.enbuild.2014.02.037>

Books:

Aleva, G. J. J. (1994). “*Laterites, Concepts, Geology, Morphology and Chemistry, International Interdisciplinary Laterite Reference Collection.*”, Wageningen, Netherlands.

Bansal, N. K., Hauser, G. and Minke, G. (1994). “*Passive building design: a handbook of natural climatic control.*” Elsevier science, Netherlands.

CIBSE. (2006). *CIBSE Environmental Design Guide-A*. 7th ed., Chartered Institution of Building services engineers, London.

Davies, M. G. (2004). “*Building Heat Transfer.*” John-Wiley & sons Ltd., U.K.

ECBC. (2009). “*Energy Conservation Building Code 2009.*” Bureau of Energy Efficiency, New Delhi, India 1-2.

GRIHA, (2011). “*Technical manual for trainers on building and system design optimization renewable energy application.*”, TERI, India.

Hall, M. R. (2010). “*Materials for energy efficiency and thermal comfort in buildings.*”, CRC Press. U.K.

IS: 1077. (1992). “*Common Burnt Clay building bricks-Specification CED 30: Clay and Stabilized Soil Products for Construction.*” Bureau of Indian standards, New Delhi.

IS: 3792. (1978). “*Indian standard guide for heat insulation of non industrial buildings.*” Indian standards institution, New Delhi., India pp.1-39.

IS:3620. (1979). “*Indian standard specification for laterite stone block for masonry*” Bureau of Indian standards. New Delhi.

IS: 3952. (1988). “*Specification for burnt clay hollow bricks for walls and partitions.*” Bureau of Indian standards, New Delhi., India 1-5.

Koo, J. H. (2006). *“Polymer nano composites- Processing, characterization and applications.”* McGraw –Hill., U.S.A.

NBC. (2005). *“National Building Code of India 2005, Section 1 Building and Services Lighting and Ventilation- Part 8”* Bureau of Indian Standards, New Delhi., India 1-47.

Trechsel, H. R. (2001). *“Moisture analysis and condensation control in building envelopes.”* ASTM., U.S.A.

Trechsel, H. R. and Bomberg, M. T. (2009). *“Moisture control in buildings: the key factor in mold prevention.”* ASTM., U.S.A.

Conference proceedings:

Valovirta, I. and Vinha, J. (2004). *“Water vapour permeability and thermal conductivity as a function of temperature and relative humidity.”* Proc., int. on DOE/ORNL/ASHRAE/BETEC/CIBSE/SBSE, Florida, USA., 1-16.

APPENDIX-I

BUILDING ENCLOSURES FOR REDUCING COOLING LOADS

Table I.1 Various recommended building enclosures/envelopes for reduced cooling loads from lower decrement factor and higher time lag perspective

S.No.	Building enclosure	Configuration
1.	Optimum air space thickness within wall to be maintained for reduced cooling loads.	<p style="text-align: center;">C-C₆</p> <p style="text-align: center;">P – Plaster A- Air space BM – Building material</p>
2.	Optimum air space location within wall for reduced heat gain through walls.	<p style="text-align: center;">C-D₆</p>
3.	Optimum insulation location within roof for reducing heat gain in building through roof.	<p style="text-align: center;">OUTSIDE CONDITIONS C-E₅ INSIDE CONDITIONS</p>
4.	Energy efficient hollow brick as compared to the conventional hollow bricks (The best suited for Composite climates).	<p style="text-align: center;">C-F₆</p>
5.	Energy efficient stuffed brick as compared to the conventional stuffed bricks (The best suited for Hot and humid climates).	<p style="text-align: center;">C-G₆</p>
6.	Energy efficient wall enclosure with optimum location of insulation (Energy efficient at any wind speed velocity).	<p style="text-align: center;">C-H₆</p> <p style="text-align: center;">0.0125P+0.01 EP+0.1 BM+0.01 EP+0.1 BM+0.0125P</p>



SHAIK SABOOR

■ Personal Data

Date of Birth: 03.08.1987

Address: H.No: 12-1-94, Sai Nagar, 7th Cross
Anantapur- 515001, Andhra Pradesh, India.

Mobile: +91 9880452903

Email: ssa.me11f05@nitk.edu.in , saboornitk@gmail.com

Website: <http://shaiksaboornitk.wix.com/scientist-site>

Nationality: Indian

■ Education

COURSE	INSTITUTION	YEAR OF PASSING	% OF MARKS
Ph.D (Mechanical Engineering)	National Institute of Technology Karnataka (NITK), Surathkal, Karnataka, India.	2016	8.75 (CGPA)
M-Tech (Refrigeration and Air-Conditioning)	JNT University, Anantapur, Andhra Pradesh, India.	Jun 2011	89.26%
B-Tech (Mechanical Engineering)	S.K. University, Anantapur, Andhra Pradesh, India.	Apr 2008	81.26%

■ Skills

Green Energy Building Simulation Software's: ECOTECT ANALYSIS, Architectural REVIT, Design Builder, Energy plus and STAR CCM+

PUBLICATIONS FROM PRESENT RESEARCH WORK

1. PEER REVIEWED INTERNATIONAL JOURNALS

1. Saboor, S. and Ashok Babu, T.P. (2016) “Influence of Ambient Air Relative Humidity and Temperature on Thermal Properties and Unsteady Thermal Response Characteristics of Laterite Wall Houses“ *Building and Environment* 99 170-183. <http://doi.org/10.1016/j.buildenv.2016.01.030> (Publisher: Elsevier; Index: SCI; Impact factor:3.83).
2. Saboor, S. and Ashok Babu, T.P. (2015) “Optimizing the Position of Insulating Materials in Flat Roof Exposed to Sun Shine to Gain Minimum Heat into Building under Periodic Heat Transfer Conditions” *Environmental Science and Pollution Research* 23(10) 9334-9344. <http://doi.org/10.1007/s11356-015-5316-7> (Publisher: Springer; Index: SCI; Impact factor: 2.83).
3. Saboor, S. and Ashok Babu, T.P. (2015) “Effects of Air Space Thickness within the External Walls on Dynamic Thermal Behavior of Building Envelopes for Energy Efficient Building Construction” *Energy Procedia* 79 766-771. <http://doi.org/10.1016/j.egypro.2015.11.564> (Publisher: Elsevier; Index: Scopus; SNIP:0.8).
4. Kirankumar, G., Saboor, S. and Ashok Babu, T.P., (2016) “Simulation of Various Wall and Window Glass Material for Energy Efficient Building Design“ *Key Engineering materials* 692 9-16. doi:10.4028/www.scientific.net/KEM.692.9 (Publisher: Transtech; Index:Scopus; Impact factor:0.2).
5. Saboor, S., Kirankumar, G. and Ashok Babu, T.P., (2016) “ Investigation of Building Walls Exposed to Periodic Heat Transfer Conditions for Green and Energy Efficient Building Construction“ *Procedia Technology* 23 496-503. <http://doi.org/10.1016/j.protcy.2016.03.055> (Publisher: Elsevier)
6. Saboor, S., Kirankumar, G. and Ashok Babu, T.P., (2016) “ Effect of Window Overhang shade on Heat gain of Various Single Glazing Window glasses for Passive Cooling“ *Procedia Technology* 23 439-446. <http://doi.org/10.1016/j.protcy.2016.03.048> (Publisher: Elsevier).
7. Kirankumar, G., Saboor, S. and Ashok Babu, T.P., (2016) “ Investigation of Different Window and Wall Materials for Solar Passive Building Design“ has been accepted for publication in journal of *Procedia Technology*. <http://doi.org/10.1016/j.protcy.2016.05.090> (Publisher: Elsevier) (Note: Peer-reviewed).
8. Saboor, S. and Ashok Babu, T.P. (2015) “Investigation of unsteady diurnal thermal behaviour of building walls exposed to periodic solar thermal excitation” *Journal of Renewable Energy Science, Technology & Economics.*, 1(1) 20-29. (ISSN: 2395-2644)

http://www.csrinstitute.co.in/yahoo_site_admin/assets/docs/S_Saboor.173151001.pdf

2. Papers Published in Reputed International Building Conferences

9. Ashok Babu, T.P. and Saboor, S. (2016) “Investigation of Dynamic Thermal Parameters of Various Insulation Filled Bricks Exposed to Periodic Thermal Variations for Energy Efficient Stuffed Bricks Design” Proceedings of 4th International High Performance Buildings Conference, Jul 11-14th, Purdue University, U.S.A. (Paper ID: 3416) (Note: Peer-reviewed).
10. Saboor, S. and Ashok Babu, T.P. (2015) “Investigation of Unsteady Thermal Response Characteristics of Various Hollow Bricks Exposed to Sinusoidal Solar Thermal Excitation” Proceedings of 14th International Conference of the International Building Performance Simulation Association IBPSA-2015, Dec 7-9th, 2015, IIIT Hyderabad, Telangana, India. (Paper ID: 2313) (Note: Peer-reviewed).
11. Saboor, S. and Ashok Babu, T.P. (2014) “Analytical computation of thermal response characteristics of homogeneous and composite walls of Building and Insulating materials used in India” Proceedings of 30th International PLEA Conference (Passive and Low Energy Architecture Conference), Volume 1, 516-523, Dec 16-18, CEPT University, Ahmedabad, Gujarat, India. (Paper ID: 2482) (ISBN (E-Book, Proceedings): 978-93-83184-03-3) <http://doi.org/10.13140/2.1.4717.9847> (Note: Peer-reviewed).
12. Ashok Babu, T.P. and Saboor, S. (2014) “Study of Unsteady State Thermal Characteristics of Homogeneous and Composite Walls of Building and Insulating Materials for Passive Cooling” Proceedings of 3rd International High Performance Buildings Conference, Purdue University, U.S.A. (Paper code: 3629; Available online in Purdue e-pubs) <http://doi.org/10.13140/2.1.3459.0402> (Note: Peer-reviewed).

■ Papers Published in Peer Reviewed International Conferences

13. Saboor, S. and Ashok Babu, T.P., (2016) “ Optimizing Vertical Air Space Location within the Wall for Energy Efficient Building Enclosure Design Based on Unsteady Heat Transfer Characteristics“ Proceedings of the International Conference on Recent Trends in Engineering and Material Sciences, Mar 17-19, 2016, Jaipur National University, Jaipur, Rajasthan, India. (Paper No: 981) ISBN:978935254230
14. Saboor, S., Kirankumar, G. and Ashok Babu, T.P., (2016) “ The Effect of Wall Orientation on Dynamic Thermal Characteristics of Laterite and Concrete Buildings in Four Different Indian Climatic Zones“ Proceedings of the International Conference on Recent Trends in Engineering and Material

- Sciences, Mar 17-19, 2016, Jaipur National University, Jaipur, Rajasthan, India. (Paper No: 1585) ISBN:978935254230
15. Kirankumar, G., Saboor, S. and Ashok Babu, T.P., (2016) “ Thermal Analysis of Wall and Window Glass Materials for Cooling Load Reduction in Green Energy Building Design“ Proceedings of the International Conference on Recent Trends in Engineering and Material Sciences, Mar 17-19, 2016, Jaipur National University, Jaipur, Rajasthan, India. (Paper No: 3013) ISBN:978935254230
 16. Kirankumar, G., Saboor, S. and Ashok Babu, T.P., (2016) “ Study of Various Solar and Thermal Control Reflective Glass materials for Energy Efficient Façade Glazing Design in Indian Climates“ Proceedings of the International Conference on Recent Trends in Engineering and Material Sciences, Mar 17-19, 2016, Jaipur National University, Jaipur, Rajasthan, India. (Paper No: 1615) ISBN:978935254230
 17. Kirankumar, G., Saboor, S. and Ashok Babu, T.P., (2015) “Effects of Single, Double, Triple and Quadruple Window Glazing of Various Glass Materials on Heat Gain in Green Energy Buildings“ Proceedings of the International Conference on Advances in Chemical Engineering, Dec 20-22, 2015, National Institute of Technology Karnataka, Surathkal, Karnataka, India. (Paper No: 70) (Note: Peer-reviewed).
 18. Kirankumar, G., Saboor, S. and Ashok Babu, T.P., (2015) “Investigation of Various Wall and Window Glass Material Buildings in Different Climatic Zones of India for Energy Efficient Building Construction” Proceedings of 5th International Conference on Advances in Energy Research ICAER-2015, Dec 15-17th, 2015, Indian Institute of Technology Bombay, Mumbai, India. (Paper No: 304) (Note: Peer-reviewed).
 19. Saboor, S. and Ashok Babu, T.P., (2015) “Investigation of Unsteady Heat Transfer Characteristics of Building Walls for Green Energy Building Construction” Proceedings of International Conference on New Frontiers in Chemical, Energy and Environmental Engineering INCEEE-2015, Mar 20-21st, NIT Warangal, Telangana, India. (ISBN: 978-81-928314-1-1, Page: 107) (Note: Peer-reviewed).
 20. Saboor, S. and Ashok Babu, T.P. (2014) “Effects of vertical air space location within the wall on thermal response characteristics of composite walls for green energy building construction applications” International conference on green technologies for environmental pollution control and prevention, NIT Tiruchirappalli, Tamilnadu, India (Note: Peer-reviewed).
 21. Saboor, S. and Ashok Babu, T.P. (2013) “Analytical computation of admittance, decrement factor, timelag and surface factors for different exterior wall materials of the buildings in Dakshina Kannada District” Proceedings of the 22nd National and 11th International ISHMT-ASME heat and mass transfer conference, IIT Kharagpur, West bengal, India. (HMTC: 1300782) <http://doi.org/10.13140/2.1.3196.8965> (Note: Peer-reviewed).
 22. Kirankumar, G., Saboor, S. and Ashok Babu, T.P., (2016) “Experimental and Theoretical Studies of Window Glazing Materials of Green Energy Building in Indian Climatic Zones “International Conference on Recent Advancements in Air-conditioning and Refrigeration (RAAR) to be held in November 10-

12 at CV Raman College of Engineering, Bhubaneswar. (Accepted to be presented)

3. NATIONAL CONFERENCES

23. Kirankumar, G., Saboor, S. and Ashok Babu, T.P., (2015) “Effects of thermal and optical properties of building wall and window glass materials on heat gain into the buildings for passive building design“ Proceedings of 4th National Conference on Refrigeration and Air Conditioning NCRAC 2015 28-30th October 2015 organized by Rajalakshmi Engineering College and IIT Madras, Chennai, India.
24. Saboor, S. and Ashok Babu, T.P., (2015) “Investigation of Building Walls Exposed to Sinusoidal Periodic Heat Transfer Conditions for Green and Energy Efficient Building Construction“ Proceedings of National conference on Trends in Mechanical Engineering (TIME-15) 23rd September-2015 JNT University, Anantapur, Andhra pradesh, India.

■ BOOK CHAPTER PUBLICATIONS

25. Kirankumar, G., Saboor, S. and Ashok Babu, T.P., (2016) “ Effects of Single, Double, Triple and Quadruple Window Glazing of Various Glass Materials on Heat Gain in Green Energy Buildings” has been accepted for book publication : Materials, Energy and Environment Engineering by Springer Publication (Note: Peer-reviewed). ISBN 978-981-10-2675-1

4. THE BEST RESEARCH PAPER AWARDS RECEIVED

1. Saboor, S. and Ashok Babu, T.P. (2015) “Investigation of Unsteady Heat Transfer Characteristics of Building Walls for Green Energy Building Construction” International Conference on New Frontiers in Chemical, Energy and Environmental Engineering INCEEE-2015, Mar 20-21st, NIT Warangal, India.
2. Saboor, S. and Ashok Babu, T.P. (2015) “Investigation of unsteady diurnal thermal behaviour of building walls exposed to periodic solar thermal excitation” International Conference on Renewable Energy Science, Technology & Economics, Feb 13-14, organized by Chandradeep solar research institute at Jadavpur University, Kolkata, West Bengal, India.
3. KiranKumar, G., Saboor, S. and Ashok Babu, T.P. (2016) “ Investigation of Various Low Emissivity Glass Materials for Green Energy Building Construction in Indian Climatic Zones ” International conference on Advancements in aeromechanical materials for manufacturing (ICAAMM-2016), Jul 7th – 9th , organized by MLRIT Hyderabad, India and Elsevier materials today.

■ PUBLICATIONS IN POST GRADUATION LEVEL

1. Yohan, M., Prasanthi, G. and Saboor, S. (2011) “An experimental approach to reduce the effect of starving on compressor in vapour compression refrigeration system” *Technology today* 3(2) 173-178. (ISSN: 2180-0987)
2. Govinda Rajulu, K., Kirankumar, G. and Saboor, S. (2011)“Experimental analysis of the effect of coiled capillary tube height on vapor compression refrigeration system performance” *Engineering today* 13 (6) 151-158. (ISSN: 0974-8377)
3. Yohan, M., Prasanthi, G., Saboor, S. and Kirankumar, G. (2011) “Experimental Analysis of Vapour Compression Refrigeration system by the Evaporator inlet Nozzle concept” *Engineering today* 13 (5) 131-136. (ISSN: 0974-8377)
4. Yohan, M. and Saboor, S. (2011) “Experimental Analysis of Vapour Compression Refrigeration system by the Condenser inlet Diffuser concept” *Engineering today* 13 (4) 129-134. (ISSN: 0974-8377)
5. Saboor, S., Yohan, M. and Kirankumar, G. (2011) “Experimental Analysis of Vapour Compression Refrigeration System by the Condenser Inlet Diffuser Concept” Proceedings of 5th International Conference on Advances in Mechanical Engineering ICAME-2011, S.V. National Institute of Technology, Surat, Gujarat, India. (Paper code: TF-65; Page: 857) <http://doi.org/10.13140/2.1.1820.6406>

■ AWARDS RECEIVED IN NATIONAL LEVEL TECHNICAL SYMPOSIUMS IN UNDER GRADUATION LEVEL

1. A National conference paper on “Analysis of quality control by six sigma concept” was awarded with **First prize** in JNT University, Anantapur, in 2007.
2. A National conference paper on “Practical implementation of six sigma concept in steel plant” was awarded with **First prize** in G.Pulla Reddy Engineering College, Kurnool in 2007.
3. A National conference poster on “Cam less I.C. engines” was awarded with **Second prize** in SV University, Tirupati in 2007.
4. A National Level Technical Paper presentation at SRTIST Nalgonda on “Analysis of quality control by six sigma concept” was awarded with **Second prize**.

■ ACADEMIC ACHIEVEMENTS

1. M-Tech project on “Analysis of Vapor Compression Refrigeration system by the condenser inlet diffuser concept“ is awarded as **Excellent** thesis of the batch by JNT University, Anantapur, Andhra Pradesh, India.
2. M-Tech (Refrigeration & Air-Conditioning) **Topper** from JNT University, Anantapur, Andhra Pradesh, India.
3. B-Tech **Gold Medalist** from G. Pulla Reddy Engineering College (Autonomous), Kurnool, Andhra Pradesh, India.
4. **Topper** in Diploma in Mechanical Engineering pursued at Govt.polytechnic, Anantapur, Andhra Pradesh, India.
5. Received Merit Scholarships/Certificates for securing highest aggregate percentage in academics.
6. Received Awards/Certificates in competitions such as Just a minute, Debates and Seminars.

■ Experience

1. Currently working as Lecturer (Asst.) in Mechanical Engineering Department of National Institute of Technology Karnataka since 11-07-2016.
2. Having one year of experience from 2008 to 2009 in teaching Mechanical subjects (thermodynamics, introduction to aero space engineering and Engg.mechanics) in Vignan institute of technology and sciences, Deshmukhi, Hyderabad, Telangana, India.
3. Having experience of teaching (Part time) Engg.mechanics to no.of students of various colleges in Anantapur, Andhra pradesh, India.

■ Declaration

I hereby solemnly declare that the above furnished information is true to the best of my knowledge and belief.

Place: Surathkal, India.

Date: 15-10-2016

(S. SABOOR)